

ANALYSIS OF THE RELATIONSHIP BETWEEN  
METEOROLOGY AND AIR POLLUTION  
AT DEUSELBACH, WEST GERMANY

by

Captain Stephen Robert Messina

Thesis submitted to the Faculty of the Graduate School  
of the University of Maryland in partial fulfillment  
of the requirements for the degree of  
Master of Science  
1985

SEC

AD-A171 425

(Entered)

PAGE		READ INSTRUCTIONS BEFORE COMPLETING FORM	
1. REPORT NUMBER		3. RECIPIENT'S CATALOG NUMBER	
AFIT/CI/NR 86- 116T			
4. TITLE (and Subtitle) Analysis of the Relationship Between Meteorology and Air Pollution at Deuselbach, West Germany		5. TYPE OF REPORT & PERIOD COVERED THESIS/DISSERTATION	
		6. PERFORMING ORG. REPORT NUMBER	
7. AUTHOR(s) Stephen Robert Messina		8. CONTRACT OR GRANT NUMBER(s)	
9. PERFORMING ORGANIZATION NAME AND ADDRESS AFIT STUDENT AT: University of Maryland		10. PROGRAM ELEMENT, PROJECT, TASK AREA & WORK UNIT NUMBERS	
11. CONTROLLING OFFICE NAME AND ADDRESS AFIT/NR WPAFB OH 45433-6583		12. REPORT DATE 1985	
		13. NUMBER OF PAGES 187	
14. MONITORING AGENCY NAME & ADDRESS (if different from Controlling Office)		15. SECURITY CLASS. (of this report) UNCLAS	
		15a. DECLASSIFICATION/DOWNGRADING SCHEDULE	
16. DISTRIBUTION STATEMENT (of this Report) APPROVED FOR PUBLIC RELEASE; DISTRIBUTION UNLIMITED			
17. DISTRIBUTION STATEMENT (of the abstract entered in Block 20, if different from Report)			
18. SUPPLEMENTARY NOTES APPROVED FOR PUBLIC RELEASE: IAW AFR 190-1 LYNN E. WOLAVER Dean for Research and Professional Development AFIT/NR			
19. KEY WORDS (Continue on reverse side if necessary and identify by block number)			
20. ABSTRACT (Continue on reverse side if necessary and identify by block number) ATTACHED. FILE COPY			

DD FORM 1 JAN 73 1473

EDITION OF 1 NOV 65 IS OBSOLETE

SECURITY CLASSIFICATION OF THIS PAGE (When Data Entered)

## **DISCLAIMER NOTICE**

**THIS DOCUMENT IS BEST QUALITY  
PRACTICABLE. THE COPY FURNISHED  
TO DTIC CONTAINED A SIGNIFICANT  
NUMBER OF PAGES WHICH DO NOT  
REPRODUCE LEGIBLY.**

112

## ABSTRACT

Title of Thesis: Analysis of the Relationship between  
Meteorology and Air Pollution at  
Deuselbach, West Germany

Stephen Robert Messina, Master of Science, 1985

Thesis directed by: Dr. Russell R. Dickerson  
Assistant Professor  
Department of Meteorology

During the period, January to August 1982, in cooperation with the German Environmental Bureau, meteorological and air pollution data were gathered at a clean air monitoring station near the West German village of Deuselbach. The meteorological data consisted of measurements in the following areas: temperature, relative humidity, wind direction and speed, rainfall and UV radiation. Air pollution measurements of nitric oxide, nitrogen dioxide, total reactive nitrogen, sulfur dioxide, carbon dioxide, ozone and total suspended particles were recorded as well.

It is the intention of this thesis to examine thoroughly how each of these meteorological parameters either enhances or diminishes the levels of atmospheric pollutants. Additionally, the relationships among the pollutants will also be examined. This is a desired aspect since correlation among pollutants could point to a common source region.

A

442

A comparison of two techniques (Chemiluminescent and Saltzman) for the measurement of nitrogen dioxide will also be considered. A discussion of nitrogen dioxide is necessary in the air pollution problem, since it is a primary pollutant, which can affect both human and plant life as well as being one of the catalysts in smog formation.

Finally, the theory of the photostationary state will be studied. This theory addresses the relationships among nitric oxide, nitrogen dioxide, ozone and UV radiation. The interaction of these constituents within the framework of the photostationary state is responsible for photochemical smog.



10-13  
10-13  
10-13

A-1	23	DDC
-----	----	-----

**c Copyright Stephen Robert Messina 1985**

## DEDICATION

In striving to achieve a worthwhile goal some sacrifice should always be expected. However, it is unfortunate that this sacrifice must be shared by those who will receive little or no credit when this goal is finally reached. Due to the demanding nature of this work, there were many missed opportunities to share time with both my wife and daughter. Therefore, I affectionately dedicate this work to my loving wife Michelle, without whose love, constant encouragement, and loyalty I would never have persevered and to my daughter Jennifer, who had to do "without daddy" on so many occasions.

## ACKNOWLEDGEMENTS

I would like to express my sincerest thanks to Dr. Russell R. Dickerson for his guidance, encouragement and endless patience in the preparation of this thesis. I would like to thank Mr. Henry Black for his many helpful suggestions and the loan of many books and pamphlets from his own personal collection. I wish to express my appreciation to Dr. Zwanzig of the University of Maryland Molecular Physics Department for allowing me the use of the department's computer. The initial drafts of this thesis were typed by my wife, Michelle and then finalized by Mrs. Edward Hougendobler. I would like to thank both of them very much. The opportunity to engage in this work was provided by the U.S. Air Force Institute of Technology.



## TABLE OF CONTENTS

Section	Page
DEDICATION	ii
ACKNOWLEDGEMENTS	iii
LIST OF TABLES	v
LIST OF FIGURES	ix
I. INTRODUCTION	1
II. CHEMICAL AND METEOROLOGICAL FACTORS	10
A. Atmospheric Photochemistry	10
B. Photostationary State	24
C. Meteorological Parameters	29
III. DATA	36
IV. ANALYSIS	45
A. Sulfur Dioxide	45
B. Nitrogen Dioxide	67
C. Ozone	85
D. Carbon Dioxide	98
E. Photostationary State	102
1. Clear Skies	103
2. Cloudy Skies	112
V. CONCLUSIONS	117
APPENDIX A. SALTZMAN VS CHEMILUMINESCENCE DATA	119
APPENDIX B. STATISTICS DATA	122
APPENDIX C. PHOTOSTATIONARY STATE DATA	131
APPENDIX D. SAMPLE PROGRAMS	178
SELECTED BIBLIOGRAPHY	182

# LIST OF TABLES

Table		Page
1	Composition of a Typical Smog.	2
2	Composition of Clean, Dry Surface Air.	5
3	Average Lifetimes, Major Sources and Major Sinks of Atmospheric Constituents.	6
4	Federal Ambient Air Quality Standards.	7
5	Predicted Equilibrium Composition of NO and NO <sub>2</sub> at Various Temperatures.	17
A-1	Concentrations of NO <sub>2</sub> in ppb for the Saltzman and Chemiluminescent Methods for January 23-31, 1982.	119
A-2	Concentrations of NO <sub>2</sub> in ppb for the Saltzman and Chemiluminescent Methods for March 1-31, 1982.	119
A-3	Concentrations of NO <sub>2</sub> in ppb for the Saltzman and Chemiluminescent Methods for May 1-13, 1982.	120
A-4	Concentrations of NO <sub>2</sub> in ppb for the Saltzman and Chemiluminescent Methods for August 20-24, 1982.	121
B-1	Linear Correlation Coefficients for January.	122

# LIST OF TABLES

Table		Page
B-2	Linear Correlation Coefficients for February.	123
B-3	Linear Correlation Coefficients for March.	124
B-4	Linear Correlation Coefficients for April.	125
B-5	Linear Correlation Coefficients for May.	126
B-6	Linear Correlation Coefficients for August.	127
B-7	Standard Deviations.	128
B-8	Variance.	128
B-9	Covariance with SO <sub>2</sub> .	129
B-10	Covariance with O <sub>3</sub> .	129
B-11	Covariance with CO <sub>2</sub> .	130
B-12	Covariance with NO <sub>2</sub> .	130

# LIST OF TABLES

Table		Page
C-1	Photostationary State (PSS) data for March 24, 1982.	138
C-2	Photostationary State (PSS) data for March 25, 1982.	141
C-3	Photostationary State (PSS) data for March 26, 1982.	144
C-4	Photostationary State (PSS) data for March 27, 1982.	147
C-5	Photostationary State (PSS) data for May 11, 1982.	150
C-6	Photostationary State (PSS) data for May 12, 1982.	152
C-7	Photostationary State (PSS) data for May 13, 1982.	154
C-8	Photostationary State (PSS) data for January 26, 1982.	156
C-9	Photostationary State (PSS) data for January 27, 1982.	159

## LIST OF TABLES

Table		Page
C-10	Photostationary State (PSS) data for March 20, 1982.	162
C-11	Photostationary State (PSS) data for March 21, 1982.	165
C-12	Photostationary State (PSS) data for May 1, 1982.	168
C-13	Photostationary State (PSS) data for May 4, 1982.	170
C-14	Photostationary State (PSS) data for August 20, 1982.	172
C-15	Photostationary State (PSS) data for August 24, 1982.	175

## LIST OF FIGURES

Figure		Page
1	Diurnal Variation of Shortwave and Ultraviolet Solar Radiation on a "Polluted" and on a "Clean" Day in Downtown Cincinnati.	9
2	Diurnal Variation of NO, NO <sub>2</sub> , and O <sub>3</sub> Concentrations in Los Angeles, July 19, 1965.	26
3	Values of the Photostationary State /Number P Calculated from Values of NO, NO <sub>2</sub> , O <sub>3</sub> and j(NO <sub>2</sub> ) for April 14, 1979 at Niwot Ridge.	28
4	The Photolysis of NO <sub>2</sub> , j(NO <sub>2</sub> ) and the Ambient Temperature at Niwot Ridge on April 14, 1979.	28
5	Political Map of Central Europe.	37
6	Daily Values of Chemiluminescence vs Saltzman for: 23-31 January, 1-31 March, 1-13 May, and 20-24 August 1982.	40
7	SO <sub>2</sub> Wind Rose.	47
8	January versus the Daily Means of SO <sub>2</sub> and (a) Wind Direction and (b) Dust.	48
9	January versus the Daily Means of SO <sub>2</sub> and (a) Precipitation and (b) Relative Humidity.	50
10	February versus the Daily Means of SO <sub>2</sub> and (a) Wind Direction and (b) Dust.	53
11	February versus the Daily Means of SO <sub>2</sub> and (a) Precipitation and (b) Relative Humidity.	54
12	0700Z Atlantic/European Surface Analysis on February 21, 1982.	55

# LIST OF FIGURES

Figure		Page
13	Simplified Skew-T Log P Diagram from Deuselbach area on February 21, 1982.	56
14	March versus the Daily Means of SO <sub>2</sub> and (a) Wind Direction and (b) Dust.	58
15	March versus the Daily Means of SO <sub>2</sub> and (a) Precipitation and (b) Relative Humidity.	59
16	April versus the Daily Means of SO <sub>2</sub> and (a) Wind Direction and (b) Dust.	61
17	April versus the Daily Means of SO <sub>2</sub> and (a) Precipitation and (b) Relative Humidity.	62
18	May versus the Daily Means of SO <sub>2</sub> and (a) Wind Direction and (b) Dust.	63
19	May versus the Daily Means of SO <sub>2</sub> and (a) Precipitation and (b) Relative Humidity.	64
20	August versus the Daily Means of SO <sub>2</sub> and (a) Wind Direction and (b) Dust.	65
21	August versus the Daily Means of SO <sub>2</sub> and (a) Precipitation and (b) Relative Humidity.	66
22	NO <sub>2</sub> Wind Rose.	69
23	January versus the Daily Means of NO <sub>2</sub> and (a) Wind Direction and (b) Temperature.	71
24	1200Z Surface Analysis of North Central Europe on January 21, 1982.	72

# LIST OF FIGURES

Figure		Page
25	February versus the Daily Means of NO <sub>2</sub> and (a) Wind Direction and (b) Temperature.	73
26	March versus the Daily Means of NO <sub>2</sub> and (a) Wind Direction and (b) Temperature.	75
27	0700Z Atlantic/European Surface Analysis on March 5, 1982.	76
28	0700Z Atlantic/European Surface Analysis on March 13, 1982.	77
29	April versus the Daily Means of NO <sub>2</sub> and (a) Wind Direction and (b) Temperature.	79
30	May versus the Daily Means of NO <sub>2</sub> and (a) Wind Direction and (b) Temperature.	81
31	1200Z Surface Analysis of North Central Europe on May 30, 1982.	82
32	August versus the Daily Means of NO <sub>2</sub> and (a) Wind Direction and (b) Temperature.	84
33	January versus the Daily Means of O <sub>3</sub> and (a) Wind Direction and (b) Temperature.	87
34	1200Z Surface Analysis of North Central Europe on January 4, 1982.	88
35	February versus the Daily Means of NO <sub>2</sub> and (a) Wind Direction and (b) Temperature.	90
36	March versus the Daily Means of NO <sub>2</sub> and (a) Wind Direction and (b) Temperature.	92



# LIST OF FIGURES

Figure		Page
37	April versus the Daily Means of O <sub>3</sub> and (a) Wind Direction and (b) Temperature.	93
38	May versus the Daily Means of NO <sub>2</sub> and (a) Wind Direction and (b) Temperature.	95
39	August versus the Daily Means of O <sub>3</sub> and (a) Wind Direction and (b) Temperature.	97
40	(a) January and (b) February versus the Daily Means of CO <sub>2</sub> and Dust.	99
41	(a) March and (b) April versus the Daily Means of CO <sub>2</sub> and Dust.	100
42	(a) May and (b) August versus the Daily Means of CO <sub>2</sub> and Dust.	101
43	Daily Values of (a) P and (b) j(NO <sub>2</sub> ) for Clear Skies on March 24, 1982.	104
44	Daily Values of (a) P and (b) j(NO <sub>2</sub> ) for Clear Skies on March 25, 1982.	105
45	Daily Values of (a) P and (b) j(NO <sub>2</sub> ) for Clear Skies on March 26, 1982.	106
46	Daily Values of (a) P and (b) j(NO <sub>2</sub> ) for Clear Skies on March 27, 1982.	107
47	Daily Values of NO, NO <sub>2</sub> , and O <sub>3</sub> under Clear Skies on May 13, 1982.	110
48	Daily Values of (a) P and (b) j(NO <sub>2</sub> ) for Clear Skies on January 26, 1982.	113
49	Daily Values of (a) P and (b) j(NO <sub>2</sub> ) for Clear Skies on January 27, 1982.	114
50	Daily Values of (a) P and (b) j(NO <sub>2</sub> ) for Clear Skies on May 1, 1982.	115

# LIST OF FIGURES

Figure		Page
51	Daily Values of (a) P and (b) $j(\text{NO}_2)$ for Clear Skies on August 24, 1982.	116
C-1	Daily values of (a) P and (b) $j(\text{NO}_2)$ for Clear Skies on May 11, 1982.	131
C-2	Daily values of (a) P and (b) $j(\text{NO}_2)$ for Clear Skies on May 12, 1982.	132
C-3	Daily values of (a) P and (b) $j(\text{NO}_2)$ for Clear Skies on May 13, 1982.	133
C-4	Daily values of (a) P and (b) $j(\text{NO}_2)$ for Cloudy Skies on March 20, 1982.	134
C-5	Daily values of (a) P and (b) $j(\text{NO}_2)$ for Cloudy Skies on March 21, 1982.	135
C-6	Daily values of (a) P and (b) $j(\text{NO}_2)$ for Cloudy Skies on May 4, 1982.	136
C-7	Daily values of (a) P and (b) $j(\text{NO}_2)$ for Cloudy Skies on August 20, 1982.	137

## SECTION I

### INTRODUCTION

The concept of air pollution is not new to any of us. We are constantly reminded of its presence through various forms of media and personal observations. The roots of our current dilemma can be traced back to the Industrial Revolution of the early 1800's and enhanced by the proliferation of the internal combustion engine. Therefore the rewards of a technologically advancing community are tempered by the side effect of polluting our environment (Wark and Warner, 1981).

Attempts to control or eliminate pollutants are not new. As far back as 1272, King Edward I of England attempted to clear up the smokey skies of London by banning the use of "sea coal". This effort was serious enough to cause the British Parliament to order the torture and hanging of a man who defied the King by selling and burning this "sea coal" (Wark and Warner, 1981).

Since that time there have been numerous pollution episodes in our history, but none more dramatic and devastating than the December 5-8, 1952 episode in London. The 500 foot deep blanket of smog that settled over the city had the composition seen in Table 1.

TABLE 1.--Composition of a Typical Smog (Petterssen, 1969)

Components	Weight	
	Tons/mi <sup>3</sup>	Tons/km <sup>3</sup>
Dry Air	2,000,000	500,000
Liquid Water	18,000	4,500
Water Vapor	68,000	17,000
Smoke Particles	40	10
Sulfur Dioxide	40	10

Despite the fact that the weight of the smoke and sulfur dioxide amounted to only about 0.4 percent of the weight of the liquid water, the effect was both repulsive and deadly. The death toll rose to 4,000 with the majority of the victims having histories of heart or respiratory trouble (Petterssen, 1969).

Atmospheric pollutants are harsh on vegetation as well as on people. According to the National Crop Loss Assessment Network, ozone, sulfur dioxide and nitrogen dioxide cause about 90% of the crop damage induced by gaseous air pollutants in the United States (Hileman, 1982). In order to compensate for their losses, farmers charge a higher price for their goods and the end result is increased consumer prices. Therefore, pollutants can have a distinct economic impact as well.

There are many descriptions or definitions of the term "air pollution." Wark and Warner, (1981) state that,

Air pollution may be defined as the presence in the outdoor atmosphere of one or more contaminants or combinations thereof in such quantities and of such duration as may be or may tend to be injurious to human, plant or animal life, or property or which unreasonably interferes with the comfortable enjoyment of life or property or the conduct of business.

The inverse question now would be to define what is meant by a clean atmosphere. It is defined by the contents of Table 2, which shows the major and trace constituents of clean dry air near sea level. Any other substance or concentrations above the amounts specified in Table 2 would be considered an air pollutant.

Table 3 discusses the average lifetimes, major sources and sinks of the pollutants discussed in this thesis.

Table 4 lists the U.S. Federal Ambient Air Quality Standards of most of the atmospheric constituents discussed in this work.

Meteorological parameters do exert a strong influence on atmospheric chemistry. According to the World Survey of Climatology (Volume 6, Climates of Central and Southern Europe),

The upper Rhine Valley is prone to the formation of temperature inversions and air stagnation resulting in detrimental pollution effects due to the trapping of noxious fumes, particularly in the densely populated industrial centers of Mannheim and Ludwigshafen as well as the Rhine-Main Basin.

However, atmospheric pollutants can also affect such parameters as visibility and short wave radiation.

TABLE 2.-- Composition of Clean, Dry, Surface Air  
(National Science Foundation, 1972)

Component	Content	
	% By Volume	ppm
Nitrogen	78.09	780,900
Oxygen	20.94	209,400
Argon	0.93	9,300
Carbon Dioxide	0.0318	360
Neon	0.0018	18
Helium	0.00052	5.2
Krypton	0.0001	1.0
Xenon	0.000008	0.08
Nitrous Oxide	0.00003	0.3
Hydrogen	0.00005	0.5
Methane	0.00017	1.7
Nitrogen Dioxide	0.00000001	0.0001
Ozone	0.000002	0.02
Sulfur Dioxide	0.00000002	0.0002
Carbon Monoxide	0.00001	0.1
Ammonia	0.000001	0.0001

TABLE 3.-- Average Lifetimes, Major Sources and Major Sinks of Atmospheric Constituents (Average lifetimes vary depending on the rate constant and concentration). The \* represents interconvergence reactions which do not affect  $\text{NO}_x$  concentrations.

	Major Sources	Major Sinks
$\text{NO}_x$	Fossil fuel burning (temp > 1800K)  $\text{N}_2 + \text{O}_2 \rightarrow 2\text{NO}$ $\text{NO}_2 + h\nu \rightarrow \text{NO} + \text{O}^*$ $\text{NO} + \text{O}_3 \rightarrow \text{NO}_2 + \text{O}_2^*$ Soil Nitrification  Lightning	Dry Deposition  $\text{NO}_2 + \text{OH} + \text{M} \rightarrow \text{HNO}_3 + \text{M}$
$\text{O}_3$	Tropospheric Photo-chemistry  Stratospheric Diffusion	$\text{NO} + \text{O}_3 \rightarrow \text{NO}_2 + \text{O}_2$ $\text{NO}_2 + \text{OH} + \text{M} \rightarrow \text{HNO}_3 + \text{M}$ $\text{HO}_2 + \text{O}_3 \rightarrow \text{OH} + 2\text{O}_2$ $\text{OH} + \text{O}_3 \rightarrow \text{HO}_2 + \text{O}_2$  Dry Deposition
$\text{SO}_2$	Fossil fuel burning  Oxidation of Reduced Sulfur Compounds  Emissions From Marine & Coastal Areas  Volcanoes	Dry deposition to vegetation and soil  Wet deposition  $\text{SO}_2 + \text{OH} + \text{O}_2 + \text{H}_2\text{O} \rightarrow \text{H}_2\text{SO}_4 + \text{HO}_2$
$\text{CO}_2$	Fossil fuel/wood burning  Release from vegetation  Decay	Absorption by vegetation and oceans



TABLE 4.-- Federal Ambient Air Quality Standards  
(Federal Register 36, No. 84, Part II, April  
30, 1971, pp. 8186-8201 (11); 43, September,  
1978, p. 46246)

Pollutant	Averaging Time	Primary Standard	Measurement Method
Nitrogen Dioxide	Annual Average	10 ug/m <sup>3</sup> (50 ppb)	Colorimetric Using NaOH
Sulfur Dioxide	Annual Average 24Hr	80 ug/m <sup>3</sup> (30 ppb)  365 ug/m <sup>3</sup> (140 ppb)	Pararosaniline Method
Suspended Particulate Matter	Annual Geometric Mean	75 ug/m <sup>3</sup>	High Volume Sampling
Ozone	1 Hr	240 ug/m <sup>3</sup> (120 ppb)	Chemilumines- cent Method

For example, a polluted city may receive on the average of 10 to 20 percent less solar radiation than the surrounding rural areas (Bach, 1972). This is illustrated in Figure 1.

This work will analyze the photostationary state and the relationship between meteorology and selected atmospheric constituents which are a part of the air pollution problem. A comparison of two techniques (Chemiluminescence and Saltzman) used in the measurement of nitrogen dioxide will also be considered. A discussion of nitrogen dioxide is necessary in the air pollution problem, since it is a primary pollutant, which can affect both human and plant life as well as being one of the catalysts in smog formation. By analyzing the meteorology in conjunction with the chemistry we will show that meteorology can have either positive or negative effects on atmospheric chemistry. Examining the photostationary state is necessary to further an understanding of the mechanism which is responsible for generating photochemical smog. A combination of empirical and statistical methods will be employed in this work.

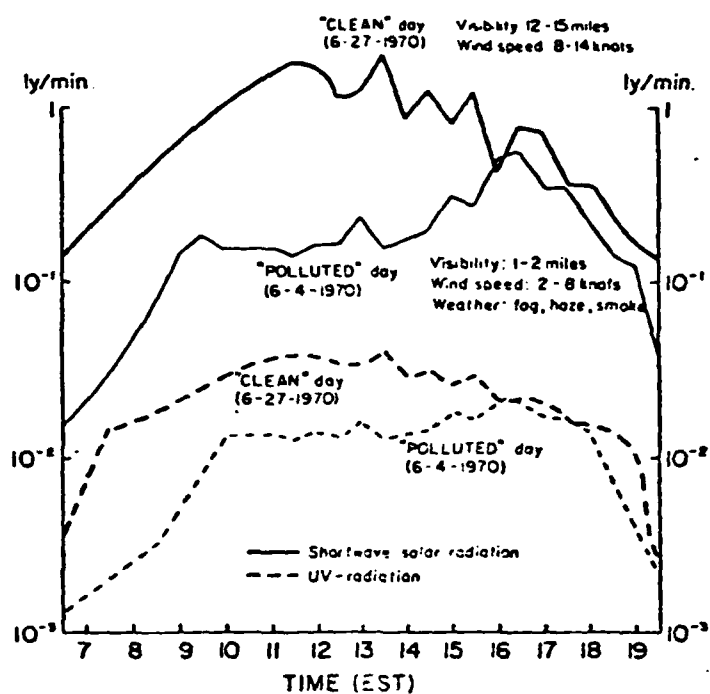


Figure 1. Diurnal Variation of Shortwave and Ultraviolet Solar Radiation on a "Polluted" and on a "Clean" Day in Downtown Cincinnati (Bach, 1972).

## SECTION II

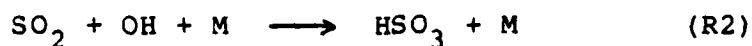
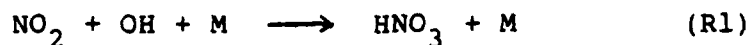
### CHEMICAL AND METEOROLOGICAL FACTORS

#### A. Atmospheric Photochemistry

Photochemical processes, which begin with the photodissociation of ozone through the absorption of UV radiation, play a dominant role in governing the transformation of tropospheric carbon, nitrogen and sulfur compounds (Crutzen, 1983). Through a chain of succeeding reactions other constituents are produced, which then react with many tropospheric compounds which, would otherwise be inert. Photochemical processes are also vital in the tropospheric removal of many important compounds (Leighton, 1961; Levy, 1971; Crutzen, 1983). Photochemistry involves the absorption and excitation of a constituent by light or more specifically solar radiation. Altering this light source will impact on the photochemical process. For example, the advent of sunset will halt photochemistry, while increasing cloud cover will only retard it. Photochemistry is also important in causing the formation of secondary pollutants (Finlayson and Pitts, 1976).

Some photochemical processes in an industrial air mass involving one primary pollutant can indirectly influence the oxidation cycle of another primary pollutant. This point was put forward by Rodhe et al.

(1981) for the case of  $\text{NO}_2$  and  $\text{SO}_2$ . Reaction R1 is approximately ten times faster than Reaction R2. M is any third body which serves to carry away energy but does not take part in the reaction.



In a situation where photochemistry plays a significant role, the oxidation of  $\text{SO}_2$  may be delayed. Hahn and Crutzen (1982) suggest that since R1 is significantly faster than R2, the formation of  $\text{HNO}_3$  (nitric acid), could function as a sink for OH, providing that the mixing ratio of  $\text{NO}_x$  (discussed later) is of the order of a few nanolitres per litre or more. Therefore, the oxidation of  $\text{SO}_2$  may be delayed, until  $\text{NO}_2$  concentrations fall below 1 nl/l. In the final analysis  $\text{HNO}_3$  will form significantly faster than  $\text{H}_2\text{SO}_4$  (sulfuric acid) (Rodhe et al., 1981). The exact path taken by  $\text{SO}_2$  to form  $\text{H}_2\text{SO}_4$  will be illustrated later in R14 - R16.

Photochemical reactions are responsible for the generation of the type of smog seen in cities such as Los Angeles and in other cities or regions where no large scale heavy industry occurs (Calvert, 1976 and Schjoldager, 1978).

The photostationary state, which is critical to understanding this type of smog generation will be dealt with later in this section.

Many of the photochemical reactions covered in this work involve constituents which will either receive only passing mention or be entirely ignored. This in no way diminishes their importance or significance in such reactions. They do not however, lie within the scope of this effort.



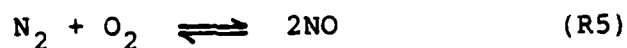
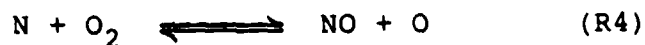
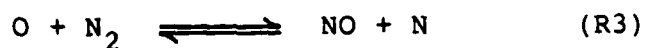
The symbol  $\text{NO}_x$  is used to define the combination of nitric oxide (NO) and nitrogen dioxide ( $\text{NO}_2$ ) such that  $\text{NO}_x = \text{NO} + \text{NO}_2$ . Anthropogenic sources, such as fossil fuel combustion and biomass burning, dominate the tropospheric input of  $\text{NO}_x$  (Garnett, 1979; Glasston, 1981; Crutzen, 1983; Fishman, 1983; Logan, 1983). NO and  $\text{NO}_2$  are the most important N species in atmospheric photochemistry. They serve as the catalysts in many atmospheric reaction chains as well as controlling the distribution of atmospheric ozone (Chameides and Walker, 1973 and Crutzen, 1973). Photochemistry of the polluted troposphere will develop around the nitrogen oxides. The key reaction in this photochemical process is the photodissociation of  $\text{NO}_2$ .

This reaction results in the production of NO and O i.e., atomic oxygen (Hanst, 1978). Photochemistry also affects the proportionality of NO<sub>x</sub> constituents, since the levels of NO and NO<sub>2</sub> are seen to shift during the day. In the study of smog formation an understanding of O<sub>3</sub> (ozone) is vital, but NO<sub>x</sub> still remains the prime factor. Therefore the key to understanding the importance of photochemical production of tropospheric O<sub>3</sub> is the attainment of tropospheric NO<sub>x</sub> distribution (Kelly et al., 1980; Crutzen and Gidel, 1983; Fishman, 1983; Logan, 1983).

#### Nitric Oxide

Nitric oxide (NO) is a colorless gas whose ambient concentration is usually well below 0.5 ppm (parts per million) which is the limit for health effects. NO acts catalytically to produce ozone by a series of reactions which will be discussed later. The end result of these reactions (initiated by NO) is a photochemical smog episode, which could occur in urban, rural or remote locations.

NO will form, as a side effect of the burning of fossil fuels, when the temperature is in excess of 1800 K. The primary reactions which describe this formation are known as the Zeldovich Mechanism and are as follows:



This mechanism will continue as long as an elevated temperature is accompanied by a source of nitrogen and oxygen (Wark and Warner, 1981). The most significant factor in the production of NO under normal combustion conditions is temperature. At high temperatures both kinetics and thermodynamics favor the formation of NO. In short, the higher the temperature, the greater the production of NO (Spedding, 1974).

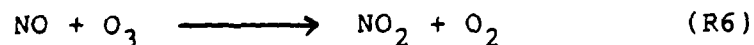
It therefore seems to follow that fossil fueled power plants and internal combustion engines, which all operate at high temperatures, would be dominant sources of atmospheric NO in industrial areas.

#### Nitrogen Dioxide

Nitrogen dioxide ( $\text{NO}_2$ ) is a brownish gas and a primary pollutant.  $\text{NO}_2$  is not very soluble and does not react quickly with water (Lee and Schwartz, 1981). Depending upon the concentration level and an individual's current pulmonary condition, it could induce chemical pneumonia.

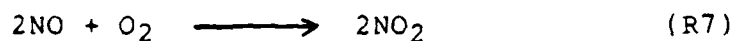


The oxidation of NO to NO<sub>2</sub> continues the smog generating process. In the presence of appreciable amounts of O<sub>3</sub>, the reaction is as follows:



This is a primary mechanism for NO<sub>2</sub> formation. Although some NO<sub>2</sub> is initially produced by the same combustion processes that generate NO, the amount of NO<sub>2</sub> produced is small compared with the amount of NO formed (Yocum, 1982). This point is also illustrated in Table 5.

Another possible photochemical reaction involving NO which produces NO<sub>2</sub> is:



The differential equations describing R6 and R7 are respectively:

$$d[\text{NO}_2]/dt = k[\text{NO}][\text{O}_3] \quad (1)$$

$$d[\text{NO}_2]/dt = 2k[\text{NO}]^2[\text{O}_2] \quad (2)$$

Equation (2) shows that (R7) is kinetically unfavorable, except in pure exhaust gases, since it is dependent upon [NO]<sup>2</sup>. However, equation (1) shows (R6) to

be kinetically favorable. Therefore, (R7) is significantly slower and of minor importance compared to (R6).

Additionally, other primary pollutants such as hydrocarbons, carbon monoxide (CO) and organic compounds can add to NO<sub>2</sub> production. The R in (R11) represents any organic compound. These reactions are as follows:

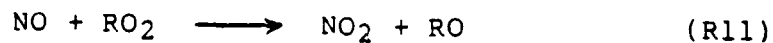
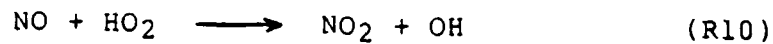
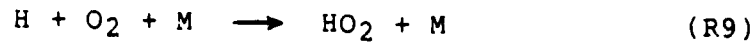
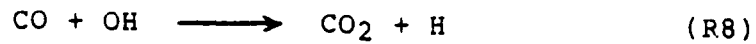


TABLE 5.-- Predicted Equilibrium Compositions of NO and NO<sub>2</sub> at Various Temperatures for the Simultaneous Reactions  $\text{N}_2 + \text{O}_2 \rightleftharpoons 2\text{NO}$  and  $\text{NO} + 1/2\text{O}_2 \rightleftharpoons \text{NO}_2$  for an initial Composition of 3.3 percent O<sub>2</sub> and 76 percent N<sub>2</sub> (JANAF Thermochemical Tables, Dow Chemical Company)

T		NO (ppm)	NO <sub>2</sub> (ppm)
(K)	(F)		
300	80	$1.1 \times 10^{-10}$	$3.3 \times 10^{-5}$
800	980	0.77	0.11
1400	2060	250	0.87
1873	2912	2000	1.8

### Ozone

Ozone ( $O_3$ ) is a secondary, rather than a primary pollutant. Simply stated,  $O_3$  is produced through the photochemical reactions of many pollutants such as  $NO$ ,  $NO_2$ ,  $NO_x$ ,  $HC$  and  $CO$ . In sufficient concentrations  $O_3$  is irritating to the respiratory tract, can impair lung functions, has the dubious distinction of being able to dissociate rubber, is an extremely reactive pollutant and is one of the most powerful oxidizers in nature (Yocum, 1982).

Photochemical production of  $O_3$  begins with the photodissociation of  $NO_2$ , as illustrated in R12. Ultraviolet radiation with wavelengths less than 420 nm will accomplish this photodissociation (Dickerson et al., 1982).



The symbol  $h\nu$  represents the light energy and  $O(^3P)$  represents a ground state oxygen atom. This oxygen atom will then react with the most common reactive molecule it can find in the atmosphere: oxygen ( $O_2$ ). This reaction will then produce ozone as follows.



Ozone values do not remain static. During the night the values are low, with a sharp increase occurring in the morning hours. The maximum levels are reached during the afternoon and then decline throughout the evening and early morning hours (Schjoldager, 1979 and Evans, 1983). These diurnal variations can be strongly linked to the diurnal stability variations that occur within the planetary boundary layer.

The transfer of stratospheric  $O_3$  across the tropopause into the troposphere is another source of tropospheric  $O_3$ . This transfer mechanism is most probably a major global source but not a significant source of elevated ozone level episodes. This does not, however, preclude occasional specific episodes of elevated  $O_3$  concentrations from being related to intrusions of stratospheric  $O_3$  into the troposphere (Shapiro, 1980). Derwent (1978) cites two such incidents in the United Kingdom. Under anticyclonic conditions, which had accounted for all episodes of elevated ozone levels reported in the United Kingdom as of 1978, the maximum hourly ozone concentrations often exceeded 100 ppb (parts per billion). In both of the above two incidents, Derwent observes that the anticyclone was missing and in its place were cold fronts with an upper level jet stream roughly parallel to the fronts at a height of 9 to 10 km. The meteorological

and chemical conditions were extremely unfavorable for photochemical ozone production (little solar UV and accumulation of photochemical precursors). However, rural monitoring sites reported marked periods during which 100 ppb was exceeded for several hours.

Junge (1963) states that there is a close association between springtime maxima in lower tropospheric ozone and stratospheric fallout. Stratospheric and tropospheric air undergo continuous exchange, which is significantly enhanced at the trailing edge of jet streams associated with cold fronts in mid-latitudes. It can be inferred that the two episodes cited by Derwent were the result of an intrusion of stratospheric ozone.

The importance of local photochemical reactions to the global ozone budget remains an area of intense research (Calvert, 1976).

#### Sulfur Dioxide

Sulfur dioxide ( $\text{SO}_2$ ) is a colorless gas, primary pollutant and a major pollutant in London type smog. It affects humans by acting as an eye and lung irritant. However, in sufficient concentrations its effects, previously described in Section I, can be deadly.

SO<sub>2</sub> is emitted into the atmosphere in many industrial and domestic processes, chiefly through the burning of fossil fuels, both in and around cities (Smith, 1974; Spedding, 1974; Chameides and Davis, 1982; Crutzen, 1983). Coal and petroleum are the chief culprits accounting for 62% and 25% (based on 1976 figures) respectively (Cullis, 1980). Other significant sources of SO<sub>2</sub> could come from biomass burning and volcanic eruptions (Crutzen, 1983).

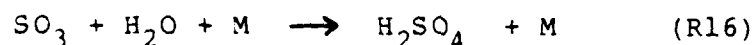
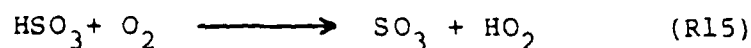
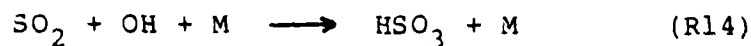
Globally, anthropogenic sources account for approximately 40% of SO<sub>2</sub>, but in urban areas this figure could be in excess of 90%. Although with respect to amount SO<sub>2</sub> is a minor pollutant, its effects are major, particularly after it is converted to fine sulfate particles (Junge, 1963).

A photochemically produced source of SO<sub>2</sub> comes from the oxidation of hydrogen sulfide (H<sub>2</sub>S), which is released to the atmosphere via the decomposition of anthropogenic organic waste (Crutzen, 1974 and Spedding, 1974).

Once SO<sub>2</sub> is in the atmosphere, it may be removed by 3 major routes: chemical transformation, scavenging by precipitation (wet deposition) and absorption at the surface by soil and vegetation (dry deposition).

The contribution of each route depends on a region's climate, geography and land use (Spedding, 1974; Pack, 1977; Milne, 1978). The chemical transformation route is described in R14, R15, and R16.

Here we see  $\text{SO}_2$  involved in the formation of sulfuric acid ( $\text{H}_2\text{SO}_4$ ). The following reactions illustrate one possible path (Calvert and Stockwell, 1983).



Sulfuric acid is very soluble and one of the main constituents in "acid rain". The other main constituent is  $\text{HNO}_3$  (nitric acid).

The effects of acid rain on materials, aquatic life, and forests are quite pronounced. In acidified lakes, elevated concentrations of aluminum have been found on the gills of fish killed from acidification. The aluminum interferes with the normal gill functions and in all probability is the cause of death. It has been well established that acidity will cause elevated aluminum levels in surface water (Hileman, 1982).



Acid rain can also alter the chemical composition of the soil, thereby having a direct effect on forests. When soil is composed of non-calcerous acidic minerals, the amounts of calcium, magnesium and potassium, all of which are required for growth, are severely limited (Hileman, 1982). Acid precipitation can also create favorable conditions for the microorganisms responsible for foliar or stem disease in trees (Smith, 1982).

SO<sub>2</sub> is quite soluble and therefore could be precipitated out (wet deposition), so sulfates serve as condensation nuclei (Batten, 1966). SO<sub>2</sub> is also quite "sticky" and can therefore adhere easily to surface structures and vegetation (dry deposition).

#### Carbon Dioxide

Carbon dioxide (CO<sub>2</sub>) is the fourth largest gas by volume in the atmosphere and is the most abundant carbon-containing gas in our atmosphere. Concentrations have been measured which show a global increase of approximately 1.6 ppm per year (Scope 16, 1981). Rotty (1981) states that this increase is primarily the result of fossil fuel burning, with additional contributions from biomass burning (i.e., grassland and forest fires). CO<sub>2</sub> is also an indicator of combustion since it contains approximately 80% of the carbon lost from the biomass in a fire.

However,  $\text{CO}_2$  is not a photochemically active atmospheric gas and therefore its role in atmospheric photochemistry is not significant. The primary method of  $\text{CO}_2$  removal from the atmosphere is accomplished mainly through the photosynthesis of plants (Crutzen, 1983).  $\text{CO}_2$  has become known as the "greenhouse gas" since it is transparent in the UV and visible, but absorbant in the IR. Therefore, the role of  $\text{CO}_2$  in atmospheric chemistry is indirect, since it impacts on the temperature and radiation structure of our atmosphere (Hansen et al., 1981; Crutzen, 1983).

In this study  $\text{CO}_2$  will be used as an indicator of combustion.

#### B. Photostationary State

The first experiments carried out on this subject were by Jackson (1975). However, Leighton (1961) in Photochemistry of Air Pollution has made it clear that an understanding of the photostationary state (hereafter referenced as PSS) is central to an understanding of photochemical smog formation. It involves the interaction of three of the previously discussed compounds:  $\text{NO}$ ,  $\text{NO}_2$  and  $\text{O}_3$ .

$\text{NO}_2$  will photodissociate after exposure to noon-time sunlight in approximately 2 minutes. Since the steady state concentration of  $\text{NO}_2$  is not significantly changed, then there must be a dynamic system at an approximate photostationary state (Jackson, 1975; Ritter et al., 1979; Kelly et al., 1980; Shetter et al., 1983). The reactions involved are generally fast with respect to other reactions which involve oxides of nitrogen and ozone. Collecting reactions R6, R12 and R13 and applying the photostationary assumption to these three reactions yields:

$$d[\text{NO}_2]/dt = d[\text{NO}]/dt = 0 = k_3[\text{O}_3][\text{NO}] - k_1[\text{NO}_2] \quad (3)$$

$k_1$  and  $k_3$  are photolysis rates. The commonly used term for  $k_1$  is  $j(\text{NO}_2)$ , so rewriting (3) yields:

$$P = j(\text{NO}_2) [\text{NO}_2] / k_3 [\text{O}_3] [\text{NO}] \quad (4)$$

where  $P$  represents the PSS value and has an anticipated value of unity. Figure 2 shows the diurnal variation in "dirty air" of  $\text{NO}$ ,  $\text{NO}_2$ , and  $\text{O}_3$  in July in Los Angeles with respect to the PSS reactions, R6, R12, and R13.

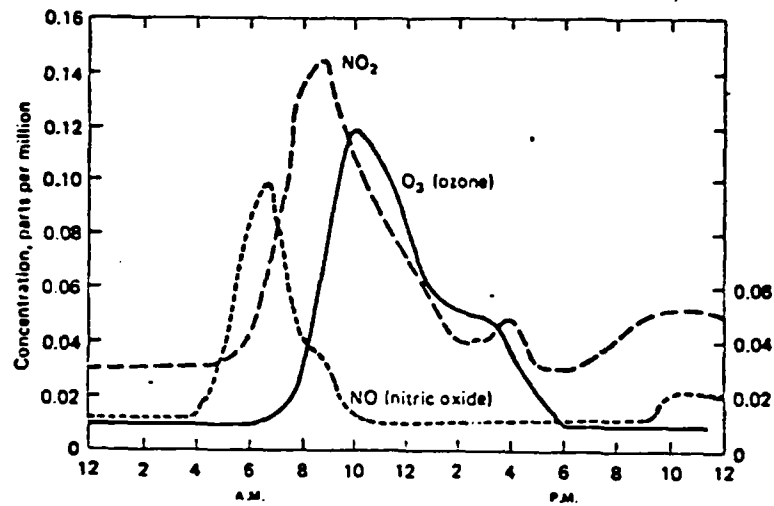


Figure 2. Diurnal Variation of NO, NO<sub>2</sub> and O<sub>3</sub> Concentrations in Los Angeles, July 19, 1965 (NACPA. Air Quality Criteria for Photochemical Oxidants; AP-63. Washington, D.C.: HEW, 1970.)

If the three reactions of the PSS did not interact with other atmospheric constituents, then the value of  $P$  would always be unity. However, this is not always the case. Therefore, other species must be involved which alter the concentrations of  $\text{NO}$ ,  $\text{NO}_2$ , or  $\text{O}_3$  forcing  $P$  away from unity. Atmospheric measurements indicate that the PSS reactions must be more complex than they seem (Ritter et al., 1979; Kelly et al., 1980). The discrepancy between the anticipated and observed  $P$  values can be attributed to the presence of peroxy radicals, which will invalidate the PSS equation in clean air. However, a systematic diurnal variation and departure from  $P = 1$  is still observed (Bottenheim et al., 1979; Kelly et al., 1980; Shetter et al., 1983). Figure 3 illustrates this point.

The intensity of solar radiation plays a significant part in the formation of photochemical air pollution (Leighton, 1961). The interactions of solar radiation and  $\text{NO}_2$  is closely related to the absolute rate of photolysis. Dickerson et al., (1982) showed  $\text{NO}_2$  photolysis frequencies to be strongly dependent on solar zenith angle, while exhibiting little dependence on temperature, pressure or altitude. This implies that the time of maximum photolysis is related to the time of maximum solar radiation (Vukovich et al., 1977). This point is illustrated in Figure 4.

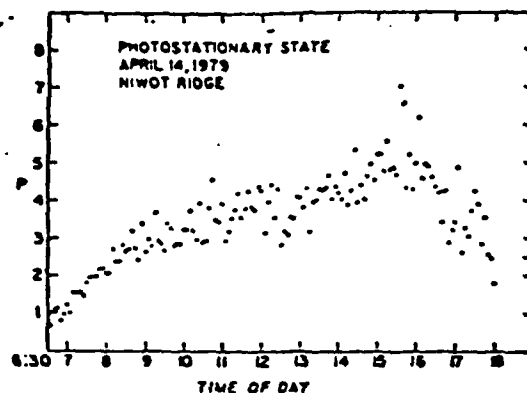


Figure 3. Values of the Photostationary State/Number  $P$  Calculated from Values of  $\text{NO}$ ,  $\text{NO}_2$ ,  $\text{O}_3$ , and  $j(\text{NO}_2)$ , for April 14, 1979, at Niwot Ridge (Kelly et al., 1979).

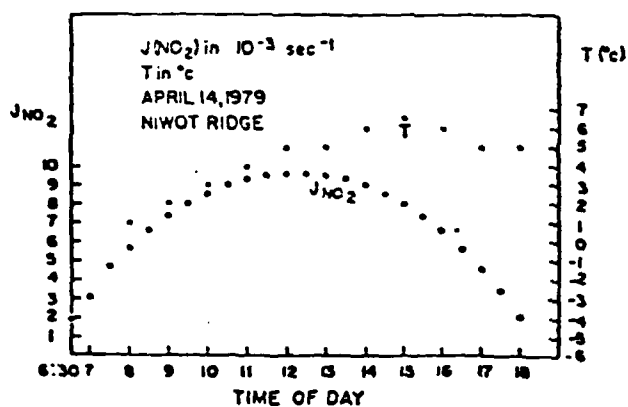


Figure 4. The Photolysis of  $\text{NO}_2$ ,  $j(\text{NO}_2)$  and the Ambient Temperature at Niwot Ridge on April 14, 1979 (Kelly et al., 1979).

### C. Meteorological Parameters

#### Temperature

The generation of photochemical pollutants is strongly related to temperature, particularly with respect to ozone. This is especially evident in the PSS where the value of P is a maximum near mid-day.

Rate constants ( $k_i$ ), which determine the speed of a photochemical reaction, are a function of temperature and are expressed by:

$$k = A \exp (-E_a/RT) \quad (5)$$

A is the Arrhenious Factor (rate of molecular collisions),  $E_a$  is the activation energy, R is the solar constant and T is temperature.

Temperature dependence is a parameter of both Los Angeles (high temperature) and London (low temperature) smog. Temperature dependence was a fairly consistent element throughout much of the literature.

### Insolation

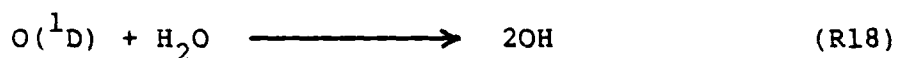
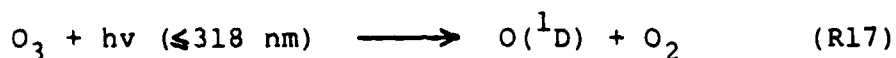
All photochemical reactions are dependent upon the solar influx of UV radiation intensity. The general diurnal variation of  $O_3$  synthesis and vertical transportation in the boundary layer is strongly related to the diurnal variation of solar intensity (Vukovich et al., 1977). Both temperature and ozone formation depend on solar radiation with a time lag of a few hours (Schjoldager, 1979). The degree of cloud cover will proportionally reduce the amount of incoming UV radiation, thereby significantly impacting on photochemical reactions. Variations in the photolysis rates due to changes in aerosol loading and albedo, other than snow, are minor when compared to changes resulting from variations in cloud cover and solar zenith angles (Dickerson et al., 1979).

### Relative Humidity

Relative humidity is one way to express the moisture content of the air.  $SO_2$ , which is very soluble, is converted to sulfates in typical industrially polluted air at a rate which seems to hinge significantly on relative humidity (Smith, 1974).  $NO_2$ , which is not very soluble, is still indirectly affected by relative humidity.



This indirect effect, which revolves around the formation of hydroxyl (OH), also involves  $\text{SO}_2$ .



$\text{O}({}^1\text{D})$  is the major source of tropospheric OH (Levy, 1971).  $\text{SO}_2$  may then be transformed by OH into  $\text{H}_2\text{SO}_4$  via R14, R15 and R16, while  $\text{NO}_2$  is transformed into  $\text{HNO}_3$  (nitric acid) via (R1).

#### Precipitation

Precipitation serves as one atmospheric removal mechanism of pollutants. It has been estimated that in about an hour, even a light rain can wash out half the particles  $\geq 10$  microns (Battan, 1966). Smaller particles may serve as nuclei. Then through a process of collision and coalescence, the resulting droplets will combine with raindrops and precipitate out. Precipitation does have an indirect effect on photochemistry since the evaporation process can alter both the temperature and relative humidity structures.

### Wind Direction and Speed

Winds are instrumental in both transporting and diffusing atmospheric pollutants. Air quality measurements have indicated an increase in industrial effluents to the point where they affect not only the immediate areas near the emissions but are also carried in significant concentrations over vast regions and, for some long-lived constituents throughout the global atmosphere (Pack, 1977). In an analysis of selected high ozone events, it was suggested that the long-range transportation of air mass ozone from urban areas contributed to the measured peak concentrations at remote sites (Evans, 1983).

The transport of pollutants from a source to a clean site is primarily a function of wind direction. However, wind speed also plays an important role. Wind speed was a significant meteorological parameter affecting pollution and exhibited an inverse relationship to the levels of pollution (Garnett, 1979).

It was determined that light wind speeds usually coincide with increased pollution and vice versa. Most pollution episodes occurred when wind speeds were less than 2.5m/sec or approximately 5 knots (Riehl, 1970 and Schjoldager, 1979).

### Atmospheric Pressure

Synoptic scale pressure systems have a definite relation to the concentrations of atmospheric pollutants. Low pressure systems will reduce these concentrations, since lows are characterized by strong convergence at the surface, good vertical mixing, relatively high winds, extensive cloud cover and precipitation. Conversely, high pressure systems have a positive effect on these concentrations. High pressure is the ideal synoptic feature to promote photochemical reactions (Vukovich et al., 1977; Evans, 1983; Fishman, 1983). Vukovich et al. (1977) gives a clear description of the effects of a high pressure system in the following:

when a synoptic high pressure system moved into the eastern portions of the United States, high concentrations of ozone were reported at a number of rural stations scattered throughout the region. This condition persisted as long as the environmental conditions (i.e., high solar radiation, low wind speed) accompanying the high pressure system remained in the eastern portions of the United States. The highest ozone concentrations were found at rural stations located near the central regions of the high pressure system. These regions were characterized by weak winds, disorganized flow, high temperatures, and relatively clear skies.

In addition to the work of Vukovich et al., Garnett (1979) comments on the effect of the stability and inversions associated with high pressure systems.

Stable conditions and long spells of hours of inversion of temperature restricting free vertical ventilation gave rise time and again to coincident peak pollution levels at all or most of the sites.

The subsiding air of a high pressure system also results in the downward transportation of ozone of stratospheric origin (Reiter, 1975; Schjoldager, 1981; Crutzen, 1983).

#### Mixing Heights

It can be stated that the greater the mixing heights, the more the effluents will be diluted. Mixing height has become a fundamental concept of air pollution forecasting (Aron, 1983). The vertical extent to which this mixing takes place varies diurnally, from season to season, as well as with topography (Wark and Warner, 1981). The depth of this mixing height times the average wind speed within it gives the rate of ventilation (Bach, 1972).

In a study conducted by Riehl (1970) it was determined that of three removal mechanisms of pollutants in Denver, ventilation was the most important parameter. Ventilation is a function of the horizontal wind speed and was determined to be the main control for the onset and termination of pollution episodes.

Although the mixing height concept is a useful one, the correlation between this concept and air pollution is currently inconsistent.

Some of the factors which could negatively influence height value, thereby degrading the correlation between mixing height and pollution levels are:

- a. method used to calculate mixing height may not yield a consistently good estimate of the actual mixing height.
- b. the mixing height may serve as an imperfect lid.
- c. location of the pollution sample and if the pollutants have had sufficient time to disperse to the mixing height.

At present the incorporation of mixing height into pollution model calculations seem to have little or no impact on improving or degrading model quality (Olson, 1974 and Aron, 1983). The exact implication of incorporating ventilation into pollution models has yet to be fully explored and documented. Continued research in the use of this factor in pollution models is needed.

### SECTION III

#### DATA

The data in this work represent a portion of the information collected from January to August, 1982 (minus June and July) in Deuselbach, West Germany (Figure 5). The monitoring ("clean air") station, where these data were taken, is operated by the Umweltbundesamt (German Environmental Bureau). The station is located about 1 km west of the village, at approximately 500 meters above sea level. The elevation had no significant effect on the measurements. The site is about 100 km west of a string of large industrialized cities (Frankfurt am Main at the northern end to Ludwigshafen at the southern end) of the upper Rhine Valley. A major industrial area (Ruhr River Valley) is about 100 km to the north. The areas to the south and west of Deuselbach are predominantly rural.

In addition to collecting  $\text{NO}_2$ ,  $\text{SO}_2$ ,  $\text{O}_3$ ,  $\text{CO}_2$ , total suspended particles, and meteorological data, a chemiluminescent  $\text{NO}_x$  detector and an Eppley UV radiometer recorded data on oxides of nitrogen and solar radiation, respectively. These last two items and their role in the PSS were discussed in Section II.

Sulfates make up a large portion of the suspended particulate matter in Deuselbach. The term particulate matter describes dispersed airborne solid and liquid particles larger than single molecules (molecules are about

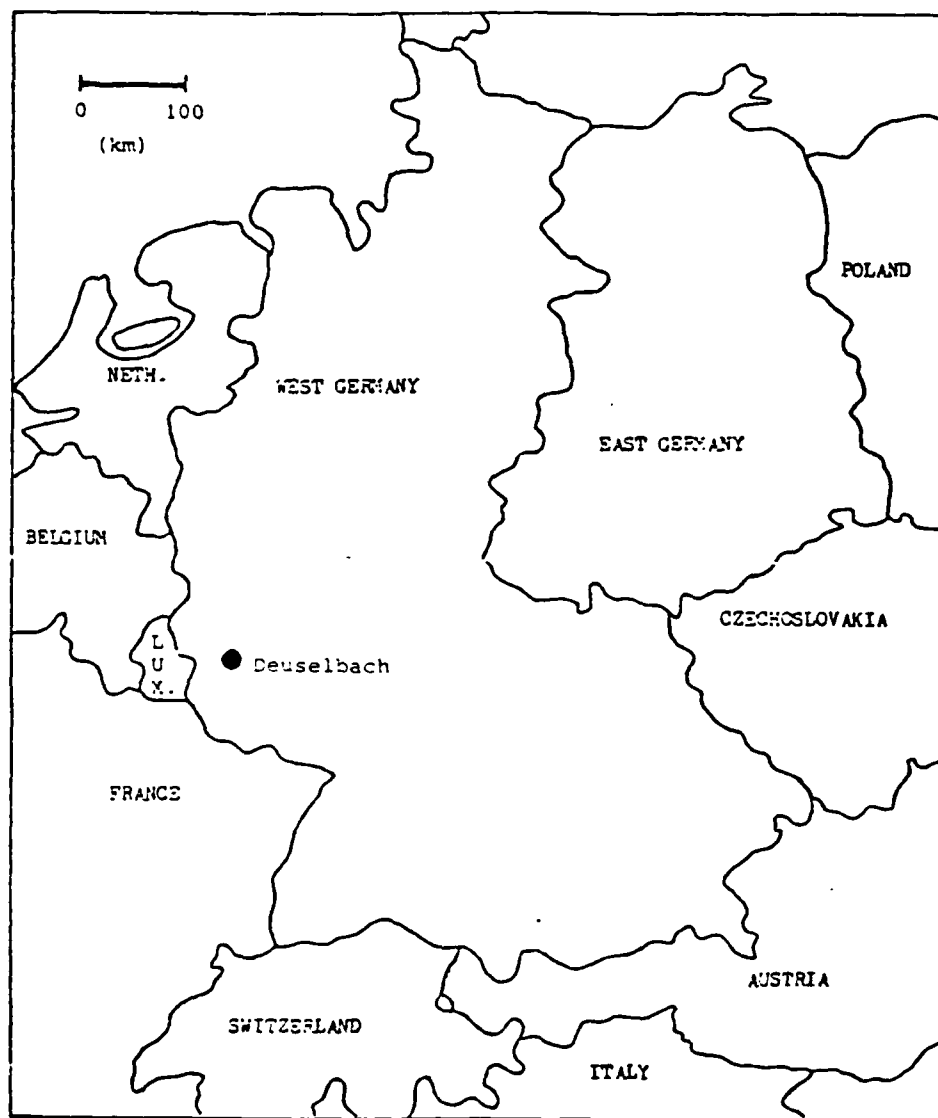


Figure 5. Political map of Central Europe.

0.0002  $\mu\text{m}$  in diameter) but smaller than 500  $\mu\text{m}$  (Wark and Warner, 1981). The filters used in Deuselbach collected particles with a diameter  $> 0.1 \mu\text{m}$ .

At Deuselbach a molybdenum converter in conjunction with a chemiluminescence instrument, converted  $\text{NO}_2$  to NO with an efficiency of about 90%. This process allows the detection of other nitrogen species provided they are converted to NO. However, this process is not as efficient in clean air.  $\text{HNO}_3$ , HONO, PAN,  $\text{N}_2\text{O}_5$ , organic nitrates and possibly other reactive nitrogen compounds are transformed in NO on hot ( $425^\circ\text{C}$ ) molybdenum. If the sample takes this path through the converter the observed signal is then referred to as total reactive nitrogen or  $\text{NO}_y$  (Dickerson et al., 1984).  $\text{NO}_y$  is defined as  $\text{NO}_x + \text{NO}_3 + 2 \times \text{N}_2\text{O}_5 + \text{HNO}_2 + \text{HNO}_3 + \text{HO}_2\text{NO}_2 + \text{PAN}$ . Exposure to high  $\text{NO}_y$  concentrations results in the converter generating a small background signal which continues for hours and even days (Dickerson et al., 1984).

Oxides of nitrogen, specifically  $\text{NO}_2$ , were collected using two techniques: Chemiluminescence (Delany et al., 1982 and Dickerson et al., 1984) and modified Saltzman (Saltzman and Wartburg, 1965). Chemiluminescence measures both NO and  $\text{NO}_2$  by constantly cycling through the detector's instrumental modes. The sensitivities of the system for NO and  $\text{NO}_2$  are acquired every six hours through calibration with standard additions of NO and  $\text{NO}_2$  at the



sampling inlet. The system background, provided no NO is present, is regularly obtained by converting NO to NO<sub>2</sub> by supplementing additional O<sub>3</sub> in a chamber which immediately precedes the NO detector. NO and NO<sub>2</sub> are now obtained through mathematical manipulation of: the instrumental signal in NO and NO<sub>x</sub> measure modes, the NO and NO<sub>2</sub> calibration modes and the zero mode (Kley and McFarland, 1980; Delany et al., 1981; Dickerson et al., 1984). Extensive measurements of NO<sub>y</sub> were made in addition to the NO<sub>x</sub> measurements. More than 50% of all the measurements of oxides of nitrogen at Deuselbach involved NO<sub>y</sub>. Measurements of NO<sub>y</sub> are important since it is another variable in the air pollution problem. The transport of these trace gases into the upper troposphere, coupled with their long lifetime permits photolysis and radical reactions to occur. This may lead to the production of significant amounts of O<sub>3</sub> in the remote atmosphere (Dickerson, 1984). However this particular aspect is not a focus of this thesis.

The Saltzman method for detecting NO<sub>2</sub> involves "wet chemistry" ( i.e., NO<sub>2</sub> reacts with an aqueous mixture). The subsequent reactions generate a product (an azo dye) which is then quantitatively measured through spectrophotometry. The agreement between Saltzman and Chemiluminescence is acceptable within the experimental errors of the

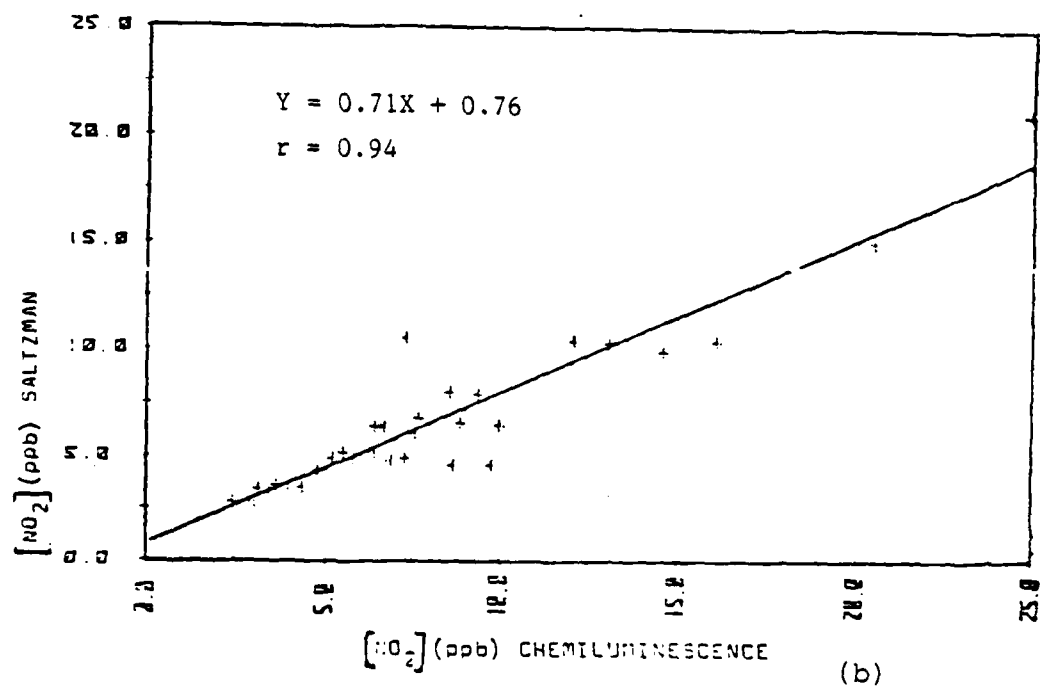
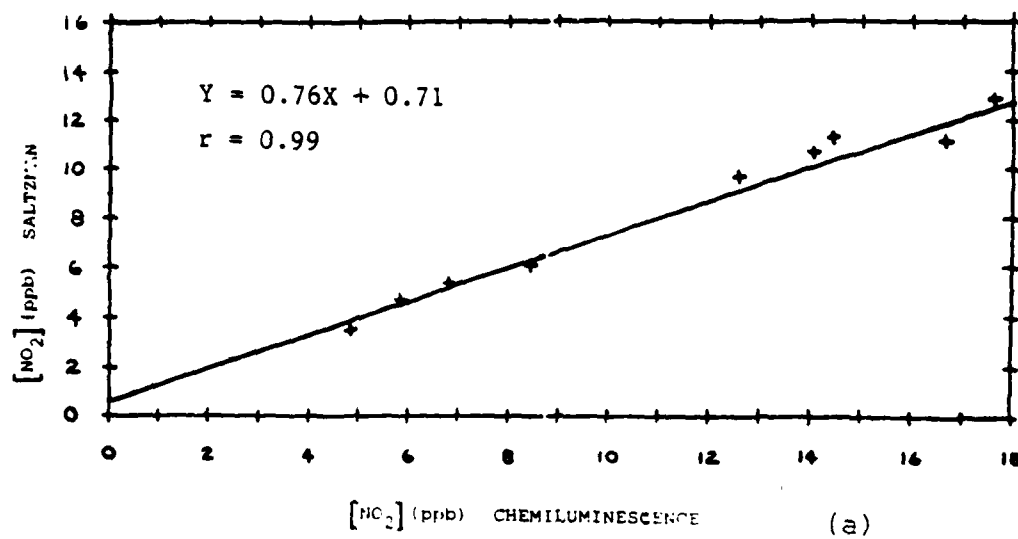


Figure 6a-b

$\text{NO}_2$  concentrations using Chemiluminescence vs Saltzman Methods for (a) January and (b) March 1982.

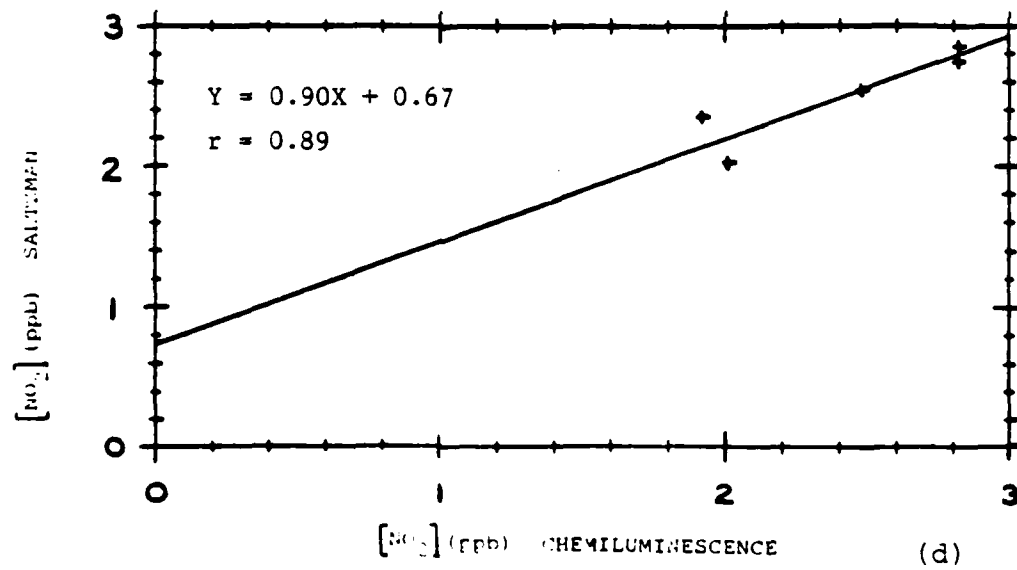
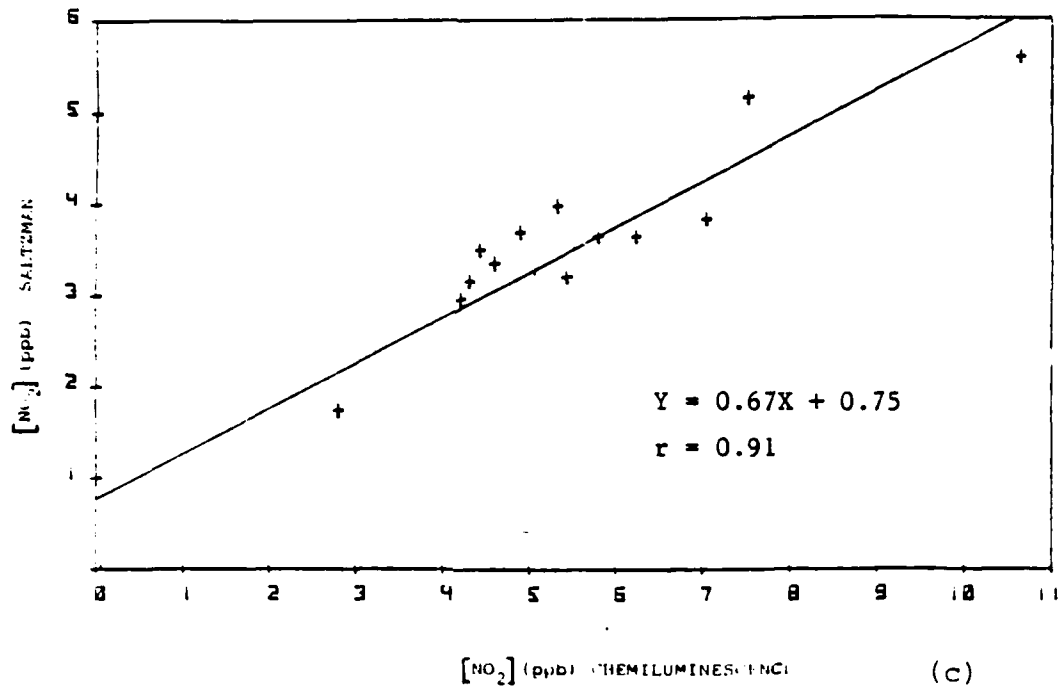


Figure 6c-d  $\text{NO}_2$  concentrations using Chemiluminescence and Saltzman Methods for (c) May and (d) August 1982.

two techniques. In "dirty air" the standard deviation for the Saltzman method is approximately 10% (Organization for Economic Cooperation and Development, 1975).

A comparison of the two methods (Figures 6a-d) shows their relationship during four pollution episodes at Deuselbach (23-31 January, 1-31 March, 1-13 May and 20-24 August 1982) and gives correlation coefficients of 0.99, 0.94, 0.91, and 0.89 respectively. In general, Saltzman values were equal to seven tenths of the chemiluminescent values for January, March and May. The August values showed almost a one to one relationship between the two methods. The August  $\text{NO}_2$  values could be distorted by  $\text{HNO}_3$  and PAN levels, which are at their highest in summer.

However, August also had the fewest data points (5), as opposed to the following: January (9 points), March (31 points) and May (13 points). It remains then to be seen at some future date, whether there is a seasonal variation in the relationship between the two methods, some unknown outside factor or simply limited August data which accounts for this discrepancy. A look at June and July data would have helped to make a determination, however, these data are unavailable.

The detection limit is greater than 1 ppb for a 24 hour sample. The result of this detection limit is a non-zero origin when the data are plotted. The data for these

figures are located in Appendix A.

Data on  $\text{NO}_x$  in this study are those obtained exclusively through the Saltzman method, except for the PSS discussions of the four pollution episodes mentioned previously. Chemiluminescent and Saltzman data are used in all four episodes. Chemiluminescent data are discussed only when such data are available. Chemiluminescence is much more reliable and accurate than Saltzman for sampling  $\text{NO}_2$ . However, the Saltzman method is much simpler and cheaper than chemiluminescence. So historically, the Saltzman method has been commercially more attractive, however chemiluminescence is currently receiving increased use. One other drawback of the Saltzman method is its unreliability in the time frame of  $< 12$  to 24 hours in moderately polluted air. Several years of data are available from numerous clear air stations in West Germany using only the Saltzman technique. Thus a comparison of the two methods was needed to reveal the degree of accuracy of the Saltzman method. Gunter Helas (private communication, 1982) was the first to compare the two methods. The results of this thesis compared favorably with his findings.

The two sources of surface and upper air charts used in this study were: Deutscher Wetterdienst (German Weather Service) and Meteorologische Abhandlungen, Institut für Meteorologie der Freien Universität Berlin (Meteorological

Data, Institute for Meteorology, Freien University, Berlin). Radiosonde data were provided from Ramstein Air Base (located about 35 km SW of Deuselbach) through the USAF Environmental Technical Applications Center (ETAC).

In attempting to establish a relationship between a specific chemical constituent and meteorological parameters, synoptic charts, graphical techniques and statistical correlation theory were used. Positive and negative correlations are referenced throughout this work as weak ( $r < 0.5$ ), good ( $r = 0.5$  to  $0.69$ ) or strong ( $r = 0.7$  to  $1.0$ ). The synoptic correlation lasts about 3 days so we have about ten degrees of freedom in a month with a value of  $r = 0.5$  significant at the 90% level, while a value of  $r = 0.7$  is significant at the 99% level (from the Two Tail Test, Pearson's Product Moment Correlation Coefficient). All statistical data are located in Appendix B.

All the meteorological parameters had some degree of effect on a particular chemical constituent. However each constituent will be discussed only in relation to selected meteorological parameters. For example,  $\text{SO}_2$  and relative humidity are strongly anticorrelated, but  $\text{O}_3$  and relative humidity are not. Therefore, in my discussions of  $\text{SO}_2$ , relative humidity is included, but excluded in the discussion of  $\text{O}_3$ . All meteorological and chemical values are representative of daily means, except for hourly values used in the PSS analysis.

## SECTION IV

### ANALYSIS

In analyzing the relationships between the chemical constituents and meteorological parameters in this work, we will see that the fluctuations and trends in the chemistry of the air in Deuselbach are due almost solely to meteorological conditions. The correlation between a particular chemical constituent and the selected meteorological factors affecting it is discussed on a monthly basis.

#### A. Sulfur Dioxide

The meteorological factors which seemed to have the most significant impact on  $\text{SO}_2$  were: wind direction, precipitation, relative humidity and dust. Although dust is not a meteorological factor it aids significantly in the discussion of wind direction.

As mentioned earlier, one of the major sources of  $\text{SO}_2$  comes from fossil fuel burning (Table 3) and since Deuselbach has neither industry nor a large population, the  $\text{SO}_2$  must be transported to the site. Hogstrom (1978) states that an analysis of data from Paris and nearby vicinity does not support the idea that a major portion of the emitted sulfur is deposited locally. Rather, most of the  $\text{SO}_2$  emitted from a heavy source area

survives the initial phase when the pollutants are confined to the atmospheric layers relatively close to the ground. The magnitude of the lifetime of  $\text{SO}_2$  is on the order of a few days (Rasool, 1973). Based upon these two statements, the wind-borne transport of sulfates, as particulate matter, from urban-industrial centers to Deuselbach becomes quite feasible. However, the lifetime of  $\text{SO}_2$  is still uncertain and seasonally dependent.

Figures 7a-f show the aggregate of daily means of  $\text{SO}_2$  levels with respect to wind direction and number of days from that direction. The value of each line on the "rose" can be found using the key beside each graph. The numbers at the end of each line on the "rose" represent the number of days when the mean wind was from that particular quadrant. Days on which the wind direction varied from the same quadrant for at least 12 hours were disregarded. The quadrants are defined as: N ( $337.5^\circ - 22.5^\circ$ ), NE ( $22.5^\circ - 67.5^\circ$ ), E ( $67.5^\circ - 112.5^\circ$ ), SE ( $112.5^\circ - 157.5^\circ$ ), S ( $157.5^\circ - 202.5^\circ$ ), SW ( $202.5^\circ - 247.5^\circ$ ), W ( $247.5^\circ - 292.5^\circ$ ), and NW ( $292.5^\circ - 337.5^\circ$ ).

#### 1. January (Figures 8-9)

The January figures show the relationships which generally held true throughout most of the period, between  $\text{SO}_2$  and wind direction, dust, relative humidity, and precipitation.  $\text{SO}_2$  levels throughout January remained



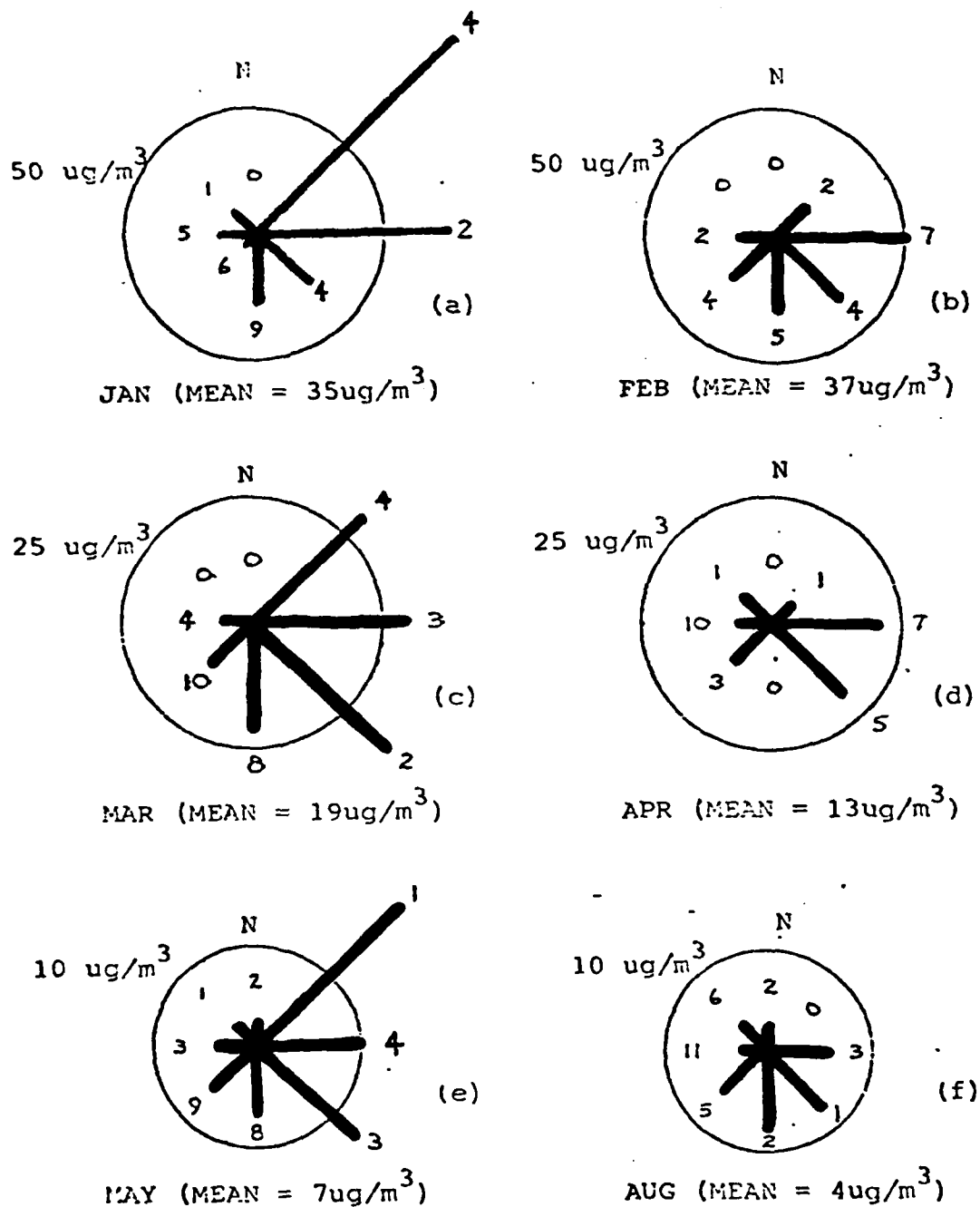


Figure 7  $\text{SO}_2$  Wind Rose. Each "rose" represents the daily means of  $\text{SO}_2$  levels with respect to wind direction. The values at the end of each line on the "rose" represents the number of days when the mean wind was from that particular quadrant.

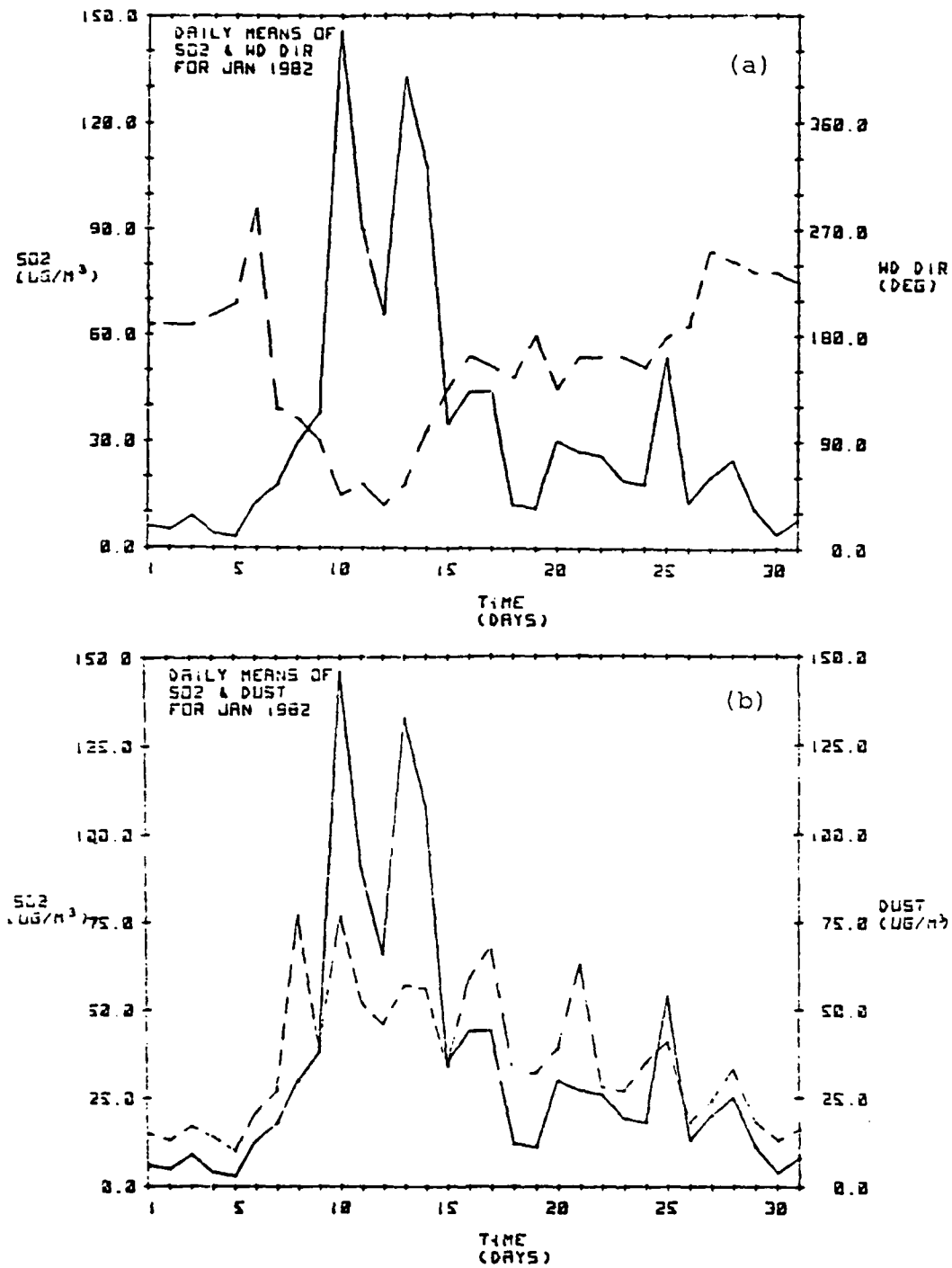


Figure 8 January versus the daily means of SO<sub>2</sub> (solid line) and (a) Wind Direction and (b) Dust. Wind Direction and Dust are represented by dashed lines.

fairly constant. An exception occurred from the 9-15th;  $\text{SO}_2$  levels rose sharply, fell, rose sharply again and then fell to the original level. Beginning on the 6-7th the wind direction shifted from the NW to a NE-SE direction (Figure 8a).

$\text{SO}_2$  levels remained high until the 14-15th when the wind direction shifted out of the NE-SE "cone". The  $\text{SO}_2$  wind rose (Figure 7a) shows that the mean wind direction from the NE-SE "cone" occurred on only 10 days, yet accounted for almost half of the aggregate daily means of  $\text{SO}_2$ . The majority of this total arrived with NE winds.

$\text{SO}_2$  and dust (Figure 8b) show a strong positive correlation ( $r = 0.72$ ). The levels of particulate matter remained low until the 6-7th, then rose as the wind shifted from the NW to a NE-SE direction. This implies a strong interdependence between dust and wind direction. Each wind direction is categorized by the quadrant boundaries defined on page 46. A strong negative correlation between particulate matter and wind direction is also implied.

Scavenging by precipitation was evident (Figure 9a) in  $\text{SO}_2$  levels (and dust). This example of wet deposition (SECTION II) was both expected and a clear indicator of  $\text{SO}_2$  washout. The sharp decline in  $\text{SO}_2$  levels from the 10-12th was attributed to precipitation on the 11th, and the rise on the 13th to a lack of wet deposition.

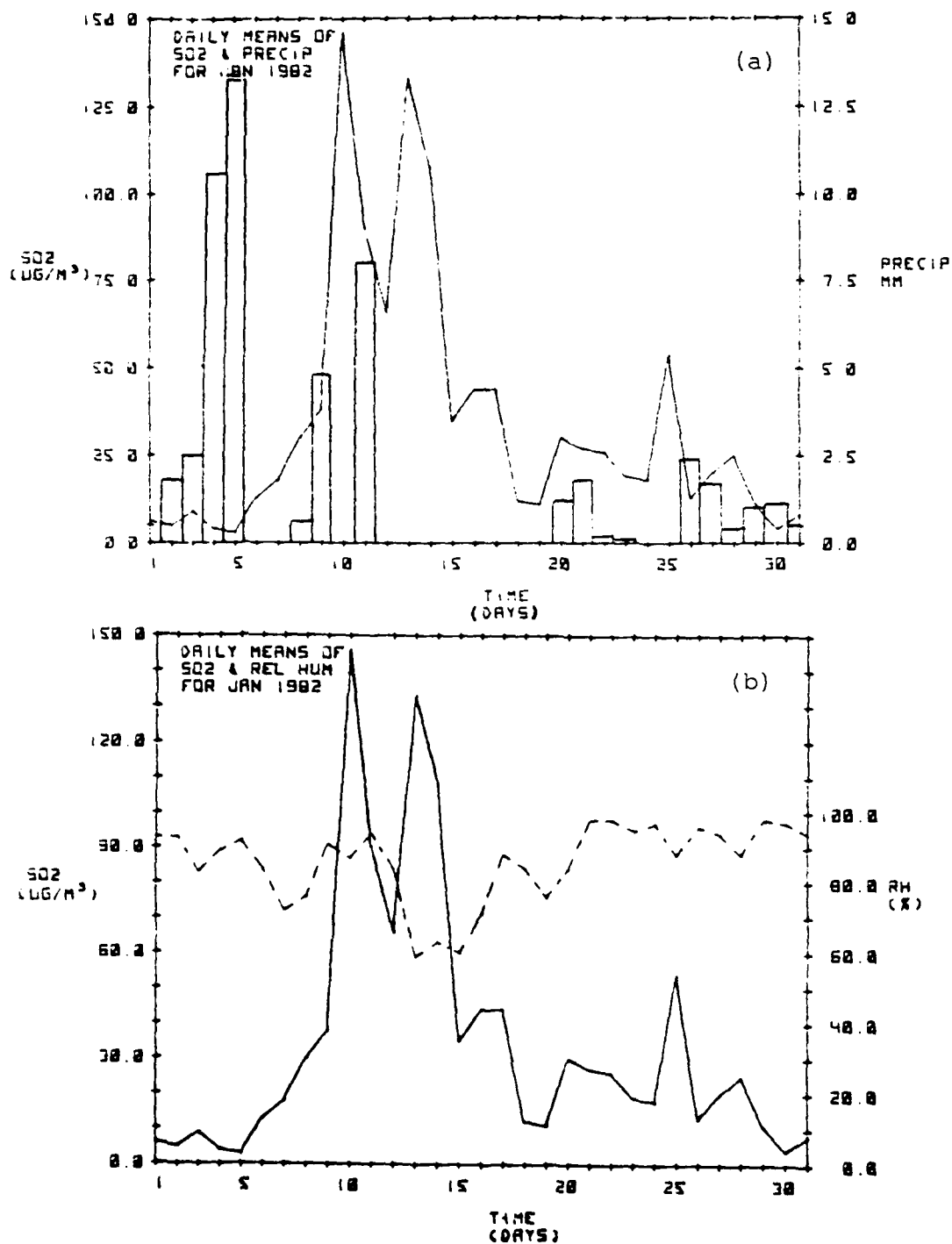


Figure 9 January versus the daily means of SO<sub>2</sub> (solid line) and (a) Precipitation (bars) and (b) Relative Humidity (dashed line).

Reductions in  $\text{SO}_2$  levels can also occur as a result of mixing clean air, brought in through convective means (i.e., thunderstorms).

Relative humidity represents the amount of water vapor actually present in the air compared with the maximum that could be contained under conditions of saturation at a given temperature and pressure. It is a factor associated with the likelihood of precipitation (i.e., 50% relative humidity is a fairly dry atmosphere, while during and for a few hours after precipitation, the relative humidity should exceed 90%). Relative humidity is also one indicator of fog, which is responsible for the heterogeneous removal of  $\text{SO}_2$ . Relative humidity and  $\text{SO}_2$  (Figure 9b) showed a good negative correlation.

According to Petterssen (1969) when the relative humidity increases above about 70%, condensation begins on the largest and most active nuclei. If the air is cooled, so that the relative humidity increases, haze thickens and changes gradually into a grayish mist. When the air is cooled further, so that the relative humidity increases to over 90%, the mist thickens into fog. The visibility is then 1 km or less. If the relative humidity is lowered, the dust particles are dry, and a dry haze results.

It appears that precipitation (wet deposition) plays an important role in controlling  $\text{SO}_2$  levels, once the wind

has advected the pollutant into the region. Dry deposition is the more dominant factor in the removal of atmospheric constituents than wet deposition. However, it was more difficult to analyze since specific information about the deposition velocities of  $\text{SO}_2$  is unavailable.

## 2. February (Figures 10-13)

February showed results similar to January with respect to precipitation, relative humidity and dust. What appears to be a deviation in the relationship between  $\text{SO}_2$  and wind direction occurs on the 26th (Figure 10a). The level rises to a peak even though the wind direction is moving away from the NE-SE "cone". This is a result of daily averaging. Hourly data show the wind direction to be E until about mid-day with the associated rising concentrations. This was expected based on previous observations. The  $\text{SO}_2$  wind rose (Figure 7b) is also affected by this same point. Although it appears that the aggregates from the S and E directions are approximately the same, one third of the S total is accounted for on the 26th. As the wind direction continued to move to the SW the levels of  $\text{SO}_2$  fell quite sharply.

The strong positive correlation ( $r = 0.93$ ) with dust is seen in Figure 10b. Scavenging by precipitation is again quite evident (Figure 11a).

A second deviation appears to be the unusual positive

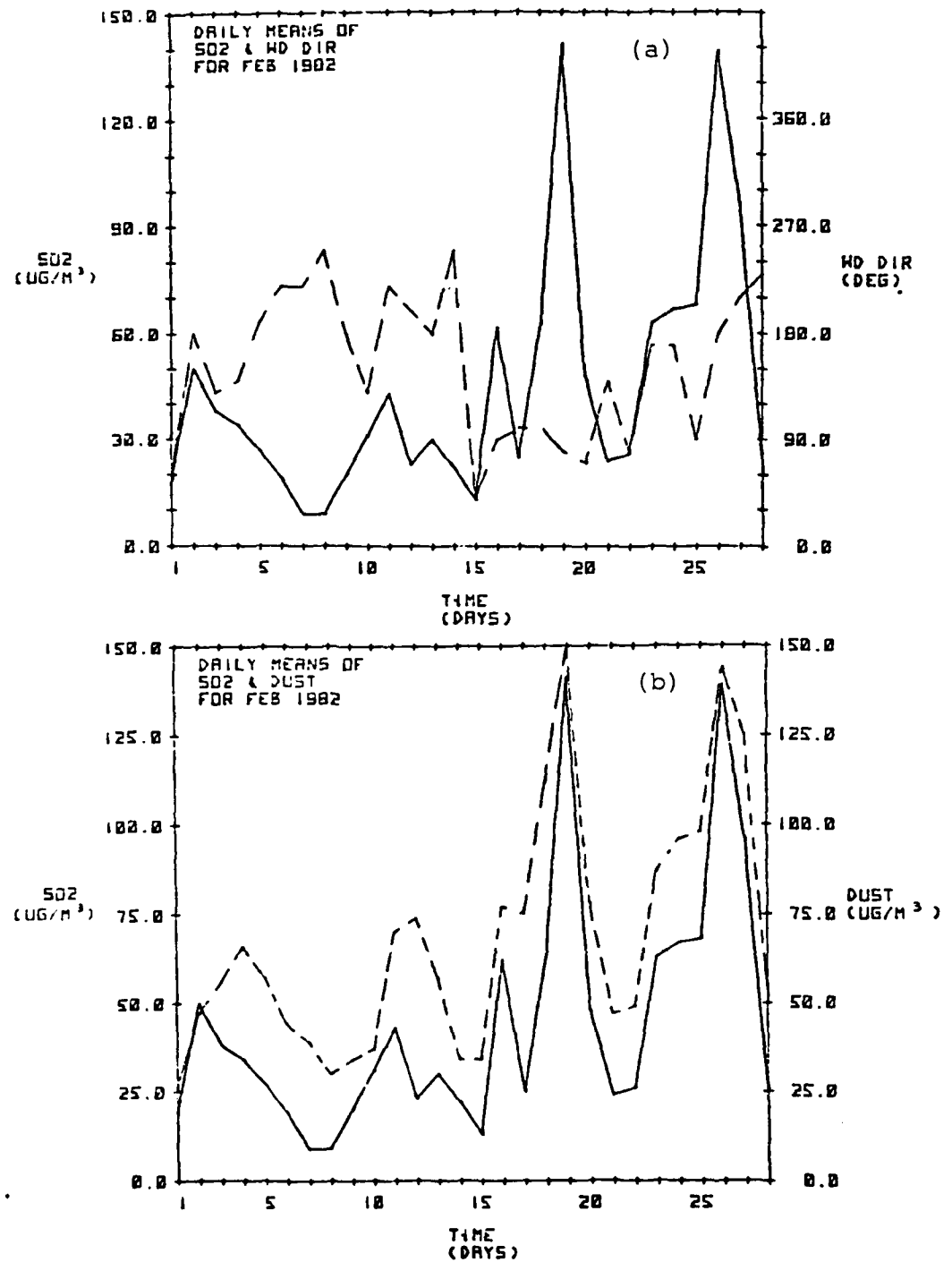


Figure 10 February versus the daily means of SO<sub>2</sub> (solid line) and (a) Wind Direction and (b) Dust. Wind Direction and Dust are represented by dashed lines.

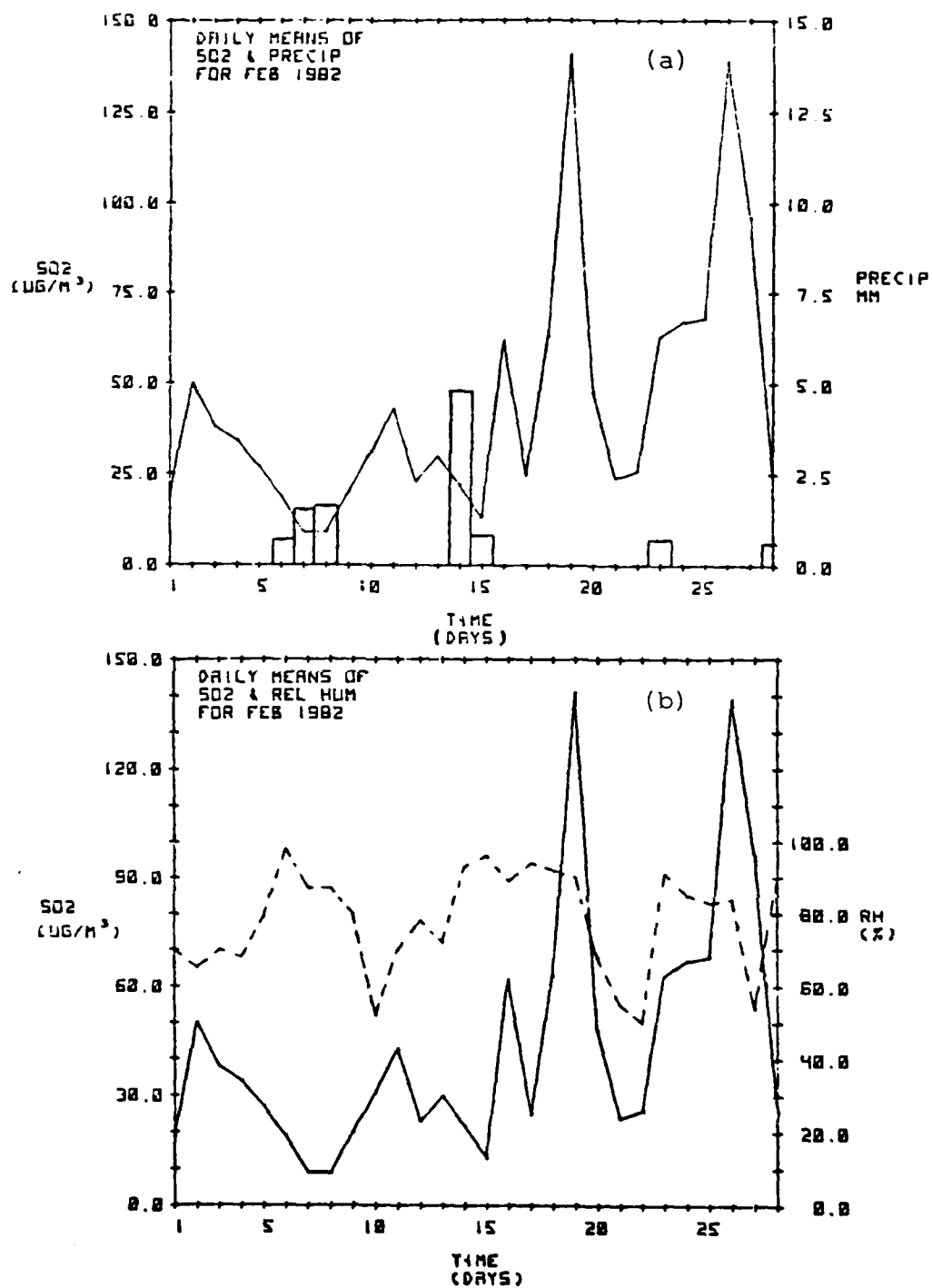


Figure 11 February versus the daily means of SO<sub>2</sub> (solid line) and (a) Precipitation (bars) and (b) Relative Humidity (dashed line).



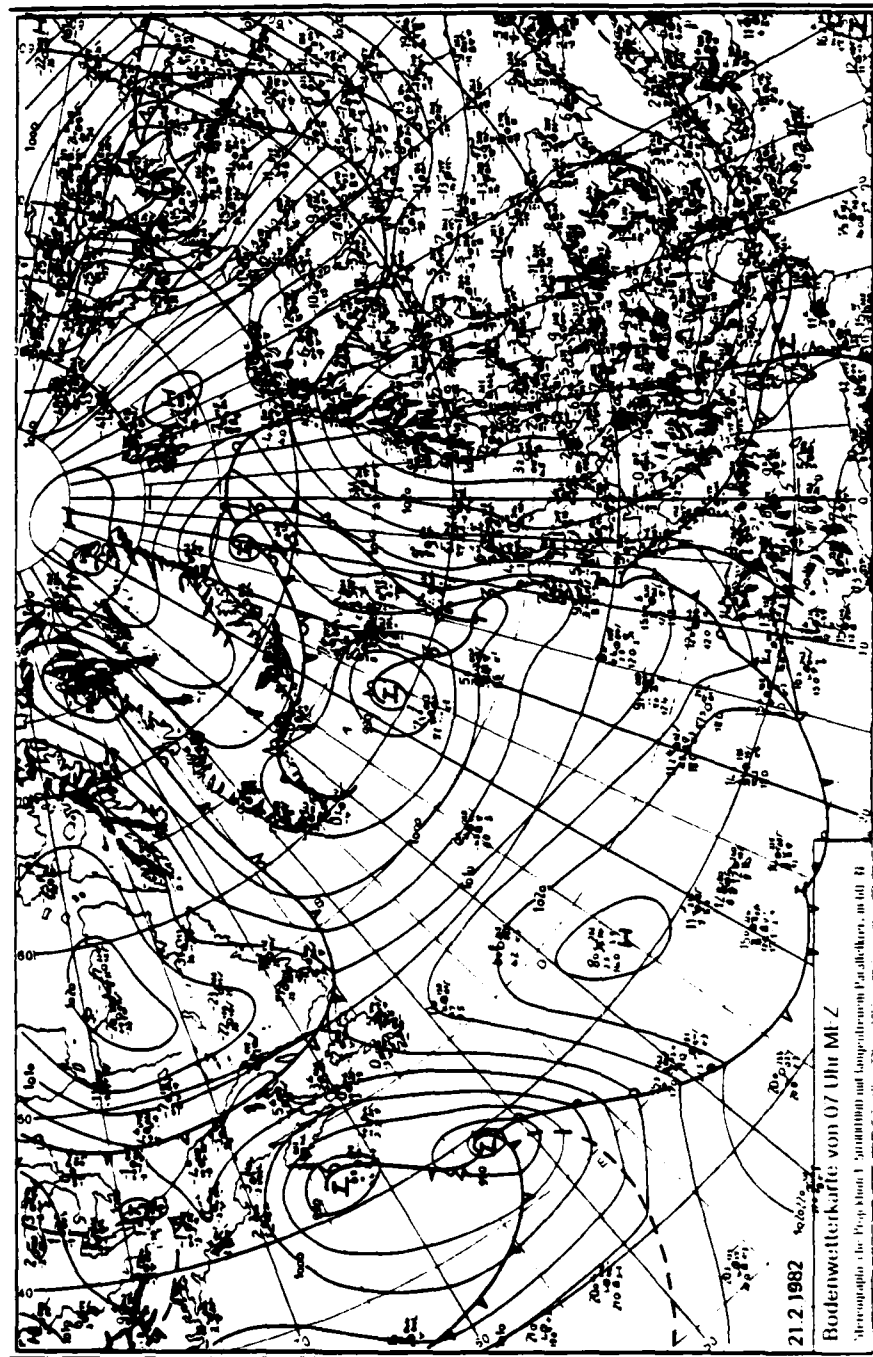


Figure 12 0700Z Atlantic/European Surface Analysis on February 21, 1982.

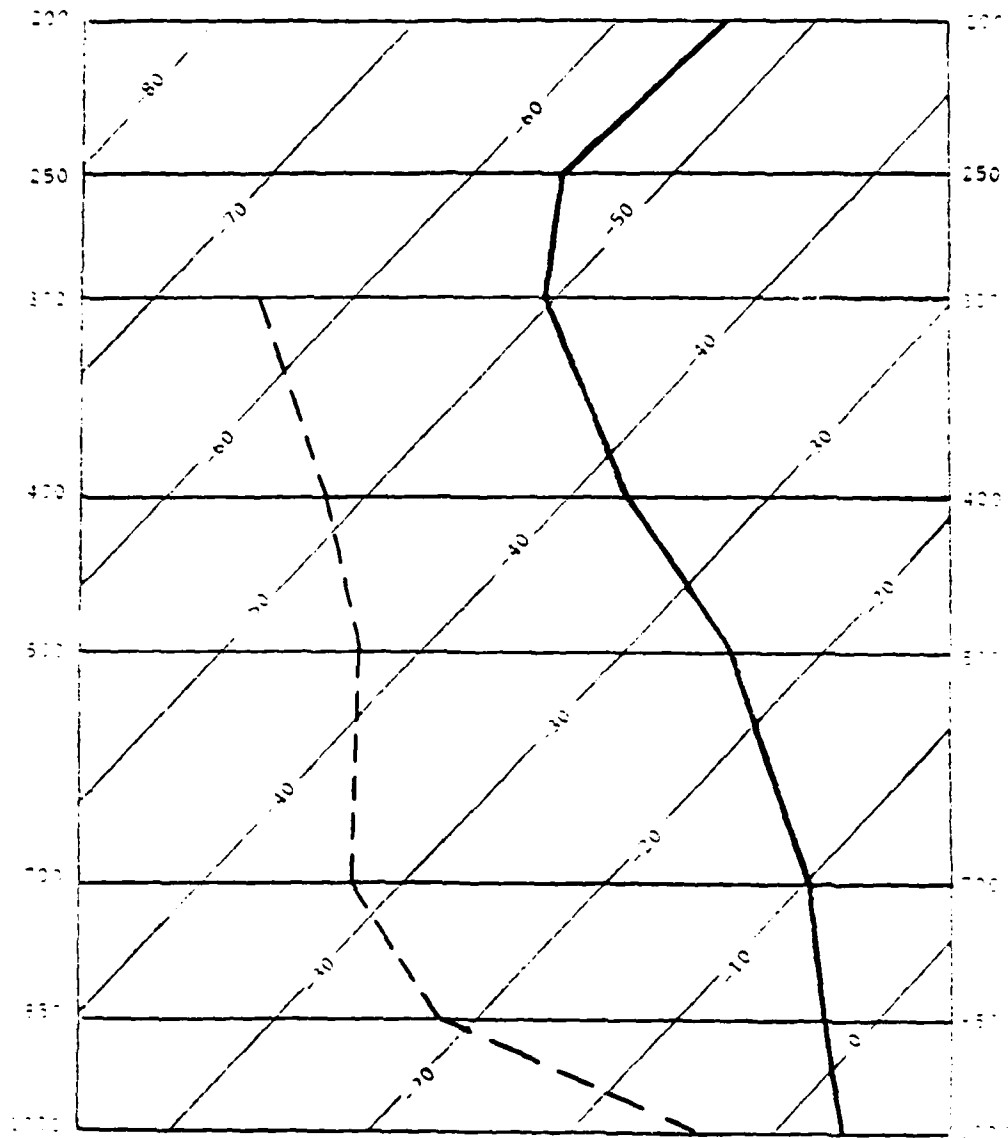


Figure 13 Simplified Skew-T Log P diagram from Deuselbach area on February 21, 1982.

correlation between  $\text{SO}_2$  and relative humidity from the 20th-23rd (Figure 11b). This period was dominated by a large subsidence inversion, which became especially pronounced on the 21st (Figures 12 and 13). The "dirty" moist surface layer was being mixed with clean, dry air from above and the end result was a reduction in  $\text{SO}_2$  and relative humidity levels.

### 3. March (Figures 14-15)

March's data coincide with the previous months' patterns. Of particular note, is the large increase in  $\text{SO}_2$  in the latter part of the month, associated with the definite wind shift and end of precipitation (Figures 14a and 15a). This large increase was part of one of the more significant pollution episodes to occur during the period when data were recorded. The major synoptic feature was a large, slow-moving high pressure system, which moved into the area on the 22nd-23rd and dominated until the 27th-28th. The restriction of vertical mixing imposed by this system contributed significantly to the build-up of  $\text{SO}_2$  levels. There was also very little horizontal mixing, which was another contributing factor to this build-up.

$\text{SO}_2$  shows excellent positive correlation ( $r = 0.87$ ) with dust (Figure 14b) and good negative correlation ( $r = 0.77$ ) with relative humidity (Figure 15b).

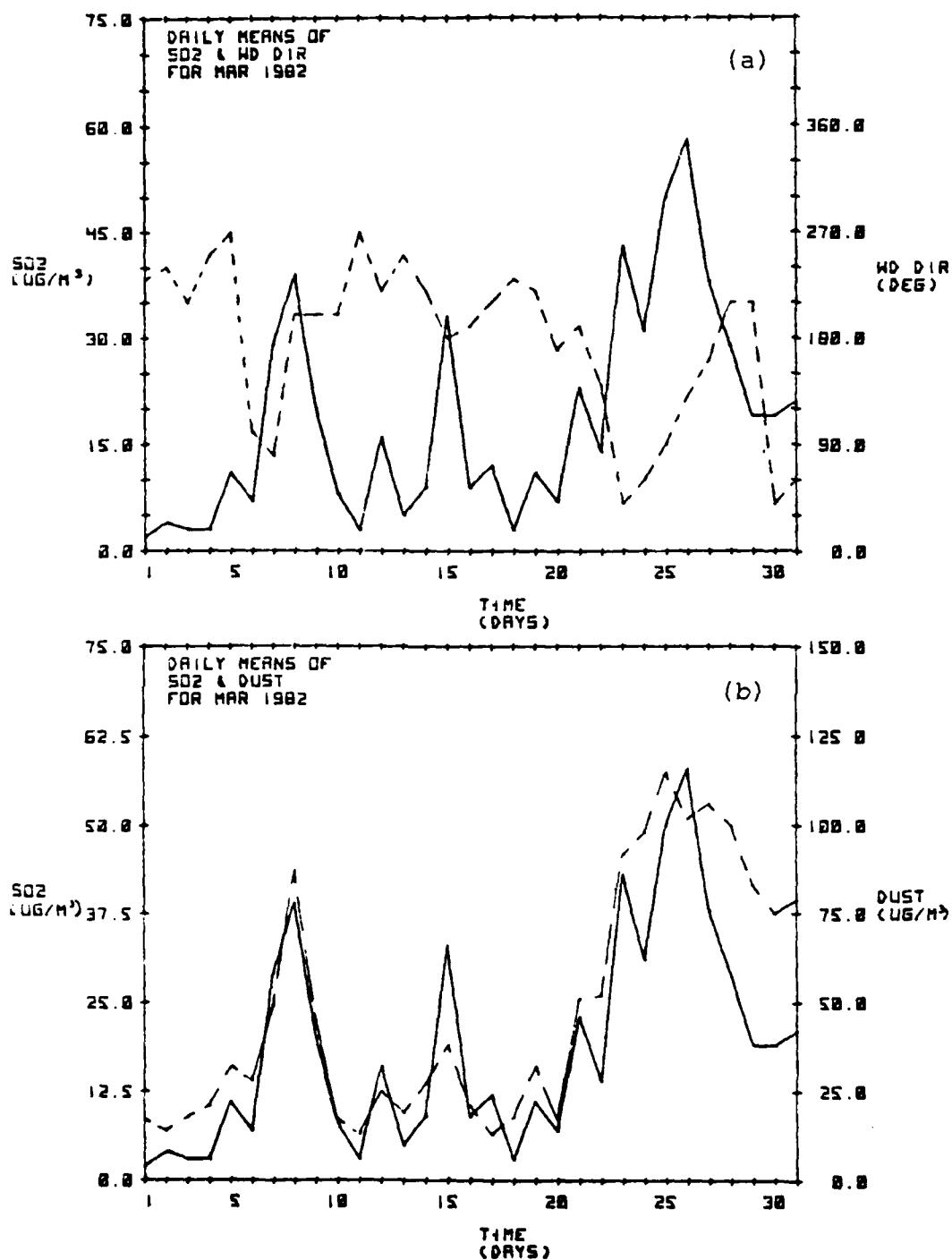


Figure 14 March versus the daily means of SO<sub>2</sub> (solid line) and (a) Wind Direction and (b) Dust. Wind Direction and Dust are represented by dashed lines.

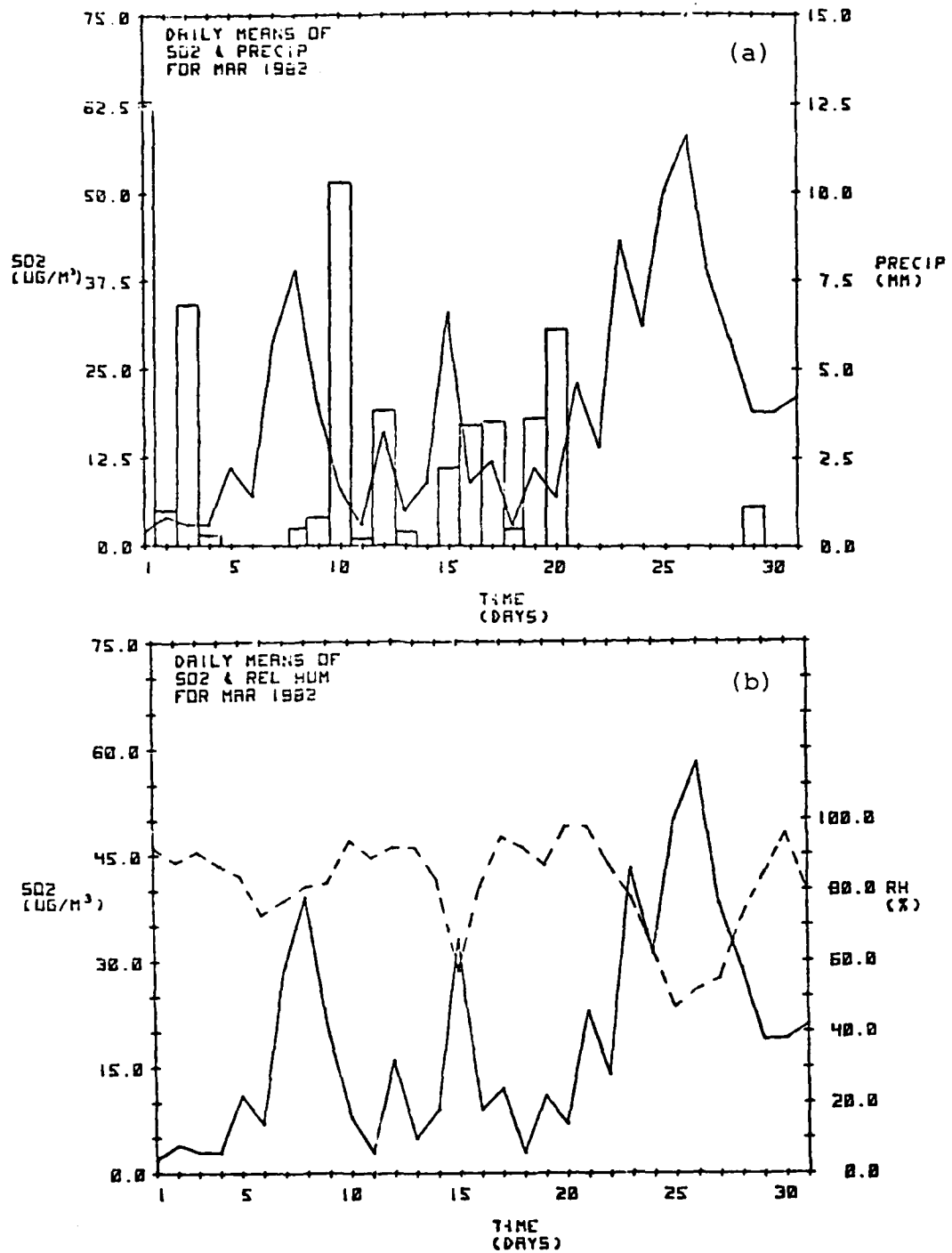


Figure 15 March versus the daily means of SO<sub>2</sub> (solid line) and (a) Precipitation (bars) and (b) Relative Humidity (dashed line).

#### 4. April (Figures 16-17)

The peak  $\text{SO}_2$  level, on the 15th, came about abruptly as once more a distinct wind shift to the E-NE occurred (Figure 16a). The continued strong positive correlation between  $\text{SO}_2$  and dust ( $r = 0.72$ ) strongly suggest a common source (Figure 16b). The negative correlations between  $\text{SO}_2$  and precipitation/relative humidity (Figure 17) are again evident.

Additionally, the overall  $\text{SO}_2$  concentrations have steadily declined (and will continue to do so) since January. This demonstrates that the stratified winter atmosphere is giving way to the more convective spring/summer atmosphere. Fall/winter inversions generally last longer and are more frequent than spring/summer inversions. Thus, there is also an increased frequency of low mixing heights in fall/winter (Fishman and Carney, 1983).

#### 5. May (Figures 18-19)

During the major pollution episode of the month, (1st-13th), the winds were again from the E (Figure 18a) and high pressure was the dominant synoptic feature. Dust continued its good positive correlation ( $r = 0.65$ ) with  $\text{SO}_2$  (Figure 18b). The inverse relationship between  $\text{SO}_2$  and precipitation/relative humidity is again evident (Figure 19).

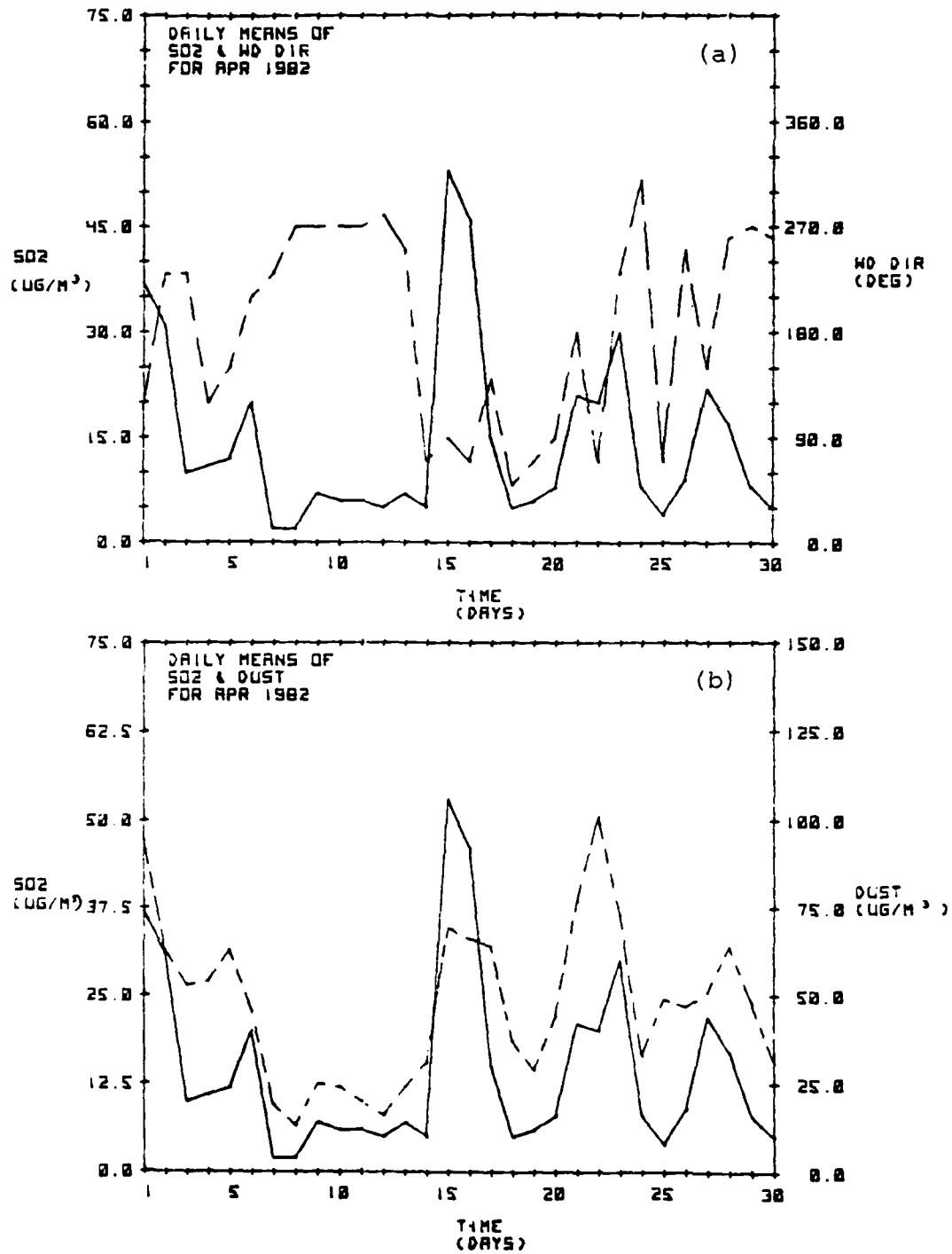


Figure 16 April versus the daily means of SO<sub>2</sub> (solid line) and (a) Wind Direction and (b) Dust. Wind Direction and Dust are represented by dashed lines.

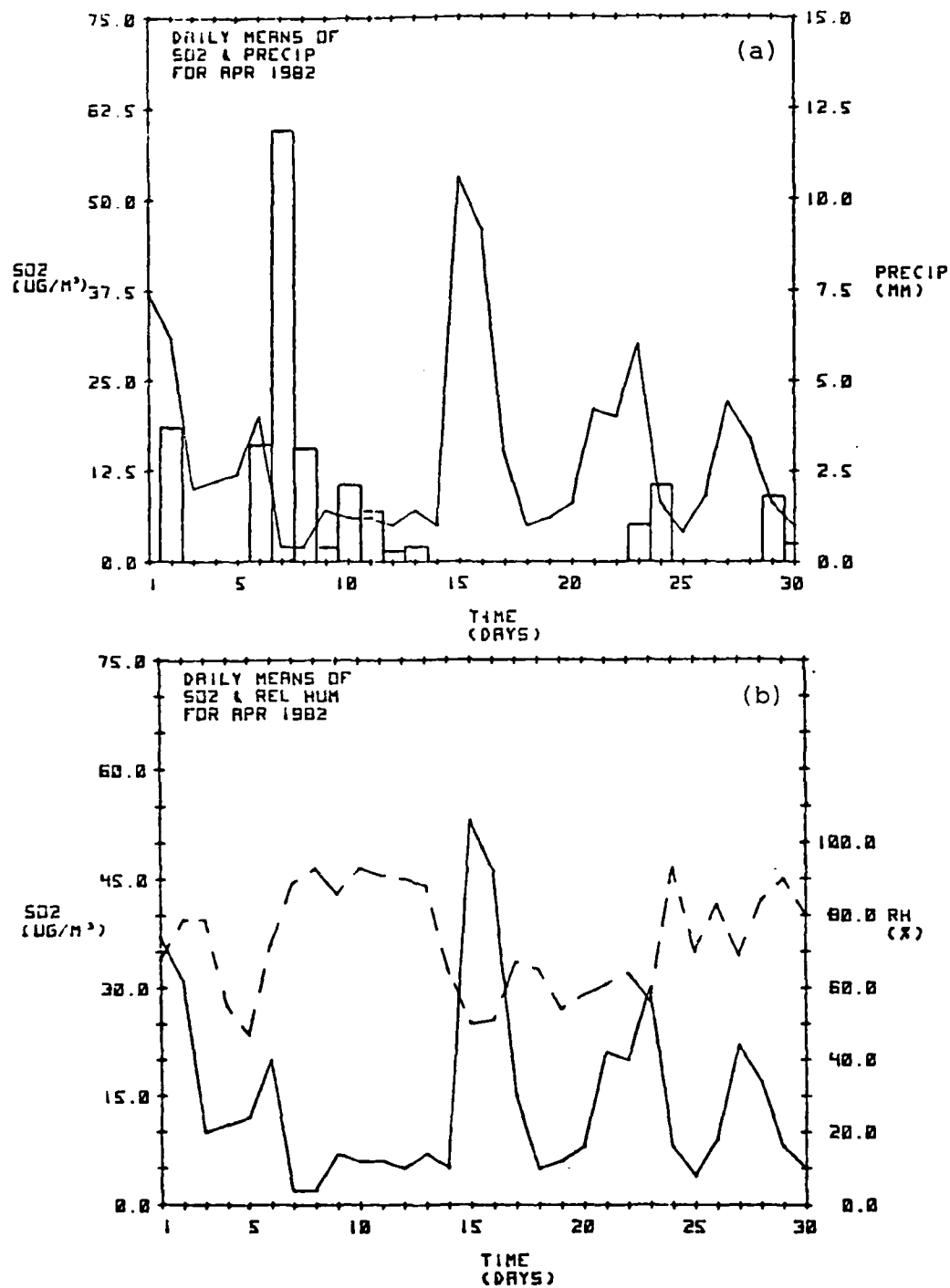


Figure 17 April versus the daily means of  $\text{SO}_2$  (solid line) and (a) Precipitation (bars) and (b) Relative Humidity (dashed line).



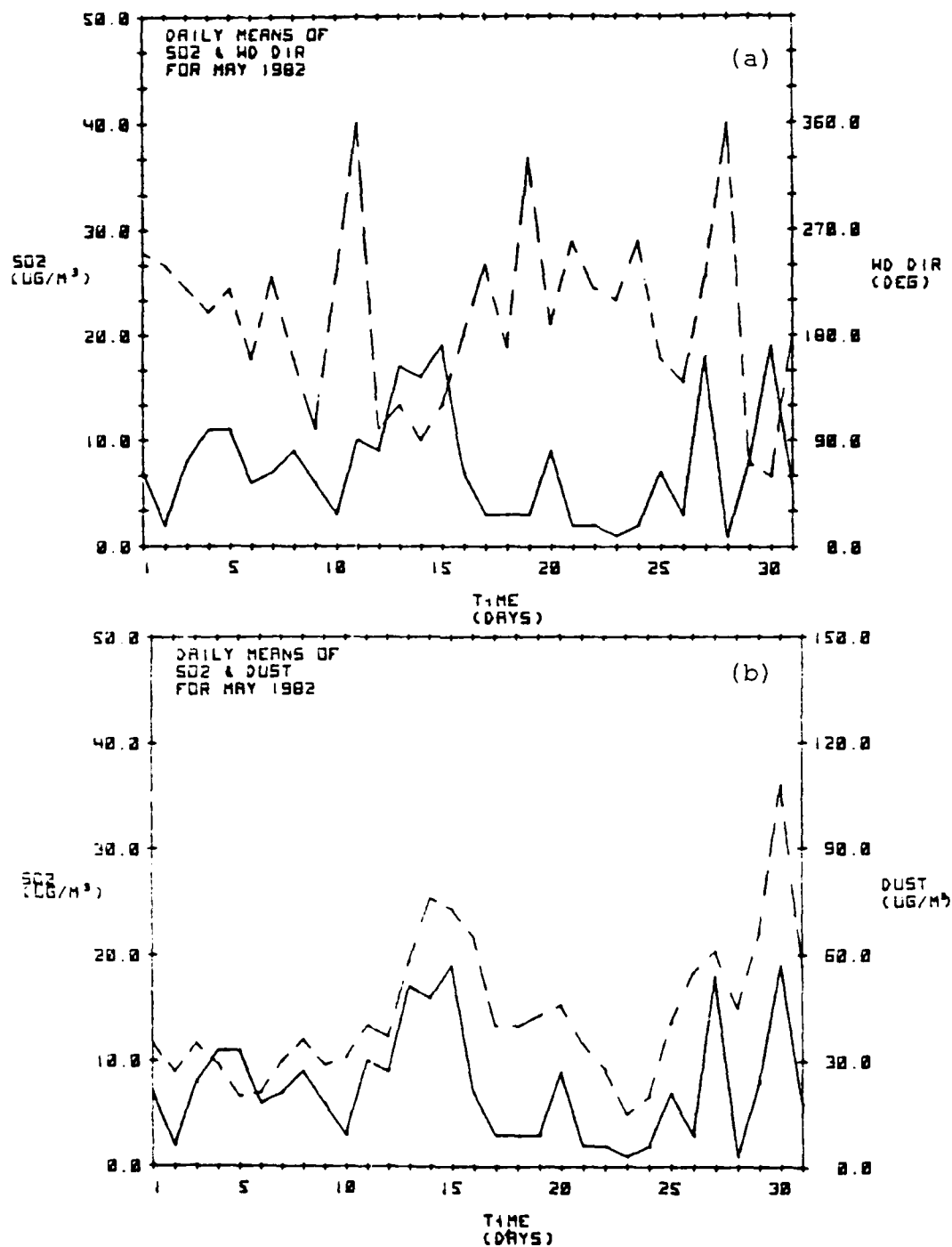


Figure 18 May versus the daily means of  $\text{SO}_2$  (solid line) and (a) Wind Direction and (b) Dust. Wind Direction and Dust are represented by dashed lines.

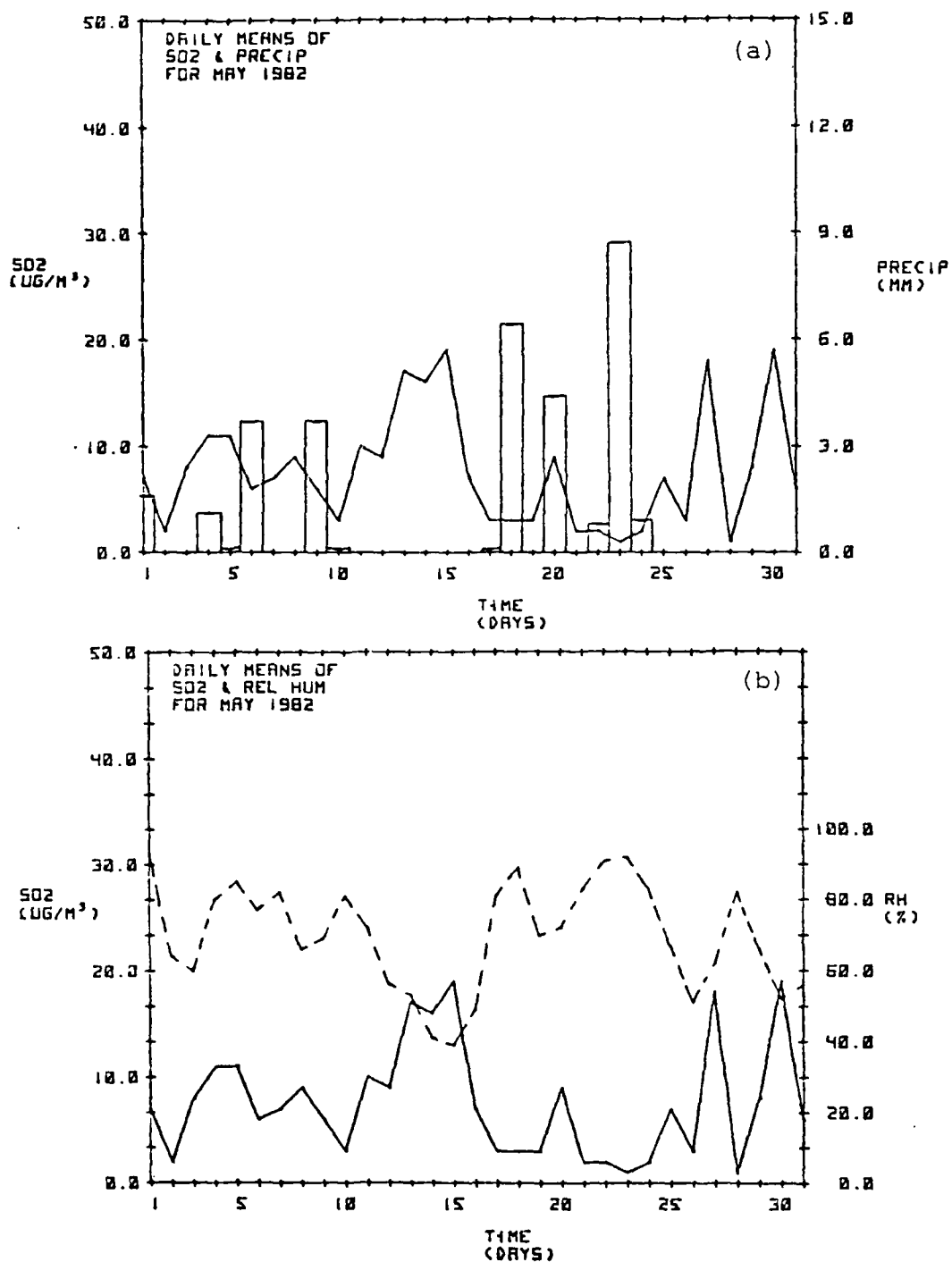


Figure 19 May versus the daily means of SO<sub>2</sub> (solid line) and (a) Precipitation (bars) and (b) Relative Humidity (dashed line).

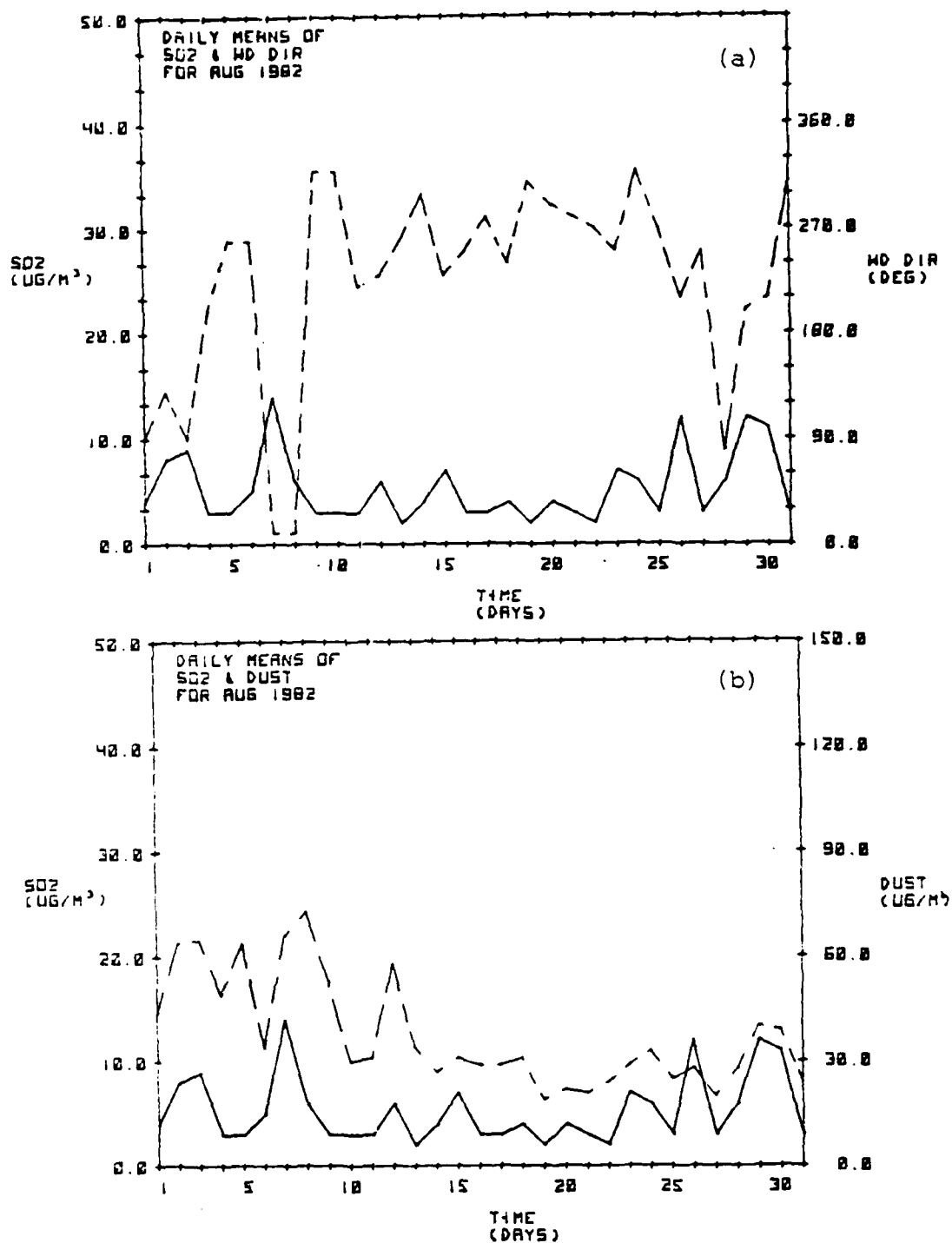


Figure 20 August versus the daily means of  $\text{SO}_2$  (solid line) and (a) Wind Direction and (b) Dust. Wind Direction and Dust are represented by dashed lines.

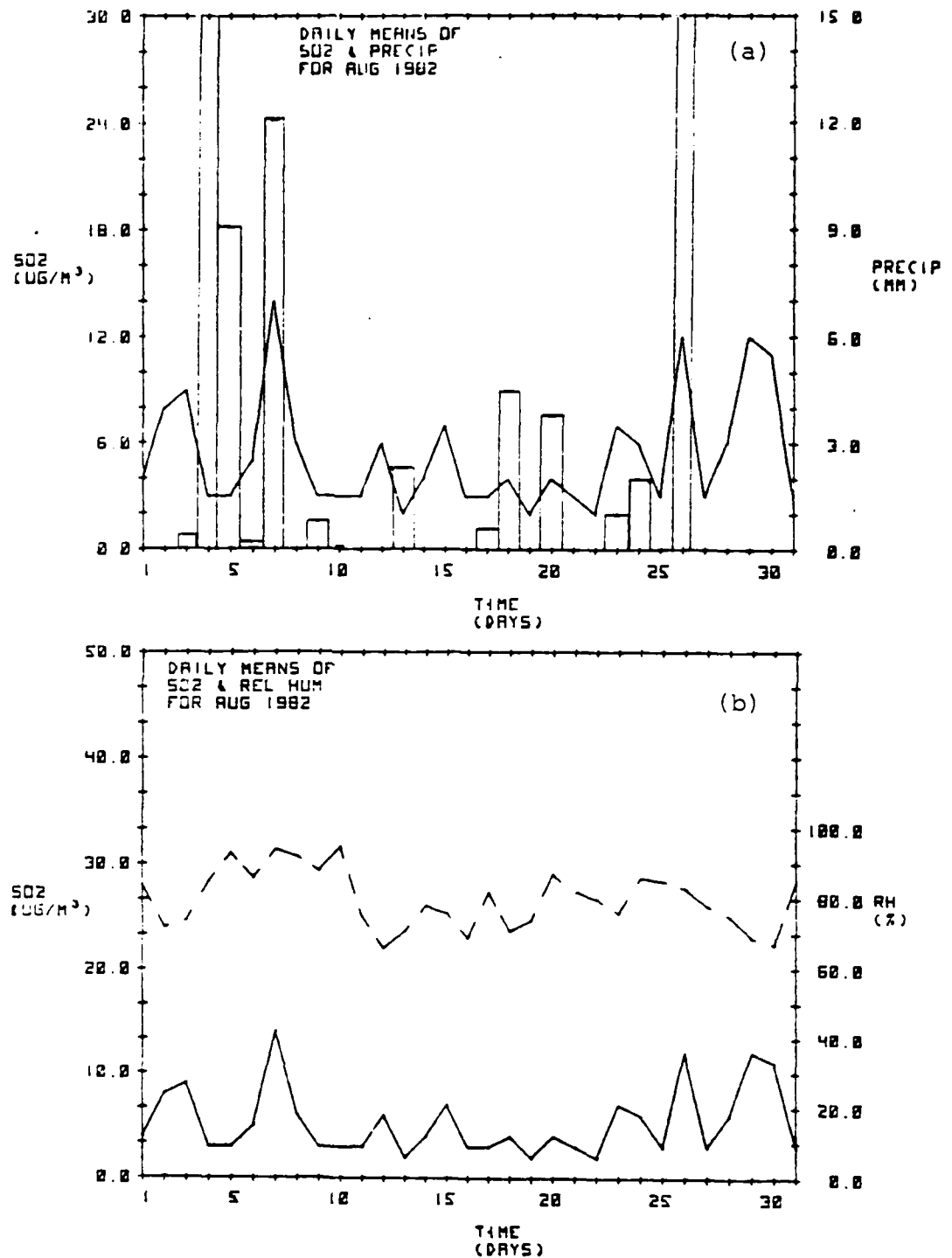


Figure 21 August versus the daily means of SO<sub>2</sub> (solid line) and (a) Precipitation (bars) and (b) Relative Humidity (dashed line).

#### 6. August (Figures 20-21)

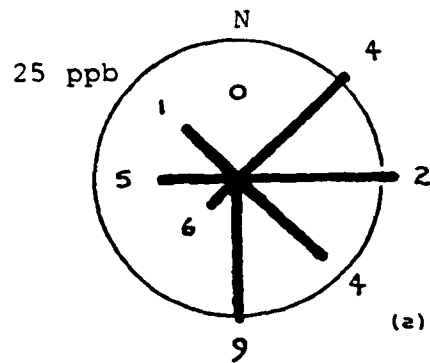
The peak level of  $\text{SO}_2$  (on the 7th) occurs again after a noticeable wind shift (Figure 20a). However it should be noted again, that the overall level of  $\text{SO}_2$  has dropped significantly since January for the reasons mentioned in April's discussion. The anticipated good correlations with dust, precipitation, and relative humidity continue to hold true (Figures 20b-21).

#### B. Nitrogen Dioxide

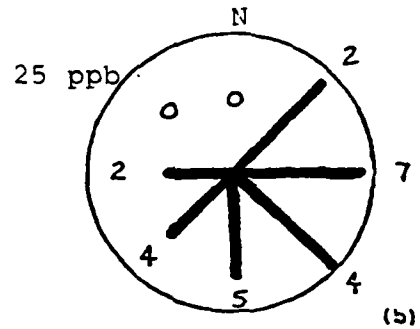
In this subsection,  $\text{NO}_2$  is treated with respect to meteorological parameters. An excellent source of  $\text{NO}_2$  comes from combustion (i.e., fossil fuel burning).  $\text{NO}_2$  is a key element in the PSS reaction and will be treated in that respect later in this thesis. Figure 22a-f represents an  $\text{NO}_2$  wind rose. It can be interpreted in the same manner as the  $\text{SO}_2$  wind rose (Figure 7).

The most significant meteorological parameters affecting  $\text{NO}_2$  are wind direction and temperature.  $\text{NO}_2$  advection is less likely than  $\text{SO}_2$  advection and therefore is generally less evident when comparing  $\text{NO}_2$  to wind direction. The atmospheric lifetime of  $\text{NO}_2$  is determined by R1 and is only about 1.5 days (Hahn and Crutzen, 1982). However,  $\text{NO}_2$  will also photodissociate in the presence of UV radiation with wavelengths less than 420 nm (Dickerson et al., 1982). This reduces its

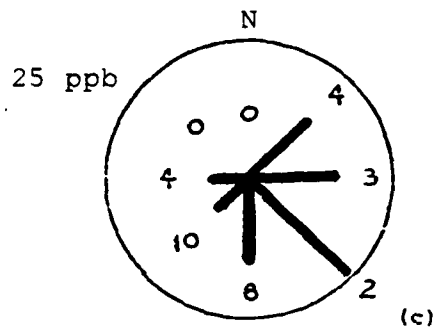
lifetime to about 1000 seconds (morning) and about 100 seconds (afternoon). Therefore photochemistry can significantly shorten the lifetime of  $\text{NO}_2$ .  $\text{NO}_2$  and  $\text{SO}_2$  show a strong positive correlation, despite the fact that  $\text{NO}_2$  is not soluble, while  $\text{SO}_2$  is very soluble. This is seen if the  $\text{NO}_2/\text{SO}_2$  levels are compared with precipitation. So, based on solubility,  $\text{NO}_2$  should not be removed from the atmosphere as readily as  $\text{SO}_2$ . On January 9th, 11th, 20th and 21st both precipitation and rising levels of  $\text{NO}_2$  occurred. This situation is less pronounced in winter than summer as a result of winter time stratification of the atmosphere. The average correlation coefficients of both  $\text{NO}_2$  and  $\text{SO}_2$  to relative humidity taken over the 6-month data period showed  $|r_{\text{NO}_2}| < |r_{\text{SO}_2}|$ , with the respective values, -0.26 and -0.41. The average correlation coefficients of both  $\text{NO}_2$  and  $\text{SO}_2$  to precipitation also revealed  $|r_{\text{NO}_2}| < |r_{\text{SO}_2}|$  but only by a small margin. The respective values were -0.19 and -0.21. Although this result seems to indicate little difference in the solubility of these two compounds, a case by case examination has shown that  $\text{SO}_2$  levels invariably drop in the presence of precipitation, while  $\text{NO}_2$  levels are variable.  $\text{NO}_2$  also converts to nitric acid ( $\text{HNO}_3$ ) much faster than  $\text{SO}_2$  converts to sulfuric acid ( $\text{H}_2\text{SO}_4$ ). Model results have shown that sulfates



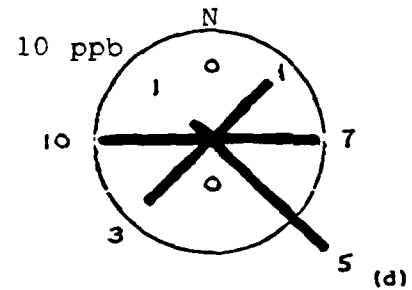
JAN (MEAN = 19 ppb)



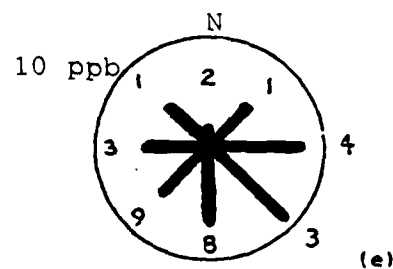
FEB (MEAN = 20 ppb)



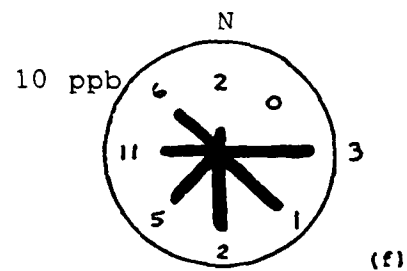
MAR (MEAN = 12 ppb)



APR (MEAN = 10 ppb)



MAY (MEAN = 6 ppb)



AUG (MEAN = 6 ppb)

**Figure 22** NO<sub>2</sub> Wind Rose. Each "rose" represents the daily means of NO<sub>2</sub> levels with respect to wind direction. The values at the end of each line on the "rose" represents the number of days when the mean wind was from that particular quadrant.

are transported over greater distances than nitrates (Rodhe et al., 1980).

To summarize, when inversions cause high  $\text{SO}_2$  levels, then  $\text{SO}_2$  and  $\text{NO}_2$  are positively correlated. When precipitation, high relative humidity and/or fog cause low  $\text{SO}_2$  levels, then  $\text{SO}_2$  and  $\text{NO}_2$  are weakly correlated.

#### 1. January (Figures 23-24)

The  $\text{NO}_2$  levels show strong negative correlation with wind direction during the first half of the month (Figure 23a). A sharp increase in  $\text{NO}_2$  levels is seen with a wind shift to the E. This point is corroborated by the  $\text{NO}_2$  wind rose (Figure 22a). The remainder of January shows little relationship between the two. This is particularly evident on the 20th when a large peak is observed with S winds. A possible explanation lies in the fact that precipitation occurred from the 20th-23rd. If some  $\text{NO}_2$  had attached itself to any suspended dust, it could have easily been precipitated out. It is also possible that mixing with mid-tropospheric air helped reduce the levels. However a much more reasonable explanation is found in the correlation ( $r = -0.59$ ) between  $\text{NO}_2$  and temperature (Figure 23b).

During periods of warming the  $\text{NO}_2$  levels decline while during periods of cooling  $\text{NO}_2$  levels rise. The overall temperature rise that begins on the 21st is



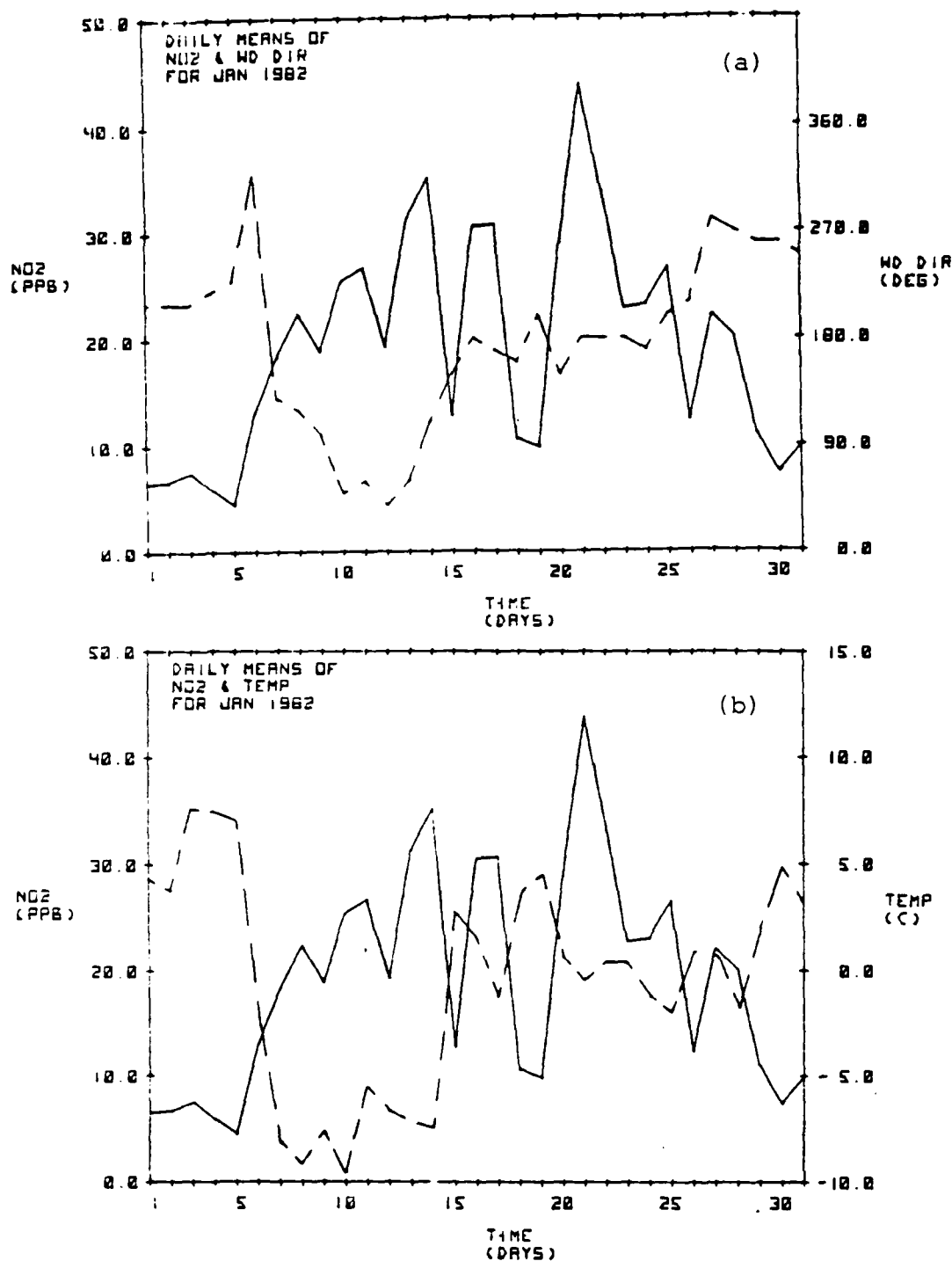


Figure 23 January versus the daily means of NO<sub>2</sub> (solid line) and (a) Wind Direction and (b) Temperature. Wind Direction and Temperature are represented by dashed lines.

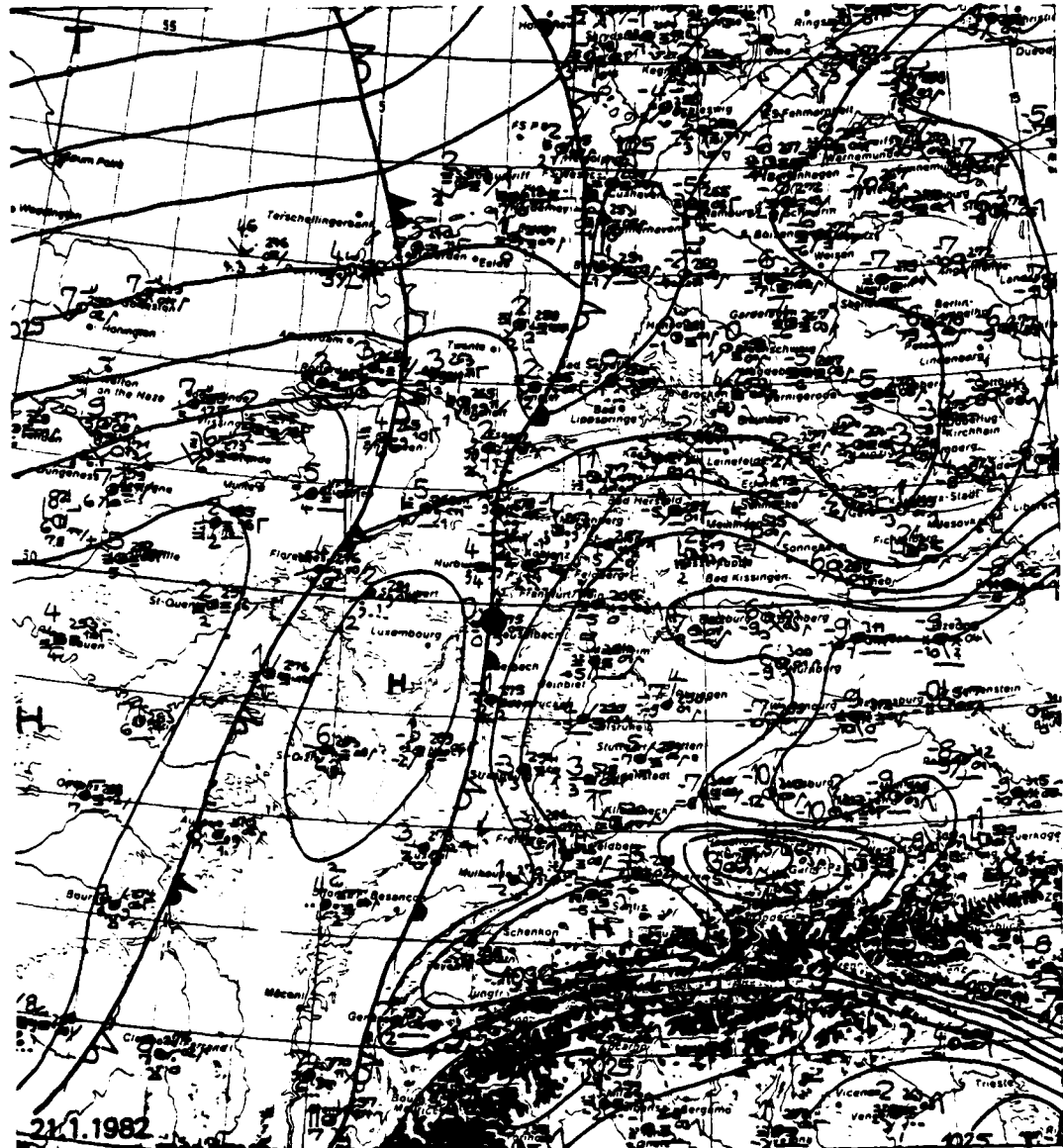


Figure 24 1200Z Surface Analysis of North Central Europe on January 21, 1982.

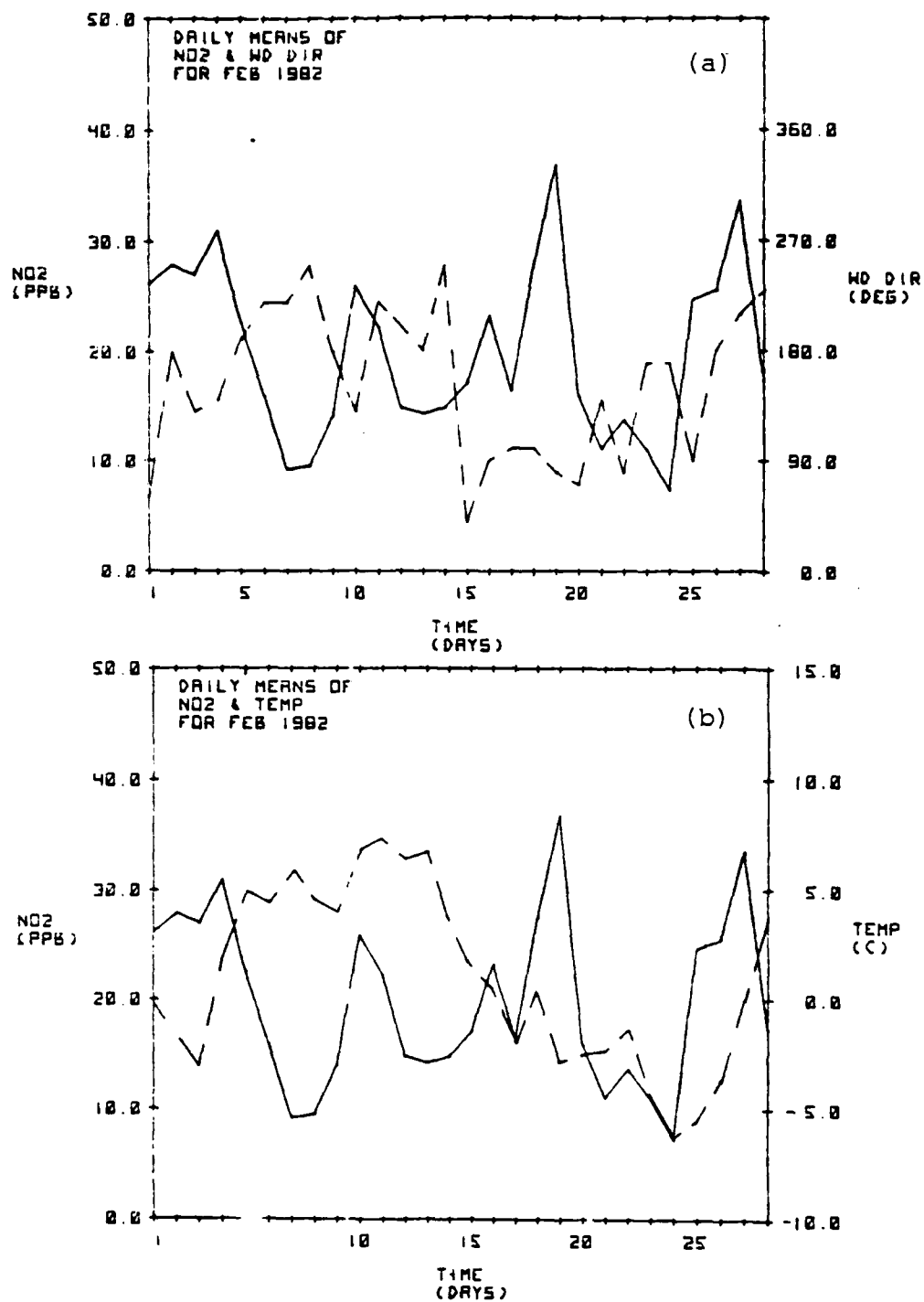


Figure 25 February versus the daily means of NO<sub>2</sub> (solid line) and (a) Wind Direction and (b) Temperature. Wind Direction and Temperature are represented by dashed lines.

accompanied by an overall decline in  $\text{NO}_2$  levels from its highest monthly level (21st) to its lowest monthly level (30th). Figure 24 clearly shows the temperature contrast across the frontal boundary.

The relationship between  $\text{NO}_2$  and temperature is very well defined. The significant cooling trend from the 5-14th coincides well with the rise in  $\text{NO}_2$ . Colder temperatures result in more local space heating (residential heating). This factor when coupled with a stratified atmosphere, or inversions, will increase  $\text{NO}_2$  levels in the lower levels. This is illustrated when, with the exception of the 11th, the Deuselbach area received warm overrunning air from a warm front to the south. The region was generally dominated by high pressure centered north of the area.

## 2. February (Figure 25)

February began with a shift to E-SE winds and an ensuing high concentration of  $\text{NO}_2$  (Figure 25a). The wind direction then shifted to the W and  $\text{NO}_2$  levels showed a rapid drop-off. The major peak of the month is associated with E winds.  $\text{NO}_2$  and temperature (Figure 25b) showed a transition from negative correlation (first half of the month) to positive correlation (second half of the month).

## 3. March (Figures 26-28)

March continued to show fairly good correlation between peak levels of  $\text{NO}_2$  and E winds (Figure 26a).

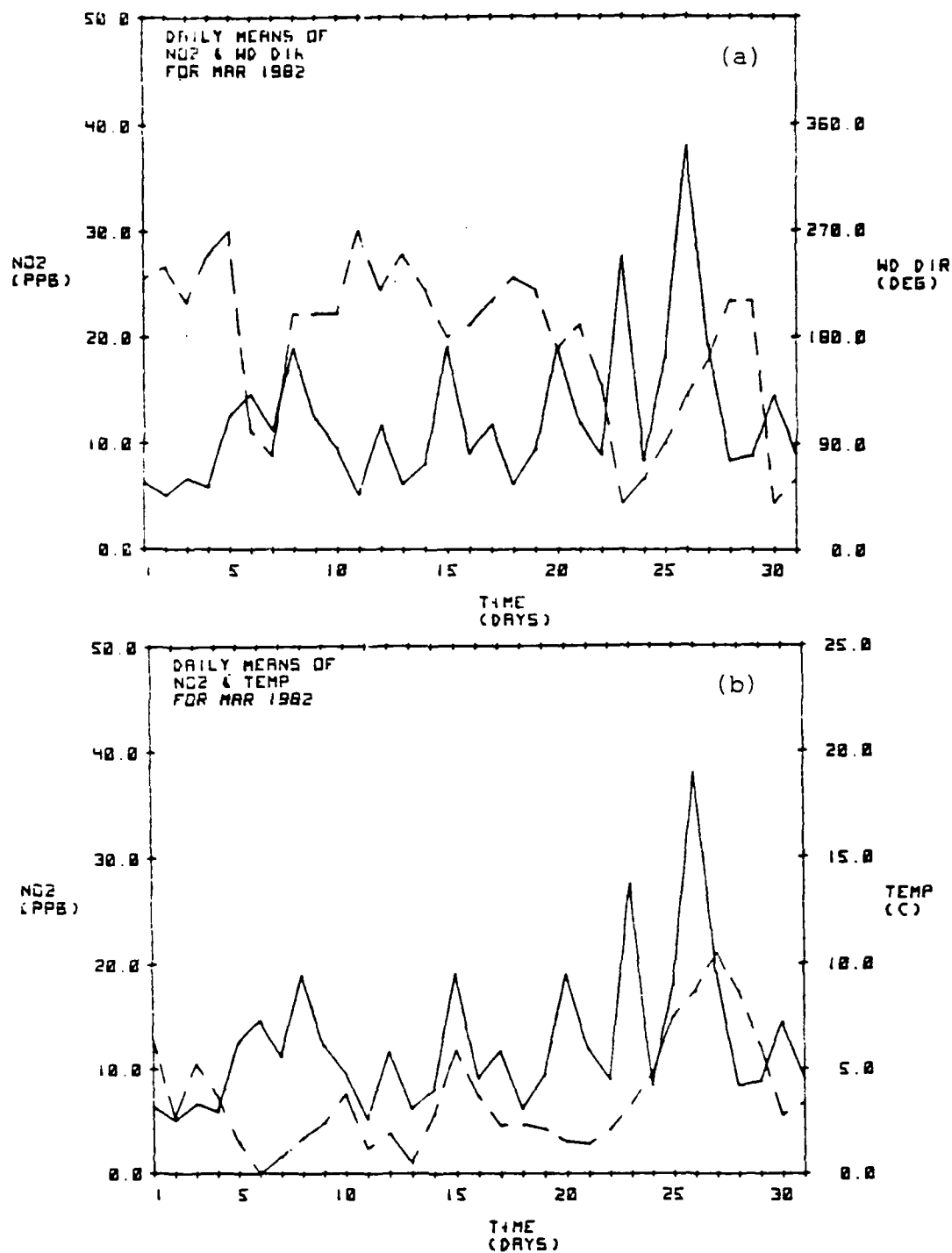


Figure 26 March: versus the daily means of NO<sub>2</sub> (solid line) and (a) Wind Direction and (b) Temperature. Wind Direction and Temperature are represented by dashed lines.

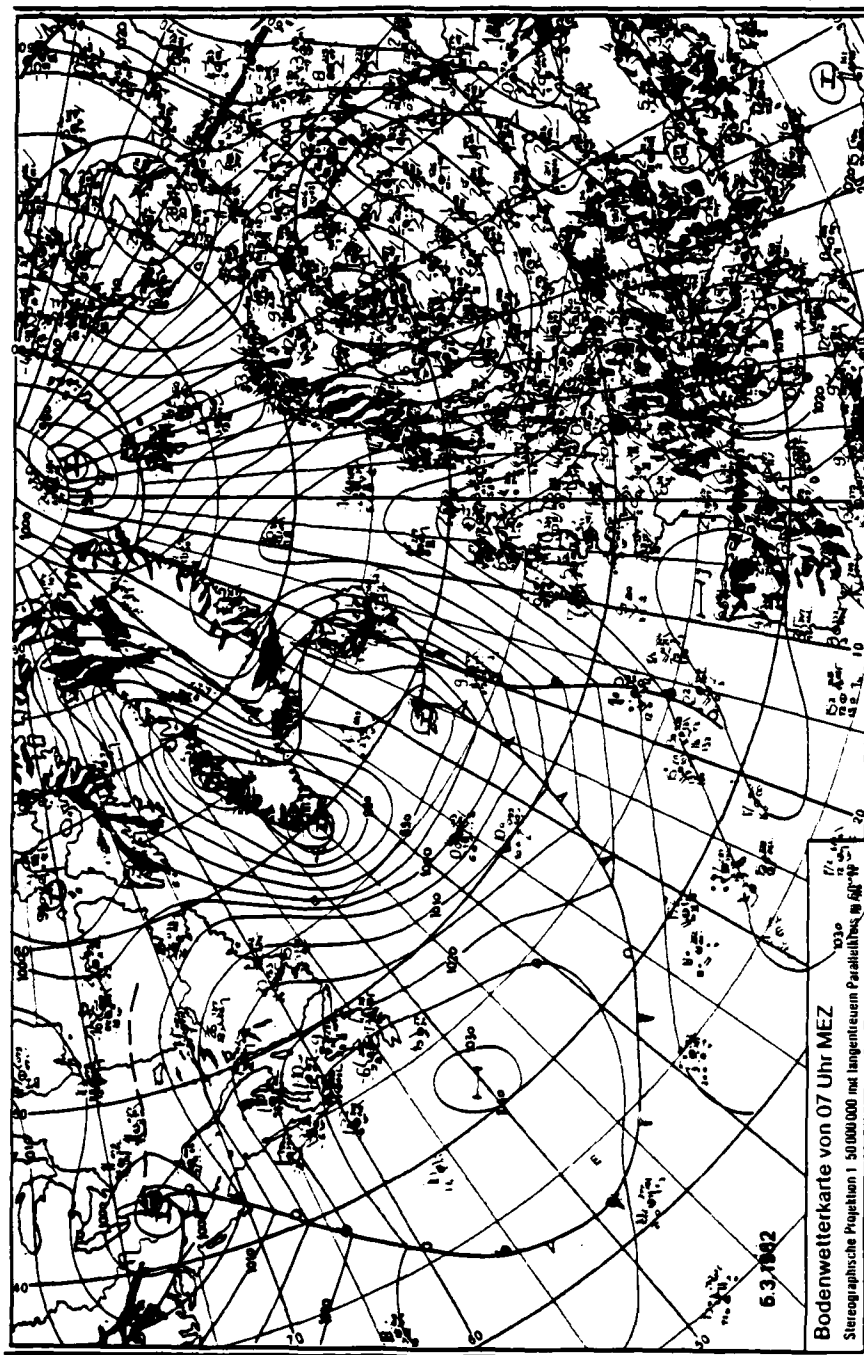


Figure 27 0700Z Atlantic/European Surface Analysis on March 5, 1982.

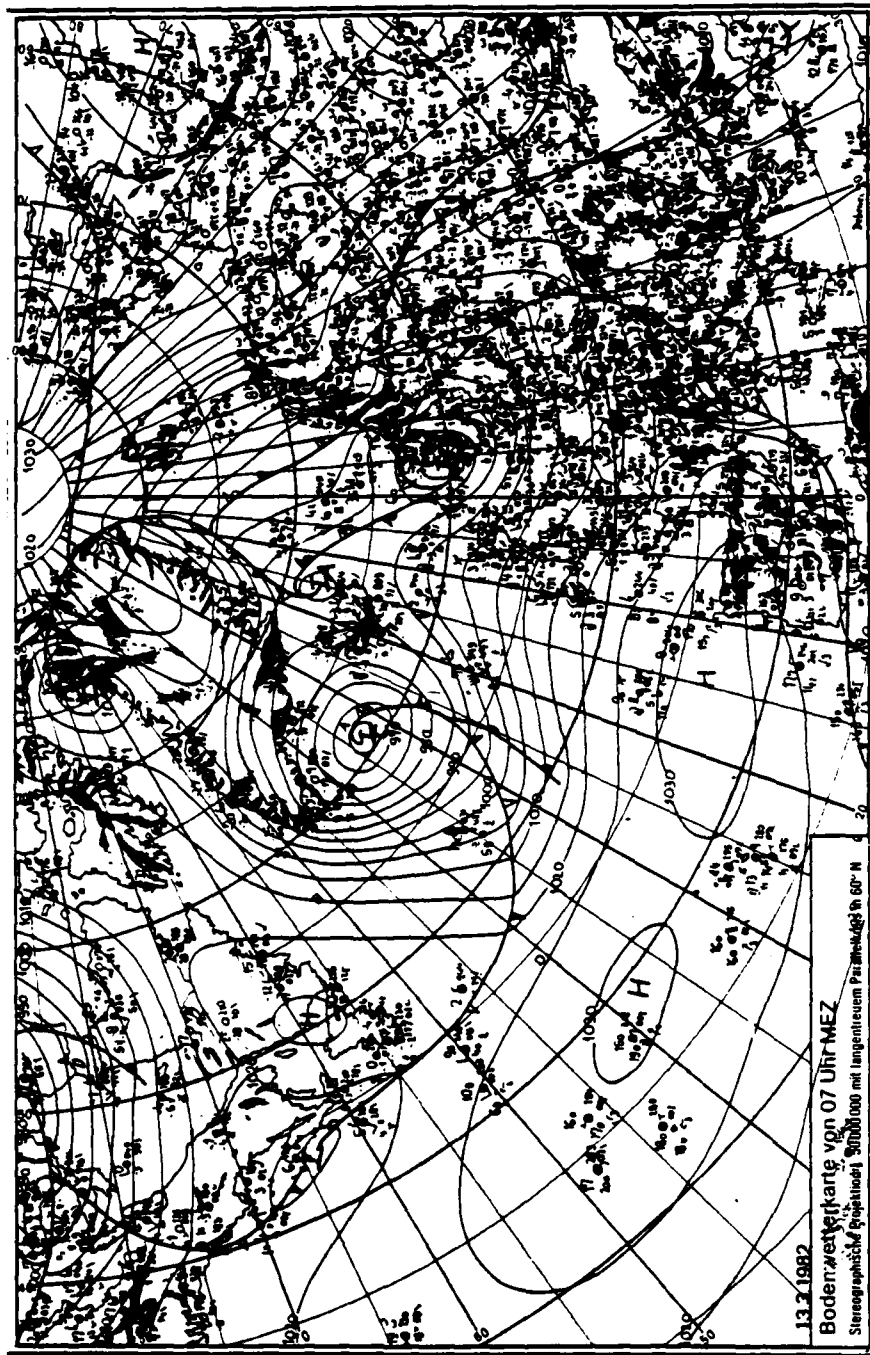


Figure 28 0700Z Atlantic/European Surface Analysis on March 13, 1982.

The correlation with temperature (Figure 26b) is now positive. By the end of the first week, the negative correlation between  $\text{NO}_2$  and temperature was replaced by a positive one. The temperature peaks on the 10th and 15th are the result of high pressure which had moved into the region from the SW (Figures 27 and 28).

#### 4. April (Figure 29)

The period with the lowest  $\text{NO}_2$  levels in April (6-12th) occurred when the winds were from the W (Figure 29a). This demonstrates a preferred wind direction for the advection of  $\text{NO}_2$ . However, the second half of April does not seem to follow the previously established pattern.  $\text{NO}_2$  levels show occasional rises despite a W wind. A possible explanation for this discrepancy could be the increased fertilization of the soil by local farmers, since Deuselbach does lie in a rural area. Soil nitrification produces NO (Slemr, Dickerson and Seiler, 1983).

However, it appears that the synoptic situation dominated the  $\text{NO}_2$  levels during the last half of April. A continuation of E winds from the 16-17th accounted for increased  $\text{NO}_2$  levels. The period from the 17-19th showed decreasing levels of  $\text{NO}_2$  as a large high pressure system expanded across central Europe. The winds during this period were consistently from the E-NE. This



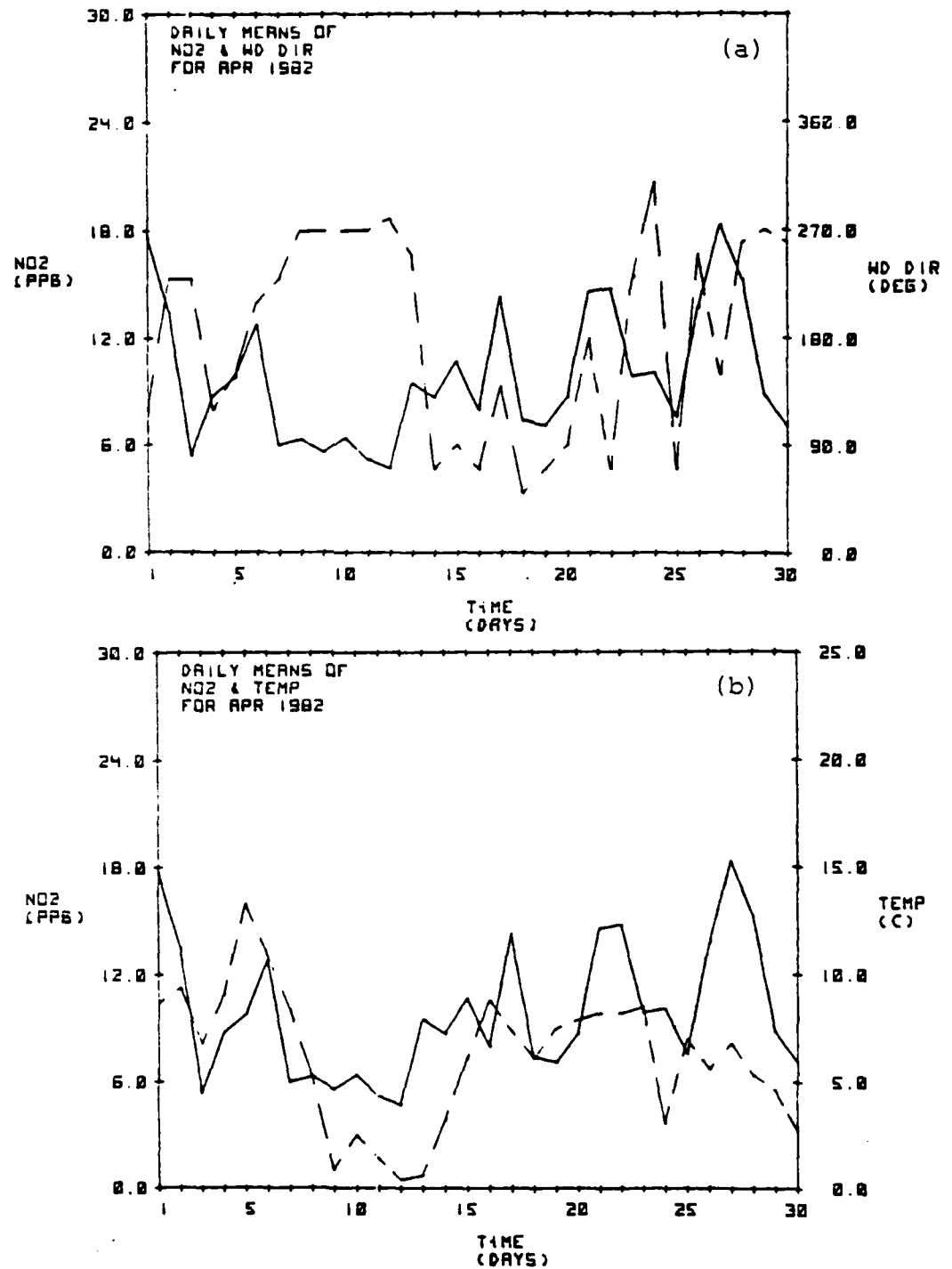


Figure 29 April versus the daily means of NO<sub>2</sub> (solid line) and (a) Wind Direction and (b) Temperature. Wind Direction and Temperature are represented by dashed lines.

should have signaled elevated levels of  $\text{NO}_2$ , yet a decrease was observed. However, the relatively clear skies, reduced wind speed and  $\text{O}_3$  precursors advected from the E-NE, most likely enhanced photochemical activity and reduced mean daily  $\text{NO}_2$  levels. During this same period, the mean daily levels of  $\text{O}_3$  rose. The period from 22nd-28th was marked by a series of stationary fronts, generally oriented N-S, in the Deuselbach area. The almost daily wind shifts during this period are symptomatic of the fluctuations of a stationary front through the region.  $\text{NO}_2$  levels also fluctuated depending on wind direction (i.e., increased levels with an E wind). A wind shift to the W at the end of April caused the observed decline in  $\text{NO}_2$  levels. Thus,  $\text{NO}_2$  levels showed declines over several days, but daily levels seemed to respond to diurnal wind fluctuations.  $\text{NO}_x$  data, on an hourly time scale, showed similar changes in concentration with wind shifts.

Temperature and  $\text{NO}_2$  also showed a strong positive correlation for the first half of April (Figure 29b).

#### 5. May (Figures 30-31)

The convective nature of the atmosphere during the month is most probably the cause of the variability between  $\text{NO}_2$  and wind direction. The most significant pollution episode of the month (11-13th) did occur with an E wind (Figure 30a).

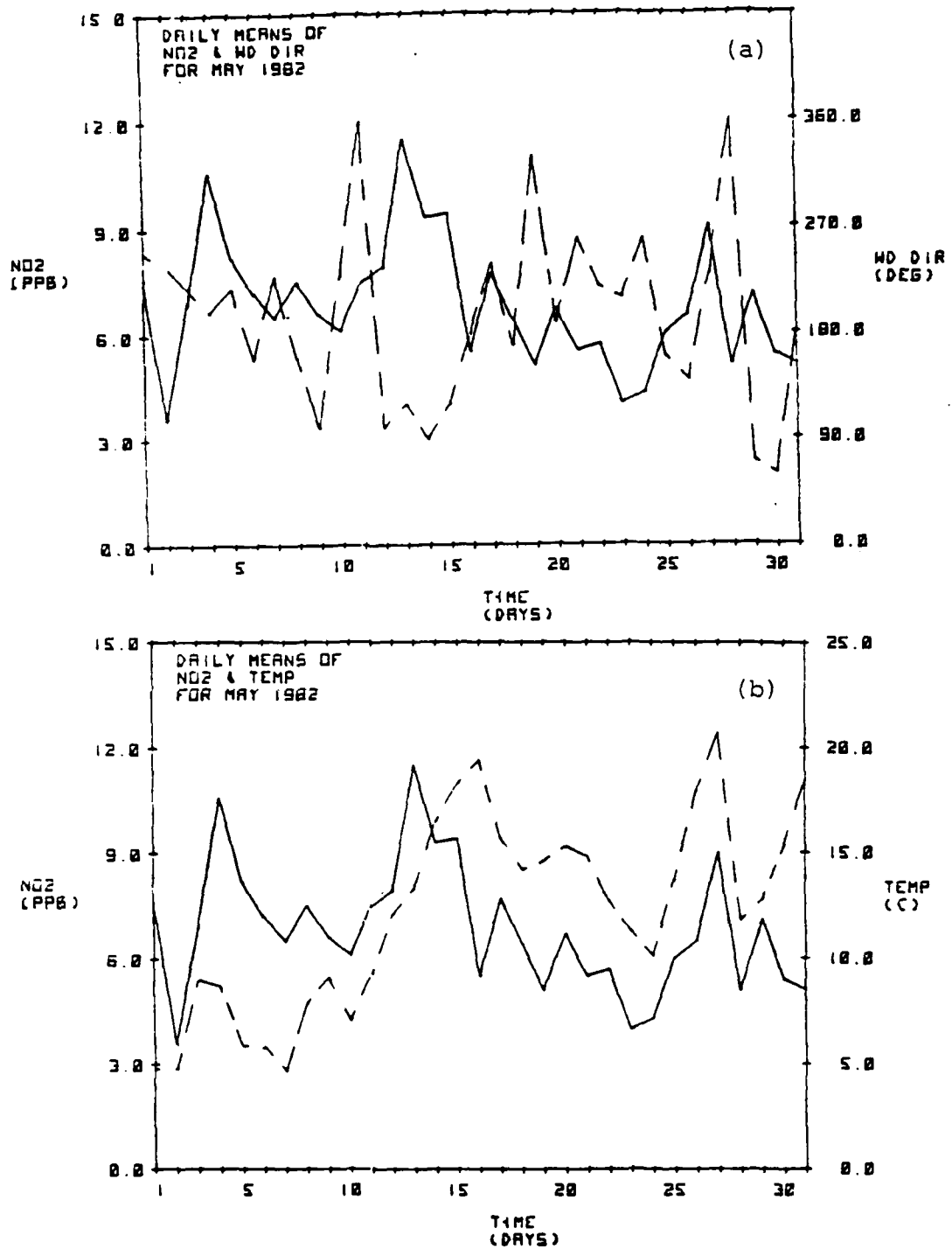


Figure 30 May versus the daily means of NO<sub>2</sub> (solid line) and (a) Wind Direction and (b) Temperature. Wind Direction and Temperature are represented by dashed lines.

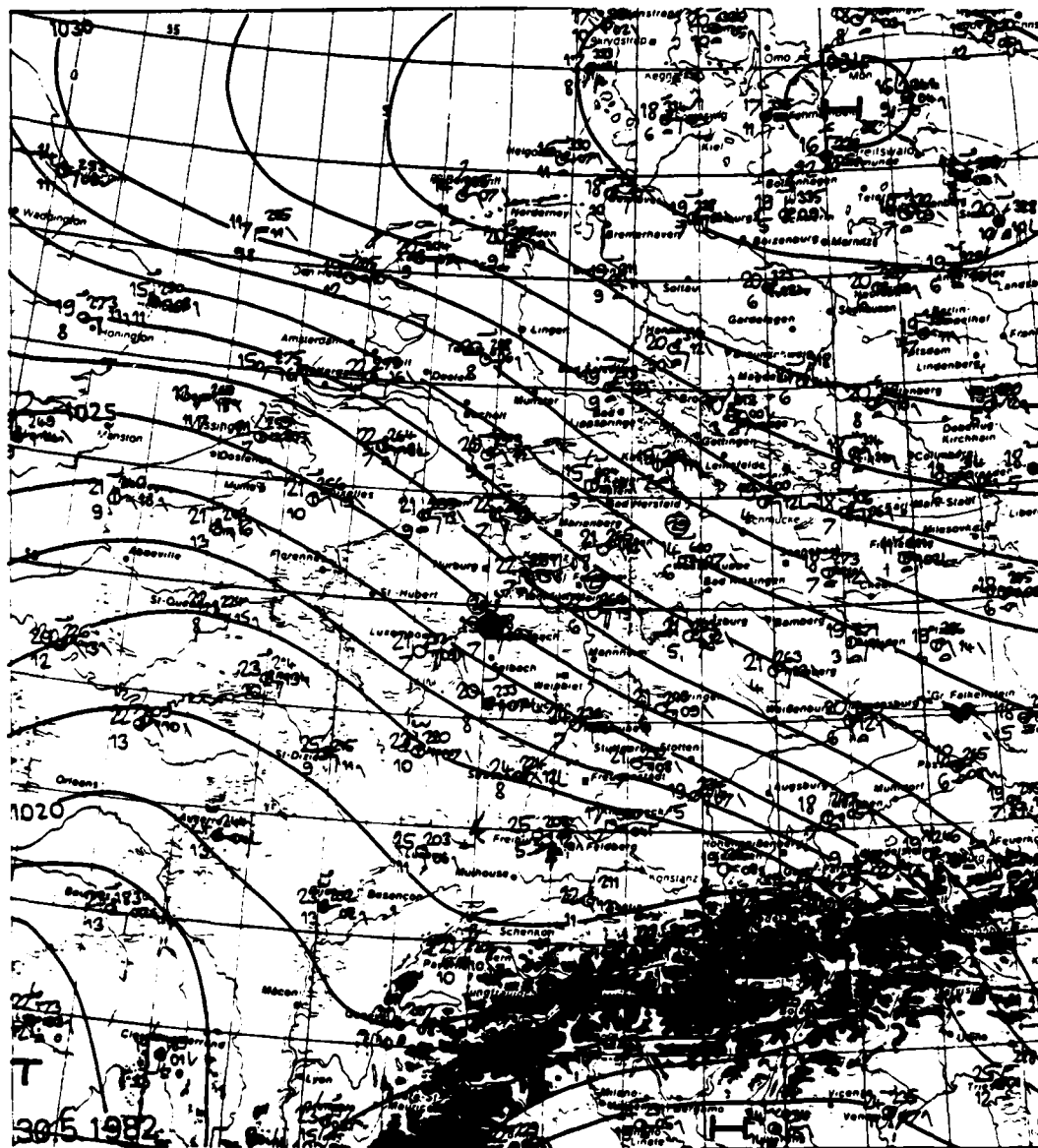


Figure 31 1200Z Surface Analysis of North Central Europe on May 30, 1982.

The other outstanding feature is the decrease of  $\text{NO}_2$  levels on the 29-30th, despite a definite E wind. Upper air soundings of the period showed a large subsidence inversion along with the associated high pressure system over the area. Although skies were generally clear, the decrease in the  $\text{NO}_2$  levels does not appear related to photochemistry. A surface analysis (Figure 31) showed a tightening gradient and subsequent increase in the mean daily winds from 2.9 m/sec (29th) to 5.0 m/sec (30th). The combination of increased wind speed and hilly terrain most probably resulted in sufficient low level turbulent mixing to drive the mean daily levels down as the clean overlying air was mixed down. This synoptic feature also accounted for the only significant negative correlation of temperature and  $\text{NO}_2$  in a month that had shown only positive correlation (Figure 30b). The decrease in cloud cover and increase in solar insolation helped raise the ambient air temperature.

#### 6. August (Figure 32)

$\text{NO}_2$  peaks occurred during the first and last weeks of August and were associated with E winds (Figure 32a).  $\text{NO}_2$  levels during the middle of the month remained fairly low as a result of a consistent W wind direction.

The peak on the 27th is again illustrative of the non-solubility of  $\text{NO}_2$ . The second largest amount of precipitation for the month fell on this day, yet  $\text{NO}_2$

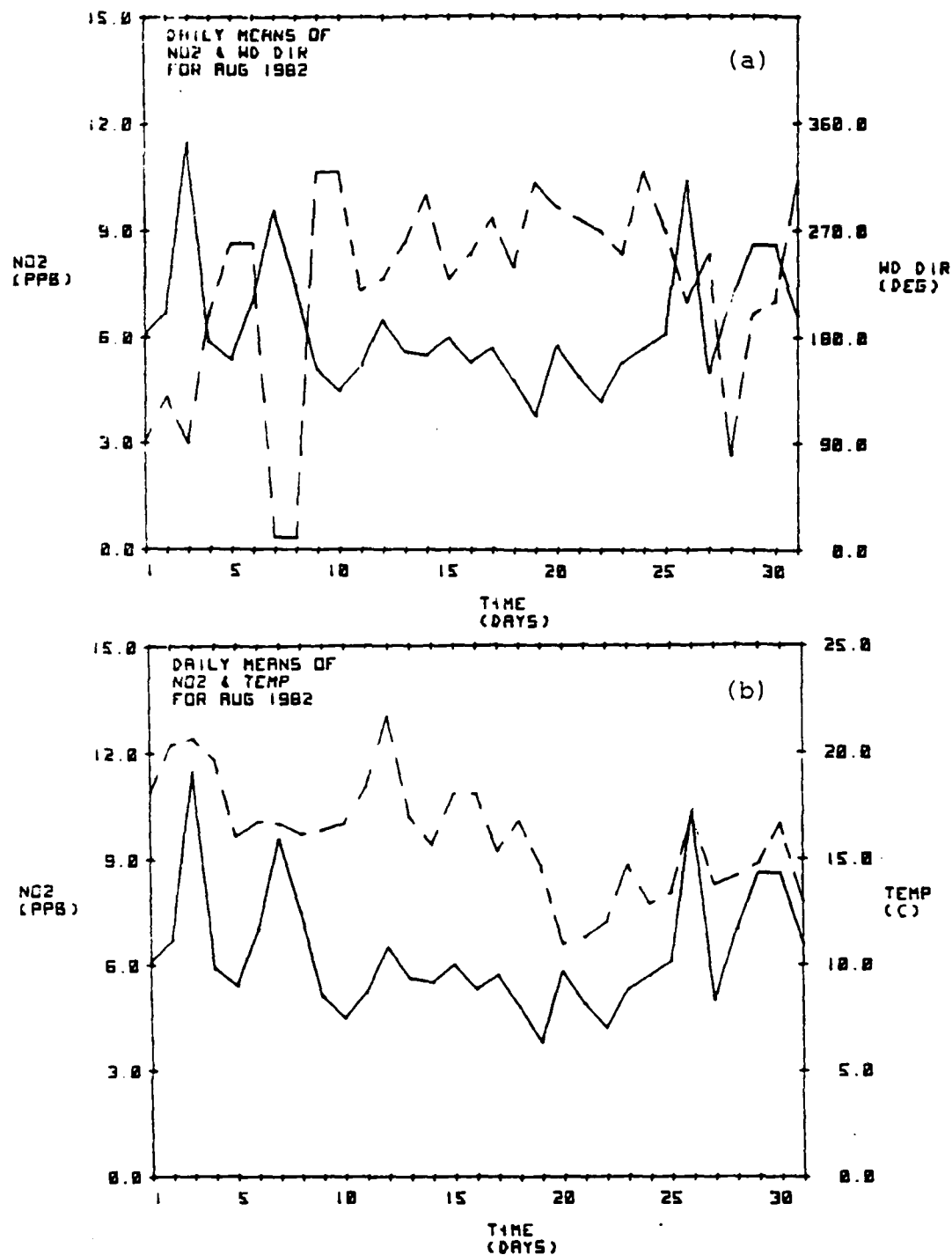


Figure 32 August versus the daily means of NO<sub>2</sub> (solid line) and (a) Wind Direction and (b) Temperature. Wind Direction and Temperature are represented by dashed lines.

levels rose while  $\text{SO}_2$  levels fell near the detection limit. The correlation with temperature was positive for the month (Figure 32b).

### C. Ozone

Ozone is highly reactive and has a short lifetime, so it must be formed in situ photochemically, or transported a short distance. Some elevated  $\text{O}_3$  concentrations did occur with an E wind, however it is generally the  $\text{O}_3$  precursors (i.e.,  $\text{NO}$ ,  $\text{NO}_2$  and hydrocarbons) that are advected into a region and not the  $\text{O}_3$  itself.  $\text{O}_3$  may also be transported from the upper troposphere to the surface via the subsiding air of a high pressure system (Shapiro, 1980). The production of photochemically produced  $\text{O}_3$  also takes place faster under the influence of high pressure.

During winter, there is also so much  $\text{NO}$  present and so little  $h\nu$ , especially UV radiation, that emissions of  $\text{NO}$  consume a large fraction of the available  $\text{O}_3$ , and  $\text{O}_3$  is actually titrated out of the atmosphere. This is typical of large cities and shows that in this particular scenario it is simple chemistry and not the meteorology that is controlling  $\text{O}_3$  levels.  $\text{NO}$  levels will decrease to at or near zero at night as  $\text{NO}$  titrates out. Typically, the lifetime of  $\text{O}_3$  in clean air is about one month or more, however in the presence of polluted air it can

be significantly shortened. This is evident from the negative correlation of  $O_3$  and  $NO_x$ .  $O_3$  formation is also very temperature dependent, which in turn is dependent on solar radiation. Therefore, the most significant meteorological parameters that affected  $O_3$  were: high pressure (with its associated light winds and clear skies), temperature and wind direction.

Another factor controlling  $O_3$  levels is not meteorological, but chemical.  $O_3$  is consumed by NO, which is typical in an urban-like atmosphere. This phenomenon was observed at Deuselbach. This is atypical for a rural village. Therefore, the atmosphere of a small rural village behaved like that of a large industrialized city.

#### 1. January (Figures 33-34)

January  $O_3$  levels were generally very low, but the most significant peak levels of  $O_3$  occurred during two completely different synoptic situations. The mid-month peak occurred after a high pressure system had moved into the area and the winds shifted to the E (Figure 33a), bringing in the  $O_3$  precursors. The peak on the 5th was of equal magnitude, but it occurred after the passage of a cold front (Figure 34). It would seem that the subsiding air behind the front was responsible for bringing stratospheric  $O_3$  to the surface. The event on the 5th appears to be the only winter time example of this



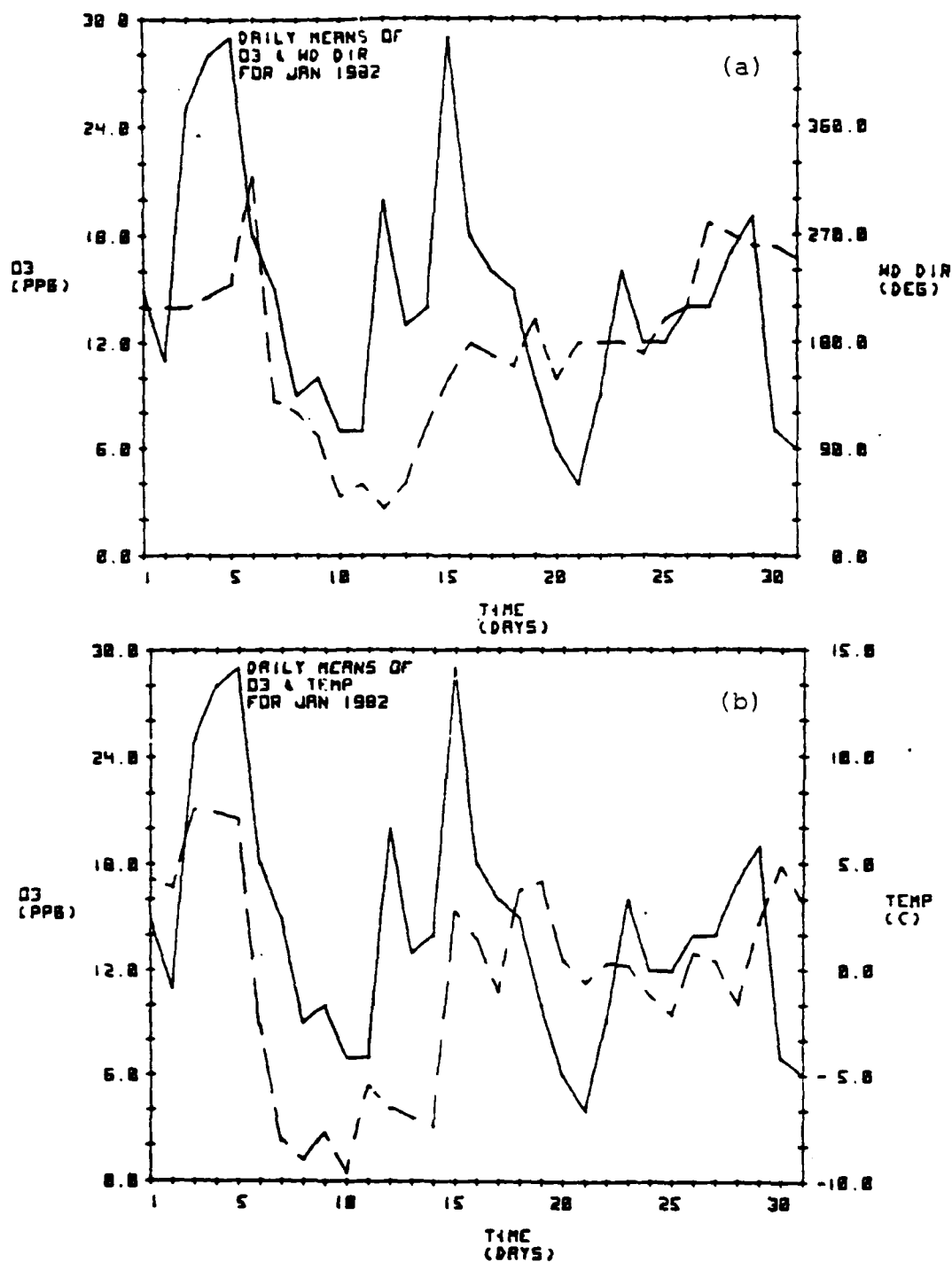


Figure 33 January versus the daily means of  $O_3$  (solid line) and (a) Wind Direction and (b) Temperature. Wind Direction and Temperature are represented by dashed lines.

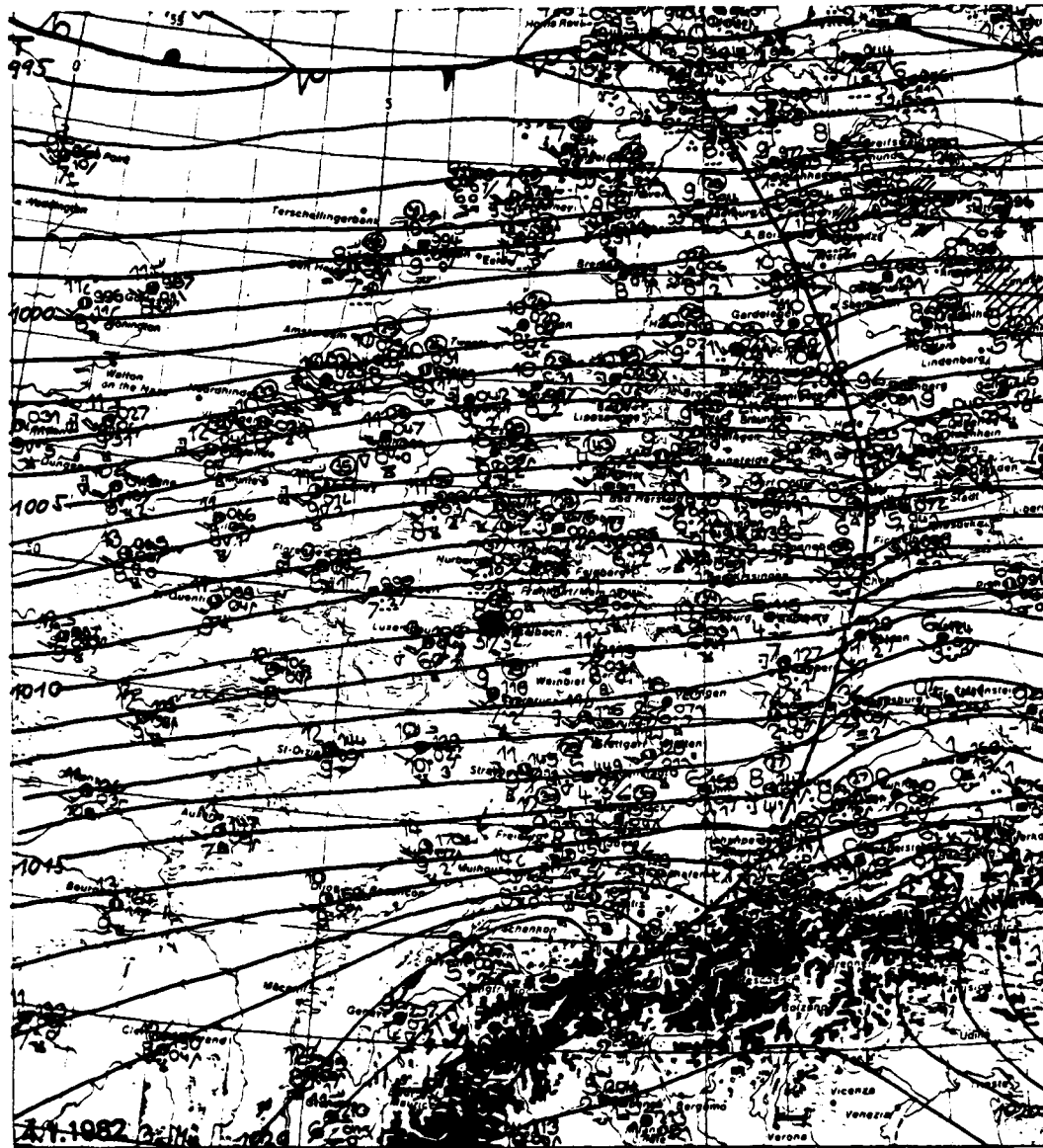


Figure 34 1200Z Surface Analysis of North Central Europe on January 4, 1982.

phenomenon that could be found. Low  $O_3$  levels could also result from abundant NO consuming the available  $O_3$ .  $O_3$  would then titrate out of the atmosphere.

Temperature correlation during the first half of the month was quite good (Figure 33b). High pressure S of Deuselbach and the resulting S winds kept the temperature relatively high. The passage of a cold front on the 4th is clearly defined in Figures 33a and 34 as the temperature showed a marked drop in values. High pressure returned to the area on the 12-13th, but it was not until the center of the high moved to the E of Deuselbach did the return flow on "the backside" cause a significant temperature rise. However, during the second half of January the overall synoptic situation of rapidly moving fronts and weak ridges, dominated the situation and the correlation deteriorated.

## 2. February (Figure 35)

February exhibited the expected patterns. The peak  $O_3$  levels were achieved under high pressure with a prior wind shift to the E (Figure 35a). Two large high pressure systems dominated the beginning of the month and a third system from the 19-20th onward. Although the temperature did not correlate as well in February (Figure 35b) as it did in January, this can be explained. The high pressure system dominating the beginning of the

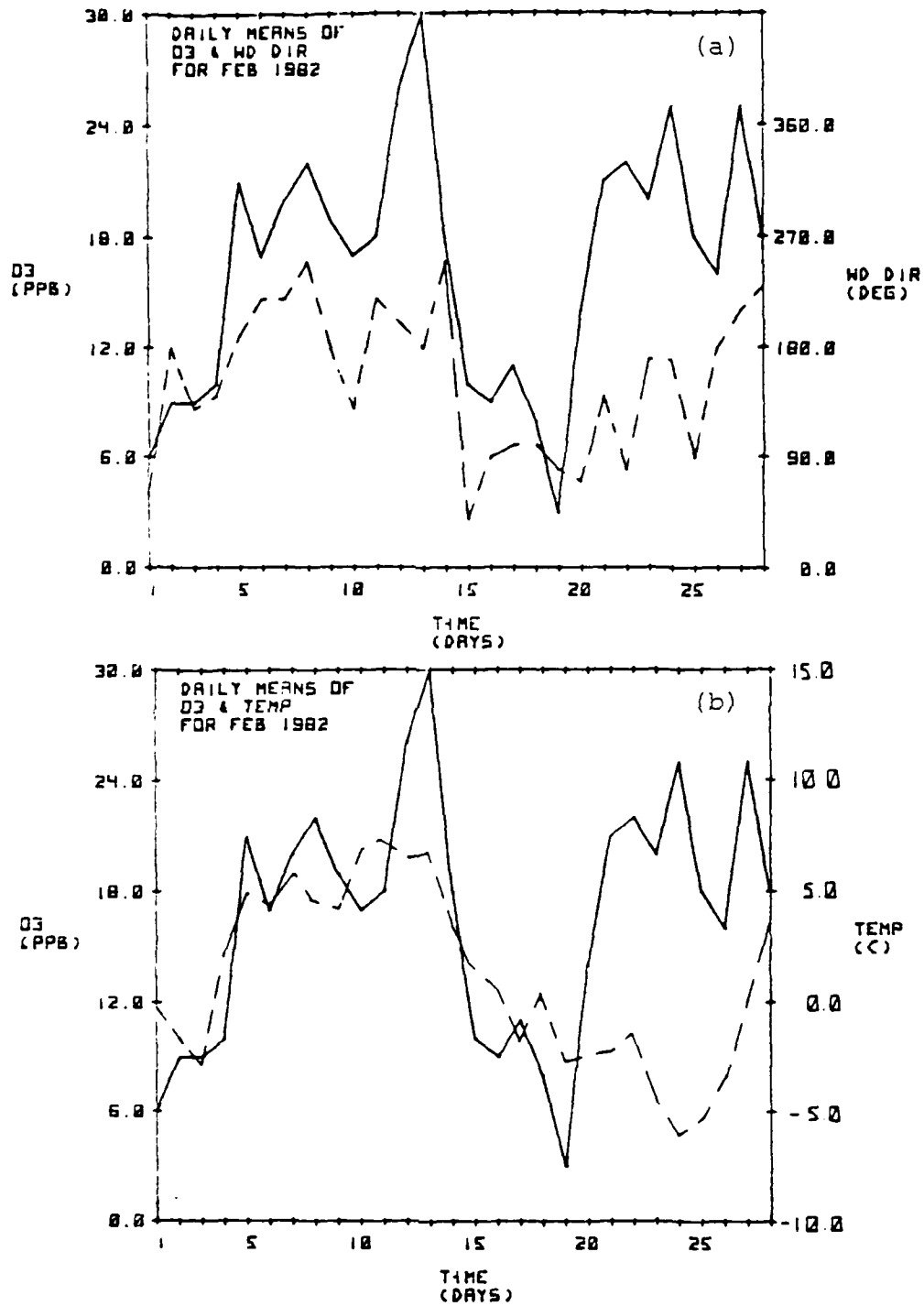


Figure 35 February versus the daily means of O<sub>3</sub> (solid line) and (a) Wind Direction and (b) Temperature. Wind Direction and Temperature are represented by dashed lines.

month passed south of Deuselbach and was responsible for warm advection into the region. The high which was dominant at the end of the month was centered over Scandanavia and responsible for cold advection.

### 3. March (Figure 36)

The  $O_3$  levels remained fairly constant during the first 3 weeks of March as a series of 9 frontal passages dominated the synoptic situation. Precipitation occurred on 16 of the first 20 days of the month. It was not until the 22nd-23rd, when high pressure moved into the region and established itself over the North Sea, that  $O_3$  levels climbed. Once more, the climb (under high pressure) was preceded by an E wind (Figure 36a). Temperature showed a similar tendency (Figure 36b). The predominantly cloudy skies which prevailed during the first 3 weeks, gave way to clear skies and the anticipated temperature rise was achieved.

This particular period of clear skies will receive further attention later in the analysis of the PSS for clear skies.

### 4. April (Figure 37)

It should be pointed out that with the advent of spring, the overall monthly level of  $O_3$  increased since January. As discussed previously, the winter time stratification ended and was replaced by a more convective

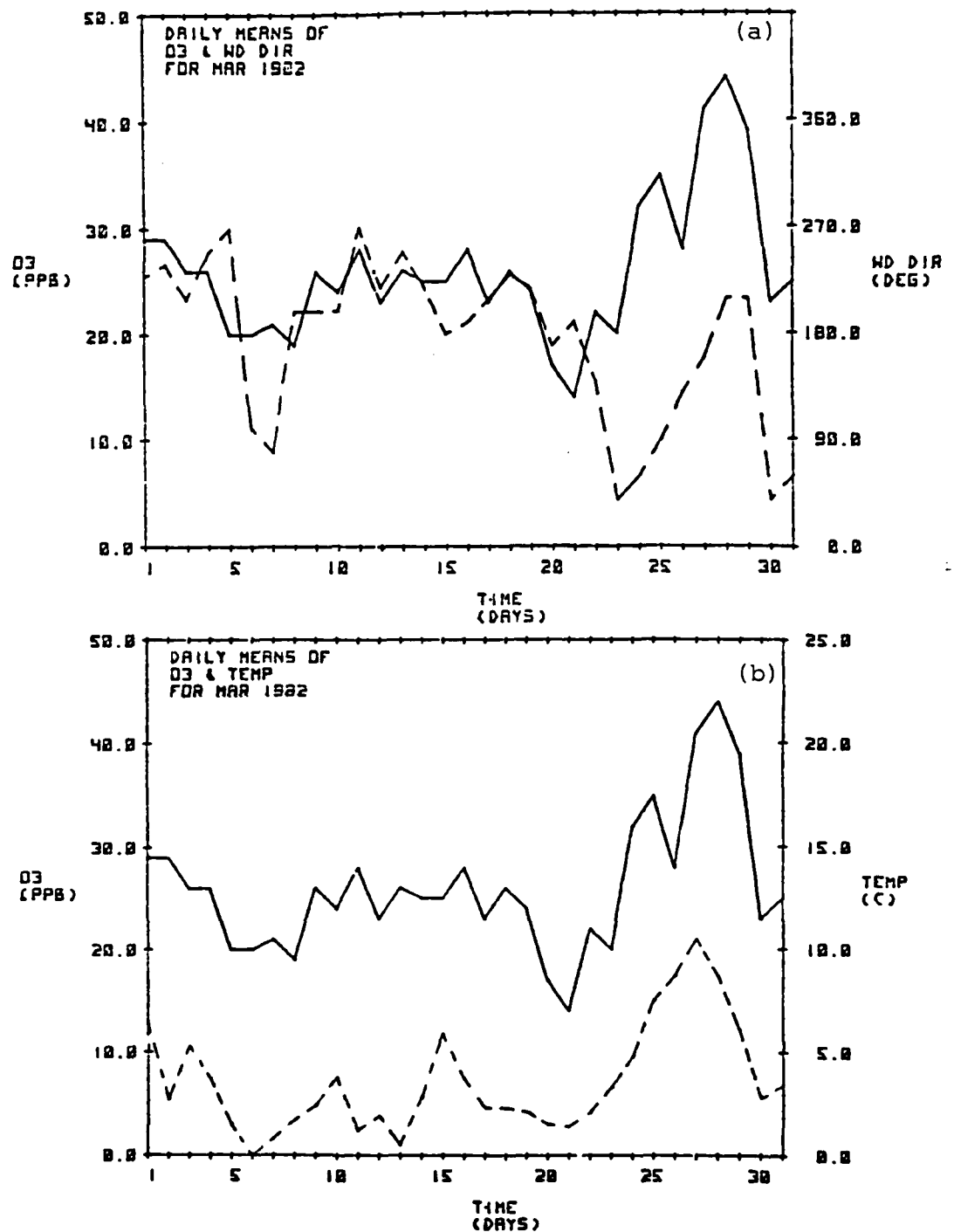


Figure 36 March versus the daily means of O<sub>3</sub> (solid line) and (a) Wind Direction and (b) Temperature. Wind Direction and Temperature are represented by dashed lines.

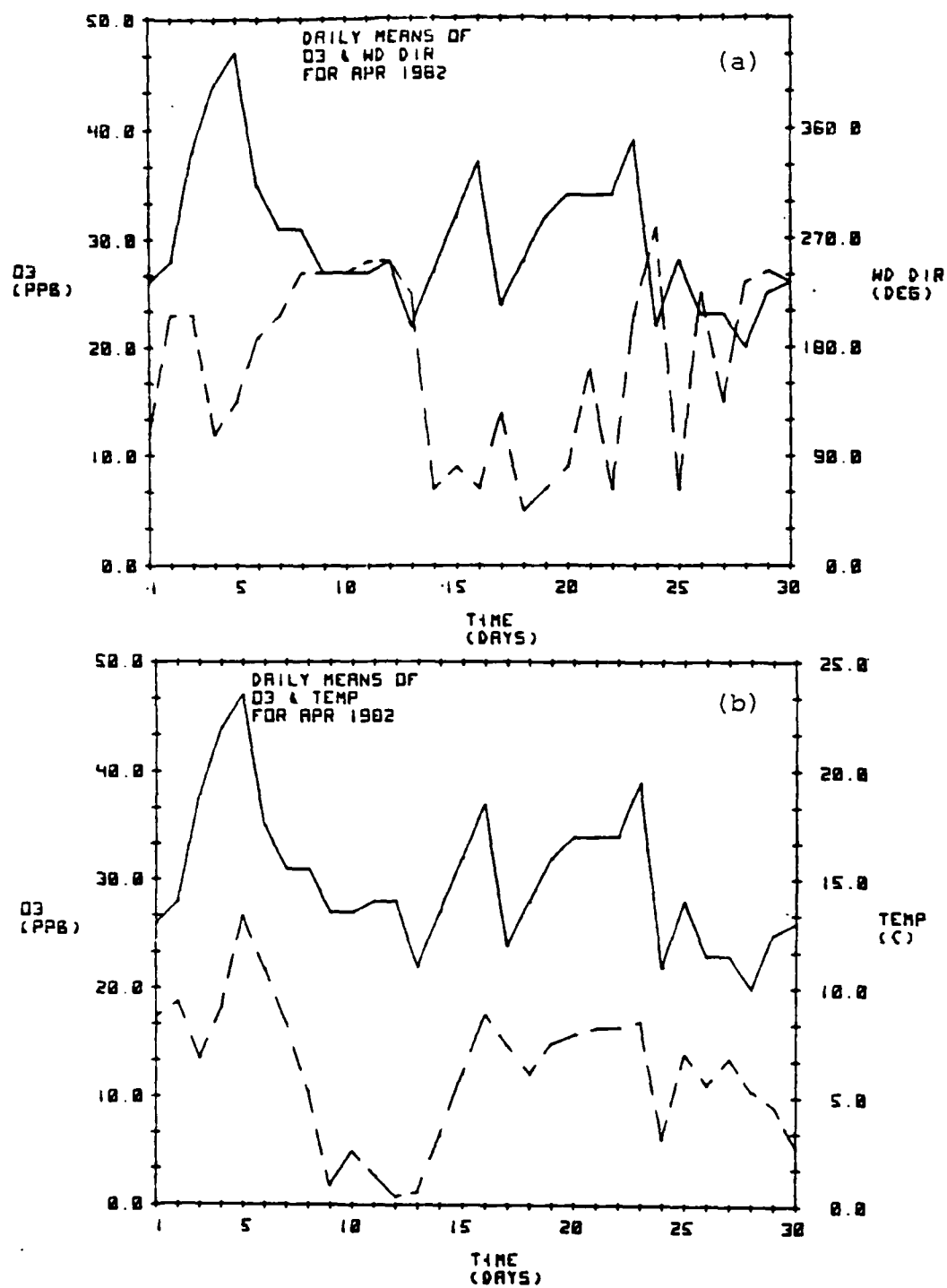


Figure 37 April versus the daily means of O<sub>3</sub> (solid line) and (a) Wind Direction and (b) Temperature. Wind Direction and Temperature are represented by dashed lines.

atmosphere. Periods of high  $O_3$  levels (2nd, 7th and 13th-22nd) occurred under high pressure. The wind direction during all periods of elevated  $O_3$  levels had an E component (Figure 37a), indicating the advection of  $O_3$  precursors. Temperature correlation (Figure 37b) with  $O_3$  continued to be positive ( $r = 0.64$ ), particularly under conditions of high pressure. High pressure ridges began influencing the area on the 3rd, 13th, and 24th, with each case showing temperature maximums shortly after each of these days.

#### 5. May (Figure 38)

The first 10 days show consistently low  $O_3$  levels as frontal systems and the associated cloud cover dominated. The noticeable peak around the 15th was preceded by the onset of a high pressure system which became firmly entrenched over the North Sea by the 11th.  $O_3$  precursors also had a chance to build up in the area, as the wind made a sharp change from the NW to the E (Figure 38a). This particular episode will also receive further attention in the PSS analysis for clear skies. There is a great potential to generate more photochemical  $O_3$  in Central Europe if the region had more cloud-free days (hence more UV radiation).

The strong positive correlation with temperature (Figure 38b) during May was remarkable ( $r = 0.83$ ).



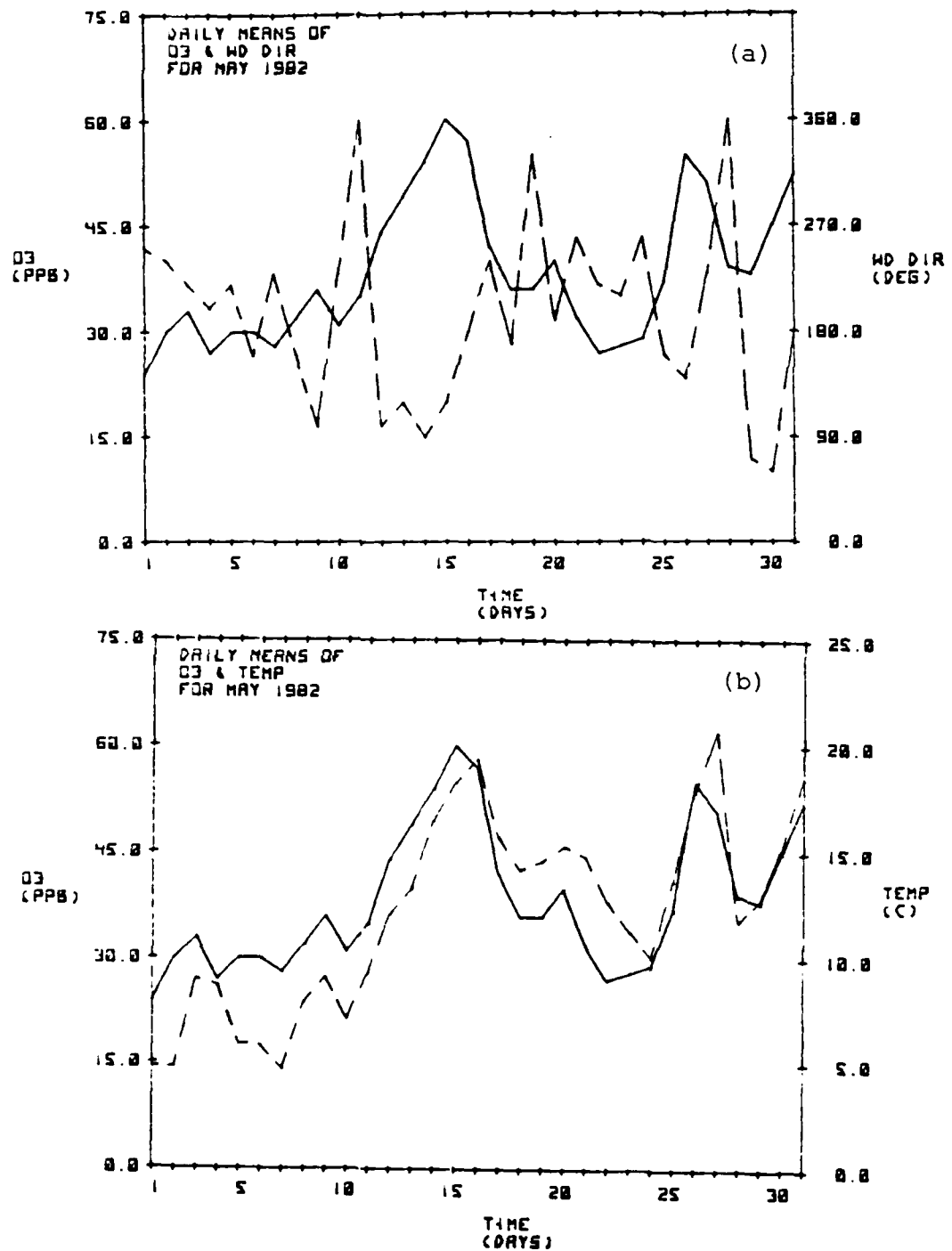


Figure 38 May versus the daily means of O<sub>3</sub> (solid line) and (a) Wind Direction and (b) Temperature. Wind Direction and Temperature are represented by dashed lines.

#### 6. August (Figure 39)

It should be noted that the average monthly  $O_3$  level for August was approximately three times the average monthly  $O_3$  level from January and February. The increased convective activity of summer can bring upper tropospheric  $O_3$  to the surface.  $NO_x$  levels are substantially less than  $O_3$  in August than in January or February. This condition does not permit  $O_3$  to titrate out as it so easily does in January or February. Additionally, the covariance from January to August gets weaker and changes sign from negative to positive. The increased duration and intensity of photochemical  $O_3$  producing episodes also contributed to this overall trend. Synoptically no one particular air mass dominated for any length of time, rather, there were a series of weak highs and fronts alternating for most of August. A weak high pressure system was in the area at the beginning of the month, when E winds and peak concentrations of  $O_3$  were found (Figure 39a). The peak on the 12th also occurred when a weak high pressure system was present, despite the absence of an E wind. It is possible in this case that sufficient  $O_3$  precursors had been able to build up during the period from 6-9th when the wind was from the E, creating an opportunity for the photochemical generation of  $O_3$ .

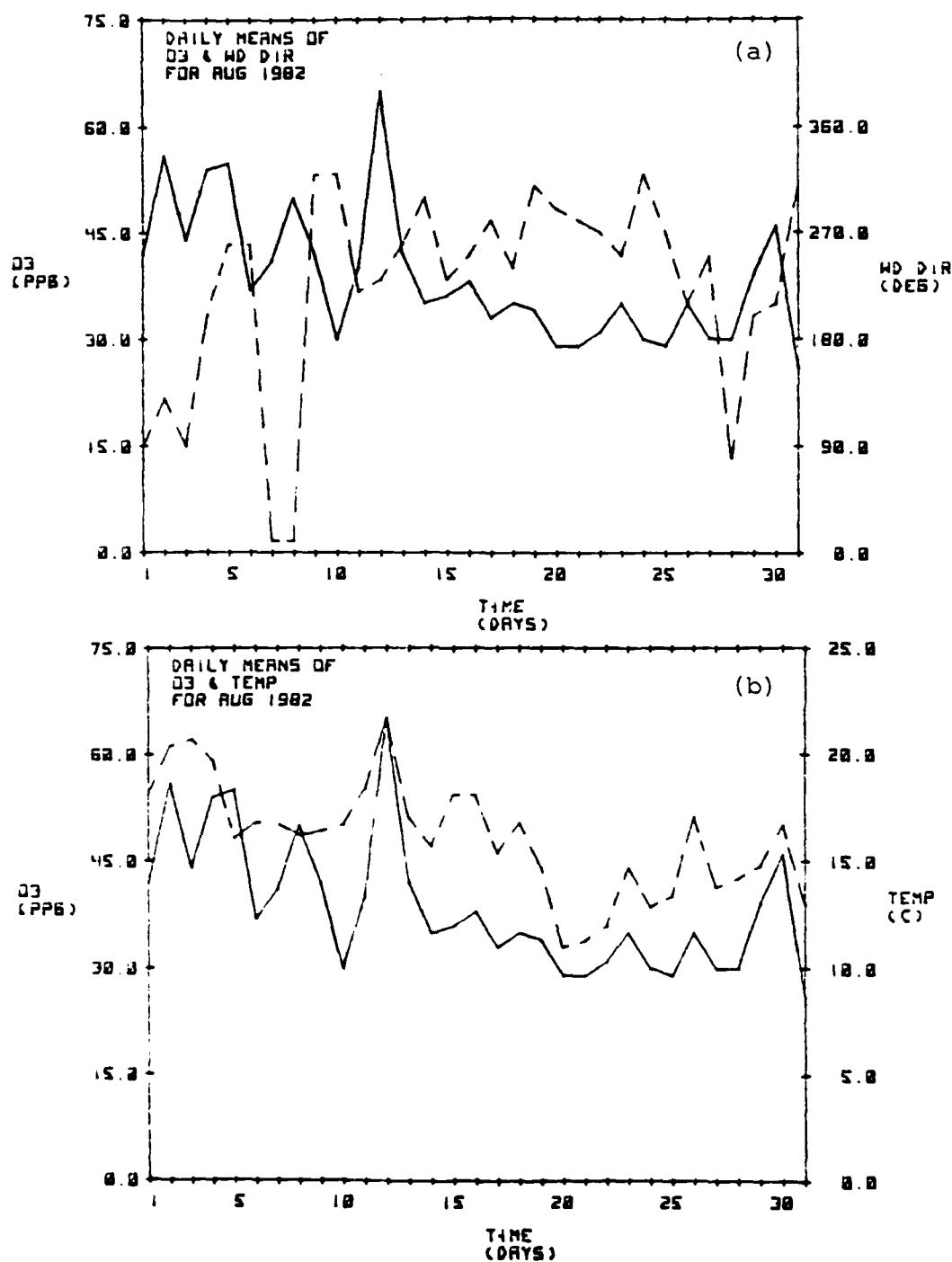


Figure 39 August versus the daily means of O<sub>3</sub> (solid line) and (a) Wind Direction and (b) Temperature. Wind Direction and Temperature are represented by dashed lines.

Temperature and  $O_3$  (Figure 39b) continued their strong positive correlation ( $r = 0.76$ ), except during the period 3rd-10th, when extensive cloud cover and occasionally heavy precipitation reduced the amount of solar radiation received at the surface.

#### D. Carbon Dioxide

The parameter with the highest correlation to  $CO_2$  is dust. Correlation with other parameters varied greatly from month to month. The principle source of  $CO_2$  in Germany is fossil fuel combustion, (i.e., anthropogenic source) and not from vegetation exhalation (Crutzen, 1983). This places a large amount of soot (or dust) into the atmosphere, so it is reasonable to expect a correlation between  $CO_2$  and dust.

##### 1. January, February, March (Figures 40-41a)

All three months showed a strong positive correlation between  $CO_2$  and dust ( $r = 0.59, 0.78, 0.74$  respectively), since the stratified winter atmosphere and associated low mixing heights tended to keep all combustion products within the lower layers. However, the strong positive correlation exhibited thus far does begin to show signs of reversing itself by late March.

##### 2. April, May (Figures 41b-42a)

The strong convective nature of the springtime atmosphere with its overturning tendencies mixed the lower

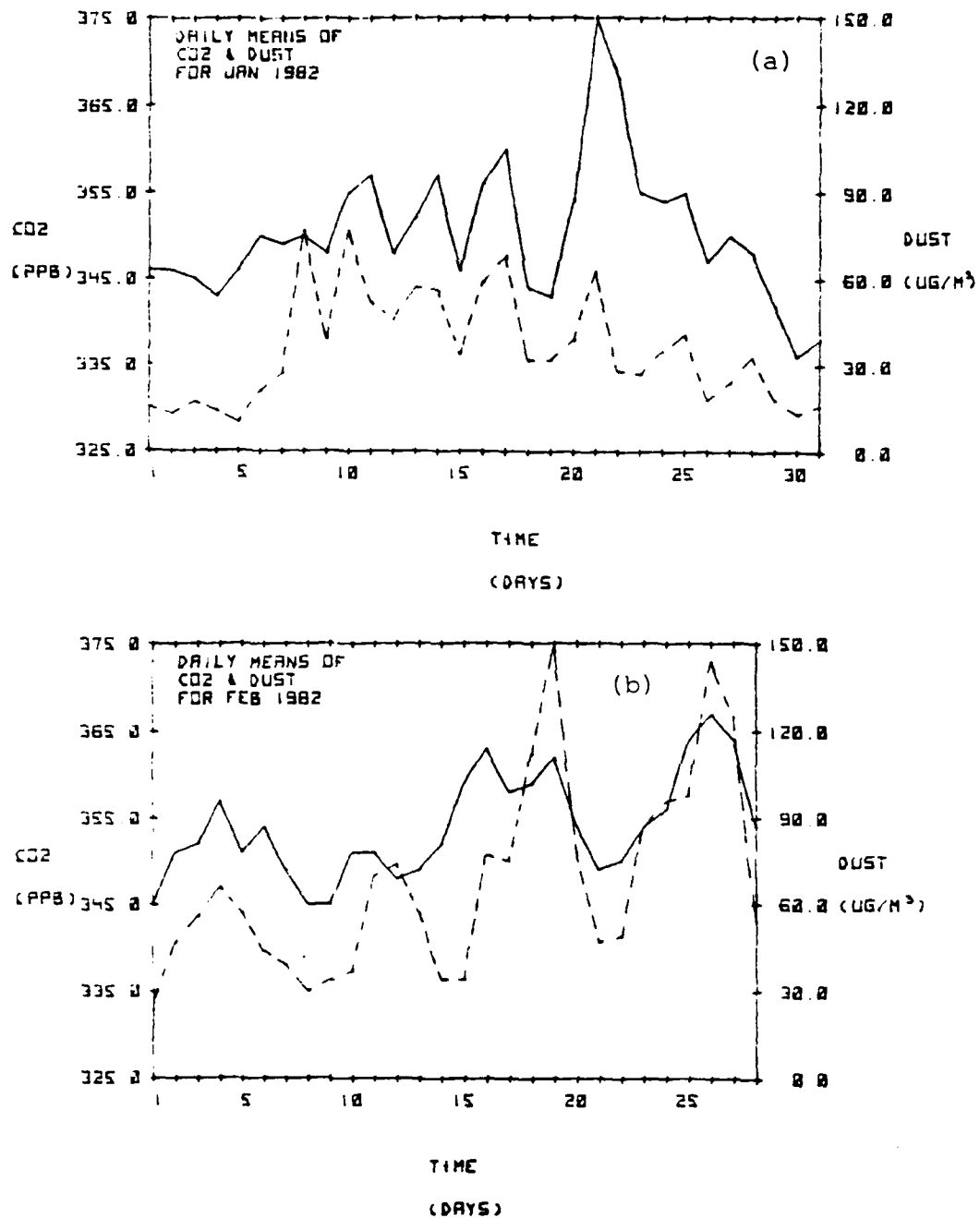


Figure 40 (a) January and (b) February versus the daily means of CO<sub>2</sub> (solid line) and Dust (dashed line).

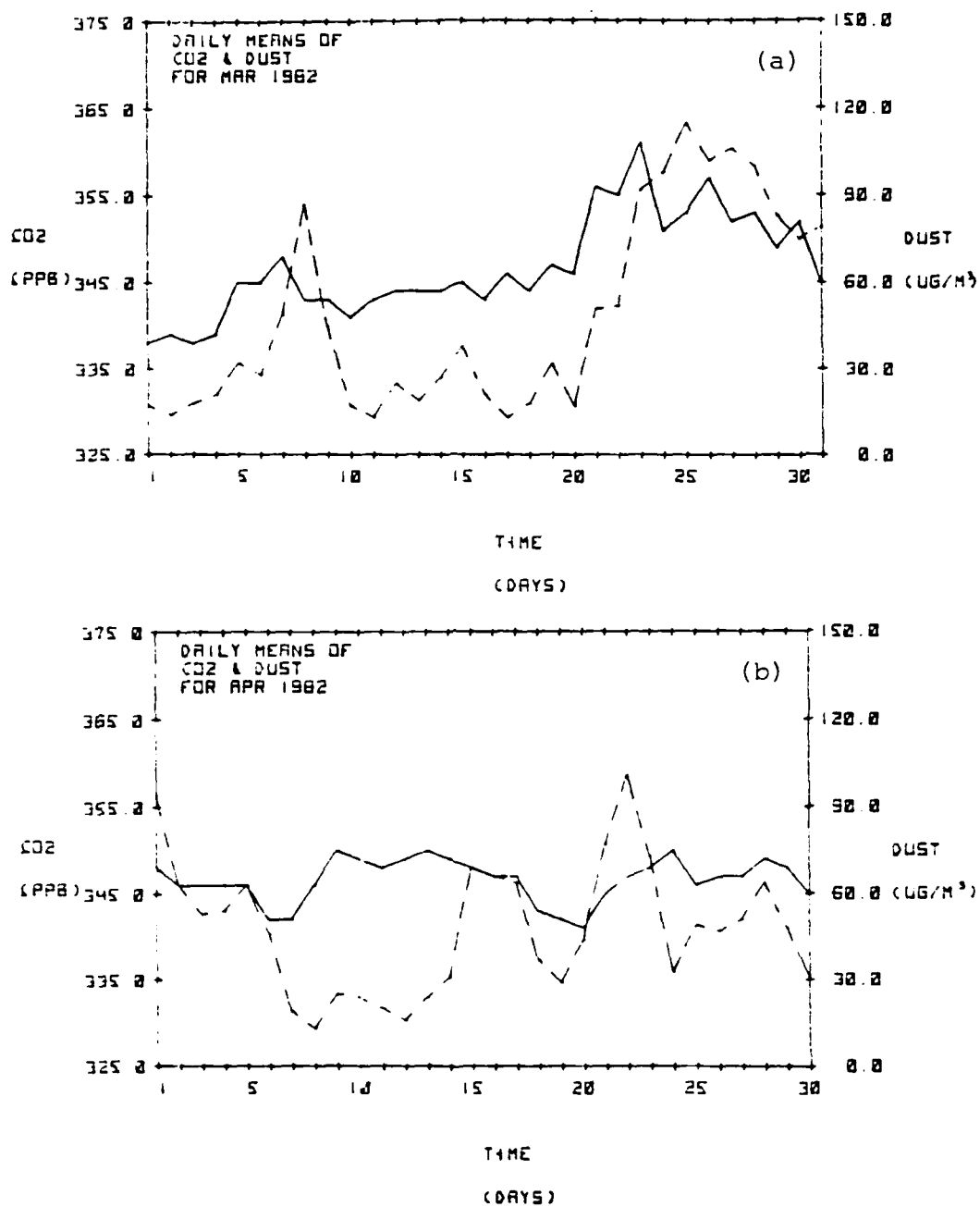


Figure 41 (a) March and (b) April versus the daily means of CO<sub>2</sub> (solid line) and Dust (dashed line).

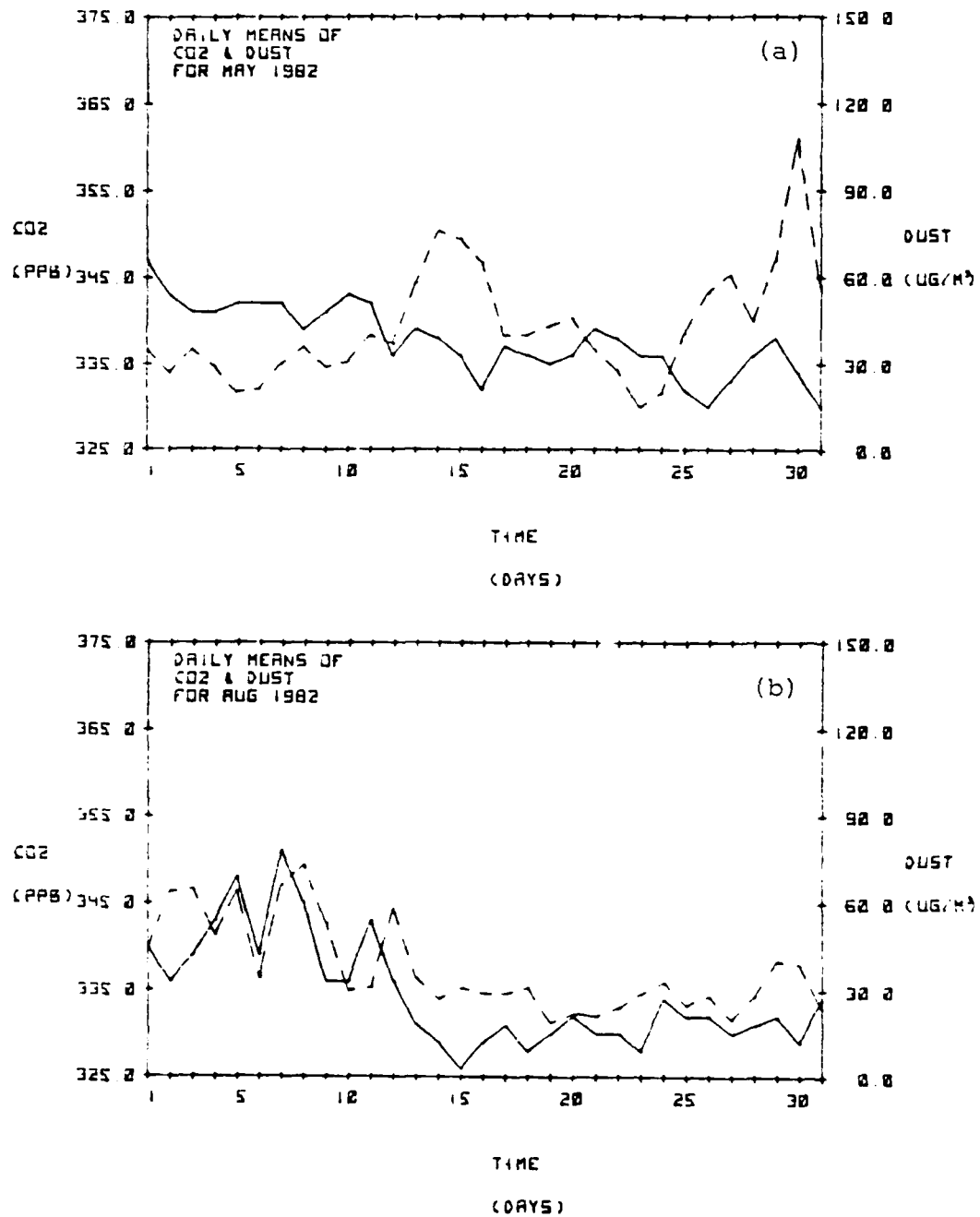


Figure 42 (a) May and (b) August versus the daily means of CO<sub>2</sub> (solid line) and Dust (dashed line).

layers. This disrupted the strong positive correlation, established over the three previous months, between CO<sub>2</sub> and dust. This is reflected in the April and May correlation coefficients ( $r = +0.27$  and  $-0.48$  respectively).

### 3. August (Figure 42b)

The strong positive correlation of the first three months returned ( $r = 0.74$ ). One possible explanation for this could be that the series of weak high pressure systems throughout the month kept the CO<sub>2</sub> trapped in the lower layers by means of temperature inversions.

### E. Photostationary State

As previously stated (SECTION II B) the photostationary state (PSS) involves reactions between nitric oxide (NO), nitrogen dioxide (NO<sub>2</sub>) and ozone (O<sub>3</sub>) in the presence of UV radiation and was defined earlier in this paper by expression (4) as

$$P = j(\text{NO}_2) [\text{NO}_2] / k_3 [\text{O}_3][\text{NO}]$$

P represents the PSS and has an anticipated value of unity. UV radiation at Deuselbach was monitored with an Eppley UV photometer. The PSS equation will be treated with respect to two periods dominated by clear skies : 24-27 March and 11-13 May 1982. The 24-27 March episode was an especially "dirty one", with large concentrations



of  $\text{NO}_2$  present particularly on the 26th. The PSS equation will also be treated with respect to four periods dominated by cloudy skies: 26-27 January, 20-21 March, 1 and 4 May, and 20 and 24 August 1982. All the data used in the analyses of all these episodes are located in Appendix C.

#### 1. Clear Skies (Figures 43-46)

Due to its rural location and name "clean air station", it can be assumed that the Deuselbach area should have relatively clean air. If the PSS assumption holds true then there should be no deviation of  $P$  from unity. However, since  $P$  does deviate significantly, as evidenced by Figures 43a-46a, the PSS assumption is not valid at Deuselbach. Similar discrepancies in the PSS have been found by Ritter et al., (1979), Kelly et al., (1980) and Shetter et al., (1983). With the exception of the PSS curve of 24 March, all other curves show a fairly uniform departure from unity with values generally ranging from about 1 to 3. All curves showed a steady increase in values and generally peaked between the hours of 1300-1500. This peak corresponds with the time of day when the maximum temperature is reached (i.e., a few hours after the maximum sunlight). This suggests both a temperature dependence of the PSS and a photochemical cause fueled by the process represented in Figures 43b-46b.

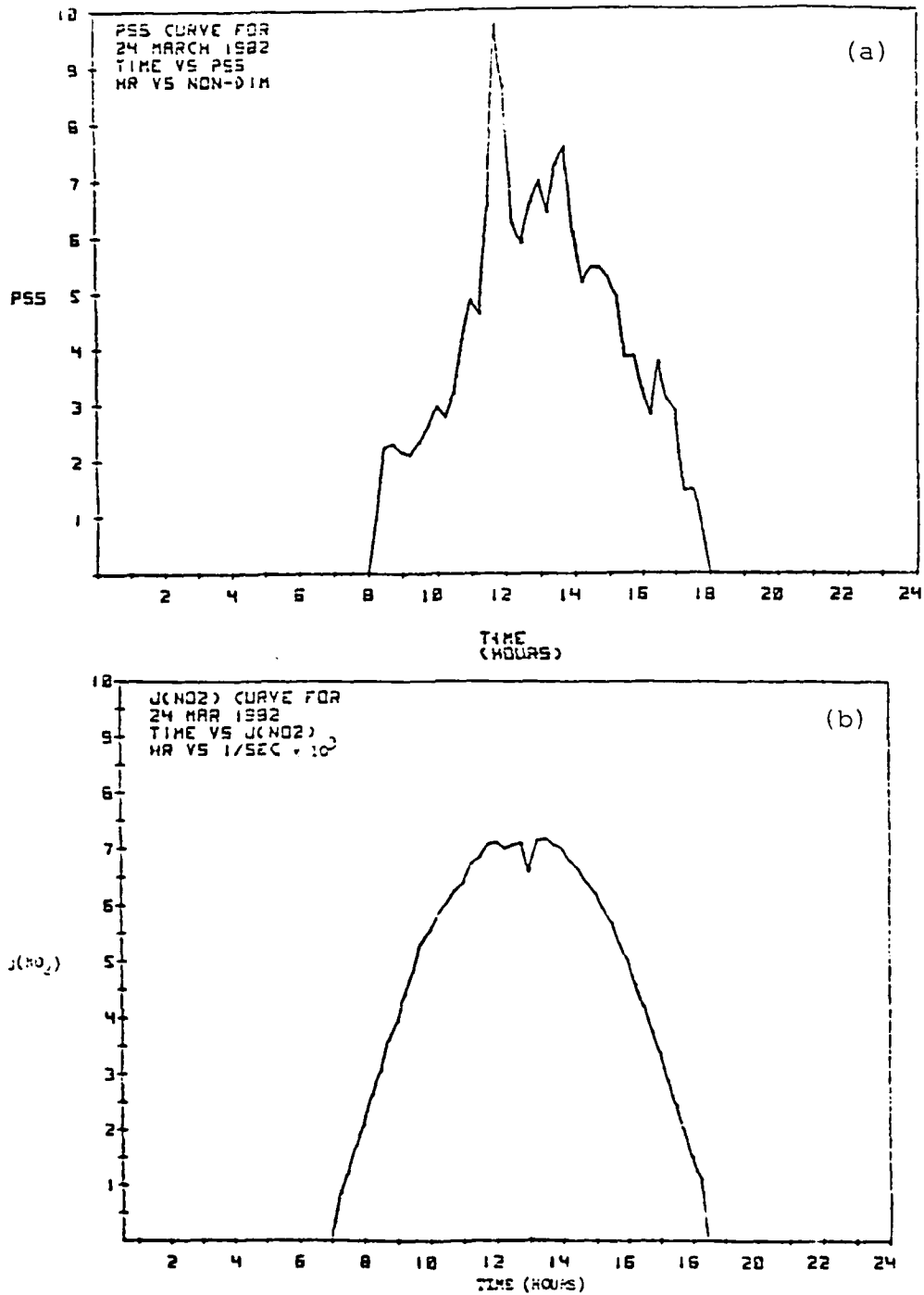


Figure 43 Daily values of (a) P and (b)  $j(\text{NO}_2)$  for clear skies on March 24, 1982.

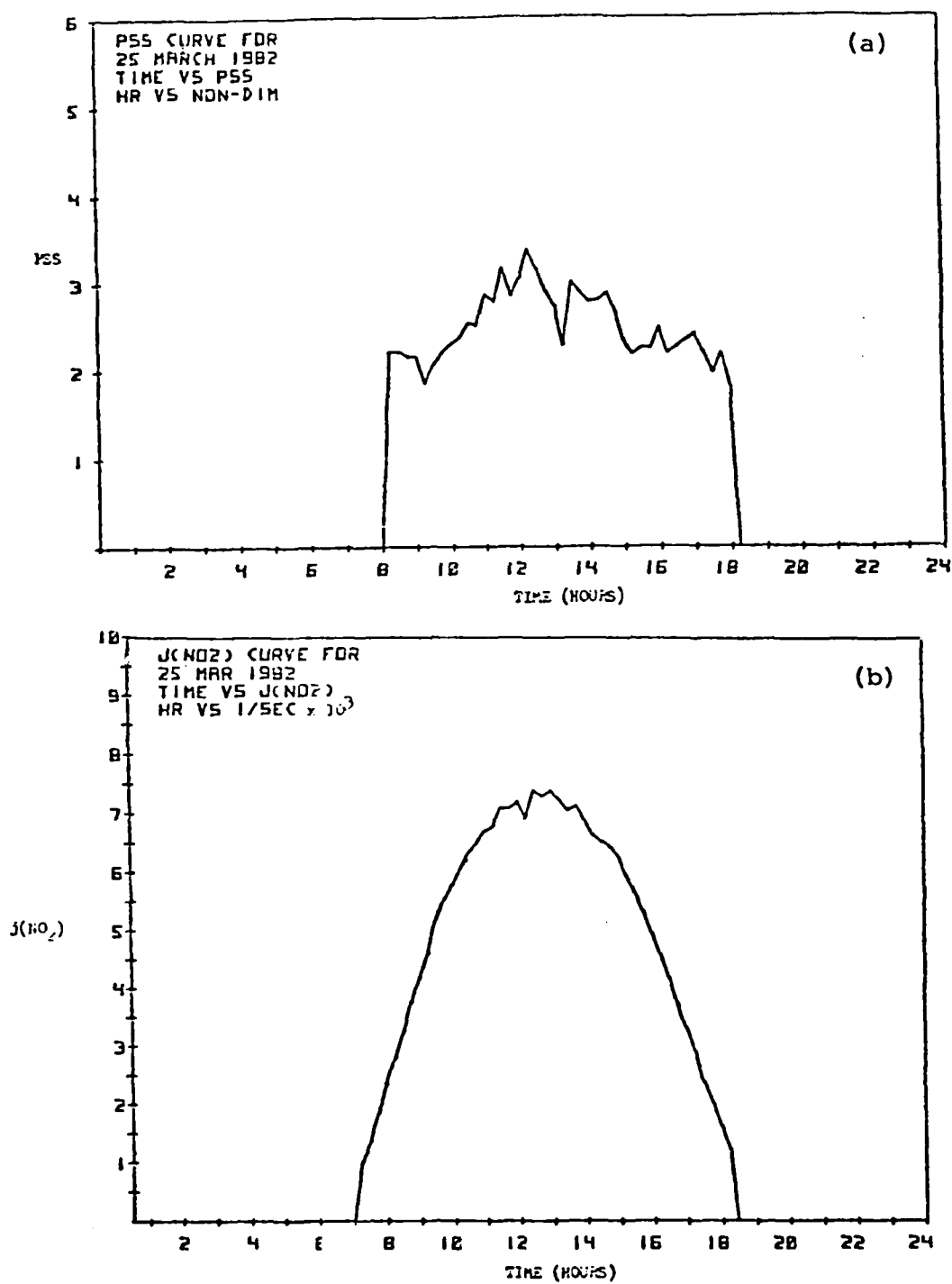


Figure 44 Daily values of (a) P and (b)  $j(\text{NO}_2)$  for clear skies on March 25, 1982.

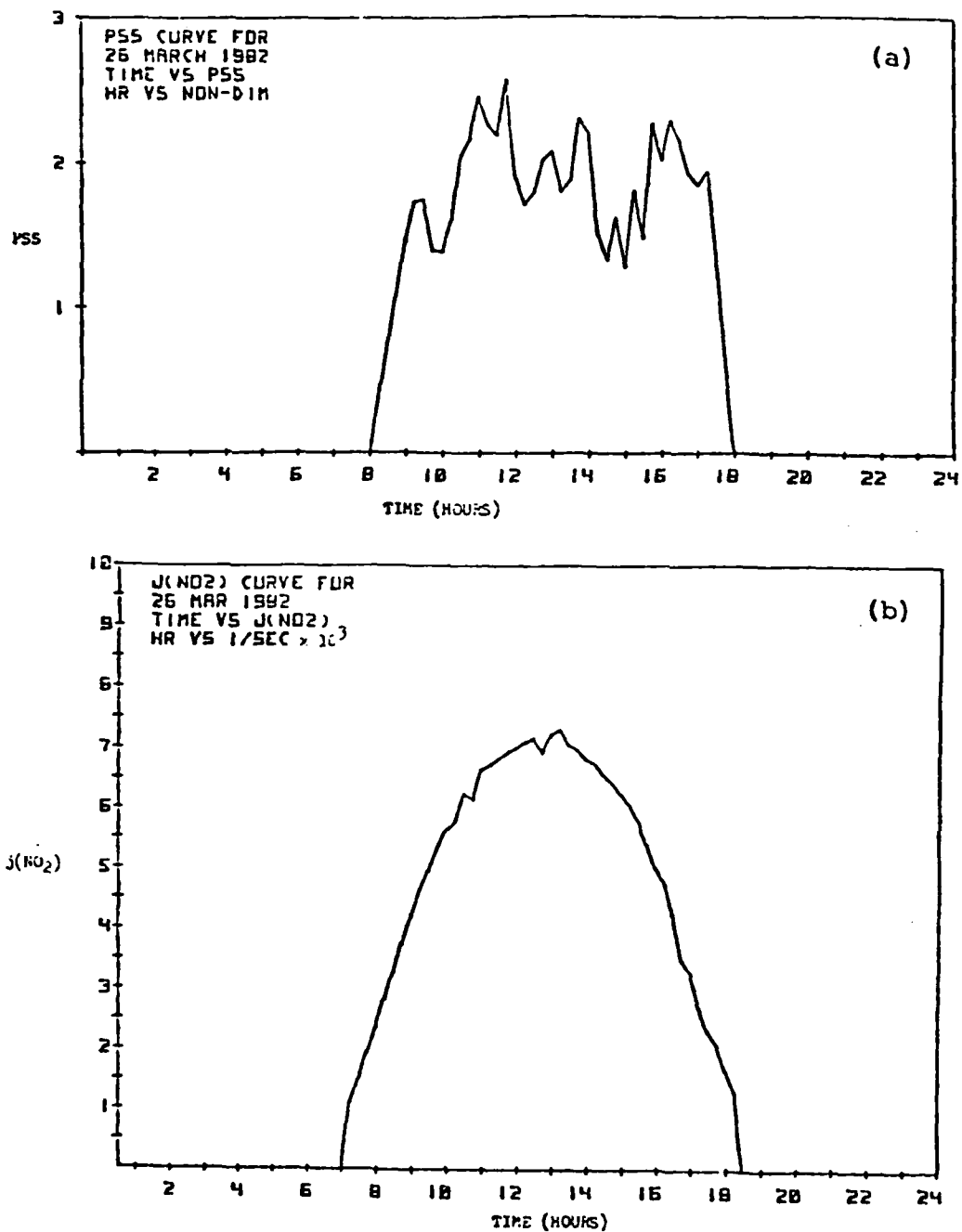


Figure 45 Daily values of (a) P and (b)  $j(\text{NO}_2)$  for clear skies on March 26, 1982.

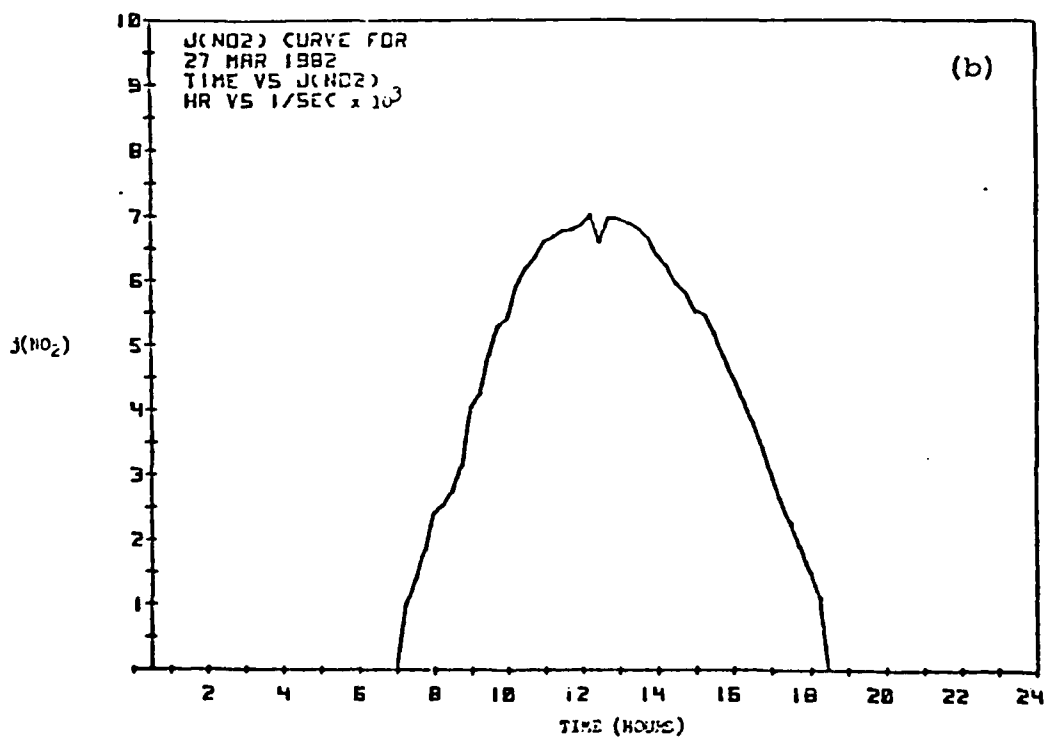
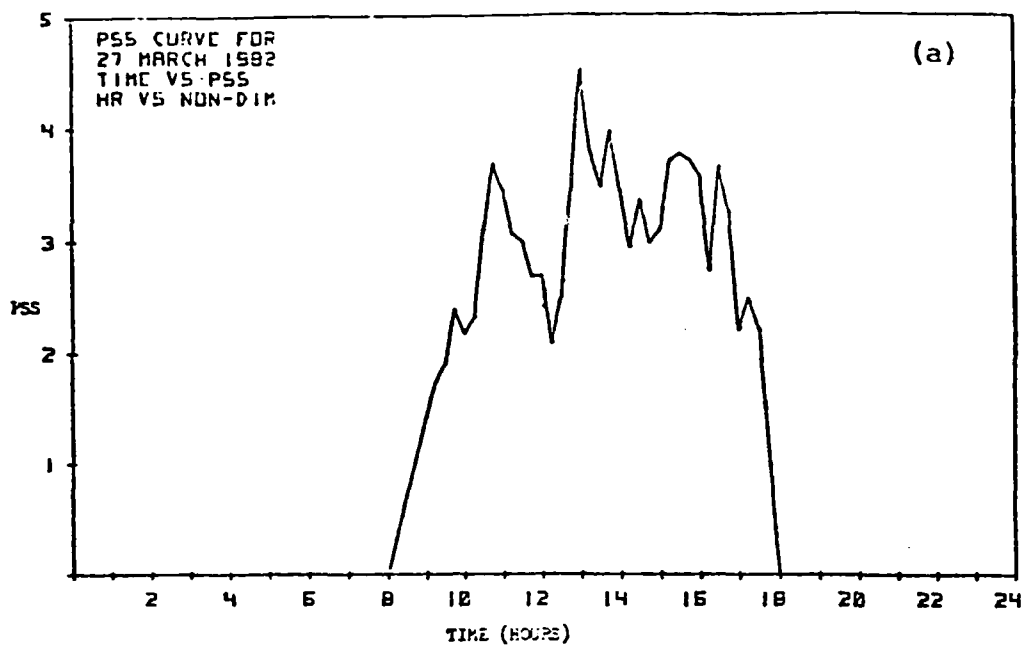


Figure 46 Daily values of (a) P and (b)  $j(\text{NO}_2)$  for clear skies on March 27, 1982.

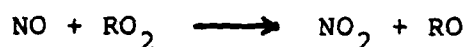
These figures show the photolysis rate of  $\text{NO}_2$  or  $j(\text{NO}_2)$ , which is a function of incoming UV radiation. The bell curve shape of these figures results from the dependence of  $j(\text{NO}_2)$  on solar radiation. The Eppley radiometer, used to gather these data, was calibrated with direct measurements of  $j(\text{NO}_2)$  (Harvey et al., 1977; Dickerson et al., 1982).

The remainder of the figures used in the analysis of clear sky conditions are located in Appendix D.

In all these studies, the  $j(\text{NO}_2)$  curves clearly indicate which periods of the day had cloud cover, by displaying "V-notches" when cloud cover reduced the amount of UV radiation reaching the site. Days with extensive cloud cover will be dealt with later in this section.

The failure of the PSS, particularly as it approaches mid-day, seemed to stem from an apparent interference with the  $\text{NO}_2$  level. Since no interferences in the measurements of  $\text{O}_3$  and  $\text{NO}$  were known, which could have accounted for the high PSS values, the deviation must have been from variations in  $\text{NO}_2$  concentrations. The failure of the PSS equation with respect to high PSS values are probably the result of some species competing with  $\text{O}_3$  in the oxidation of  $\text{NO}$  to  $\text{NO}_2$  (Levy, 1973; O'Brian, 1974; Ritter et al., 1979; Kelly et al., 1980; and Shetter et al., 1983). Such a species would have to react quickly

with NO in order to compete with  $O_3$ . It should also have a source which is light intensity dependent, to account for the shape exhibited by the PSS values throughout the day. A possible explanation lies in the previously mentioned reaction (R11).



$RO_2$  is any organic peroxy radical or  $HO_2$  radical, which converts NO to  $NO_2$  without consuming  $O_3$ . The presence of PAN and organic nitrates could also result in a deviation from the PSS.

The presence of these radicals could lead to larger amounts of tropospheric  $O_3$  than can be accounted for by known tropospheric  $O_3$  destruction mechanisms. If the reaction involving peroxy radicals is the only process causing high PSS values, then an  $RO_2$  concentration between  $3.0$  and  $3.5 \times 10^9/cm$  would be required (Kelly et al., 1980; Shetter et al., 1983). Bottenheim and Strausz (1979) predicted that the PSS equation will not be valid in clean air because of the presence of peroxy radicals at model predicted concentrations of  $10^8$  to  $10^9/cm^3$ . Additionally, if  $O_3$ ,  $HNO_3$  or organic nitrates are present, they can interfere with  $NO_2$  concentrations. This would also result in artificially high values of P.

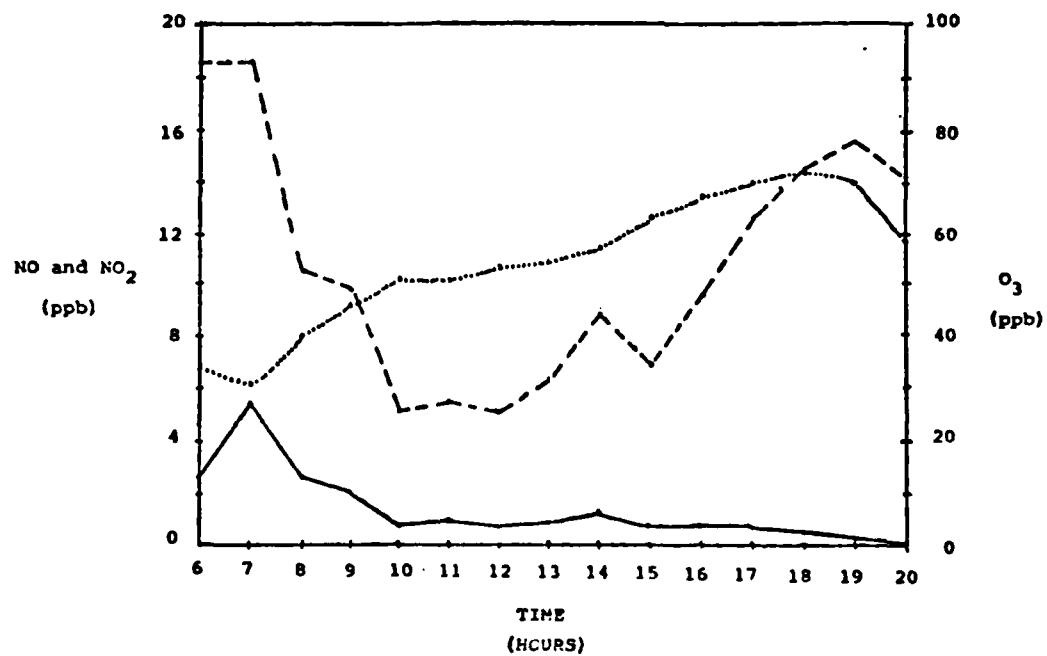


Figure 47 Daily values of NO (solid line), NO<sub>2</sub> (dashed line), and O<sub>3</sub> (dotted line) under clear skies on May 13, 1982.



Figure 47, is illustrative of this "tampering" with the PSS. Photochemical processes began with the introduction of UV radiation. The first few hours showed an increase in NO and NO<sub>2</sub> levels. Then NO was consumed and NO<sub>2</sub> was photolyzed, driving both levels down. Simultaneously, O<sub>3</sub> generation was taking place. Eventually, NO<sub>2</sub> levels also began to rise. Increasing amounts of both O<sub>3</sub> and NO<sub>2</sub> support the concept of a competing species. The production of both O<sub>3</sub> and NO<sub>2</sub> also began decreasing near sunset, further supporting a photochemical argument. Although transport remains the more dominant factor in affecting NO<sub>x</sub> concentrations, photochemical reactions are still a definite contributing factor in the concentration of these levels.

One final comment on the subject of high PSS values comes from the works of Zimmerman (1977), Tingey et al., (1978) and Kelly et al., (1980) and is at best, speculative on my part. Pine forests are an excellent emitting source of reactive terpene hydrocarbons whose emission rate is known to correlate with temperature. Since Deuselbach is located in a region with extensive tracts of pine forests, it is possible that the interactions among NO, NO<sub>2</sub>, O<sub>3</sub> and these terpene hydrocarbons and their products during the warmest part of the day help maintain the high PSS values.

## 2. Cloudy Skies (Figures 48-51)

Under cloudy skies, the PSS curves also showed a fairly uniform departure from unity. However, values of  $P$  deviated only slightly from unity with daily means varying from 0.6 to 1.4 during the 8 days that were examined. Generally, the peak values occurred between the hours of 1200-1500, which was similar to clear sky conditions. Still, the effect of extensive cloud cover on  $P$  values was quite evident. Under overcast skies, such as on 26-27 January (Figures 48-49), the  $P$  values remained near unity throughout the day. However, with occasional breaks in the overcast  $P$  values showed almost immediate increases, such as on 1 May and 24 August (Figures 50-51). The values then decreased with the onset of increased cloud cover, hence decreased solar radiation reaching the surface.

The average daily value of  $P$  taken over the 8 cloudy days was almost unity ( $P = 1.1$ ). The amount of solar radiation received at the surface is inversely proportional to the amount of cloud cover that is present. Since solar radiation is the "triggering mechanism" for photochemistry, it therefore appears to substantiate the argument that the PSS will generally hold true under cloudy skies.

The remainder of the figures used in the analysis of cloudy sky conditions is located in Appendix D.

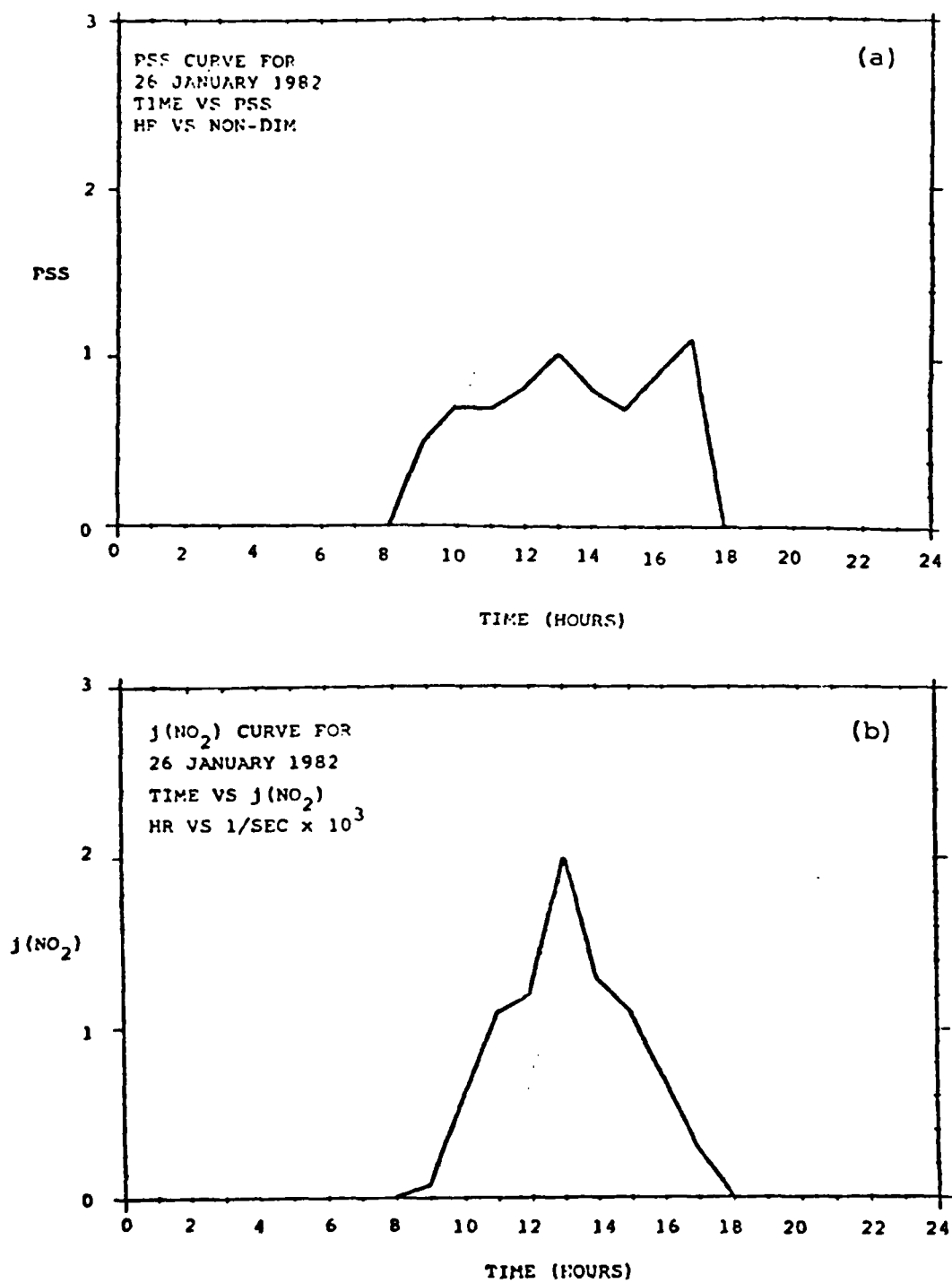


Figure 48 Daily values of (a) P and (b)  $j(\text{NO}_2)$  for cloudy skies on January 26, 1982.

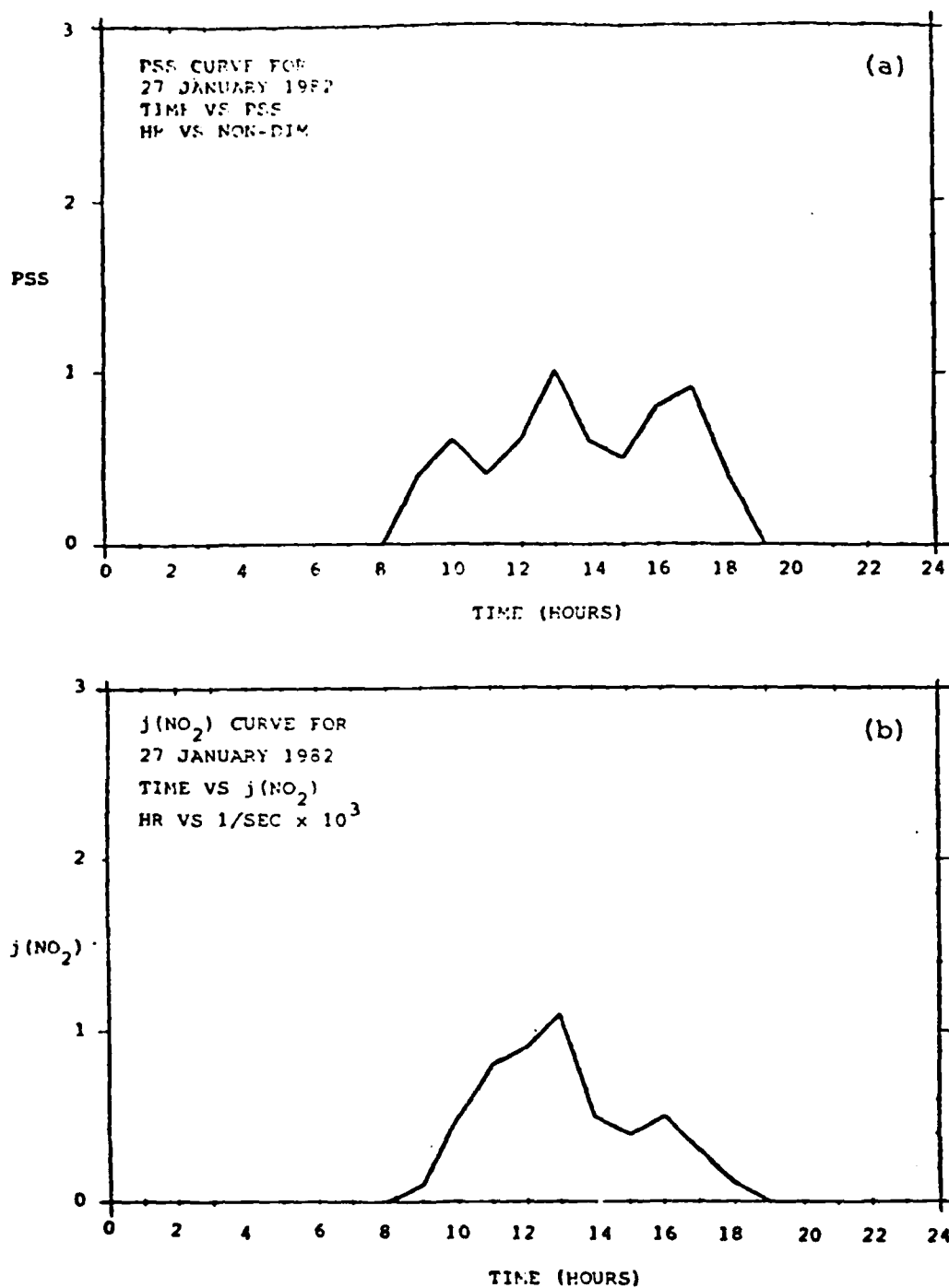


Figure 49 Daily values of (a) P and (b)  $j(\text{NO}_2)$  for cloudy skies on January 27, 1982.

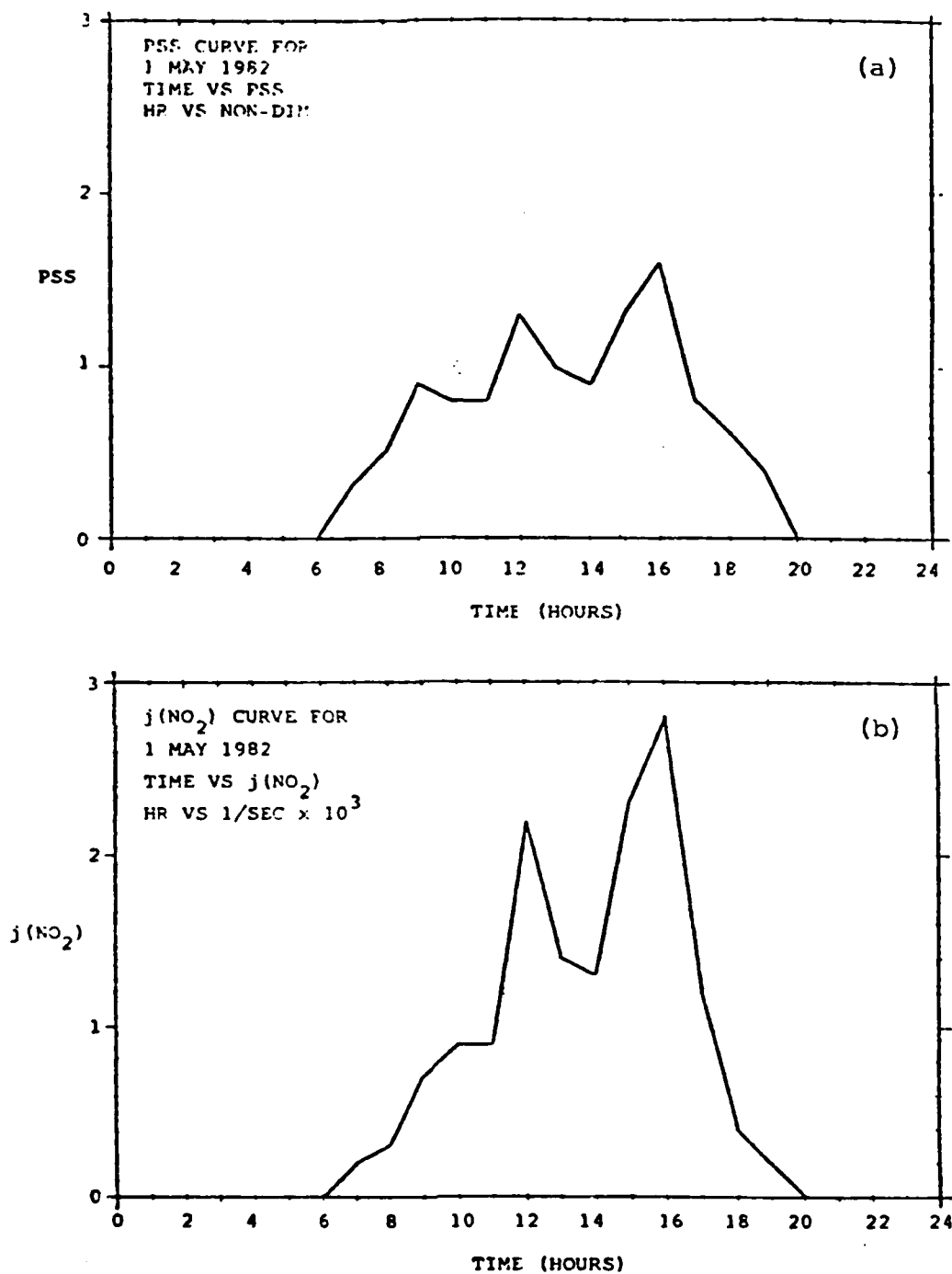


Figure 50 Daily values of (a) P and (b)  $j(\text{NO}_2)$  for cloudy skies on May 1, 1982.

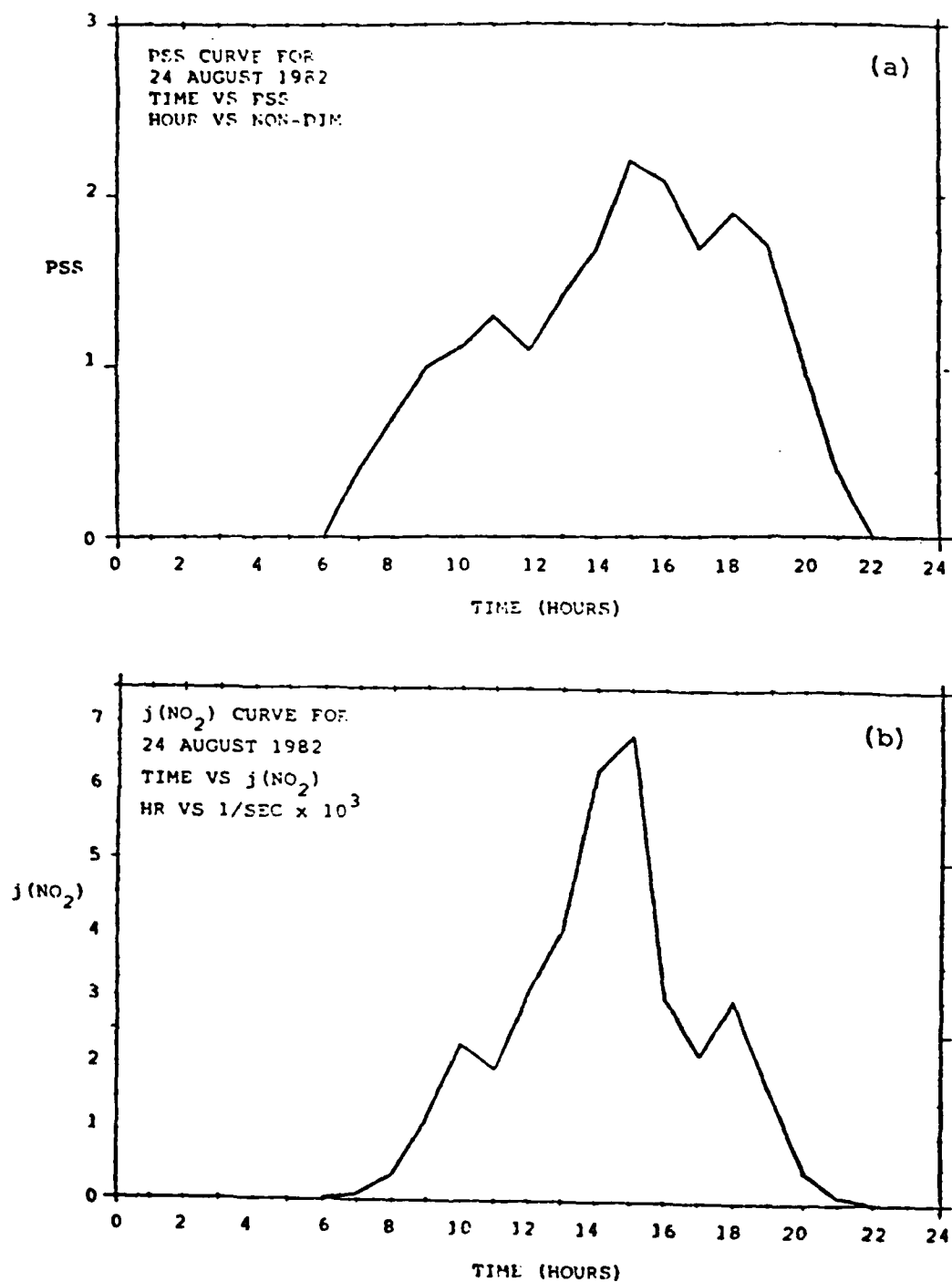


Figure 51 Daily values of (a) P and (b)  $j(\text{NO}_2)$  for cloudy skies on August 24, 1982.

## SECTION V

### CONCLUSIONS

Meteorology does influence air pollution in varying degrees through several means: wind direction and speed, temperature, precipitation, relative humidity, insolation, mixing height, and atmospheric pressure.

The prevailing wind direction at Deuselbach is from the SW. However, pollutant levels are significantly increased only when NE-SE winds are recorded.

Although the dry deposition rate is greater than the wet deposition rate for both  $\text{NO}_2$  and  $\text{SO}_2$  (Rodhe et al., 1981), the effect of wet deposition is quite dramatic on  $\text{SO}_2$  and much less noticeable on  $\text{NO}_2$ .  $\text{SO}_2$  showed a marked decrease in the presence of precipitation while  $\text{NO}_2$  failed to show any consistent behavior with respect to precipitation.  $\text{NO}_2$  rose during some periods of precipitation and fell during others. Although this supports  $\text{SO}_2$  solubility and  $\text{NO}_2$  non-solubility, the inconsistent behavior of  $\text{NO}_2$  in the presence of precipitation requires explanation.  $\text{NO}_2$  reacts with OH to form  $\text{HNO}_3$ , which is very soluble and easily precipitated out. This reaction may be responsible for the reduction of  $\text{NO}_2$  levels during precipitation.  $\text{NO}_2$  adhering to suspended particulates, which are also easily precipitated out, is another possibility for reduced  $\text{NO}_2$  in the presence of precipitation.

The  $\text{CO}_2$  analysis showed that recorded levels of  $\text{CO}_2$  were due to anthropogenic sources and not vegetation exhalation since  $\text{CO}_2$  varied even in January when there was little photosynthesis and decay of vegetative matter.

In general, the Saltzman values were found to be equal to seven-tenths of the Chemiluminescent values.

The PSS and  $\text{O}_3$  generation are dependent upon a variety of meteorological factors. The build-up of  $\text{O}_3$  precursors ( $\text{NO}$ ,  $\text{NO}_2$ , hydrocarbons and their products) is dependent on their advection from the NE-SE quadrants. High pressure must supply clear skies, warm temperatures and low wind speeds. The photodissociation of  $\text{NO}_2$  (a key factor in the PSS) is a function of UV radiation, so a near cloudless sky is imperative for  $\text{O}_3$  generation. Inversely, cloudy skies will severely hamper any photochemistry and hence greatly retard  $\text{O}_3$  generation.

The consumption of  $\text{O}_3$  by  $\text{NO}_2$  was seen at Deuselbach. This is typical of an urban-like atmosphere and is atypical for a rural village. It illustrates the effect on a rural location when it is in close proximity to large urban-industrial complexes, such as with Deuselbach in the highly concentrated population and industrial centers of Western Europe.

Episodes of  $\text{O}_3$  of stratospheric origin reaching the surface is believed to have occurred only once during this study. This agrees with others who have noted the infrequency of this type of episodic occurrence.



# APPENDIX A

## SALTZMAN VS CHEMILUMINESCENCE DATA

Table A-1. Concentrations of NO<sub>2</sub> in ppb for the Saltzman and Chemiluminescent Methods for January 23-31, 1982.

	Saltzman	Chemiluminescence
January 23	11.1	16.6
24	11.3	14.4
25	13.0	17.6
26	6.0	8.4
27	10.8	14.0
28	9.8	12.5
29	5.4	6.8
30	3.6	4.8
31	4.8	5.8

Table A-2. Concentrations of NO<sub>2</sub> in ppb for the Saltzman and Chemiluminescent Methods for March 1-31, 1982.

	Saltzman	Chemiluminescence
March 1	3.5	4.4
2	2.8	3.1
3	3.6	3.7
4	3.2	3.5
5	6.8	7.7
6	8.0	8.6
7	6.1	7.6
8	10.3	13.1
9	6.6	8.9
10	5.2	5.5
11	2.8	2.5
12	6.4	6.7
13	3.4	3.2
14	4.3	4.8

Table A-2 (continued)

		Saltzman	Chemiluminescence
March	15	10.4	12.1
	16	4.9	5.2
	17	6.4	6.4
	18	3.4	4.0
	19	5.2	6.4
	20	6.5	7.3
	21	10.5	10.0
	22	4.9	7.3
	23	15.0	20.5
	24	4.6	9.8
	25	9.9	14.6
	26	20.9	24.9
	27	10.4	16.1
	28	4.6	8.7
	29	4.8	6.9
	30	7.9	9.4
	31	4.9	5.8

Table A-3. Concentrations of NO<sub>2</sub> in ppb for the Saltzman and Chemiluminescent Methods for May 1-13, 1982.

		Saltzman	Chemiluminescence
May	1	3.7	4.9
	2	1.8	2.8
	3	3.4	4.6
	4	5.2	7.5
	5	4.0	5.3
	6	3.5	4.4
	7	3.2	4.3
	8	3.7	5.8
	9	3.2	5.4
	10	3.0	4.2
	11	3.7	6.3
	12	3.9	7.1
	13	5.6	10.7

Table A-4. Concentrations of NO<sub>2</sub> in ppb for the Saltzman and Chemiluminescent Methods for August 20-24, 1982.

		Saltzman	Chemiluminescence
August	20	2.8	2.8
	21	2.4	1.9
	22	2.0	2.0
	23	2.6	2.5
	24	2.8	2.8

# APPENDIX B

## STATISTICS DATA

Table B-1. Linear Correlation Coefficients for January.

	SO <sub>2</sub>	O <sub>3</sub>	CO <sub>2</sub>	NO <sub>2</sub>
RH	-0.446	-0.269	+0.059	-0.166
TT	-0.706	+0.402	-0.363	-0.590
dd	-0.742	+0.209	-0.303	-0.451
ff	-0.154	+0.196	-0.535	-0.527
SO <sub>2</sub>	XXXXX	-0.234	+0.346	+0.579
O <sub>3</sub>	-0.234	XXXXX	-0.335	-0.457
CO <sub>2</sub>	+0.346	-0.335	XXXXX	+0.876
NO <sub>2</sub>	+0.579	-0.457	+0.876	XXXXX
dd <sub>850</sub>	-0.514	-0.089	-0.031	-0.184
ff <sub>850</sub>	-0.407	+0.437	-0.576	-0.664
Dust	+0.723	-0.359	+0.585	+0.757
Rain	-0.163	+0.369	-0.130	-0.316

### LEGEND:

RH	Relative Humidity.
TT	Temperature (F).
dd	Wind Direction.
ff	Wind Speed (knots).
dd <sub>850</sub>	Wind Direction at 850 mb.
ff <sub>850</sub>	Wind Speed at 850 mb.

Table B-2. Linear Correlation Coefficients for February.

	SO <sub>2</sub>	O <sub>3</sub>	CO <sub>2</sub>	NO <sub>2</sub>
RH	+0.038	-0.216	+0.257	-0.222
TT	-0.552	+0.307	-0.511	-0.153
dd	-0.164	+0.582	-0.301	-0.303
ff	-0.278	-0.151	-0.333	-0.077
SO <sub>2</sub>	XXXXX	-0.226	+0.751	+0.563
O <sub>3</sub>	-0.226	XXXXX	-0.299	-0.590
CO <sub>2</sub>	+0.751	-0.299	XXXXX	+0.501
NO <sub>2</sub>	+0.563	-0.590	+0.501	XXXXX
dd <sub>850</sub>	-0.363	+0.567	-0.304	-0.352
ff <sub>850</sub>	-0.481	+0.232	-0.513	-0.293
Dust	+0.926	-0.119	+0.784	+0.473
Rain	-0.282	+0.112	-0.173	-0.335

LEGEND:

RH	Relative Humidity.
TT	Temperature (F).
dd	Wind Direction.
ff	Wind Speed (knots).
dd <sub>850</sub>	Wind Direction at 850 mb.
ff <sub>850</sub>	Wind Speed at 850 mb.

Table B-3. Linear Correlation Coefficients for March.

	SO <sub>2</sub>	O <sub>3</sub>	CO <sub>2</sub>	NO <sub>2</sub>
RH	-0.773	-0.495	+0.409	-0.543
TT	+0.525	+0.781	+0.270	+0.326
dd	-0.570	+0.071	-0.602	-0.461
ff	-0.535	-0.022	-0.665	-0.427
SO <sub>2</sub>	XXXXX	+0.223	+0.715	+0.783
O <sub>3</sub>	+0.223	XXXXX	+0.076	-0.124
CO <sub>2</sub>	+0.715	+0.076	XXXXX	+0.601
NO <sub>2</sub>	+0.783	-0.124	+0.601	XXXXX
dd <sub>850</sub>	-0.479	+0.233	-0.664	-0.504
ff <sub>850</sub>	-0.415	+0.007	-0.633	-0.373
Dust	+0.872	+0.447	+0.728	+0.538
Rain	-0.404	-0.082	-0.498	-0.190

LEGEND:

RH	Relative Humidity.
TT	Temperature (F).
dd	Wind Direction.
ff	Wind Speed (knots).
dd <sub>850</sub>	Wind Direction at 850 mb.
ff <sub>850</sub>	Wind Speed at 850 mb.

Table B-4. Linear Correlation Coefficients for April.

	SO <sub>2</sub> *	O <sub>3</sub>	CO <sub>2</sub>	NO <sub>2</sub>
RH	-0.524	-0.632	+0.351	-0.260
TT	+0.416	+0.644	-0.570	+0.417
dd	-0.319	-0.338	+0.390	+0.198
ff	+0.005	-0.134	-0.027	-0.310
SO <sub>2</sub>	XXXXX	+0.197	+0.132	+0.503
O <sub>3</sub>	+0.197	XXXXX	+0.390	-0.220
CO <sub>2</sub>	+0.132	+0.390	XXXXX	+0.074
NO <sub>2</sub>	+0.503	-0.220	+0.074	XXXXX
dd <sub>850</sub>	-0.131	+0.052	+0.111	-0.161
ff <sub>850</sub>	-0.265	-0.338	+0.095	-0.185
Dust	+0.707	+0.279	+0.028	+0.714
Rain	-0.187	-0.021	-0.305	-0.213

\* only 28 days of SO<sub>2</sub> data were available.

LEGEND:

RH	Relative Humidity.
TT	Temperature (F).
dd	Wind Direction.
ff	Wind Speed (knots).
dd <sub>850</sub>	Wind Direction at 850 mb.
ff <sub>850</sub>	Wind Speed at 850 mb.

Table B-5. Linear Correlation Coefficients for May.

	SO <sub>2</sub>	O <sub>3</sub>	CO <sub>2</sub>	NO <sub>2</sub>
RH	-0.618	-0.842	+0.444	-0.298
TT	+0.279	+0.826	-0.849	+0.078
dd	-0.485	-0.423	+0.224	-0.320
ff	+0.202	-0.169	+0.222	-0.001
SO <sub>2</sub>	XXXXX	+0.505	-0.051	+0.707
O <sub>3</sub>	+0.505	XXXXX	-0.675	+0.283
CO <sub>2</sub>	-0.051	-0.675	XXXXX	+0.208
NO <sub>2</sub>	+0.707	+0.283	+0.208	XXXXX
dd <sub>850</sub>	-0.490	-0.413	+0.157	-0.388
ff <sub>850</sub>	-0.117	-0.397	+0.180	-0.070
Dust	+0.653	+0.763	-0.485	+0.219
Rain	-0.285	-0.294	+0.045	-0.211

LEGEND:

RH	Relative Humidity.
TT	Temperature (F).
dd	Wind Direction.
ff	Wind Speed (knots).
dd <sub>850</sub>	Wind Direction at 850 mb.
ff <sub>850</sub>	Wind Speed at 850 mb.



Table B-6. Linear Correlation Coefficients for August.

	SO <sub>2</sub>	O <sub>3</sub>	CO <sub>2</sub>	NO <sub>2</sub>
RH*	-0.125	-0.185	+0.564	-0.045
TT	+0.251	+0.764	+0.347	+0.339
dd	-0.559	-0.402	-0.513	-0.619
ff	-0.269	-0.256	-0.659	-0.296
SO <sub>2</sub>	XXXXX	+0.217	+0.165	+0.835
O <sub>3</sub>	+0.217	XXXXX	+0.513	+0.239
CO <sub>2</sub>	+0.165	+0.513	XXXXX	+0.300
NO <sub>2</sub>	+0.835	+0.239	+0.300	XXXXX
dd <sub>850</sub> *	-0.509	-0.359	-0.542	-0.583
ff <sub>850</sub> *	-0.189	-0.156	-0.623	-0.283
Dust	+0.401	+0.811	+0.736	+0.474
Rain	+0.051	+0.303	+0.346	+0.117

\* only 30 days of data were available.

LEGEND:

RH	Relative Humidity.
TT	Temperature (F).
dd	Wind Direction.
ff	Wind Speed (knots).
dd <sub>850</sub>	Wind Direction at 850 mb.
ff <sub>850</sub>	Wind Speed at 850 mb.

Table B-7. Standard Deviations.

	Jan	Feb	Mar	Apr	May	Aug
RH	11.08	13.91	13.60	14.63	14.94	8.07
TT	4.96	3.98	2.58	3.14	4.55	2.63
dd	6.93	6.05	6.75	8.26	7.53	8.58
ff	2.78	1.36	2.36	1.47	1.31	1.42
SO <sub>2</sub>	36.75	33.65	14.95	12.87	5.36	3.23
O <sub>3</sub>	6.60	6.58	6.54	6.40	9.93	9.27
CO <sub>2</sub>	8.44	6.00	5.75	2.47	4.02	6.17
NO <sub>2</sub>	101.59	77.40	69.87	37.73	18.08	17.57
dd <sub>850</sub>	7.77	8.18	9.23	11.94	7.18	7.49
ff <sub>850</sub>	5.42	2.77	6.02	3.38	3.91	3.59
Dust	19.33	33.21	33.57	22.39	19.63	15.55
Rain	31.92	9.59	31.25	22.87	20.98	110.30

Table B-8. Variance.

	Jan	Feb	Mar	Apr	May	Aug
RH	122.84	193.45	184.89	214.07	223.06	65.22
TT	24.65	15.80	6.66	9.83	20.67	6.90
dd	48.03	36.59	45.52	68.18	56.76	73.53
ff	7.74	1.86	5.55	2.16	1.73	2.02
SO <sub>2</sub>	1350.31	1132.24	223.57	165.57	28.70	10.46
O <sub>3</sub>	43.58	43.32	42.77	40.93	98.66	85.97
CO <sub>2</sub>	71.21	36.00	33.09	6.11	16.19	38.06
NO <sub>2</sub>	10321.31	5990.87	4882.35	1423.66	326.76	308.74
dd <sub>850</sub>	60.31	66.97	85.14	142.56	51.59	56.05
ff <sub>850</sub>	29.43	7.66	36.20	11.45	15.30	12.92
Dust	373.73	1102.90	1127.15	501.51	385.37	241.73
Rain	1018.74	91.93	976.82	523.03	440.09	12166.30

Table B-9. Covariance with SO<sub>2</sub>

	Jan	Feb	Mar	Apr	May	Aug
RH	-181.68	16.08	-157.12	-98.57	-49.44	-3.27
TT	-128.73	-66.67	20.27	16.80	6.80	2.14
dd	-189.00	-30.10	-57.47	-33.89	-19.58	-15.51
ff	-15.78	-11.50	-18.82	0.09	1.42	-1.24
O <sub>3</sub>	-56.80	-45.15	21.76	16.23	26.90	6.52
CO <sub>2</sub>	107.31	136.87	61.47	4.19	-1.11	3.30
NO <sub>2</sub>	2161.66	1325.36	818.13	244.31	68.45	47.46
dd850	-146.81	-90.27	-73.06	-20.11	-18.84	-12.32
ff850	-81.18	-40.45	-37.34	-11.52	-2.45	-2.20
Dust	513.44	934.77	437.59	203.71	68.70	20.16
Rain	-190.89	-82.27	-188.64	-55.08	-32.02	18.03

Table B-10. Covariance with O<sub>3</sub>.

	Jan	Feb	Mar	Apr	May	Aug
RH	-19.68	-17.87	-44.00	-59.13	-124.88	-13.83
TT	13.19	7.25	13.18	12.93	37.28	18.61
dd	9.55	20.94	3.15	-17.87	-31.68	-31.98
ff	3.59	-1.22	-0.33	1.26	-2.21	-3.37
SO <sub>2</sub>	-56.80	-45.15	21.76	16.23	26.90	6.52
CO <sub>2</sub>	-18.66	-10.66	2.86	-6.17	-26.99	29.34
NO <sub>2</sub>	-306.84	-271.55	-56.66	-53.10	50.74	38.91
dd850	-4.54	27.60	14.09	3.97	-29.50	-24.95
ff850	15.64	3.82	0.27	-7.31	-15.43	-5.19
Dust	-45.80	-23.40	98.06	40.00	148.79	116.87
Rain	77.82	6.37	-16.67	-3.10	-61.19	310.11

Table B-11. Covariance with CO<sub>2</sub>

	Jan	Feb	Mar	Apr	May	Aug
RH	5.52	19.35	-32.03	12.70	26.66	28.10
TT	-15.20	-11.01	4.00	-4.42	-15.52	5.62
dd	-17.73	-9.85	-23.35	7.95	6.79	-27.15
ff	-12.57	-2.46	-9.01	-0.10	1.17	-5.77
SO <sub>2</sub>	107.31	136.87	61.47	4.19	-1.11	3.30
O <sub>3</sub>	-18.66	-10.66	2.86	-6.17	-26.99	29.34
NO <sub>2</sub>	750.83	209.91	241.57	6.87	15.12	32.55
dd850	-2.04	-13.48	-35.26	3.29	4.55	-25.04
ff850	-26.38	-7.69	-21.92	0.79	2.84	-13.82
Dust	95.41	140.94	140.68	1.53	-38.28	70.56
Rain	-34.88	-8.99	-89.54	-17.26	3.79	235.43

Table B-12. Covariance with NO<sub>2</sub>.

	Jan	Feb	Mar	Apr	May	Aug
RH	-187.16	-216.35	-516.04	-143.50	-80.38	-6.37
TT	-297.61	-42.42	58.83	49.34	6.42	15.63
dd	-317.50	-128.08	-217.16	-61.70	-43.70	-93.27
ff	-148.93	-7.29	-70.33	-17.22	-0.03	-7.38
SO <sub>2</sub>	2161.66	1325.36	818.13	244.31	68.45	47.46
O <sub>3</sub>	-306.84	-271.55	-56.66	-53.10	50.74	38.91
CO <sub>2</sub>	750.83	209.91	241.57	6.87	15.12	32.55
dd850	-145.18	-201.21	-325.05	-72.54	-50.31	-76.67
ff850	-366.03	-56.69	-156.98	-23.65	-4.97	-17.89
Dust	1487.63	1099.31	1262.48	603.64	77.68	129.60
Rain	-1025.78	-224.83	-414.98	-183.62	-80.14	227.47

APPENDIX C  
PHOTOSTATIONARY STATE DATA  
CLEAR SKIES

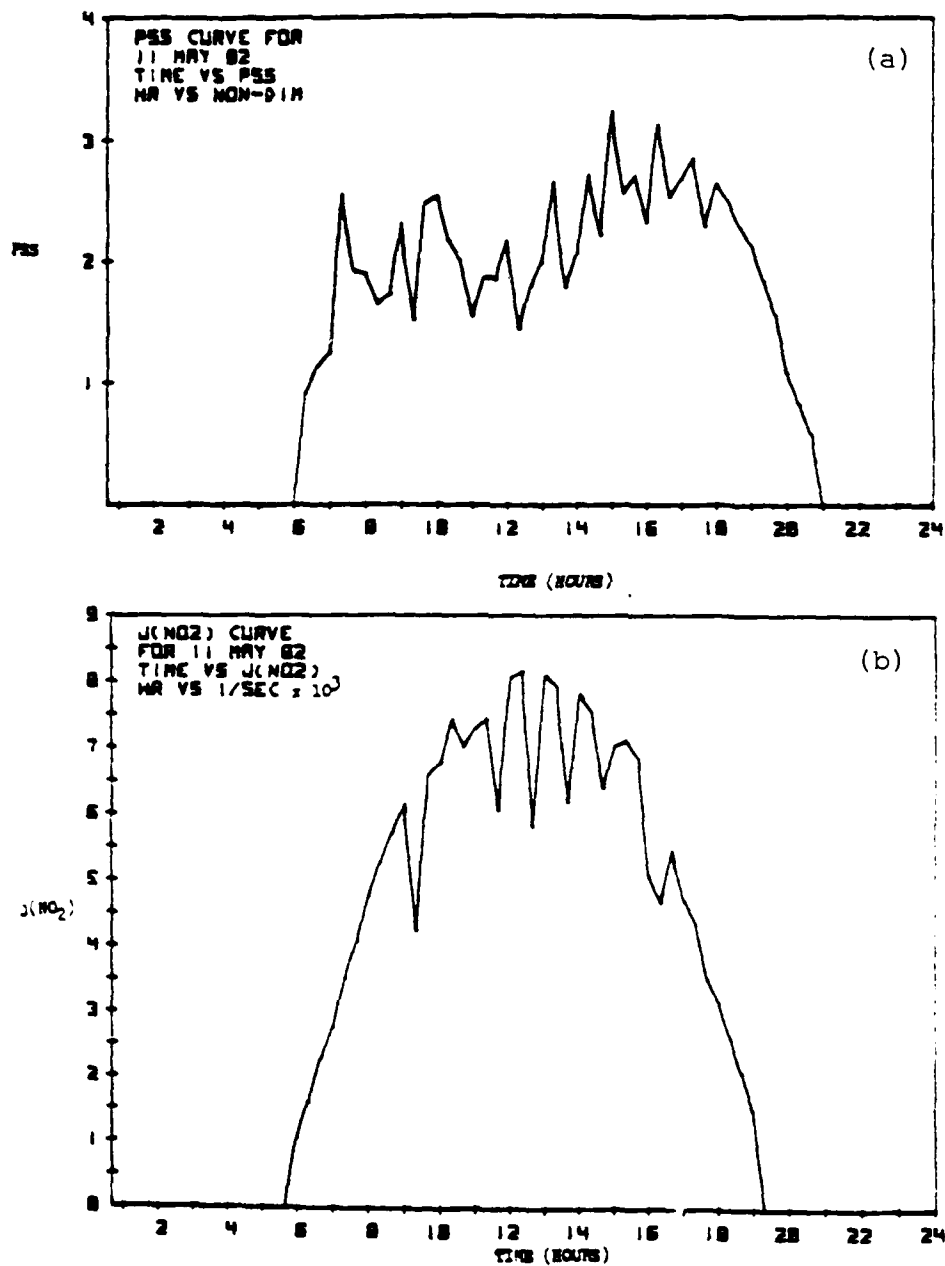


Figure C-1. Daily values of (a) P and (b)  $j(\text{NO}_2)$  for clear skies on May 11, 1982.

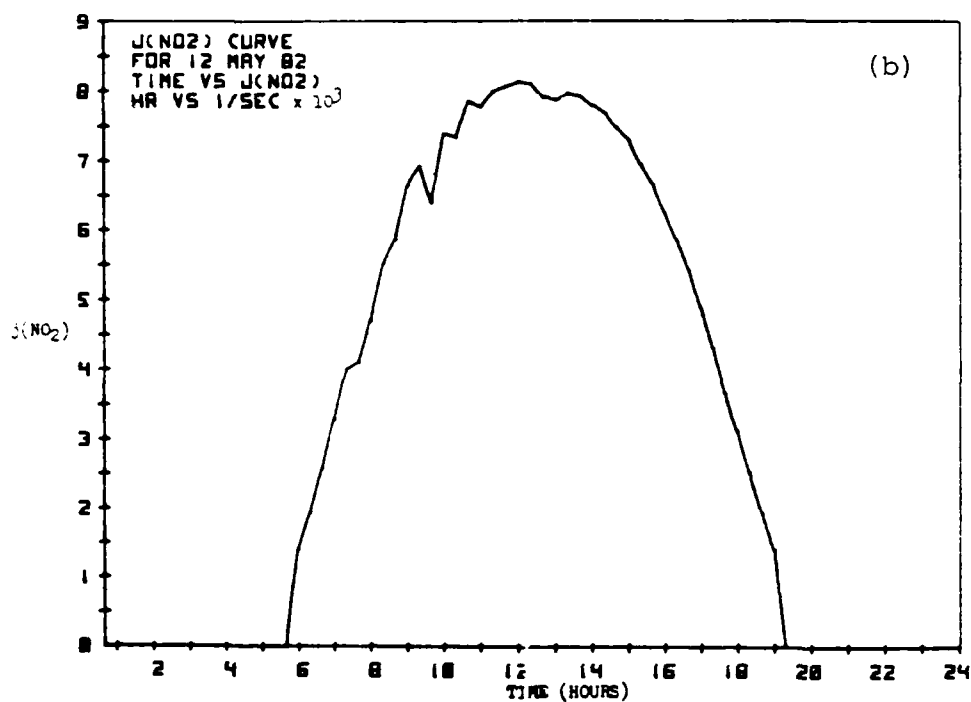
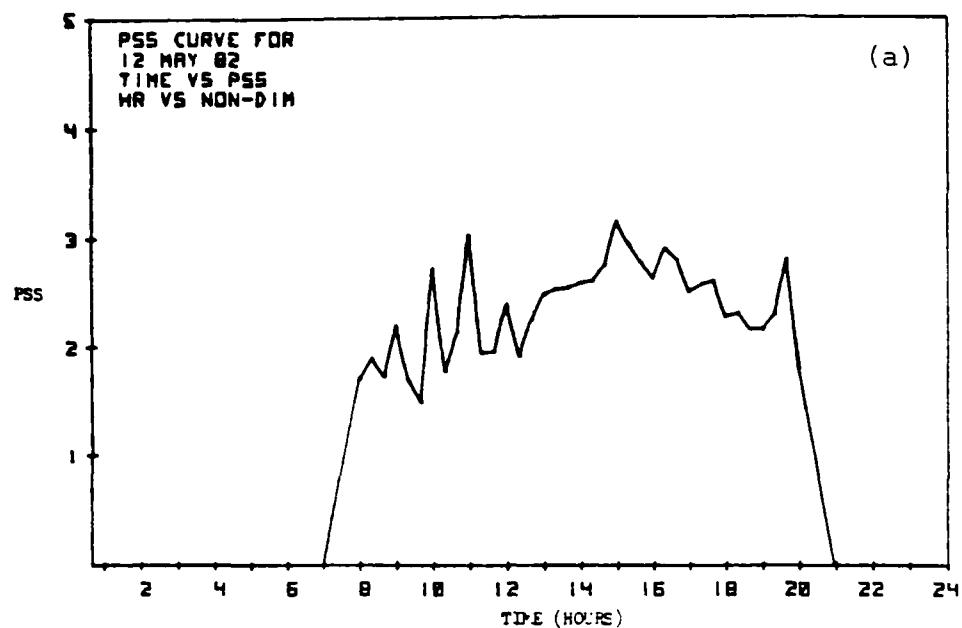


Figure C-2. Daily values of (a) P and (b)  $j(\text{NO}_2)$  for clear skies on May 12, 1982.

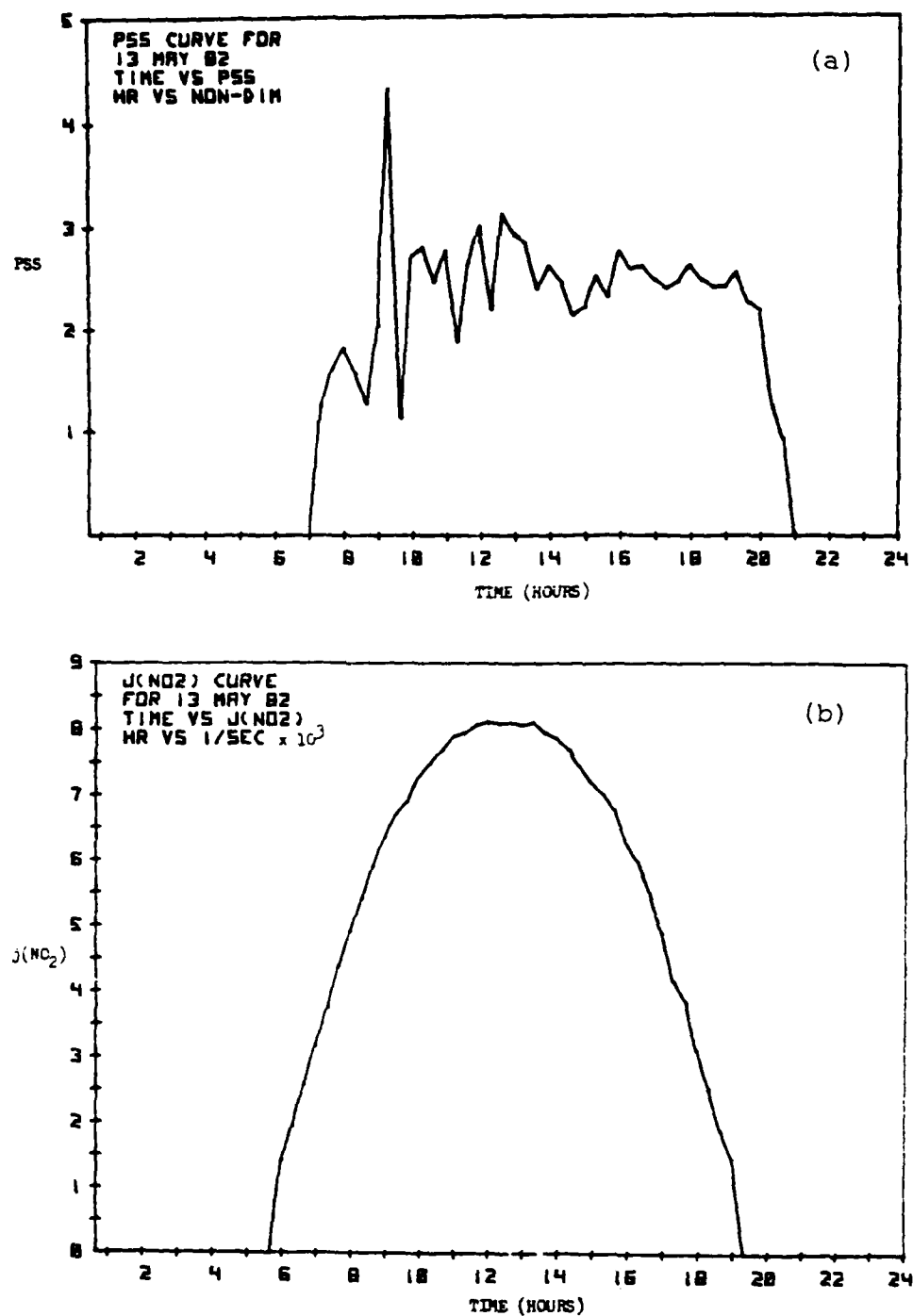


Figure C-3. Daily values of (a) P and (b)  $j(\text{NO}_2)$  for clear skies on May 13, 1982.

## CLOUDY SKIES

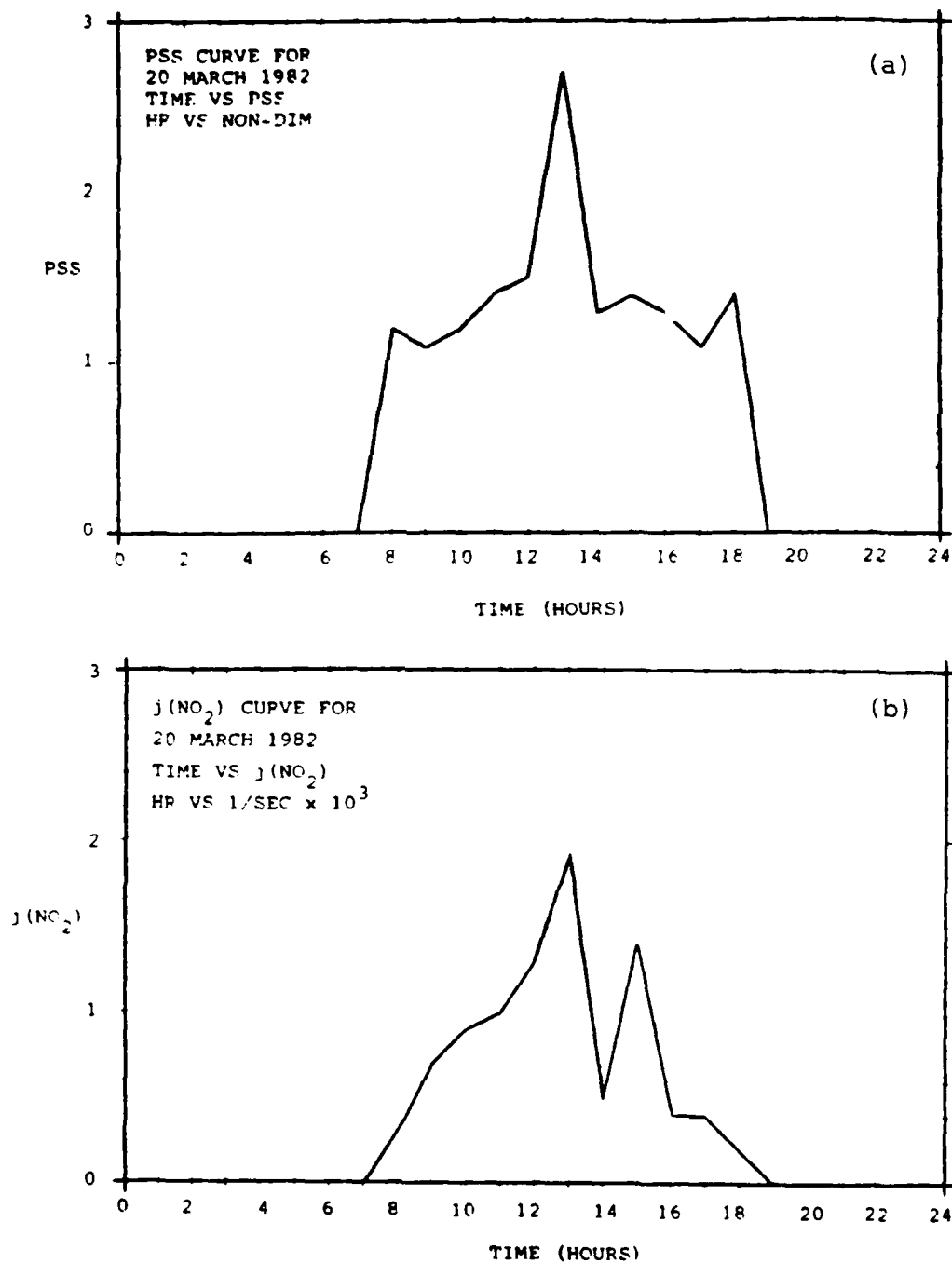


Figure C-4. Daily values of (a) P and (b)  $j(\text{NO}_2)$  for cloudy skies on March 20, 1982.



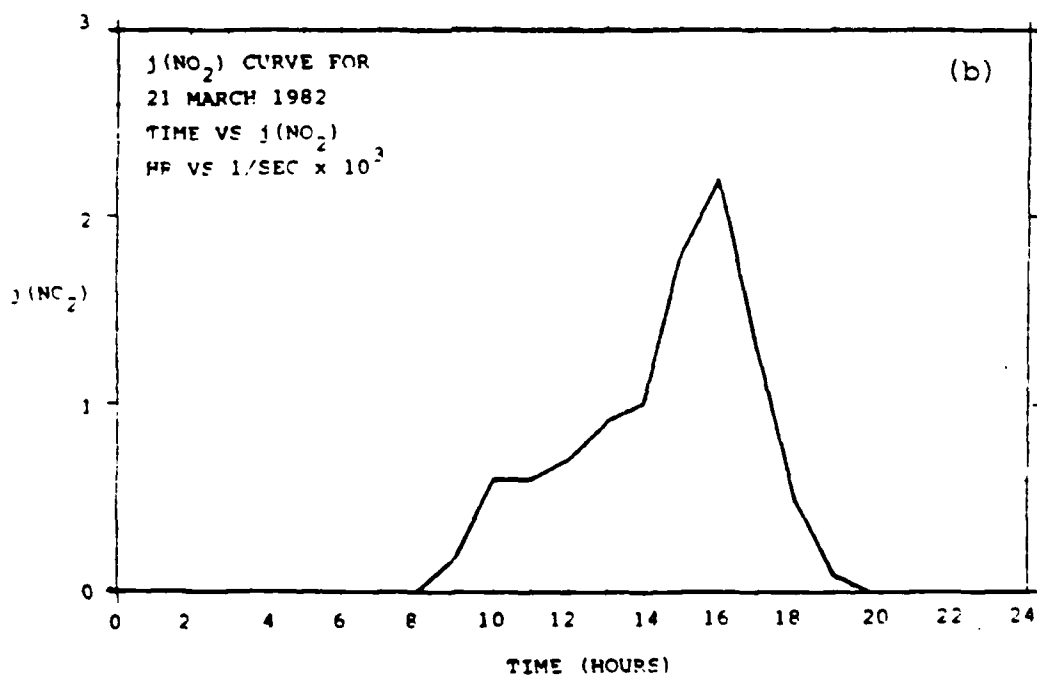
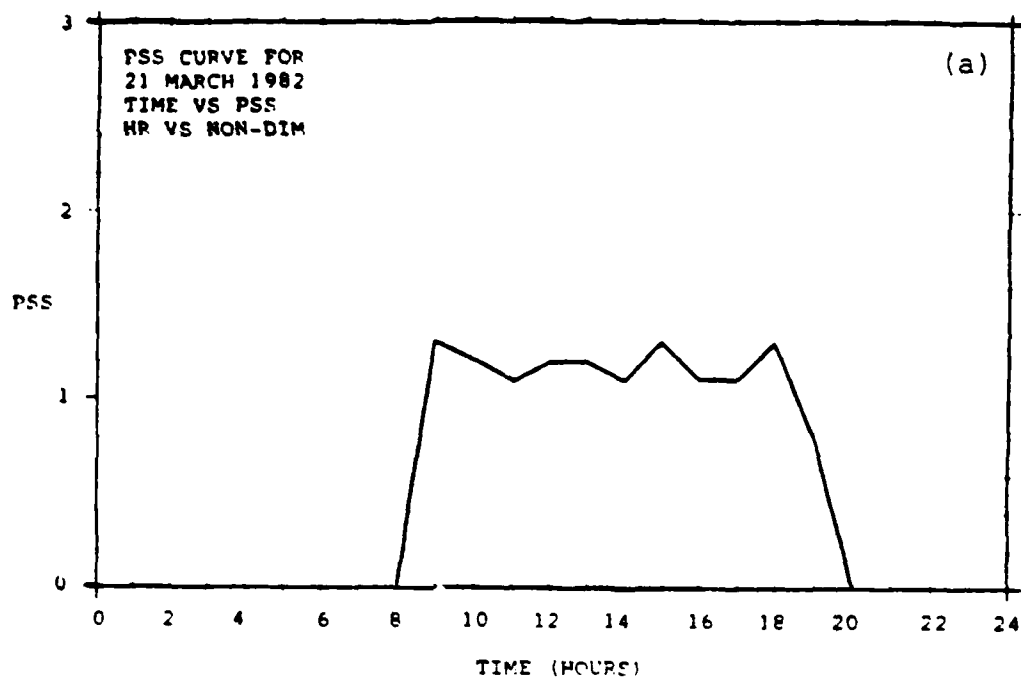


Figure C-5. Daily values of (a) P and (b)  $j(\text{NO}_2)$  for cloudy skies on March 21, 1982.

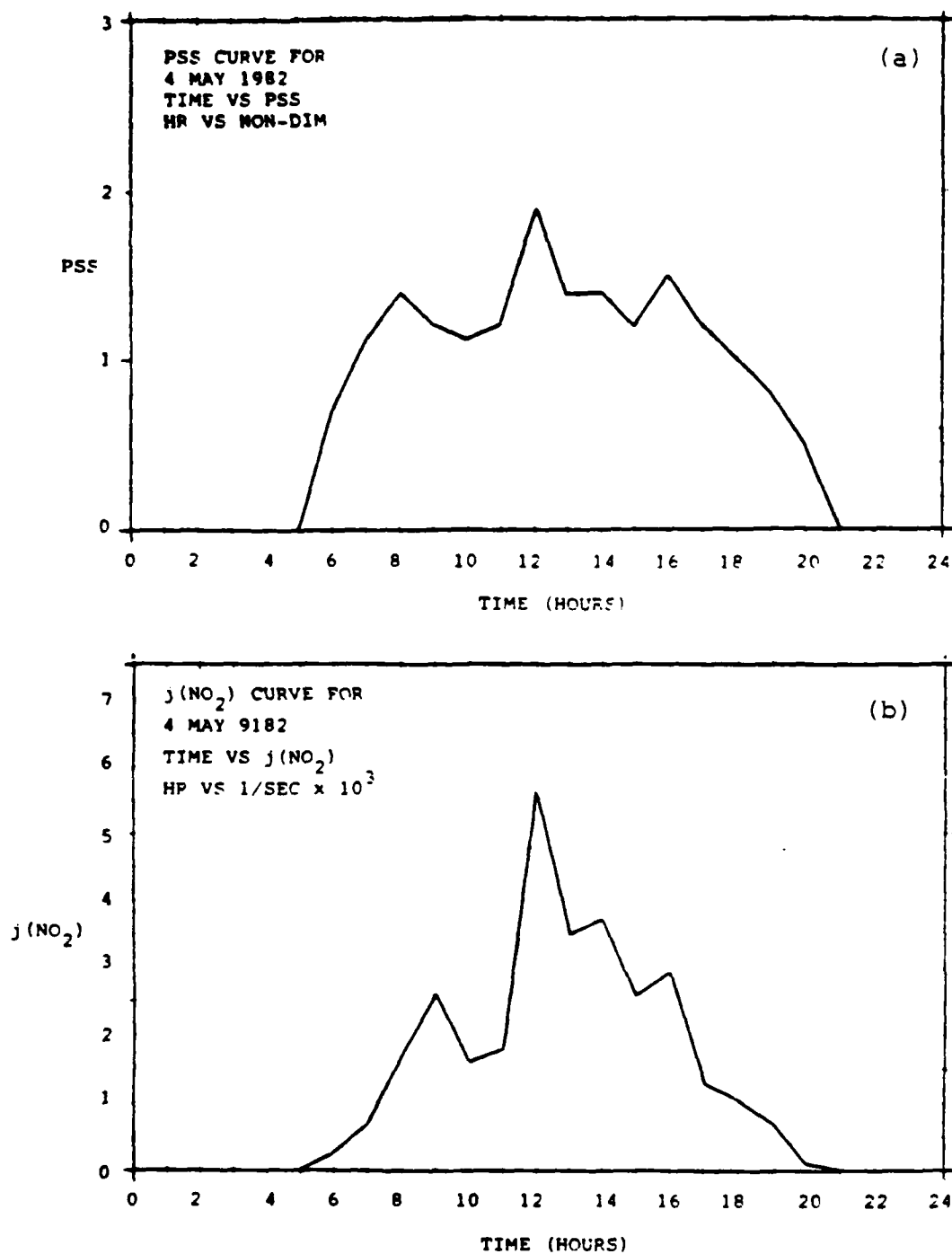


Figure C-6. Daily values of (a) P and (b)  $j(\text{NO}_2)$  for cloudy skies on May 4, 1982.

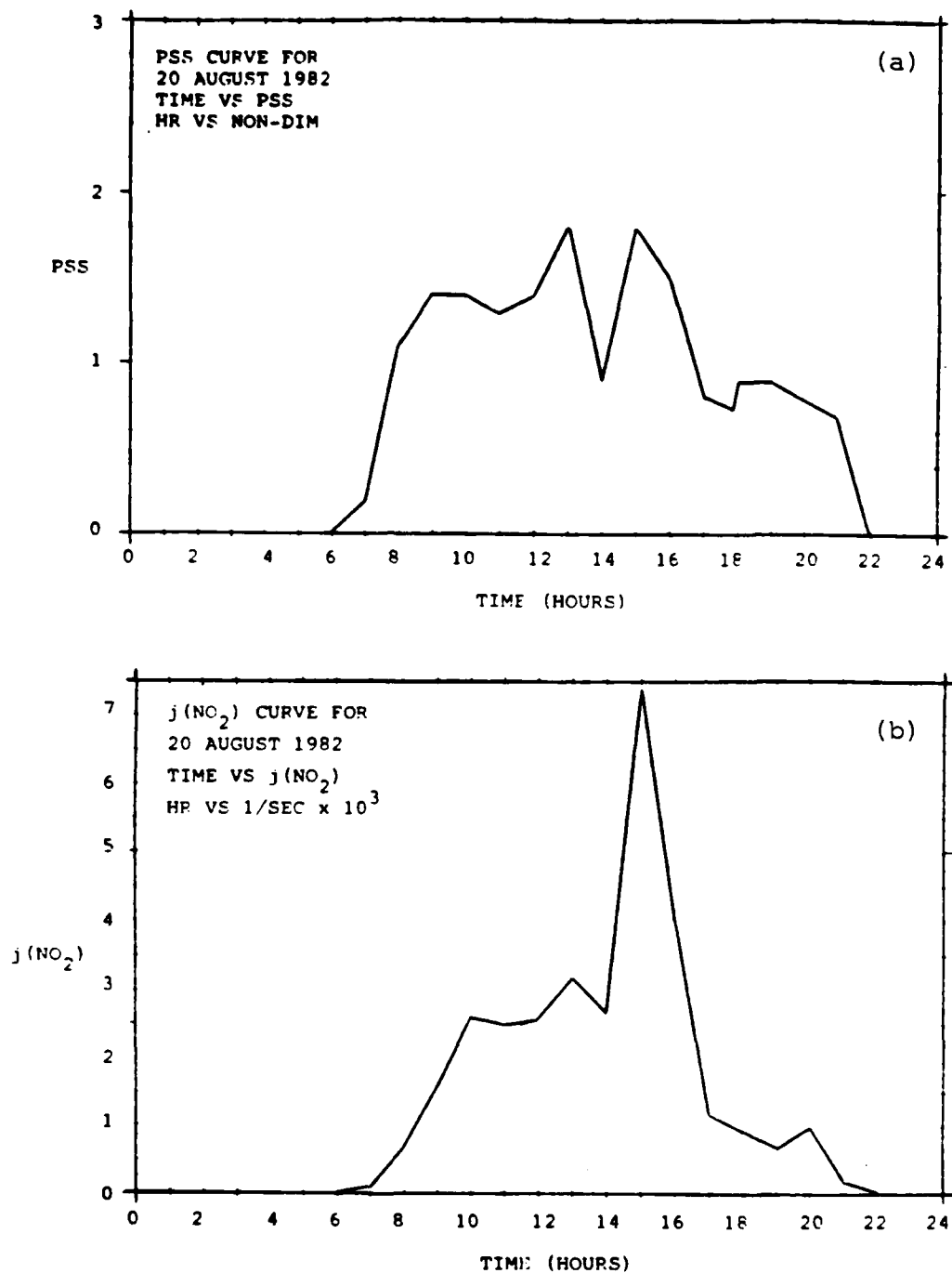


Figure C-7. Daily values of (a) P and (b) j(NO<sub>2</sub>) for cloudy skies on August 20, 1982.

## CLEAR SKIES

Table C-1. Photostationary State (PSS) Data for March 24, 1982. Units of PSS are non-dimensional.

NO PPB	NO <sub>2</sub> PPB	j(NO <sub>2</sub> ) 1/SEC	O <sub>3</sub> PPB	TEMP C	PSS
0.160	9.851	0.000E+00	23.0	2.3	0.000
0.000	10.274	0.000E+00	23.0	2.3	0.000
0.000	11.011	0.000E+00	23.0	2.3	0.000
0.030	12.138	0.000E+00	23.0	2.3	0.000
0.000	11.126	0.000E+00	21.0	1.2	0.000
0.020	7.622	0.000E+00	21.0	1.2	0.000
0.050	8.403	0.000E+00	21.0	1.2	0.000
0.010	10.264	0.000E+00	21.0	1.2	0.000
0.000	8.105	0.000E+00	23.0	1.0	0.000
0.010	7.716	0.000E+00	23.0	1.0	0.000
0.020	7.212	0.000E+00	23.0	1.0	0.000
0.010	8.116	0.000E+00	23.0	1.0	0.000
0.000	9.284	0.000E+00	23.0	0.5	0.000
0.020	6.854	0.000E+00	23.0	0.5	0.000
0.020	7.212	0.000E+00	23.0	0.5	0.000
0.020	7.033	0.000E+00	23.0	0.5	0.000
0.000	6.084	0.000E+00	23.0	0.4	0.000
0.000	7.947	0.000E+00	23.0	0.4	0.000
0.040	8.918	0.000E+00	23.0	0.4	0.000
0.000	8.495	0.000E+00	23.0	0.4	0.000
0.010	9.390	0.000E+00	21.0	-0.1	0.000
0.020	8.180	0.000E+00	21.0	-0.1	0.000
0.000	7.547	0.000E+00	21.0	-0.1	0.000
0.000	7.284	0.000E+00	21.0	-0.1	0.000
0.000	6.884	0.000E+00	21.0	-0.9	0.000
0.040	7.613	0.000E+00	21.0	-0.9	0.000
0.090	7.352	1.958E-04	21.0	-0.9	2.386
0.160	7.198	4.729E-04	21.0	-0.9	3.171
0.590	10.021	8.492E-04	21.0	-0.1	2.125
0.860	9.466	1.212E-03	21.0	-0.1	1.963
1.150	9.839	1.708E-03	21.0	-0.1	2.147
1.420	10.012	2.087E-03	21.0	-0.1	2.158
1.330	8.091	2.625E-03	19.0	1.2	2.545
1.860	8.593	3.046E-03	19.0	1.2	2.237
2.170	8.756	3.599E-03	19.0	1.2	2.305
2.270	7.856	3.931E-03	19.0	1.2	2.154
2.360	8.093	4.381E-03	21.0	3.5	2.094
2.430	8.454	4.787E-03	21.0	3.5	2.327
2.330	8.249	5.294E-03	21.0	3.5	2.614
2.260	8.719	5.510E-03	21.0	3.5	2.969

Table C-1. (Continued)

NO PPB	NO <sub>2</sub> PPB	j(NO <sub>2</sub> ) 1/SEC	O <sub>3</sub> PPB	TEMP C	PSS
2.110	9.153	5.915E-03	26.0	5.7	2.778
1.970	10.035	6.006E-03	26.0	5.7	3.210
1.870	11.298	6.231E-03	26.0	5.7	4.160
1.830	12.696	6.359E-03	26.0	5.7	4.880
1.750	13.734	6.716E-03	32.0	8.0	4.619
1.350	14.766	6.926E-03	32.0	8.0	6.555
0.940	14.744	7.067E-03	32.0	8.0	9.747
1.070	14.804	7.100E-03	32.0	8.0	8.633
1.240	14.676	6.966E-03	37.0	8.4	6.235
1.270	14.046	7.051E-03	37.0	8.4	5.895
1.110	13.679	7.100E-03	37.0	8.4	6.618
0.940	13.239	6.562E-03	37.0	8.4	6.994
0.950	12.461	7.132E-03	40.0	9.9	6.438
0.800	11.800	7.164E-03	40.0	9.9	7.276
0.730	11.433	7.034E-03	40.0	9.9	7.590
0.800	10.137	6.966E-03	40.0	9.9	6.074
0.860	9.887	6.753E-03	41.0	10.2	5.193
0.800	9.884	6.601E-03	41.0	10.2	5.457
0.760	9.756	6.359E-03	41.0	10.2	5.462
0.760	9.682	6.187E-03	41.0	10.2	5.274
0.750	9.861	5.912E-03	43.0	10.7	4.932
0.920	9.859	5.666E-03	43.0	10.7	3.850
0.820	9.422	5.294E-03	43.0	10.7	3.958
0.890	9.142	5.008E-03	43.0	10.7	3.261
0.920	9.122	4.577E-03	44.0	10.7	2.811
0.630	9.149	4.177E-03	44.0	10.7	3.764
0.630	9.025	3.748E-03	44.0	10.7	3.086
0.650	8.971	3.367E-03	44.0	10.7	2.883
1.000	8.368	2.881E-03	45.0	10.2	1.466
0.890	8.868	2.449E-03	45.0	10.2	1.486
0.380	9.357	1.994E-03	45.0	10.2	2.999
0.350	9.103	1.513E-03	45.0	10.2	2.404
0.160	9.819	1.110E-03	45.0	8.8	4.231
0.140	9.860	7.431E-04	45.0	8.8	3.252
0.170	10.398	4.181E-04	45.0	8.8	1.589
0.140	12.113	1.958E-04	45.0	8.8	1.053
0.050	10.992	0.000E+00	40.0	6.5	0.000
0.000	8.126	0.000E+00	40.0	6.5	0.000
0.000	7.684	0.000E+00	40.0	6.5	0.000
0.000	7.905	0.000E+00	40.0	6.5	0.000

Table C-1. (Continued)

NO PPB	NO <sub>2</sub> PPB	j(NO <sub>2</sub> ) 1/SEC	O <sub>3</sub> PPB	TEMP C	PSS
0.000	7.400	0.000E+00	38.0	4.7	0.000
0.000	7.221	0.000E+00	38.0	4.7	0.000
0.020	7.138	0.000E+00	38.0	4.7	0.000
0.000	6.989	0.000E+00	38.0	4.7	0.000
0.000	7.105	0.000E+00	39.0	3.7	0.000
0.000	7.432	0.000E+00	39.0	3.7	0.000
0.000	7.453	0.000E+00	39.0	3.7	0.000
0.000	7.484	0.000E+00	39.0	3.7	0.000
0.000	7.789	0.000E+00	39.0	3.7	0.000
0.040	7.781	0.000E+00	39.0	3.7	0.000
0.030	7.759	0.000E+00	39.0	3.7	0.000
0.000	7.611	0.000E+00	39.0	3.7	0.000
0.040	7.455	0.000E+00	38.0	3.4	0.000
0.080	7.141	0.000E+00	38.0	3.4	0.000
0.000	7.234	0.000E+00	38.0	3.4	0.000
0.000	7.821	0.000E+00	38.0	3.4	0.000

Table C-2. Photostationary State (PSS) Data for  
March 25, 1982. Units of PSS are  
non-dimensional.

NO PPB	NO <sub>2</sub> PPB	j(NO <sub>2</sub> ) 1/SEC	O <sub>3</sub> PPB	TEMP C	PSS
0.000	7.463	0.000E+00	37.0	3.0	0.000
0.150	8.850	0.000E+00	37.0	3.0	0.000
0.000	10.305	0.000E+00	37.0	3.0	0.000
0.000	10.358	0.000E+00	37.0	3.0	0.000
0.020	9.791	0.000E+00	35.0	3.0	0.000
0.040	10.949	0.000E+00	35.0	3.0	0.000
0.000	11.000	0.000E+00	35.0	3.0	0.000
0.000	11.947	0.000E+00	35.0	3.0	0.000
0.000	12.773	0.000E+00	32.0	3.0	0.000
0.000	13.726	0.000E+00	32.0	3.0	0.000
0.040	13.855	0.000E+00	32.0	3.0	0.000
0.000	13.236	0.000E+00	32.0	3.0	0.000
0.040	13.371	0.000E+00	29.0	2.7	0.000
0.060	13.003	0.000E+00	29.0	2.7	0.000
0.000	13.095	0.000E+00	29.0	2.7	0.000
0.030	13.947	0.000E+00	29.0	2.7	0.000
0.000	13.600	0.000E+00	28.0	2.2	0.000
0.010	13.337	0.000E+00	28.0	2.2	0.000
0.010	11.706	0.000E+00	28.0	2.2	0.000
0.000	12.032	0.000E+00	28.0	2.2	0.000
0.000	10.526	0.000E+00	29.0	2.6	0.000
0.000	11.663	0.000E+00	29.0	2.6	0.000
0.050	12.887	0.000E+00	29.0	2.6	0.000
0.000	10.726	0.000E+00	29.0	2.6	0.000
0.070	11.530	0.000E+00	31.0	2.3	0.000
0.010	13.358	1.396E-04	31.0	2.3	18.134
0.020	14.022	2.518E-04	31.0	2.3	17.171
0.180	14.504	5.818E-04	31.0	2.3	4.557
0.390	14.547	1.006E-03	28.0	3.4	3.985
0.710	14.595	1.364E-03	28.0	3.4	2.973
0.950	14.597	1.852E-03	28.0	3.4	3.015
1.290	14.131	2.360E-03	28.0	3.4	2.735
1.690	14.394	2.796E-03	31.0	5.5	2.218
1.890	13.899	3.249E-03	31.0	5.5	2.223
2.170	13.504	3.748E-03	31.0	5.5	2.167
2.390	13.357	4.177E-03	31.0	5.5	2.167
2.600	13.025	4.577E-03	33.0	8.7	1.868
2.600	12.899	5.153E-03	33.0	8.7	2.082
2.610	12.537	5.510E-03	33.0	8.7	2.222
2.730	13.049	5.766E-03	33.0	8.7	2.314

Table C-2. (Continued)

NO PPB	NO <sub>2</sub> PPB	j(NO <sub>2</sub> ) 1/SEC	O <sub>3</sub> PPB	TEMP C	PSS
2.370	12.304	6.052E-03	36.0	10.0	2.385
2.380	12.641	6.317E-03	36.0	10.0	2.548
2.410	12.327	6.483E-03	36.0	10.0	2.517
2.030	11.507	6.678E-03	36.0	10.0	2.876
1.730	10.628	6.753E-03	40.0	11.6	2.799
1.510	10.079	7.067E-03	40.0	11.6	3.174
1.580	9.515	7.067E-03	40.0	11.6	2.861
1.540	9.765	7.164E-03	40.0	11.6	3.056
1.290	9.942	6.897E-03	42.0	12.2	3.388
1.260	8.551	7.348E-03	42.0	12.2	3.176
1.260	7.908	7.258E-03	42.0	12.2	2.899
1.400	8.221	7.348E-03	42.0	12.2	2.744
1.560	7.819	7.196E-03	42.0	12.1	2.293
1.120	7.543	7.017E-03	42.0	12.1	3.013
0.570	7.219	7.100E-03	42.0	12.1	5.753
0.380	6.273	6.862E-03	42.0	12.1	2.798
1.080	7.299	6.601E-03	42.0	13.1	2.813
1.210	8.569	6.483E-03	42.0	13.1	2.896
1.250	8.287	6.401E-03	42.0	13.1	2.676
1.400	8.368	6.231E-03	42.0	13.1	2.346
1.330	8.228	5.912E-03	44.0	13.5	2.191
1.320	8.880	5.615E-03	44.0	13.5	2.264
1.310	9.301	5.294E-03	44.0	13.5	2.254
1.030	8.696	4.919E-03	44.0	13.5	2.493
0.970	8.188	4.545E-03	46.0	13.5	2.203
0.940	8.965	4.143E-03	46.0	13.5	2.271
0.880	9.688	3.711E-03	46.0	13.5	2.350
0.780	9.999	3.288E-03	46.0	13.5	2.426
0.710	9.437	2.881E-03	46.0	13.0	2.215
0.650	9.424	2.360E-03	46.0	13.0	1.981
0.510	9.732	1.994E-03	46.0	13.0	2.304
0.470	9.151	1.611E-03	46.0	13.0	1.818
0.560	9.735	1.213E-03	45.0	11.8	1.264
0.300	10.363	7.963E-04	45.0	11.8	1.652
0.010	10.822	4.729E-04	45.0	11.8	30.786
0.000	11.200	2.518E-04	45.0	11.8	0.000
0.000	12.137	0.000E+00	40.0	10.0	0.000
0.000	12.204	0.000E+00	40.0	10.0	0.000
0.000	12.274	0.000E+00	40.0	10.0	0.000
0.000	13.432	0.000E+00	40.0	10.0	0.000



Table C-2. (Continued)

NO PPB	NO <sub>2</sub> PPB	J(NO <sub>2</sub> ) 1/SEC	O <sub>3</sub> PPB	TEMP C	PSS
0.000	15.400	0.000E+00	33.0	7.0	0.000
0.000	14.139	0.000E+00	33.0	7.0	0.000
0.000	13.505	0.000E+00	33.0	7.0	0.000
0.040	13.992	0.000E+00	33.0	7.0	0.000
0.060	14.445	0.000E+00	33.0	5.3	0.000
0.080	13.794	0.000E+00	33.0	5.3	0.000
0.000	13.105	0.000E+00	33.0	5.3	0.000
0.000	13.032	0.000E+00	33.0	5.3	0.000
0.020	13.201	0.000E+00	32.0	5.2	0.000
0.000	13.789	0.000E+00	32.0	5.2	0.000
0.030	24.133	0.000E+00	32.0	5.2	0.000
0.080	29.109	0.000E+00	32.0	5.2	0.000
0.040	60.192	0.000E+00	26.0	4.5	0.000
0.140	59.407	0.000E+00	26.0	4.5	0.000
0.140	59.081	0.000E+00	26.0	4.5	0.000
0.290	59.636	0.000E+00	26.0	4.5	0.000

Table C-3. Photostationary State (PSS) Data for March 26, 1982. Units of PSS are non-dimensional.

NO PPB	NO <sub>2</sub> PPB	j(NO <sub>2</sub> ) 1/SEC	O <sub>3</sub> PPB	TEMP C	PSS
2.170	55.104	0.000E+00	7.0	4.5	0.000
2.790	54.810	0.000E+00	7.0	4.5	0.000
2.430	55.223	0.000E+00	7.0	4.5	0.000
4.000	53.453	0.000E+00	7.0	4.5	0.000
9.210	48.253	0.000E+00	1.0	4.0	0.000
8.140	49.165	0.000E+00	1.0	4.0	0.000
7.890	49.331	0.000E+00	1.0	4.0	0.000
10.680	46.594	0.000E+00	1.0	4.0	0.000
8.990	48.273	0.000E+00	1.0	3.8	0.000
8.770	48.904	0.000E+00	1.0	3.8	0.000
8.150	49.524	0.000E+00	1.0	3.8	0.000
7.660	49.940	0.000E+00	1.0	3.8	0.000
7.200	49.979	0.000E+00	1.0	3.5	0.000
5.580	51.609	0.000E+00	1.0	3.5	0.000
3.540	53.544	0.000E+00	1.0	3.5	0.000
4.240	52.655	0.000E+00	1.0	3.5	0.000
2.020	55.296	0.000E+00	1.0	2.8	0.000
0.670	58.425	0.000E+00	1.0	2.8	0.000
0.040	58.107	0.000E+00	1.0	2.8	0.000
0.000	55.042	0.000E+00	1.0	2.8	0.000
0.000	46.158	0.000E+00	2.0	2.4	0.000
0.000	38.737	0.000E+00	2.0	2.4	0.000
0.000	46.674	0.000E+00	2.0	2.4	0.000
0.000	32.579	0.000E+00	2.0	2.4	0.000
0.000	18.905	0.000E+00	8.0	2.4	0.000
0.000	17.347	1.396E-04	8.0	2.4	0.000
0.090	13.205	3.629E-04	8.0	2.4	20.039
0.450	14.434	6.896E-04	8.0	2.4	8.314
0.740	14.744	1.110E-03	20.0	3.6	3.275
0.810	14.853	1.513E-03	20.0	3.6	4.108
1.780	14.831	1.947E-03	20.0	3.6	2.393
2.880	17.120	2.360E-03	20.0	3.6	2.065
4.580	20.694	2.838E-03	23.0	5.0	1.610
4.750	21.071	3.288E-03	23.0	5.0	1.831
5.210	20.285	3.748E-03	23.0	5.0	1.829
6.370	17.809	4.177E-03	23.0	5.0	1.456
7.050	19.813	4.641E-03	21.0	7.6	1.728
7.230	19.254	4.949E-03	21.0	7.6	1.745
9.390	18.821	5.294E-03	21.0	7.6	1.395
11.150	20.987	5.615E-03	21.0	7.6	1.387

Table C-3. (Continued)

NO PPB	NO <sub>2</sub> PPB	j(NO <sub>2</sub> ) 1/SEC	O <sub>3</sub> PPB	TEMP C	PSS
9.790	21.568	5.766E-03	21.0	11.5	1.604
7.470	19.383	6.231E-03	21.0	11.5	2.049
6.220	17.275	6.143E-03	21.0	11.5	2.165
3.930	11.470	6.640E-03	21.0	11.5	2.461
3.170	12.304	6.716E-03	30.0	14.0	2.266
3.520	13.017	6.826E-03	30.0	14.0	2.193
2.870	12.246	6.932E-03	30.0	14.0	2.574
2.910	9.069	7.000E-03	30.0	14.0	1.890
3.150	12.008	7.100E-03	41.0	14.5	1.712
2.840	11.202	7.164E-03	41.0	14.5	1.788
2.270	10.414	6.932E-03	41.0	14.5	2.016
1.850	8.392	7.227E-03	41.0	14.5	2.078
1.980	8.504	7.304E-03	45.0	15.2	1.798
1.890	8.784	7.051E-03	45.0	15.2	1.879
1.540	8.849	6.966E-03	45.0	15.2	2.301
1.770	9.967	6.826E-03	45.0	15.2	2.209
2.590	10.736	6.753E-03	48.0	15.3	1.502
2.600	9.916	6.562E-03	48.0	15.3	1.341
2.010	9.464	6.422E-03	48.0	15.3	1.624
2.390	9.242	6.231E-03	48.0	15.3	1.291
2.490	12.673	6.052E-03	44.0	15.3	1.807
2.000	9.789	5.766E-03	44.0	15.3	1.484
1.320	9.417	5.404E-03	44.0	15.3	2.268
1.160	7.956	5.008E-03	44.0	15.3	2.020
1.060	9.793	4.766E-03	45.0	14.8	2.289
1.040	9.149	4.246E-03	45.0	14.8	2.163
1.030	9.812	3.484E-03	45.0	14.8	1.923
1.090	10.552	3.288E-03	45.0	14.8	1.845
0.780	10.062	2.711E-03	48.0	13.0	1.939
0.570	9.672	2.315E-03	48.0	13.0	2.180
0.460	9.845	2.087E-03	48.0	13.0	2.480
0.450	10.287	1.660E-03	48.0	13.0	2.108
0.360	10.619	1.314E-03	47.0	11.7	2.230
0.130	12.428	8.492E-04	47.0	11.7	4.679
0.010	13.422	4.729E-04	47.0	11.7	36.598
0.220	14.327	2.518E-04	47.0	11.7	0.945
0.170	15.083	0.000E+00	43.0	9.8	0.000
0.090	15.068	0.000E+00	43.0	9.8	0.000
0.050	14.876	0.000E+00	43.0	9.8	0.000
0.100	14.626	0.000E+00	43.0	9.8	0.000

Table C-3. (Continued)

NO PPB	NO <sub>2</sub> PPB	j(NO <sub>2</sub> ) 1/SEC	O <sub>3</sub> PPB	TEMP C	PSS
0.000	14.832	0.000E+00	39.0	8.0	0.000
0.000	15.211	0.000E+00	39.0	8.0	0.000
0.000	15.400	0.000E+00	39.0	8.0	0.000
0.000	15.400	0.000E+00	39.0	8.0	0.000
0.000	16.642	0.000E+00	41.0	7.3	0.000
0.030	17.675	0.000E+00	41.0	7.3	0.000
0.090	18.626	0.000E+00	41.0	7.3	0.000
0.020	19.885	0.000E+00	41.0	7.3	0.000
0.040	19.149	0.000E+00	36.0	7.5	0.000
0.040	20.539	0.000E+00	36.0	7.5	0.000
0.000	19.116	0.000E+00	36.0	7.5	0.000
0.080	19.352	0.000E+00	36.0	7.5	0.000
0.020	20.117	0.000E+00	31.0	7.8	0.000
0.050	22.213	0.000E+00	31.0	7.8	0.000
0.070	23.351	0.000E+00	31.0	7.8	0.000
0.040	24.339	0.000E+00	31.0	7.8	0.000

**Table C-4. Photostationary State (PSS) Data for  
March 27, 1982. Units of PSS are  
non-dimensional.**

NO PPB	NO <sub>2</sub> PPB	j(NO <sub>2</sub> ) 1/SEC	O <sub>3</sub> PPB	TEMP C	PSS
0.220	25.791	0.000E+00	27.0	8.4	0.000
0.020	25.685	0.000E+00	27.0	8.4	0.000
0.010	24.758	0.000E+00	27.0	8.4	0.000
0.020	22.275	0.000E+00	27.0	8.4	0.000
0.000	21.600	0.000E+00	24.0	8.0	0.000
0.010	22.443	0.000E+00	24.0	8.0	0.000
0.000	23.842	0.000E+00	24.0	8.0	0.000
0.000	24.326	0.000E+00	24.0	8.0	0.000
0.000	22.895	0.000E+00	23.0	6.8	0.000
0.000	25.863	0.000E+00	23.0	6.8	0.000
0.000	25.726	0.000E+00	23.0	6.8	0.000
0.000	22.905	0.000E+00	23.0	6.8	0.000
0.020	22.012	0.000E+00	20.0	6.2	0.000
0.000	24.589	0.000E+00	20.0	6.2	0.000
0.000	23.474	0.000E+00	20.0	6.2	0.000
0.000	22.242	0.000E+00	20.0	6.2	0.000
0.000	23.453	0.000E+00	20.0	6.6	0.000
0.000	20.326	0.000E+00	20.0	6.6	0.000
0.000	17.737	0.000E+00	20.0	6.6	0.000
0.000	17.263	0.000E+00	20.0	6.6	0.000
0.010	17.958	0.000E+00	27.0	6.7	0.000
0.080	13.783	0.000E+00	27.0	6.7	0.000
0.000	17.989	0.000E+00	27.0	6.7	0.000
0.000	16.695	0.000E+00	27.0	6.7	0.000
0.000	16.758	0.000E+00	26.0	7.5	0.000
0.000	15.979	8.303E-05	26.0	7.5	0.000
0.020	15.422	3.075E-04	26.0	7.5	25.891
0.170	15.430	6.358E-04	26.0	7.5	6.298
0.250	15.761	1.006E-03	31.0	7.6	5.799
0.580	15.482	1.414E-03	31.0	7.6	3.441
0.850	15.876	1.852E-03	31.0	7.6	3.156
1.210	16.464	2.405E-03	31.0	7.6	2.982
1.250	20.697	2.537E-03	37.0	8.4	3.181
2.200	20.716	2.754E-03	37.0	8.4	1.959
2.690	20.889	3.128E-03	37.0	8.4	1.833
4.250	19.950	4.038E-03	37.0	8.4	1.424
4.550	20.113	4.246E-03	29.0	11.3	1.741
4.570	19.409	4.828E-03	29.0	11.3	1.901
4.260	20.687	5.294E-03	29.0	11.3	2.387
4.360	18.977	5.404E-03	29.0	11.3	2.181

Table C-4. (Continued)

NO PPB	NO <sub>2</sub> PPB	j(NO <sub>2</sub> ) 1/SEC	O <sub>3</sub> PPB	TEMP C	PSS
3.460	18.003	5.912E-03	35.0	13.1	2.322
2.060	13.656	6.187E-03	35.0	13.1	3.103
1.600	12.253	6.359E-03	35.0	13.1	3.689
1.660	11.498	6.601E-03	35.0	13.1	3.461
1.410	11.643	6.678E-03	47.0	14.4	3.069
1.420	11.296	6.771E-03	47.0	14.4	2.997
1.660	11.824	6.790E-03	47.0	14.4	2.689
1.540	10.881	6.862E-03	47.0	14.4	2.695
1.770	9.988	7.017E-03	49.0	15.0	2.094
1.390	9.926	6.601E-03	49.0	15.0	2.498
1.080	10.099	6.966E-03	49.0	15.0	3.458
0.890	10.878	6.949E-03	49.0	15.0	4.515
0.910	10.427	6.897E-03	54.0	15.8	3.779
0.960	10.261	6.826E-03	54.0	15.8	3.488
0.820	10.201	6.678E-03	54.0	15.8	3.974
0.930	10.481	6.401E-03	54.0	15.8	3.449
1.020	10.654	6.231E-03	57.0	15.8	2.947
0.910	11.353	5.959E-03	57.0	15.8	3.369
1.000	11.247	5.815E-03	57.0	15.8	2.989
0.930	11.544	5.510E-03	57.0	15.8	3.100
0.750	11.324	5.457E-03	57.0	16.3	3.718
0.650	10.497	5.182E-03	57.0	16.3	3.776
0.640	10.939	4.828E-03	57.0	16.3	3.724
0.620	10.896	4.512E-03	57.0	16.3	3.580
0.650	9.908	4.177E-03	60.0	15.8	2.744
0.540	12.007	3.822E-03	60.0	15.8	3.666
0.580	12.736	3.445E-03	60.0	15.8	3.263
0.690	11.626	3.046E-03	60.0	15.8	2.212
0.560	11.787	2.625E-03	58.0	14.8	2.491
0.530	11.407	2.270E-03	58.0	14.8	2.203
0.380	12.020	1.900E-03	58.0	14.8	2.711
0.410	12.516	1.513E-03	58.0	14.8	2.084
0.320	14.343	1.110E-03	56.0	13.3	2.363
0.180	15.273	7.963E-04	56.0	13.3	3.212
0.140	14.292	4.729E-04	56.0	13.3	2.295
0.050	14.234	2.518E-04	56.0	13.3	3.409
0.050	13.529	0.000E+00	49.0	10.5	0.000
0.040	13.328	0.000E+00	49.0	10.5	0.000
0.000	13.874	0.000E+00	49.0	10.5	0.000
0.000	13.042	0.000E+00	49.0	10.5	0.000

Table C-4. (Continued)

NO PPB	NO <sub>2</sub> PPB	J(NO <sub>2</sub> ) 1/SEC	O <sub>3</sub> PPB	TEMP C	PSS
0.160	12.082	0.000E+00	45.0	8.8	0.000
0.020	11.812	0.000E+00	45.0	8.8	0.000
0.030	11.202	0.000E+00	45.0	8.8	0.000
0.000	10.000	0.000E+00	45.0	8.8	0.000
0.000	9.305	0.000E+00	46.0	7.4	0.000
0.000	9.168	0.000E+00	46.0	7.4	0.000
0.080	9.825	0.000E+00	46.0	7.4	0.000
0.000	10.137	0.000E+00	45.0	7.4	0.000
0.010	9.422	0.000E+00	42.0	7.6	0.000
0.000	9.389	0.000E+00	42.0	7.6	0.000
0.020	9.443	0.000E+00	42.0	7.6	0.000
0.000	9.811	0.000E+00	42.0	7.6	0.000
0.000	10.000	0.000E+00	41.0	7.3	0.000
0.000	9.653	0.000E+00	41.0	7.3	0.000
0.000	9.526	0.000E+00	41.0	7.3	0.000
0.070	9.193	0.000E+00	41.0	7.3	0.000

Table C-5. Photostationary State (PSS) Data for May 11, 1982. Units of PSS are non-dimensional.

NO PPB	NO <sub>2</sub> PPB	j(NO <sub>2</sub> ) 1/SEC	O <sub>3</sub> PPB	TEMP C	PSS
0.000	3.543	2.620E-05	25.0	5.2	0.000
0.015	3.400	2.620E-05	25.0	5.2	0.485
0.015	3.206	2.620E-05	25.0	5.2	0.648
0.031	3.996	2.620E-05	25.0	5.1	0.420
0.031	3.513	2.620E-05	25.0	5.1	0.370
0.031	3.513	2.620E-05	25.0	5.1	0.370
0.031	3.996	2.620E-05	25.0	5.0	0.421
0.015	3.367	2.620E-05	25.0	5.0	0.709
0.015	3.367	2.620E-05	25.0	5.0	0.709
0.015	2.984	2.620E-05	25.0	4.6	0.610
0.015	3.528	2.620E-05	25.0	4.6	0.747
0.046	3.658	2.620E-05	25.0	4.6	0.258
0.031	4.962	2.620E-05	25.0	4.2	0.527
0.199	3.666	2.620E-05	25.0	4.2	0.060
0.031	4.640	1.396E-04	25.0	4.2	2.628
0.077	4.433	3.629E-04	25.0	5.1	2.584
0.168	4.502	7.431E-04	25.0	5.1	2.442
0.520	6.244	1.058E-03	25.0	5.1	1.561
1.561	6.170	1.611E-03	21.0	6.7	0.915
2.601	9.156	2.270E-03	21.0	6.7	1.148
2.127	6.731	2.754E-03	21.0	6.7	1.252
1.867	9.568	3.522E-03	21.0	8.1	2.552
3.902	13.009	4.073E-03	21.0	8.1	1.920
4.942	13.901	4.766E-03	21.0	8.1	1.895
4.896	12.659	5.266E-03	24.0	10.0	1.649
5.018	12.536	5.716E-03	24.0	10.0	1.729
3.657	11.331	6.143E-03	24.0	10.0	2.303
2.723	10.161	4.246E-03	30.0	11.0	1.518
2.356	9.240	6.601E-03	30.0	11.0	2.480
2.234	8.718	6.771E-03	30.0	11.0	2.532
2.341	8.289	7.421E-03	35.0	10.8	2.163
2.417	8.373	7.017E-03	35.0	10.8	2.001
4.269	11.031	7.288E-03	35.0	10.8	1.550
2.678	8.596	7.436E-03	36.0	13.3	1.859
2.188	8.603	6.052E-03	36.0	13.3	1.853
2.096	7.245	8.047E-03	36.0	13.3	2.166
1.729	4.230	8.160E-03	39.0	12.5	1.448
1.408	6.001	5.815E-03	39.0	12.5	1.736
1.499	5.104	8.092E-03	39.0	12.5	1.907
1.362	6.530	7.930E-03	40.0	13.7	2.634
1.403	5.840	6.187E-03	40.0	13.7	1.732
1.346	5.096	7.808E-03	40.0	13.7	2.063



Table C-5. (Continued)

NO PPB	NO <sub>2</sub> PPB	I(NO <sub>2</sub> ) 1/SEC	O <sub>3</sub> PPB	TEMP C	PSS
0.918	5.041	7.548E-03	43.0	13.2	2.706
0.995	5.287	6.401E-03	43.0	13.2	2.221
0.780	5.501	7.034E-03	43.0	13.2	2.237
0.949	5.494	7.115E-03	45.0	13.5	2.562
0.811	5.148	6.844E-03	45.0	13.5	2.701
0.673	4.964	5.067E-03	45.0	13.5	2.323
0.474	5.324	4.673E-03	47.0	13.4	2.125
0.643	4.994	5.457E-03	47.0	13.4	2.528
0.490	4.664	4.704E-03	47.0	13.4	2.670
0.428	4.725	4.381E-03	48.0	12.5	2.847
0.428	4.725	3.523E-03	48.0	12.5	2.289
0.352	4.963	3.169E-03	48.0	12.5	2.633
0.305	4.848	2.625E-03	48.0	11.2	2.485
0.275	5.039	2.087E-03	48.0	11.2	2.282
0.230	5.407	1.513E-03	48.0	11.2	2.138
0.184	5.292	1.006E-03	46.0	9.9	1.835
0.122	5.192	5.818E-04	46.0	9.9	1.561
0.077	5.238	2.518E-04	45.0	9.9	1.091
0.061	5.576	1.396E-04	45.0	9.0	0.830
0.061	6.542	0.303E-05	45.0	9.0	0.580
0.046	6.718	0.000E+00	45.0	9.0	0.000
0.061	7.186	0.000E+00	45.0	9.0	0.000
0.046	7.201	0.000E+00	45.0	9.0	0.000
0.046	7.040	0.000E+00	45.0	9.0	0.000
0.046	8.812	0.000E+00	42.0	9.6	0.000
0.046	9.939	0.000E+00	42.0	9.6	0.000
0.046	12.033	0.000E+00	40.0	9.6	0.000
0.061	15.883	0.000E+00	36.0	9.3	0.000
0.077	12.436	0.000E+00	36.0	9.3	0.000
0.077	9.265	0.000E+00	36.0	9.3	0.000

Table C-6. Photostationary State (PSS) Data for May 12, 1982. Units of PSS are non-dimensional.

NO PPB	NO <sub>2</sub> PPB	J(NO <sub>2</sub> ) 1/SEC	O <sub>3</sub> PPB	TEMP C	PSS
0.061	7.508	2.620E-05	39.0	8.1	0.245
0.046	5.752	2.620E-05	39.0	8.1	0.250
0.031	4.479	2.620E-05	39.0	8.1	0.292
0.031	4.318	2.620E-05	39.0	8.0	0.282
0.031	4.318	2.620E-05	39.0	8.0	0.282
0.046	3.980	2.620E-05	39.0	8.0	0.173
0.031	3.513	2.620E-05	39.0	7.9	0.229
0.031	3.352	2.620E-05	39.0	7.9	0.219
0.031	3.190	2.620E-05	39.0	7.9	0.208
0.031	3.352	2.620E-05	38.0	7.0	0.227
0.031	3.190	2.620E-05	38.0	7.0	0.216
0.015	3.367	2.620E-05	38.0	7.0	0.456
0.015	3.689	2.620E-05	36.0	6.6	0.530
0.015	3.850	2.620E-05	36.0	6.6	0.553
0.031	3.674	1.396E-04	36.0	6.6	1.405
0.061	3.643	4.181E-04	36.0	8.1	2.052
0.092	4.257	9.019E-04	36.0	8.1	3.448
0.230	4.119	1.414E-03	36.0	8.1	2.092
0.275	3.751	1.947E-03	37.0	9.9	2.085
0.321	3.544	2.581E-03	37.0	9.9	2.239
0.260	3.122	3.288E-03	37.0	9.9	3.104
0.490	3.859	4.002E-03	37.0	11.3	2.443
0.719	4.918	4.108E-03	37.0	11.3	2.175
1.423	6.630	4.704E-03	37.0	11.3	1.697
1.775	7.405	5.510E-03	34.0	13.7	1.888
2.463	8.810	5.864E-03	34.0	13.7	1.722
1.958	7.866	6.540E-03	34.0	13.7	2.190
1.561	5.204	6.932E-03	38.0	14.5	1.684
1.270	4.045	6.401E-03	38.0	14.5	1.485
0.933	4.704	7.393E-03	38.0	14.5	2.714
1.270	4.689	7.348E-03	42.0	15.1	1.777
1.285	5.318	7.858E-03	42.0	15.1	2.130
1.117	6.614	7.784E-03	42.0	15.1	3.019
1.346	5.418	8.000E-03	45.0	16.3	1.943
1.255	5.026	8.070E-03	45.0	16.3	1.952
1.102	5.341	8.137E-03	45.0	16.3	2.381
1.148	4.811	8.115E-03	48.0	16.9	1.914
1.255	6.315	7.930E-03	48.0	16.9	2.245
1.102	6.146	7.882E-03	48.0	16.9	2.473
1.056	6.192	7.977E-03	50.0	17.1	2.521
1.117	6.614	7.942E-03	50.0	17.1	2.534
1.040	6.368	7.808E-03	50.0	17.1	2.575

Table C-6. (Continued)

NO PPB	NO <sub>2</sub> PPB	j(NO <sub>2</sub> ) 1/SEC	O <sub>3</sub> PPB	TEMP C	PSS
0.887	5.877	7.707E-03	53.0	17.0	2.597
0.826	5.938	7.492E-03	53.0	17.0	2.740
0.734	6.191	7.319E-03	53.0	17.0	3.139
0.689	5.915	6.966E-03	55.0	16.9	2.937
0.750	6.337	6.678E-03	55.0	16.9	2.771
0.826	7.065	6.253E-03	55.0	16.9	2.625
0.765	7.771	5.864E-03	56.0	16.0	2.898
0.765	8.093	5.431E-03	56.0	16.0	2.796
0.811	8.530	4.889E-03	56.0	16.0	2.502
0.689	8.492	4.314E-03	57.0	15.1	2.568
0.627	9.197	3.674E-03	57.0	15.1	2.599
0.612	9.212	3.128E-03	57.0	15.1	2.272
0.536	9.772	2.537E-03	56.0	13.7	2.308
0.520	11.559	1.947E-03	56.0	13.7	2.157
0.413	12.632	1.414E-03	56.0	13.7	2.155
0.306	13.706	9.543E-04	53.0	11.9	2.296
0.153	13.698	5.818E-04	53.0	11.9	2.797
0.107	14.237	2.518E-04	53.0	11.9	1.796
0.031	13.659	1.396E-04	48.0	11.2	3.723
0.015	14.157	8.303E-05	48.0	11.2	4.591
0.015	13.996	0.000E+00	43.0	11.2	0.000
0.015	13.352	0.000E+00	43.0	9.2	0.000
0.015	12.547	0.000E+00	43.0	9.2	0.000
0.000	13.367	0.000E+00	43.0	9.2	0.000
0.015	12.386	0.000E+00	40.0	9.0	0.000
0.000	12.401	0.000E+00	40.0	9.0	0.000
0.015	13.191	0.000E+00	40.0	9.0	0.000
0.000	14.334	0.000E+00	36.0	8.9	0.000
0.000	16.427	0.000E+00	36.0	8.9	0.000
0.000	17.233	0.000E+00	36.0	8.9	0.000

THIS DOCUMENT IS BEST QUALITY PRACTICABLE.  
 THE COPY FURNISHED TO YOU CONTAINED A  
 SIGNIFICANT NUMBER OF PAGES WHICH DO NOT  
 REPRODUCE LEGIBLY.

Table C-7. Photostationary State (PSS) Data for  
May 13, 1982. Units of PSS are  
non-dimensional.

NO PPB	NO <sub>2</sub> PPB	j(NO <sub>2</sub> ) 1/SEC	O <sub>3</sub> PPB	TEMP C	PSS
0.000	18.521	2.620E-05	32.0	8.3	0.000
0.031	16.075	2.620E-05	32.0	8.3	1.274
0.015	14.640	2.620E-05	32.0	8.3	2.320
0.015	13.352	2.620E-05	34.0	7.8	2.003
0.015	12.125	2.620E-05	34.0	7.8	1.834
0.015	11.503	2.620E-05	34.0	7.8	1.786
0.015	11.580	2.620E-05	34.0	7.6	1.741
0.000	10.952	2.620E-05	34.0	7.6	0.000
0.000	11.113	2.620E-05	34.0	7.6	0.000
0.000	11.113	2.620E-05	34.0	7.3	0.000
0.000	11.596	2.620E-05	34.0	7.3	0.000
0.000	10.791	2.620E-05	34.0	7.3	0.000
0.015	11.097	2.620E-05	34.0	7.1	1.678
0.015	12.386	2.620E-05	34.0	7.1	1.873
0.031	10.931	1.958E-04	34.0	7.1	6.171
0.122	11.634	4.729E-04	35.0	7.6	3.834
0.331	12.402	9.019E-04	35.0	7.6	2.969
0.474	11.283	1.414E-03	35.0	7.6	2.869
0.765	12.290	1.947E-03	33.0	11.0	2.722
1.333	16.041	2.531E-03	33.0	11.0	1.964
2.192	27.112	3.169E-03	33.0	11.0	1.442
5.792	14.710	3.748E-03	31.0	14.6	1.244
7.792	14.710	4.381E-03	31.0	14.6	1.611
7.792	14.710	4.319E-03	31.0	14.6	1.819
11.611	15.654	5.404E-03	40.0	15.6	1.726
11.611	9.663	5.912E-03	40.0	15.6	1.726
11.611	6.108	6.338E-03	40.0	15.6	1.726
11.641	12.542	6.716E-03	46.0	16.3	4.335
4.284	11.932	6.897E-03	46.0	16.3	1.139
0.750	4.727	7.286E-03	46.0	16.3	2.712
0.714	5.125	7.478E-03	51.0	17.4	2.661
0.704	4.727	7.694E-03	51.0	17.4	3.473
0.714	5.125	7.894E-03	51.0	17.4	3.737
0.750	5.125	7.954E-03	51.0	17.8	1.835
0.757	5.125	8.070E-03	51.0	17.8	1.749
0.714	5.125	8.115E-03	51.0	17.8	2.006
0.704	5.125	8.104E-03	53.0	18.3	2.197
0.750	5.125	8.104E-03	53.0	18.3	3.115
0.750	5.125	8.070E-03	53.0	18.3	2.929
0.750	5.114	8.115E-03	54.0	18.4	2.846
0.750	5.125	7.954E-03	54.0	18.4	2.398
0.750	5.114	7.870E-03	54.0	18.4	2.621

Table C-7. (Continued)

NO PPB	NO <sub>2</sub> PPB	j(NO <sub>2</sub> ) 1/SEC	O <sub>3</sub> PPB	TEMP C	PSS
		7.707E-03	57.0	18.8	2.468
		7.450E-03	57.0	18.8	2.141
		7.212E-03	57.0	18.8	2.217
		7.034E-03	63.0	18.7	2.525
		6.790E-03	63.0	18.7	2.317
		6.274E-03	63.0	18.7	2.787
		6.006E-03	67.0	18.2	2.596
		5.310E-03	67.0	18.9	2.625
		4.9E-03	67.0	18.2	2.498
		4.5E-03	70.0	17.4	2.434
		4.2E-03	70.0	17.4	2.474
		4.0E-03	70.0	17.4	2.528
		3.7E-03	72.0	15.7	2.482
		1.900E-02	72.0	15.7	2.415
		1.454E-03	72.0	15.7	2.411
		1.006E-03	70.0	13.3	2.559
		9.813E-04	70.0	13.3	2.358
		1.518E-04	70.0	13.3	2.198
		1.395E-04	59.0	11.6	1.259
		1.201E-05	59.0	11.6	0.937
		0.000E+00	59.0	11.6	0.000
		0.000E+00	59.0	11.8	0.000
		0.000E+00	59.0	11.8	0.000
		0.000E+00	59.0	11.8	0.000
		0.000E+00	59.0	10.2	0.000
		0.000E+00	59.0	10.2	0.000
		0.000E+00	59.0	10.2	0.000
		0.000E+00	59.0	10.5	0.000
		0.000E+00	59.0	10.5	0.000
		0.000E+00	59.0	10.5	0.000

THIS DOCUMENT IS BEST QUALITY PRACTICABLE.  
 THE COPY FURNISHED TO DDC CONTAINED A  
 SIGNIFICANT NUMBER OF PAGES WHICH DO NOT  
 REPRODUCE LEGIBLY.

## CLOUDY SKIES

Table C-8. Photostationary State (PSS) Data for January 26, 1982. Units of PSS are non-dimensional.

NO PPB	NO <sub>2</sub> PPB	j(NO <sub>2</sub> ) 1/SEC	O <sub>3</sub> PPB	TEMP C	PSS
0.000	22.358	0.000E+00	1.0	-0.8	0.000
0.000	21.181	0.000E+00	1.0	-0.8	0.000
0.000	18.828	0.000E+00	1.0	-0.8	0.000
0.000	17.651	0.000E+00	1.0	-0.8	0.000
0.000	16.474	0.000E+00	4.0	-0.7	0.000
0.000	15.298	0.000E+00	4.0	-0.7	0.000
0.000	14.121	0.000E+00	4.0	-0.7	0.000
0.000	12.944	0.000E+00	4.0	-0.7	0.000
0.000	12.944	0.000E+00	6.0	-0.6	0.000
0.000	10.591	0.000E+00	6.0	-0.6	0.000
0.000	9.414	0.000E+00	6.0	-0.6	0.000
0.000	10.591	0.000E+00	6.0	-0.6	0.000
0.000	11.767	0.000E+00	6.0	-0.3	0.000
0.000	10.591	0.000E+00	6.0	-0.3	0.000
0.000	10.591	0.000E+00	6.0	-0.3	0.000
0.000	10.591	0.000E+00	6.0	-0.3	0.000
0.000	10.591	0.000E+00	6.0	-0.1	0.000
0.000	10.591	0.000E+00	6.0	-0.1	0.000
0.000	9.414	0.000E+00	6.0	-0.1	0.000
0.000	9.414	0.000E+00	6.0	-0.1	0.000
0.000	10.591	0.000E+00	6.0	0.2	0.000
0.000	8.237	0.000E+00	6.0	0.2	0.000
0.000	8.237	0.000E+00	6.0	0.2	0.000
0.000	7.060	0.000E+00	6.0	0.2	0.000
0.000	7.060	0.000E+00	8.0	0.4	0.000
0.000	7.060	0.000E+00	8.0	0.4	0.000
0.000	7.060	0.000E+00	8.0	0.4	0.000
0.000	5.884	0.000E+00	8.0	0.4	0.000
0.000	7.060	0.000E+00	8.0	0.4	0.000
0.000	7.060	0.000E+00	6.0	0.3	0.000
0.000	7.060	0.000E+00	6.0	0.3	0.000
0.000	7.060	0.000E+00	6.0	0.3	0.000
0.000	7.060	0.000E+00	6.0	0.3	0.000
0.000	7.060	0.000E+00	12.0	0.1	0.000
0.118	6.942	3.005E-05	12.0	0.1	0.456
0.118	6.942	6.010E-05	12.0	0.1	0.911
0.354	7.883	1.202E-04	12.0	0.1	0.689
0.590	6.470	3.606E-04	17.0	0.2	0.716
0.826	6.204	4.808E-04	17.0	0.2	0.655
1.062	5.998	7.211E-04	17.0	0.2	0.734
1.298	5.762	7.211E-04	17.0	0.2	0.575

Table C-8. (Continued)

NO PPB	NO <sub>2</sub> PPB	j(NO <sub>2</sub> ) 1/SEC	O <sub>3</sub> PPB	TEMP C	PSS
1.888	6.349	6.610E-04	17.0	0.9	0.395
1.652	5.408	1.322E-03	17.0	0.9	0.768
1.534	5.526	1.202E-03	17.0	0.9	0.770
1.534	5.526	1.082E-03	17.0	0.9	0.693
1.416	5.644	1.082E-03	18.0	1.2	0.722
1.534	5.526	1.022E-03	18.0	1.2	0.616
1.416	5.821	1.683E-03	18.0	1.2	1.361
2.360	5.877	1.142E-03	18.0	1.2	0.472
2.242	5.995	2.224E-03	19.0	1.6	0.933
2.006	5.054	1.983E-03	19.0	1.6	0.783
1.652	5.408	2.163E-03	19.0	1.6	1.115
1.298	5.762	1.803E-03	19.0	1.6	1.356
1.534	5.526	1.082E-03	19.0	2.0	0.612
1.534	5.526	1.743E-03	19.0	2.0	0.985
1.180	5.880	1.322E-03	19.0	2.0	1.038
1.416	5.644	1.082E-03	19.0	2.0	0.678
1.416	5.644	1.022E-03	18.0	1.8	0.677
1.298	5.762	1.082E-03	18.0	1.8	0.800
1.770	5.290	9.014E-04	18.0	1.8	0.446
1.298	5.762	1.262E-03	18.0	1.8	0.933
1.180	7.057	3.413E-04	17.0	2.0	0.888
1.062	7.175	7.211E-04	17.0	2.0	0.861
0.826	6.234	5.409E-04	17.0	2.0	0.722
0.708	7.529	4.808E-04	17.0	2.0	0.906
0.590	7.647	4.808E-04	17.0	2.1	1.103
0.354	9.060	3.605E-04	17.0	2.1	1.537
0.236	9.178	1.202E-04	17.0	2.1	0.830
0.236	9.178	1.202E-04	17.0	2.1	0.830
0.236	9.178	9.014E-05	15.0	1.6	0.710
0.236	10.355	6.010E-05	15.0	1.6	0.534
0.118	10.473	0.000E+00	15.0	1.6	0.000
0.118	10.473	0.000E+00	15.0	1.6	0.000
0.118	9.296	0.000E+00	16.0	1.7	0.000
0.000	9.237	0.000E+00	16.0	1.7	0.000
0.000	8.237	0.000E+00	16.0	1.7	0.000
0.000	8.237	0.000E+00	16.0	1.7	0.000
0.000	8.237	0.000E+00	21.0	1.6	0.000
0.000	8.237	0.000E+00	21.0	1.6	0.000
0.000	7.060	0.000E+00	21.0	1.6	0.000
0.000	7.060	0.000E+00	21.0	1.6	0.000

Table C-8. (Continued)

NO PPB	NO <sub>2</sub> PPB	J(NO <sub>2</sub> ) 1/SEC	O <sub>3</sub> PPB	TEMP C	PSS
0.000	5.884	0.000E+00	28.0	1.4	0.000
0.000	5.884	0.000E+00	28.0	1.4	0.000
0.000	4.707	0.000E+00	28.0	1.4	0.000
0.000	4.707	0.000E+00	28.0	1.4	0.000
0.000	4.707	0.000E+00	28.0	1.5	0.000
0.000	5.884	0.000E+00	28.0	1.5	0.000
0.000	5.884	0.000E+00	28.0	1.5	0.000
0.000	5.884	0.000E+00	28.0	1.5	0.000
0.000	7.060	0.000E+00	22.0	0.8	0.000
0.000	8.237	0.000E+00	22.0	0.8	0.000
0.000	9.414	0.000E+00	22.0	0.8	0.000
0.000	10.591	0.000E+00	22.0	0.8	0.000
0.000	9.414	0.000E+00	18.0	1.1	0.000
0.000	10.591	0.000E+00	18.0	1.1	0.000
0.000	7.060	0.000E+00	18.0	1.1	0.000
0.000	7.060	0.000E+00	18.0	1.1	0.000



Table C-9. Photostationary State (PSS) Data for January 27, 1982. Units of PSS are non-dimensional.

NO PPB	NO <sub>2</sub> PPB	j(NO <sub>2</sub> ) 1/SEC	O <sub>3</sub> PPB	TEMP C	PSS
0.000	7.060	0.000E+00	24.0	1.3	0.000
0.000	7.060	0.000E+00	24.0	1.3	0.000
0.000	5.834	0.000E+00	24.0	1.3	0.000
0.000	7.060	0.000E+00	24.0	1.3	0.000
0.000	5.834	0.000E+00	25.0	1.5	0.000
0.000	4.707	0.000E+00	25.0	1.5	0.000
0.000	9.414	0.000E+00	25.0	1.5	0.000
0.000	9.414	0.000E+00	25.0	1.5	0.000
0.000	10.591	0.000E+00	17.0	1.5	0.000
0.000	11.767	0.000E+00	17.0	1.5	0.000
0.000	11.767	0.000E+00	17.0	1.5	0.000
0.000	10.591	0.000E+00	17.0	1.5	0.000
0.000	10.591	0.000E+00	15.0	1.4	0.000
0.000	10.591	0.000E+00	15.0	1.4	0.000
0.000	10.591	0.000E+00	15.0	1.4	0.000
0.000	10.591	0.000E+00	15.0	1.4	0.000
0.000	10.591	0.000E+00	15.0	1.3	0.000
0.000	11.767	0.000E+00	15.0	1.3	0.000
0.000	10.591	0.000E+00	15.0	1.3	0.000
0.000	10.591	0.000E+00	15.0	1.3	0.000
0.000	11.767	0.000E+00	14.0	1.3	0.000
0.000	11.767	0.000E+00	14.0	1.3	0.000
0.000	11.767	0.000E+00	14.0	1.3	0.000
0.000	11.767	0.000E+00	14.0	1.3	0.000
0.000	12.944	0.000E+00	12.0	1.2	0.000
0.000	12.944	0.000E+00	12.0	1.2	0.000
0.000	14.121	0.000E+00	12.0	1.2	0.000
0.000	14.121	0.000E+00	12.0	1.2	0.000
0.000	14.121	0.000E+00	11.0	1.0	0.000
0.000	14.121	0.000E+00	11.0	1.0	0.000
0.000	12.944	0.000E+00	11.0	1.0	0.000
0.000	12.944	0.000E+00	11.0	1.0	0.000
0.000	14.121	0.000E+00	11.0	0.4	0.000
0.236	15.052	3.005E-05	11.0	0.4	0.537
0.826	13.295	9.014E-05	11.0	0.4	0.406
1.298	11.646	2.404E-04	11.0	0.4	0.601
2.242	13.056	4.207E-04	11.0	0.4	0.681
2.596	12.702	4.507E-04	11.0	0.4	0.612
3.068	13.406	6.010E-04	11.0	0.4	0.728
4.720	11.754	4.507E-04	11.0	0.4	0.308

Table C-9. (Continued)

NO PPB	NO <sub>2</sub> PPB	j(NO <sub>2</sub> ) 1/SEC	O <sub>3</sub> PPB	TEMP C	PSS
6.254	12.574	7.211E-04	10.0	0.6	0.434
3.024	9.627	8.413E-04	10.0	0.6	0.297
4.484	11.990	8.413E-04	10.0	0.6	0.679
3.260	7.038	8.413E-04	10.0	0.6	0.207
3.063	11.053	9.014E-04	14.0	0.6	0.703
3.304	11.994	8.413E-04	14.0	0.6	0.662
5.310	9.988	8.413E-04	14.0	0.6	0.338
3.422	10.699	1.052E-03	14.0	0.6	0.711
2.950	9.994	1.262E-03	13.0	0.6	0.996
2.478	9.289	1.082E-03	13.0	0.6	0.946
2.714	10.230	1.022E-03	13.0	0.6	0.899
3.186	12.112	9.615E-04	13.0	0.6	0.853
6.136	17.399	7.312E-04	6.0	0.2	1.120
10.266	20.329	6.010E-04	6.0	0.2	0.597
9.204	22.566	4.207E-04	6.0	0.2	0.520
3.850	20.563	2.404E-04	6.0	0.2	0.281
5.310	20.573	3.005E-04	10.0	0.0	0.356
4.956	22.109	3.305E-04	10.0	0.0	0.452
6.013	16.340	3.906E-04	10.0	0.0	0.322
3.186	14.465	5.409E-04	10.0	0.0	0.752
2.832	17.172	6.010E-04	15.0	0.0	0.746
2.242	19.939	6.010E-04	15.0	0.0	1.043
2.124	19.057	3.606E-04	15.0	0.0	0.665
2.006	17.998	3.005E-04	15.0	0.0	0.554
1.416	17.412	3.005E-04	13.0	0.0	0.634
1.062	16.589	2.404E-04	13.0	0.0	0.644
0.590	14.703	2.404E-04	13.0	0.0	1.030
0.354	14.944	2.103E-04	13.0	0.0	1.527
0.590	14.703	1.202E-04	13.0	-0.1	0.515
0.236	15.062	9.014E-05	13.0	-0.1	0.991
0.354	15.120	0.000E+00	13.0	-0.1	0.000
0.236	15.062	0.000E+00	13.0	-0.1	0.000
0.113	14.003	0.000E+00	21.0	0.0	0.000
0.000	11.767	0.000E+00	21.0	0.0	0.000
0.000	11.767	0.000E+00	21.0	0.0	0.000
0.000	11.767	0.000E+00	21.0	0.0	0.000
0.000	11.767	0.000E+00	20.0	-0.1	0.000
0.000	11.767	0.000E+00	20.0	-0.1	0.000
0.000	11.767	0.000E+00	20.0	-0.1	0.000
0.000	12.944	0.000E+00	20.0	-0.1	0.000

Table C-9. (Continued)

NO PPB	NO <sub>2</sub> PPB	j(NO <sub>2</sub> ) 1/SEC	O <sub>3</sub> PPB	TEMP C	PSS
0.000	11.767	0.000E+00	17.0	-0.5	0.000
0.000	14.121	0.000E+00	17.0	-0.5	0.000
0.000	16.474	0.000E+00	17.0	-0.5	0.000
0.000	17.651	0.000E+00	17.0	-0.5	0.000
0.944	22.591	0.000E+00	4.0	-0.6	0.000
3.422	22.466	0.000E+00	4.0	-0.6	0.000
3.422	21.289	0.000E+00	4.0	-0.6	0.000
2.950	20.585	0.000E+00	4.0	-0.6	0.000
1.770	20.588	0.000E+00	1.0	-1.2	0.000
0.590	21.768	0.000E+00	1.0	-1.2	0.000
0.590	24.121	0.000E+00	1.0	-1.2	0.000
1.298	23.413	0.000E+00	1.0	-1.2	0.000
0.236	22.122	0.000E+00	5.0	-1.3	0.000
0.118	21.063	0.000E+00	5.0	-1.3	0.000
0.000	20.004	0.000E+00	5.0	-1.3	0.000
0.000	18.828	0.000E+00	5.0	-1.3	0.000

Table C-10. Photostationary State (PSS) Data for  
March 20, 1982. Units of PSS are  
non-dimensional.

NO PPB	NO <sub>2</sub> PPB	j(NO <sub>2</sub> ) 1/SEC	O <sub>3</sub> PPB	TEMP C	PSS
0.000	6.516	0.000E+00	23.0	0.8	0.000
0.000	7.619	0.000E+00	23.0	0.8	0.000
0.000	6.422	0.000E+00	23.0	0.8	0.000
0.000	5.186	0.000E+00	23.0	0.8	0.000
0.000	4.817	0.000E+00	24.0	0.5	0.000
0.000	5.804	0.000E+00	24.0	0.5	0.000
0.000	5.046	0.000E+00	24.0	0.5	0.000
0.000	5.963	0.000E+00	24.0	0.5	0.000
0.000	6.422	0.000E+00	23.0	0.4	0.000
0.000	5.275	0.000E+00	23.0	0.4	0.000
0.000	5.425	0.000E+00	23.0	0.4	0.000
0.000	5.585	0.000E+00	23.0	0.4	0.000
0.000	4.507	0.000E+00	24.0	0.3	0.000
0.000	4.158	0.000E+00	24.0	0.3	0.000
0.000	4.208	0.000E+00	24.0	0.3	0.000
0.000	3.909	0.000E+00	24.0	0.3	0.000
0.180	3.500	0.000E+00	24.0	0.1	0.000
0.020	3.859	0.000E+00	24.0	0.1	0.000
0.010	4.039	0.000E+00	24.0	0.1	0.000
0.030	4.238	0.000E+00	24.0	0.1	0.000
0.030	4.687	0.000E+00	22.0	0.3	0.000
0.010	4.996	0.000E+00	22.0	0.3	0.000
0.020	5.136	0.000E+00	22.0	0.3	0.000
0.020	5.285	0.000E+00	22.0	0.3	0.000
0.020	5.146	0.000E+00	20.0	0.8	0.000
0.000	5.674	0.000E+00	20.0	0.8	0.000
0.020	5.764	0.000E+00	20.0	0.8	0.000
0.100	6.262	6.010E-05	20.0	0.8	0.577
0.110	7.010	1.202E-04	19.0	1.3	1.229
0.160	6.721	1.502E-04	19.0	1.3	1.012
0.270	6.770	2.704E-04	19.0	1.3	1.087
0.330	5.274	5.709E-04	19.0	1.3	1.461
0.290	4.945	4.507E-04	21.0	1.6	1.109
0.400	4.616	6.610E-04	21.0	1.6	1.100
0.440	4.227	9.615E-04	21.0	1.6	1.330
0.480	3.868	8.413E-04	21.0	1.6	0.975
0.350	4.447	6.010E-04	19.0	2.2	1.208
0.590	4.326	8.413E-04	19.0	2.2	0.973
0.690	4.346	1.202E-03	19.0	2.2	1.193
0.460	4.526	9.615E-04	19.0	2.2	1.455

Table C-10. (Continued)

NO PPB	NO <sub>2</sub> PPB	j(NO <sub>2</sub> ) 1/SEC	O <sub>3</sub> PPB	TEMP C	PSS
0.540	4.805	1.142E-03	19.0	2.5	1.599
0.510	5.713	4.808E-04	19.0	2.5	0.849
0.470	5.813	9.014E-04	19.0	2.5	1.758
0.920	4.365	1.623E-03	19.0	2.5	1.205
0.330	5.453	7.211E-04	18.0	3.4	0.777
0.540	5.812	1.022E-03	18.0	3.4	1.809
0.540	5.334	7.912E-04	18.0	3.4	1.269
1.030	5.113	2.704E-03	18.0	3.4	2.196
0.900	7.417	4.207E-03	18.0	3.0	5.723
0.530	7.627	7.312E-04	18.0	3.0	1.861
0.790	7.128	1.322E-03	18.0	3.0	1.970
1.080	6.459	1.322E-03	18.0	3.0	1.302
0.540	7.029	1.803E-04	17.0	2.2	0.415
0.350	7.398	3.005E-04	17.0	2.2	1.125
0.410	6.880	8.413E-04	17.0	2.2	2.499
0.680	6.131	7.211E-04	17.0	2.2	1.148
0.430	7.613	3.005E-04	17.0	2.2	0.942
0.770	7.038	1.202E-03	17.0	2.2	1.940
1.760	6.916	2.163E-03	17.0	2.2	1.489
1.800	7.205	1.923E-03	17.0	2.2	1.349
0.840	5.841	3.606E-04	16.0	2.0	0.471
0.200	6.741	2.404E-04	16.0	2.0	1.530
0.370	7.010	5.409E-04	16.0	2.0	1.933
0.530	6.680	4.808E-04	16.0	2.0	1.141
0.480	7.249	4.207E-04	15.0	2.3	1.273
0.430	6.940	4.507E-04	15.0	2.3	1.457
0.680	6.520	4.808E-04	15.0	2.3	0.922
0.650	7.418	3.606E-04	15.0	2.3	0.823
0.410	6.999	3.606E-04	14.0	1.8	1.330
0.260	6.820	2.404E-04	14.0	1.8	1.363
0.180	6.970	1.502E-04	14.0	1.8	1.359
0.060	7.539	6.010E-05	14.0	1.8	1.635
0.050	8.048	6.010E-05	13.0	1.9	2.256
0.020	8.636	6.010E-05	13.0	1.9	5.054
0.020	8.476	0.000E+00	13.0	1.9	0.000
0.020	7.798	0.000E+00	13.0	1.9	0.000
0.050	7.689	0.000E+00	11.0	1.7	0.000
0.220	7.588	0.000E+00	11.0	1.7	0.000
0.100	8.307	0.000E+00	11.0	1.7	0.000
0.030	7.808	0.000E+00	11.0	1.7	0.000

Table C-10. (Continued)

NO PPB	NO <sub>2</sub> PPB	j(NO <sub>2</sub> ) 1/SEC	O <sub>3</sub> PPB	TEMP C	PSS
0.000	7.719	0.000E+00	11.0	1.4	0.000
0.000	8.387	0.000E+00	11.0	1.4	0.000
0.000	9.055	0.000E+00	11.0	1.4	0.000
0.000	9.783	0.000E+00	11.0	1.4	0.000
0.000	11.458	0.000E+00	6.0	1.4	0.000
0.000	13.891	0.000E+00	6.0	1.4	0.000
0.000	14.530	0.000E+00	6.0	1.4	0.000
0.000	17.661	0.000E+00	6.0	1.4	0.000
0.000	19.306	0.000E+00	7.0	1.2	0.000
0.000	18.189	0.000E+00	7.0	1.2	0.000
0.000	14.879	0.000E+00	7.0	1.2	0.000
0.000	15.447	0.000E+00	7.0	1.2	0.000
0.000	15.986	0.000E+00	10.0	1.0	0.000
0.000	15.178	0.000E+00	10.0	1.0	0.000
0.000	13.532	0.000E+00	10.0	1.0	0.000
0.000	11.199	0.000E+00	10.0	1.0	0.000

Table C-11. Photostationary State (PSS) Data for March 21, 1982. Units of PSS are non-dimensional.

NO PPB	NO <sub>2</sub> PPB	j(NO <sub>2</sub> ) 1/SEC	O <sub>3</sub> PPB	TEMP C	PSS
0.050	7.639	0.000E+00	18.0	0.8	0.000
0.050	7.150	0.000E+00	18.0	0.8	0.000
0.020	6.542	0.000E+00	18.0	0.8	0.000
0.040	5.923	0.000E+00	18.0	0.8	0.000
0.000	5.904	0.000E+00	20.0	0.9	0.000
0.020	5.804	0.000E+00	20.0	0.9	0.000
0.020	4.966	0.000E+00	20.0	0.9	0.000
0.010	4.497	0.000E+00	20.0	0.9	0.000
0.020	4.248	0.000E+00	23.0	1.0	0.000
0.010	4.019	0.000E+00	23.0	1.0	0.000
0.020	3.680	0.000E+00	23.0	1.0	0.000
0.030	3.520	0.000E+00	23.0	1.0	0.000
0.000	3.450	0.000E+00	24.0	1.1	0.000
0.040	3.211	0.000E+00	24.0	1.1	0.000
0.020	3.161	0.000E+00	24.0	1.1	0.000
0.010	3.181	0.000E+00	24.0	1.1	0.000
0.020	4.148	0.000E+00	21.0	1.1	0.000
0.070	4.059	0.000E+00	21.0	1.1	0.000
0.030	4.138	0.000E+00	21.0	1.1	0.000
0.040	4.428	0.000E+00	21.0	1.1	0.000
0.020	4.527	0.000E+00	19.0	1.1	0.000
0.030	4.627	0.000E+00	19.0	1.1	0.000
0.050	5.036	0.000E+00	19.0	1.1	0.000
0.010	5.265	0.000E+00	19.0	1.1	0.000
0.010	4.996	0.000E+00	18.0	1.1	0.000
0.010	5.126	0.000E+00	18.0	1.1	0.000
0.190	5.035	0.000E+00	18.0	1.1	0.000
0.010	6.273	0.000E+00	18.0	1.1	0.000
0.040	6.711	0.000E+00	11.0	1.0	0.000
0.050	10.850	0.000E+00	11.0	1.0	0.000
0.320	18.548	6.010E-05	11.0	1.0	0.969
0.540	18.348	9.014E-05	11.0	1.0	0.851
0.670	17.729	1.202E-04	8.0	1.1	1.214
1.010	16.950	2.103E-04	8.0	1.1	1.345
1.570	15.862	3.606E-04	8.0	1.1	1.386
1.970	15.132	3.906E-04	8.0	1.1	1.139
2.110	15.173	4.808E-04	9.0	1.1	1.156
2.490	14.662	6.310E-04	9.0	1.1	1.252
2.670	14.083	5.709E-04	9.0	1.1	1.013
2.700	13.555	6.610E-04	9.0	1.1	1.116

Table C-11. (Continued)

NO PPB	NO <sub>2</sub> PPB	j(NO <sub>2</sub> ) 1/SEC	O <sub>3</sub> PPB	TEMP C	PSS
2.520	13.765	6.010E-04	11.0	1.2	0.903
2.260	13.815	6.310E-04	11.0	1.2	1.062
2.040	13.816	5.409E-04	11.0	1.2	1.009
1.950	13.627	6.610E-04	11.0	1.2	1.273
2.010	13.377	6.610E-04	11.0	1.4	1.209
2.010	13.228	6.610E-04	11.0	1.4	1.196
2.280	12.888	7.812E-04	11.0	1.4	1.212
2.350	12.848	6.610E-04	11.0	1.4	0.992
2.420	12.509	1.142E-03	11.0	1.6	1.615
2.770	12.567	7.512E-04	11.0	1.6	0.931
2.740	12.857	7.211E-04	11.0	1.6	0.925
2.570	12.847	9.014E-04	11.0	1.6	1.232
2.520	12.668	6.911E-04	11.0	2.0	0.946
2.840	12.767	9.615E-04	11.0	2.0	1.175
3.440	12.067	1.202E-03	11.0	2.0	1.142
3.470	12.137	1.082E-03	11.0	2.0	1.025
3.390	12.486	1.142E-03	12.0	2.7	1.037
3.530	12.545	1.322E-03	12.0	2.7	1.158
4.220	11.835	2.163E-03	12.0	2.7	1.489
4.900	10.258	2.524E-03	12.0	2.7	1.288
4.960	9.689	2.584E-03	14.0	2.8	1.052
4.350	9.462	2.584E-03	14.0	2.8	1.174
3.470	9.644	1.562E-03	14.0	2.8	0.912
3.230	10.801	1.863E-03	14.0	2.8	1.313
3.450	10.043	2.043E-03	17.0	2.6	1.032
2.180	10.385	1.502E-03	17.0	2.6	1.251
1.690	10.127	9.014E-04	17.0	2.6	0.946
1.140	9.381	7.812E-04	17.0	2.6	1.129
0.630	9.163	5.409E-04	15.0	2.4	1.574
1.050	11.186	7.211E-04	15.0	2.4	1.535
1.150	11.525	4.908E-04	15.0	2.4	0.962
0.850	11.496	4.207E-04	15.0	2.4	1.138
0.590	11.596	2.404E-04	13.0	2.2	1.094
0.290	11.876	9.014E-05	13.0	2.2	0.856
0.160	12.216	6.010E-05	13.0	2.2	1.065
0.110	12.256	0.000E+00	13.0	2.2	0.000
0.040	11.219	0.000E+00	11.0	2.0	0.000
0.100	11.966	0.000E+00	11.0	2.0	0.000
0.020	12.794	0.000E+00	11.0	2.0	0.000
0.050	12.894	0.000E+00	11.0	2.0	0.000



Table C-11. (Continued)

NO PPB	NO <sub>2</sub> PPB	j(NO <sub>2</sub> ) 1/SEC	O <sub>3</sub> PPB	TEMP C	PSS
0.020	13.143	0.000E+00	11.0	1.5	0.000
0.110	11.927	0.000E+00	11.0	1.5	0.000
0.030	11.837	0.000E+00	11.0	1.5	0.000
0.050	12.705	0.000E+00	11.0	1.5	0.000
0.090	12.625	0.000E+00	9.0	1.2	0.000
0.060	12.395	0.000E+00	9.0	1.2	0.000
0.050	12.266	0.000E+00	9.0	1.2	0.000
0.010	12.236	0.000E+00	9.0	1.2	0.000
0.010	11.518	0.000E+00	11.0	0.0	0.000
0.040	10.890	0.000E+00	11.0	0.0	0.000
0.020	9.673	0.000E+00	11.0	0.0	0.000
0.020	8.556	0.000E+00	11.0	0.0	0.000
0.020	7.938	0.000E+00	14.0	0.0	0.000
0.030	7.798	0.000E+00	14.0	0.0	0.000
0.020	7.080	0.000E+00	14.0	0.0	0.000
0.020	7.240	0.000E+00	14.0	0.0	0.000

Table C-12. Photostationary State (PSS) Data for May 1, 1982. Units of PSS are non-dimensional.

NO PPB	NO <sub>2</sub> PPB	j(NO <sub>2</sub> ) 1/SEC	O <sub>3</sub> PPB	TEMP C	PSS
0.280	7.011	0.000E+00	22.0	4.2	0.000
0.350	7.960	0.000E+00	22.0	4.2	0.000
0.350	7.451	0.000E+00	22.0	4.2	0.000
0.350	7.783	0.000E+00	21.0	4.8	0.000
0.380	7.587	0.000E+00	21.0	4.8	0.000
0.400	7.567	0.000E+00	21.0	4.8	0.000
0.400	7.234	0.000E+00	21.0	5.0	0.000
0.400	7.057	0.000E+00	21.0	5.0	0.000
0.430	7.703	0.000E+00	21.0	5.0	0.000
0.440	8.712	0.000E+00	21.0	5.0	0.000
0.440	7.527	0.000E+00	21.0	5.0	0.000
0.380	6.461	0.000E+00	21.0	5.0	0.000
0.410	6.537	0.000E+00	21.0	5.0	0.000
0.410	7.224	0.000E+00	21.0	5.0	0.000
0.410	6.028	0.000E+00	21.0	5.0	0.000
0.430	6.351	0.000E+00	20.0	5.1	0.000
0.410	5.019	6.010E-05	20.0	5.1	0.107
0.440	5.499	6.010E-05	20.0	5.1	0.109
0.460	5.302	1.202E-04	18.0	5.1	0.224
0.540	6.241	1.803E-04	18.0	5.1	0.336
0.600	6.347	2.704E-04	18.0	5.1	0.461
0.660	7.650	3.005E-04	16.0	5.3	0.631
0.770	8.050	3.704E-04	16.0	5.3	0.512
0.780	8.040	3.704E-04	16.0	5.3	0.505
0.840	7.293	4.207E-04	18.0	5.7	0.584
0.700	6.934	3.606E-04	18.0	5.7	0.572
0.830	6.117	1.202E-03	18.0	5.7	1.416
0.960	5.655	1.022E-03	20.0	5.9	0.862
1.030	5.751	9.615E-04	20.0	5.9	0.769
0.780	6.167	7.211E-04	20.0	5.9	0.819
0.690	6.257	4.808E-04	22.0	6.7	0.564
0.630	5.309	7.211E-04	22.0	6.7	0.786
0.920	5.351	1.502E-03	22.0	6.7	1.128
0.700	4.729	1.683E-03	26.0	6.8	1.242
0.890	3.520	2.464E-03	26.0	6.8	1.058
0.610	3.634	2.344E-03	26.0	6.8	1.523
0.580	3.154	1.923E-03	27.0	7.0	1.095
0.540	4.036	1.082E-03	27.0	7.0	0.849
0.630	4.456	1.142E-03	27.0	7.0	0.848
0.610	4.310	1.322E-03	28.0	7.2	0.943

Table C-12. (Continued)

NO PPB	NO <sub>2</sub> PPB	j(NO <sub>2</sub> ) 1/SEC	O <sub>3</sub> PPB	TEMP C	PSS
0.600	4.142	1.082E-03	28.0	7.2	0.754
0.580	3.320	1.562E-03	28.0	7.2	0.902
0.430	3.470	1.502E-03	29.0	7.4	1.181
0.640	2.917	2.764E-03	29.0	7.4	1.221
0.640	3.604	2.524E-03	29.0	7.4	1.380
0.690	2.867	3.486E-03	28.0	7.2	1.455
0.630	3.946	2.464E-03	28.0	7.2	1.557
0.510	3.734	2.344E-03	29.0	7.2	1.733
0.730	3.846	1.562E-03	28.0	7.1	0.830
0.550	3.634	1.082E-03	28.0	7.1	0.734
0.430	4.312	8.413E-04	28.0	7.1	0.855
0.430	4.999	5.409E-04	27.0	4.8	0.679
0.410	4.687	4.507E-04	27.0	4.8	0.556
0.310	4.266	3.005E-04	27.0	4.8	0.447
0.260	3.806	2.404E-04	28.0	3.4	0.373
0.230	5.709	1.803E-04	28.0	3.4	0.475
0.140	4.270	1.202E-04	28.0	3.4	0.389
0.150	4.936	9.014E-05	27.0	2.4	0.330
0.150	5.279	3.005E-05	27.0	2.4	0.118
0.170	5.769	0.000E+00	27.0	2.4	0.000
0.200	5.905	0.000E+00	24.0	1.2	0.000
0.200	6.071	0.000E+00	24.0	1.2	0.000
0.180	5.925	0.000E+00	24.0	1.2	0.000
0.230	4.856	0.000E+00	24.0	1.5	0.000
0.180	4.906	0.000E+00	24.0	1.5	0.000
0.150	4.426	0.000E+00	24.0	1.5	0.000
0.200	5.905	0.000E+00	23.0	0.8	0.000
0.200	5.739	0.000E+00	23.0	0.8	0.000
0.200	4.720	0.000E+00	23.0	0.8	0.000
0.200	4.044	0.000E+00	25.0	0.5	0.000
0.200	4.376	0.000E+00	25.0	0.5	0.000
0.150	4.094	0.000E+00	25.0	0.5	0.000

Table C-13. Photostationary State (PSS) Data for May 4, 1982. Units of PSS are non-dimensional.

NO PPB	NO <sub>2</sub> PPB	j(NO <sub>2</sub> ) 1/SEC	O <sub>3</sub> PPB	TEMP C	PSS
0.000	3.734	0.000E+00	36.0	8.8	0.000
0.110	4.466	0.000E+00	36.0	8.8	0.000
0.110	3.956	0.000E+00	36.0	8.8	0.000
0.110	3.624	0.000E+00	34.0	8.4	0.000
0.110	3.790	0.000E+00	34.0	8.4	0.000
0.110	3.790	0.000E+00	34.0	8.4	0.000
0.110	4.134	0.000E+00	32.0	8.2	0.000
0.110	4.134	0.000E+00	32.0	8.2	0.000
0.120	4.124	0.000E+00	32.0	8.2	0.000
0.090	3.976	0.000E+00	31.0	7.6	0.000
0.090	4.154	0.000E+00	31.0	7.6	0.000
0.090	4.154	0.000E+00	31.0	7.6	0.000
0.110	4.466	0.000E+00	29.0	7.0	0.000
0.090	4.486	0.000E+00	29.0	7.0	0.000
0.120	4.456	0.000E+00	29.0	7.0	0.000
0.140	4.270	1.202E-04	28.0	7.4	0.371
0.180	4.740	2.404E-04	28.0	7.4	0.641
0.210	4.366	5.409E-04	28.0	7.4	1.139
0.290	4.463	8.413E-04	27.0	7.6	1.404
0.370	4.882	6.610E-04	27.0	7.6	0.912
0.320	4.256	6.610E-04	27.0	7.6	0.920
0.520	4.400	8.413E-04	26.0	8.3	0.766
0.490	4.762	1.472E-03	26.0	8.3	1.540
1.040	6.417	2.704E-03	26.0	8.3	1.790
1.060	4.879	2.284E-03	26.0	8.1	1.127
1.010	5.095	2.284E-03	26.0	8.1	1.236
0.860	4.226	2.704E-03	26.0	8.1	1.426
0.700	4.552	1.803E-03	28.0	8.3	1.169
0.430	4.490	1.082E-03	28.0	8.3	1.129
0.870	4.726	1.923E-03	28.0	8.3	1.939
0.780	4.649	2.224E-03	27.0	9.9	1.345
0.540	4.545	9.615E-04	27.0	9.9	0.823
0.730	5.209	2.103E-03	27.0	9.9	1.525
1.480	4.116	6.610E-03	28.0	10.0	1.778
1.840	6.127	7.031E-03	28.0	10.0	2.272
1.030	5.408	3.005E-03	28.0	10.0	1.540
1.150	3.426	4.026E-03	28.0	9.5	1.168
1.390	5.557	4.207E-03	28.0	9.5	1.546
1.420	8.408	2.103E-03	28.0	9.5	1.324
1.760	9.431	2.885E-03	26.0	9.3	1.538

Table C-13. (Continued)

NO PPB	NO <sub>2</sub> PPB	j(NO <sub>2</sub> ) 1/SEC	O <sub>3</sub> PPB	TEMP C	PSS
3.640	9.922	3.846E-03	26.0	9.3	1.100
3.320	11.594	4.267E-03	26.0	9.3	1.571
2.370	10.683	1.803E-03	26.0	9.5	0.858
2.680	10.040	3.365E-03	26.0	9.5	1.327
1.910	9.115	2.584E-03	26.0	9.5	1.302
2.140	9.051	4.147E-03	27.0	9.4	1.783
1.990	10.531	3.906E-03	27.0	9.4	2.107
1.270	12.802	7.211E-04	27.0	9.4	0.744
1.180	13.402	9.615E-04	26.0	9.3	1.163
1.790	11.939	1.502E-03	26.0	9.3	1.064
1.210	10.657	1.442E-03	26.0	9.3	1.351
0.860	7.960	1.562E-03	29.0	8.8	1.387
0.800	5.981	9.014E-04	29.0	8.8	0.646
0.530	7.387	6.911E-04	29.0	8.8	0.846
0.770	5.668	8.413E-04	27.0	8.9	0.636
0.960	10.741	9.014E-04	27.0	8.9	1.039
0.990	16.473	4.308E-04	27.0	8.9	0.825
0.470	14.621	2.404E-04	25.0	8.8	0.843
0.310	13.923	1.202E-04	25.0	8.8	0.609
0.150	15.784	0.000E+00	25.0	8.8	0.000
0.140	17.666	0.000E+00	24.0	7.8	0.000
0.150	14.593	0.000E+00	24.0	7.8	0.000
0.140	17.666	0.000E+00	24.0	7.8	0.000
0.140	16.400	0.000E+00	23.0	7.6	0.000
0.140	17.666	0.000E+00	23.0	7.6	0.000
0.120	18.523	0.000E+00	23.0	7.6	0.000
0.150	17.822	0.000E+00	22.0	7.4	0.000
0.120	14.794	0.000E+00	22.0	7.4	0.000
0.150	14.598	0.000E+00	22.0	7.4	0.000
0.150	16.470	0.000E+00	21.0	6.5	0.000
0.120	15.304	0.000E+00	21.0	6.5	0.000
0.770	17.712	0.000E+00	21.0	6.5	0.000

Table C-14. Photostationary State (PSS) Data for August 20, 1982. Units of PSS are non-dimensional.

NO PPB	NO <sub>2</sub> PPB	j(NO <sub>2</sub> ) 1/SEC	O <sub>3</sub> PPB	TEMP C	PSS
0.000	2.059	0.000E+00	33.0	12.7	0.000
0.000	1.765	0.000E+00	33.0	12.7	0.000
0.000	1.765	0.000E+00	33.0	12.7	0.000
0.000	2.255	0.000E+00	33.0	12.7	0.000
0.000	3.334	0.000E+00	33.0	12.5	0.000
0.000	4.217	0.000E+00	33.0	12.5	0.000
0.000	4.805	0.000E+00	33.0	12.5	0.000
0.000	4.707	0.000E+00	33.0	12.5	0.000
0.000	4.707	0.000E+00	31.0	11.7	0.000
0.000	3.922	0.000E+00	31.0	11.7	0.000
0.000	4.217	0.000E+00	31.0	11.7	0.000
0.000	4.903	0.000E+00	31.0	11.7	0.000
0.000	4.707	0.000E+00	28.0	10.7	0.000
0.000	4.609	0.000E+00	28.0	10.7	0.000
0.000	4.119	0.000E+00	28.0	10.7	0.000
0.000	4.119	0.000E+00	28.0	10.7	0.000
0.000	4.020	0.000E+00	26.0	10.8	0.000
0.000	4.217	0.000E+00	26.0	10.8	0.000
0.000	4.315	0.000E+00	26.0	10.8	0.000
0.000	4.217	0.000E+00	26.0	10.8	0.000
0.000	4.119	0.000E+00	25.0	10.9	0.000
0.000	4.119	0.000E+00	25.0	10.9	0.000
0.000	3.922	0.000E+00	25.0	10.9	0.000
0.000	3.922	0.000E+00	25.0	10.9	0.000
0.000	4.217	0.000E+00	22.0	11.7	0.000
0.000	3.922	0.000E+00	22.0	11.7	0.000
0.000	4.609	1.202E-04	22.0	11.7	0.000
0.159	4.940	1.502E-04	22.0	11.7	0.573
0.186	5.011	4.207E-04	26.0	12.4	1.171
0.274	4.923	5.709E-04	26.0	12.4	1.057
0.336	4.469	7.512E-04	26.0	12.4	1.038
0.398	4.701	9.916E-04	26.0	12.4	1.205
0.327	3.203	1.262E-03	28.0	12.2	1.182
0.274	3.060	1.322E-03	28.0	12.2	1.413
0.407	3.221	1.683E-03	28.0	12.2	1.273
0.425	3.007	2.224E-03	28.0	12.2	1.504
0.593	2.643	2.584E-03	28.0	12.0	1.098
0.398	2.642	2.524E-03	28.0	12.0	1.602
0.389	1.866	2.764E-03	28.0	12.0	1.264
0.372	2.276	2.404E-03	28.0	12.0	1.408

Table C-14. (Continued)

NO PPB	NO <sub>2</sub> PPB	j(NO <sub>2</sub> ) 1/SEC	O <sub>3</sub> PPB	TEMP C	PSS
0.336	1.919	2.764E-03	28.0	12.5	1.500
0.310	1.848	2.464E-03	28.0	12.5	1.398
0.345	2.106	2.644E-03	28.0	12.5	1.535
0.504	2.437	1.983E-03	28.0	12.5	0.969
0.540	2.402	2.865E-03	29.0	12.7	1.172
0.451	2.981	2.224E-03	29.0	12.7	1.347
0.327	2.222	2.224E-03	29.0	12.7	1.384
0.469	2.571	3.185E-03	29.0	12.7	1.598
0.531	3.391	3.906E-03	29.0	14.0	2.249
0.549	2.491	3.606E-03	29.0	14.0	1.470
0.504	1.849	2.945E-03	29.0	14.0	0.957
0.345	2.499	2.224E-03	29.0	14.0	1.452
0.310	3.122	1.202E-03	34.0	14.0	0.929
0.646	3.374	2.644E-03	34.0	14.0	1.054
1.071	2.361	3.305E-03	34.0	14.0	0.549
0.437	2.063	3.545E-03	34.0	14.0	1.144
0.522	2.125	6.791E-03	37.0	10.0	2.035
0.664	1.788	8.113E-03	37.0	10.0	1.599
0.451	1.608	7.812E-03	37.0	10.0	2.046
0.416	1.153	6.731E-03	37.0	10.0	1.366
0.310	1.259	4.207E-03	36.0	9.6	1.300
0.230	1.241	4.147E-03	36.0	9.6	1.306
0.239	1.438	3.726E-03	36.0	9.6	1.300
0.230	1.143	3.786E-03	36.0	9.6	1.433
0.263	1.598	3.005E-03	38.0	9.0	1.097
0.106	1.659	9.014E-04	38.0	9.0	1.177
0.549	1.920	3.606E-04	38.0	9.0	0.955
0.089	1.873	4.207E-04	38.0	9.0	0.745
0.204	1.660	1.022E-03	38.0	10.4	0.758
0.142	2.114	3.065E-04	38.0	10.4	0.410
0.159	1.300	8.413E-04	38.0	10.4	0.915
0.150	2.007	1.322E-03	38.0	10.4	1.610
0.195	3.434	1.262E-03	38.0	9.5	2.053
0.212	2.827	5.409E-04	38.0	9.5	0.864
0.602	3.026	7.812E-04	38.0	9.5	0.360
0.089	3.246	1.202E-04	38.0	9.5	0.407
0.389	3.043	1.382E-03	28.0	9.0	1.070
0.584	2.843	1.082E-03	29.0	9.0	0.520
0.327	3.399	9.014E-04	28.0	9.0	0.328
0.239	2.997	5.010E-04	28.0	9.0	0.748

Table C-14. (Continued)

NO PPB	NO <sub>2</sub> PPB	j(NO <sub>2</sub> ) 1/SEC	O <sub>3</sub> PPB	TEMP C	PSS
0.159	3.665	3.506E-04	25.0	8.5	0.929
0.097	3.335	2.404E-04	25.0	8.5	0.923
0.053	3.967	1.202E-04	25.0	8.5	1.008
0.035	4.083	0.000E+00	25.0	8.5	0.000
0.013	4.003	0.000E+00	24.0	8.5	0.000
0.013	3.414	0.000E+00	24.0	8.5	0.000
0.000	3.432	0.000E+00	24.0	8.5	0.000
0.000	3.538	0.000E+00	24.0	8.5	0.000
0.000	3.138	0.000E+00	23.0	8.3	0.000
0.000	3.236	0.000E+00	23.0	8.3	0.000
0.000	3.824	0.000E+00	23.0	8.3	0.000
0.000	3.814	0.000E+00	23.0	8.3	0.000
0.000	3.824	0.000E+00	24.0	7.8	0.000
0.000	3.720	0.000E+00	24.0	7.3	0.000
0.000	3.720	0.000E+00	24.0	7.3	0.000
0.000	4.111	0.000E+00	24.0	7.8	0.000



Table C-15. Photostationary State (PSS) Data for August 24, 1982. Units of PSS are non-dimensional.

NO PPB	NO <sub>2</sub> PPB	j(NO <sub>2</sub> ) 1/SEC	O <sub>3</sub> PPB	TEMP C	PSS
0.000	3.628	0.000E+00	26.0	12.5	0.000
0.000	2.942	0.000E+00	26.0	12.5	0.000
0.000	3.040	0.000E+00	26.0	12.5	0.000
0.000	3.236	0.000E+00	26.0	12.5	0.000
0.000	2.648	0.000E+00	24.0	12.2	0.000
0.000	2.452	0.000E+00	24.0	12.2	0.000
0.000	2.452	0.000E+00	24.0	12.2	0.000
0.000	2.648	0.000E+00	24.0	12.2	0.000
0.000	2.942	0.000E+00	22.0	11.8	0.000
0.000	2.844	0.000E+00	22.0	11.8	0.000
0.000	3.530	0.000E+00	22.0	11.8	0.000
0.000	2.648	0.000E+00	22.0	11.8	0.000
0.000	2.844	0.000E+00	19.0	11.6	0.000
0.000	2.550	0.000E+00	19.0	11.6	0.000
0.000	2.648	0.000E+00	19.0	11.6	0.000
0.000	2.452	0.000E+00	19.0	11.6	0.000
0.000	3.530	0.000E+00	19.0	10.8	0.000
0.000	3.334	0.000E+00	19.0	10.8	0.000
0.000	2.746	0.000E+00	19.0	10.8	0.000
0.000	2.746	0.000E+00	19.0	10.8	0.000
0.000	3.040	0.000E+00	18.0	11.0	0.000
0.000	3.236	0.000E+00	18.0	11.0	0.000
0.000	3.236	0.000E+00	18.0	11.0	0.000
0.000	3.628	0.000E+00	18.0	11.0	0.000
0.000	3.628	0.000E+00	15.0	11.1	0.000
0.000	3.922	0.000E+00	15.0	11.1	0.000
0.000	2.824	6.010E-05	15.0	11.1	0.000
0.080	4.137	1.803E-04	15.0	11.1	1.701
0.133	3.790	3.305E-04	15.0	11.6	1.703
0.177	3.647	3.305E-04	15.0	11.6	1.229
0.195	6.670	4.207E-04	15.0	11.6	2.602
0.292	4.415	6.010E-04	15.0	11.6	1.637
0.531	3.882	4.808E-04	20.0	11.7	0.473
0.487	3.730	1.202E-03	20.0	11.7	1.239
0.469	4.042	1.022E-03	20.0	11.7	1.186
0.885	3.332	2.163E-03	20.0	11.7	1.088
0.522	2.812	1.322E-03	24.0	12.8	0.787
0.549	3.275	2.043E-03	24.0	12.8	1.349
0.664	2.572	2.524E-03	24.0	12.8	1.077
0.708	1.940	3.245E-03	24.0	12.8	0.973

Table C-15. (Continued)

NO PPB	NO <sub>2</sub> PPB	j(NO <sub>2</sub> ) 1/SEC	O <sub>3</sub> PPB	TEMP C	PSS
0.310	3.319	1.803E-03	27.0	13.0	1.802
0.752	2.386	2.163E-03	27.0	13.0	0.668
0.478	2.464	2.224E-03	27.0	13.0	1.123
0.398	3.916	1.442E-03	27.0	13.0	1.396
1.195	2.728	2.284E-03	31.0	14.3	0.431
0.416	2.330	2.704E-03	31.0	14.3	1.269
0.504	3.928	3.606E-03	31.0	14.3	1.754
0.664	2.082	3.786E-03	31.0	14.3	0.987
0.575	2.955	2.835E-03	35.0	16.0	1.085
0.504	1.947	4.988E-03	35.0	16.0	1.405
0.389	2.062	3.666E-03	35.0	16.0	1.422
0.407	2.044	4.086E-03	35.0	16.0	1.502
0.513	1.742	7.812E-03	39.0	15.0	1.751
0.664	1.788	6.311E-03	39.0	15.0	1.334
0.327	2.124	3.666E-03	39.0	15.0	1.582
0.398	1.857	6.791E-03	39.0	15.0	2.100
0.398	1.661	7.392E-03	40.0	15.4	1.982
0.292	1.277	7.512E-03	40.0	15.4	2.113
0.293	1.482	7.572E-03	40.0	15.4	2.554
0.195	1.374	4.808E-03	40.0	15.4	2.194
0.150	1.419	4.507E-03	43.0	15.2	2.556
0.142	2.300	1.142E-03	43.0	15.2	1.367
0.168	2.293	2.704E-03	43.0	15.2	2.321
0.274	2.471	3.726E-03	43.0	15.2	2.026
0.265	2.284	4.086E-03	43.0	15.5	2.067
0.133	1.417	1.502E-03	44.0	15.5	1.613
0.150	2.333	1.502E-03	44.0	15.5	1.702
0.177	2.733	1.502E-03	44.0	15.5	1.383
0.254	2.274	3.005E-03	45.0	14.9	1.600
0.310	2.534	2.764E-03	45.0	14.9	1.600
0.159	2.292	2.486E-03	45.0	14.9	2.903
0.177	1.882	2.885E-03	45.0	14.9	1.776
0.354	3.563	2.284E-03	43.0	14.3	1.403
0.177	3.255	1.923E-03	43.0	14.3	2.161
0.133	2.103	1.382E-03	43.0	14.3	1.976
0.177	3.353	1.082E-03	43.0	14.3	1.252
0.195	3.139	7.312E-04	39.0	13.7	0.854
0.195	3.434	5.409E-04	39.0	13.7	0.647
0.142	4.369	3.005E-04	39.0	13.7	0.629
0.035	4.181	2.103E-04	39.0	13.7	1.639

Table C-15. (Continued)

NO PPB	NO <sub>2</sub> PPB	j(NO <sub>2</sub> ) 1/SEC	O <sub>3</sub> PPB	TEMP C	PSS
0.080	4.627	1.502E-04	35.0	11.3	0.678
0.071	3.852	9.014E-05	35.0	11.3	0.381
0.035	4.181	6.010E-05	35.0	11.3	0.552
0.027	3.895	0.000E+00	35.0	11.3	0.000
0.000	4.903	0.000E+00	32.0	11.2	0.000
0.000	4.119	0.000E+00	32.0	11.2	0.000
0.000	3.530	0.000E+00	32.0	11.2	0.000
0.000	3.725	0.000E+00	32.0	11.2	0.000
0.000	4.119	0.000E+00	30.0	11.0	0.000
0.000	4.119	0.000E+00	30.0	11.0	0.000
0.000	4.119	0.000E+00	30.0	11.0	0.000
0.000	4.119	0.000E+00	30.0	11.0	0.000
0.000	1.725	0.000E+00	30.0	11.0	0.000
0.000	4.315	0.000E+00	28.0	11.0	0.000
0.000	4.020	0.000E+00	18.0	11.0	0.000
0.000	1.510	0.000E+00	18.0	11.0	0.000
0.000	1.040	0.000E+00	18.0	11.0	0.000

## APPENDIX D

### SAMPLE PROGRAMS

#### DATA AQUITION PHOTOSTATIONARY STATE

```

10 DIM A(72,3),J(72,3),O(72,3),T(72,3),K(72,3)
20 REM *****
30 REM A=NO,NOX,NOY, J=J(NO2), O=OZONE(O3), T=TEMP(CENT), PSS=PHOTOSTATIONARY
40 REM *****
50 PRINT "DATA ACQUISITION PHOTOSTATIONARY STATE"
60 DISP "UV INT. IN MM FROM FILE"
70 INPUT B
80 LOAD DATA B:P
90 DISP "OZONE FROM FILE"
100 INPUT B
110 LOAD DATA B:O
120 DISP "TEMP FROM WHAT FILE"
130 INPUT B
140 LOAD DATA B:T
150 GOTO 450
160 DISP "WANT TO CHANGE DATA"
170 INPUT I
180 IF I#1 THEN 300
190 DISP "WHICH LINE"
200 INPUT I
210 PRINT A(I,2),A(I,3),A(I,1),J(I,1),O(I,1),T(I,1)
220 DISP "NEW VALUES"
230 INPUT A(I,2),A(I,3),A(I,1),J(I,1),O(I,1),T(I,1)
240 PRINT "NEW"
250 PRINT "A(I,2)=A(I,3),A(I,1),J(I,1),O(I,1),T(I,1)"
260 DISP "ANOTHER LINE"
270 INPUT I
280 IF I#1 THEN 300
290 GOTO 190
300 DISP "WANT TO CHANGE MM INTO PPB"
310 INPUT I1
320 IF I1#1 THEN 450
330 REM *****
340 REM CONSTANT = 0.153 PPB/MM
350 REM *****
360 FOR I=1 TO 72
370 A(I,2)=A(I,2)
380 A(I,3)=A(I,3)/0.95
390 A(I,1)=A(I,1)/0.95
400 NEXT I
410 REM *****
420 REM CONVERSION EFFICIENCY IS 95%
430 REM *****
440 PRINT "A CHANGE FROM MM INTO PPB AT 0.153 PPB/MM; CONV EFF 95%"
450 DISP "WANT TO CHANGE P INTO J(NO2)"
460 INPUT I1
470 IF I1#1 THEN 910

```

```

480 REM *****
490 REM CHANGE K INTO J WHICH IS J(N02) IN 1/SEC
500 REM K(I,1) IS FOR CLEAR SKIES
510 REM K(I,2) IS FOR CLOUDY SKIES
520 REM *****
530 FOR I=1 TO 62
540 K(I,3)=K(I,3)+0.05+0.505
550 W=0.0262
560 J(I,1)=(K(I,3)+3)*7.22E-02-(K(I,3)+2)*8.917E-01+K(I,3)+4.5123+W)-0.001
570 REM *****
580 REM 0.05 MV/MM; 0.505 MVCM-2/MV
590 REM ONLY VALID FOR EPPLLEY IN DEUSELBACH
600 REM POLYNOMIAL CONVERTS MVCM-2 INTO 1/SEC
610 REM *****
620 NEXT I
630 FOR I=63 TO 72
640 K(I,3)=0
650 J(I,1)=(K(I,3)+3)*7.22E-02-(K(I,3)+2)*8.917E-01+K(I,3)+4.5123
660 NEXT I
670 DISP "NO NOX FROM FILE";
680 INPUT B
690 LOAD DATA B.A
700 REM*****
710 REM C = RATE CONST IN PPB-1,SEC-1
720 REM*****
730 PRINT "DATE: 13 MAY 1982"
740 PRINT
750 PRINT " NO          NO2          J,N02          O3          TEMP          P55
760 PRINT " PPB          PPB          1/S          PPB          C"
770 FORMAT F6.3,5X,F7.3,5X,E10.3,4X,F5.1,5X,F5.1,8X,F6.3
780 Q=273
790 FOR I=1 TO 72
800 IF A(I,2)=0 THEN 870
810 Z=2.7E+10*(Q/(Q+T(I,3)))*2.3E-12*EXP(-1450/(T(I,3)+Q))
820 P=(J(I,1)*(A(I,3)+0.95)-A(I,2))/(A(I,2)+Q*(I,3)*(Z*(Q/(Q+T(I,3))))
830 REM*****
840 REM F=N02
850 REM*****
860 IF P#0 THEN 880
870 P=0
880 F=(A(I,3)+0.95)-A(I,2)
890 WRITE (15,770)A(I,2),F,J(I,1),Q(I,3),T(I,3),P
900 NEXT I
910 END

```

## GENERAL PLOTTING ROUTINE

```
10 DIM A[31]
20 DISP "# OF DAYS IN MONTH";
30 INPUT T
40 DISP "NORMAL RUN";
50 INPUT S
60 IF S=1 THEN 130
70 DISP "WANT TOP AXIS";
80 INPUT M
90 IF M=1 THEN 210
100 DISP "WANT RIGHT AXIS";
110 INPUT R
120 IF R=1 THEN 270
130 X=0
140 DISP "DATA FROM WHICH FILE";
150 INPUT D
160 LOAD DATA D,A
170 SCALE -5,38,-10,75
180 DISP "WANT TO SKIP LABELS";
190 INPUT R
200 IF R=1 THEN 760
210 DISP "Y-OFFSET";
220 INPUT E
230 XAXIS E,1,1,T
240 DISP "DID YOU CHANGE Y-OFFSET";
250 INPUT F
260 IF F=1 THEN 870
270 DISP "X-OFFSET";
280 INPUT G
290 YAXIS G,5,0,70
300 DISP "DID YOU CHANGE X-OFFSET";
310 INPUT H
320 IF H=1 THEN 880
330 OFFSET 0,0
340 FOR I=1 TO 5 STEP 4
350 PLOT I,0,1
360 CPLOT -2,-1.5
370 LABEL (380)I
380 FORMAT F3.0
390 NEXT I
400 FOR I=10 TO T STEP 5
410 PLOT I,0,1
420 CPLOT -2,-1.5
430 LABEL (440)I
440 FORMAT F3.0
450 NEXT I
```

```
460 FOR J=0 TO 70 STEP 10
470 PLOT 0,J,1
480 CPLOT -5,-0.3
490 LABEL (500)J
500 FORMAT F6.1
510 NEXT J
520 LABEL (530)"DAILY MEANS OF"
530 FORMAT 9X
540 LABEL (550)"SO2 & PRECIP"
550 FORMAT 9X
560 LABEL (570)"FOR MAR 1982"
570 FORMAT 9X,3B
580 PLOT -5,37
590 CPLOT -12,-0.3
600 LABEL (*)"SO2"
610 PLOT -5,35
620 CPLOT -12,-0.3
630 LABEL (*)"(PPB)"
640 PLOT (T-14),-6
650 CPLOT -1,-0.3
660 LABEL (*)"TIME"
670 PLOT (T-14),-8
680 CPLOT -1,-0.3
690 LABEL (*)"(DAYS)"
700 PLOT (T+1),37
710 CPLOT 5,-0.3
720 LABEL (*)"PRECIP"
730 PLOT (T+1),35
740 CPLOT 5,-0.3
750 LABEL (*)"(MM)"
760 FOR I=1 TO T
770 X=X+1
780 PLOT X,AC(I)
790 CPLOT -0.3,-0.3
800 LABEL (*)
810 IPLOT 0,0
820 NEXT I
830 PEN
840 DISP "WANT TO END PROGRAM";
850 INPUT Q
860 IF Q=1 THEN 960
870 GOTO 40
880 DISP "J=U TO V STEP W";
890 INPUT U,V,W
900 FOR J=U TO V STEP W
910 PLOT T,J,1
920 CPLOT 0,-0.3
930 LABEL (940)J/5
940 FORMAT F5.1
950 NEXT J
960 END
```

# SELECTED BIBLIOGRAPHY

- Aron, R., Mixing height - an inconsistent indicator of potential air pollution concentrations, Atmos. Environ., 17, 2193-2197, 1983.
- Bach, W., Atmospheric Pollution, McGraw-Hill, New York, 1972.
- Bahe, F.C., W.N. Marx, and U. Schurath, Determination of the absolute photolysis rate of ozone by sunlight,  $O_3 + h\nu \rightarrow O(^1D) + O_2(^1\Delta_g)$ , at ground level, Atmos. Environ., 13, 1515-1522, 1979.
- Battan, L.J., The Unclean Sky, a Meteorologist Looks at Air Pollution, Anchor/Doubleday, Garden City, 1966.
- Bottenheim, J., S. Bralavsky, and O. Strausz, Modelling study of seasonal effect on air pollution at 60° N latitude, Environ. Sci. Tech., 11, 801-808, 1977.
- Brooks, C., Handbook of Statistical Methods in Meteorology, AMS Press, New York, 1953.
- Calvert, J.G., Test of the theory of ozone generation in Los Angeles atmosphere, Environ. Sci. Tech., 10, 248-256, 1976.
- Carmichael, G.R., and L.K. Peters, Some aspects of SO<sub>2</sub> absorption by water-generalized treatment, Atmos. Environ., 13, 1505-1513, 1979.
- Chameides, W.L., and J.C.G. Walker, A photochemical theory of tropospheric ozone, J. Geophys. Res., 78, 8751-8760, 1973.
- Chameides, W.L., D.H. Stedman, R.R. Dickerson, D.W. Rusch, and R.J. Cicerone, NO<sub>x</sub> production in lightning, J. Atmos. Sci., 34, 143-149, 1979.
- Chameides, W.L., and D.D. Davis, Special Report, Chem. and Environ., Oct., 39-52, 1982.
- Chock, D.P., and S. Kumar, Technical note on the photo-stationary state assumption in the atmospheric nitric oxide-nitrogen dioxide-ozone system, Atmos. Environ., 13, 419-420, 1978.



- Cox, R.A., A.E.J. Eggleton, R.G. Derwent, J.E. Lovelock, and D.H. Pack, Long-range transport of photochemical ozone in north-western Europe, *Nature*, 255, 118-121, 1975.
- Crocker, J.E., and H.G. Applegate, Ozone concentrations in El Paso, Texas, *J. Air Pollut. Contr. Assoc.*, 33, 129-130, 1983.
- Crutzen, P.J., Chemical issues in atmospheric sciences with emphasis on tropospheric processes, in the 2nd International Chemistry Conference in Africa, Nairobi, Kenya, June 27 - July 2, 1983.
- Crutzen, P.J., and L.T. Gidel, A two-dimensional photochemical model of the atmosphere 2: the tropospheric budgets of the anthropogenic chlorocarbons CO, CH<sub>4</sub>, CH<sub>3</sub>Cl, and the effect of various NO<sub>x</sub> sources on tropospheric ozone, *J. Geophys. Res.*, 88, 6641-6661, 1983.
- Derwent, R.G., A.E.J. Eggleton, M.L. Williams, C.A. Bell, Elevated ozone levels from natural sources, *Atmos. Environ.*, 12, 2173-2177, 1978.
- Derwent, R.G., and O. Hov., The potential for secondary pollutant formation in the atmospheric boundary layer in a high pressure situation over England, *Atmos. Environ.*, 16, 655-665, 1982.
- Dickerson, R.R., Measurements of reactive nitrogen compounds in the free troposphere, *Atmos. Environ.*, 18, 2585-2593, 1984.
- Dickerson, R.R., and D.H. Stedman, Measurements of solar ultraviolet radiation and atmospheric photolysis rates, *Atmos. Tech.*, 12, 56-62, 1980.
- Dickerson, R.R., D.H. Stedman, and A.C. Delaney, Direct measurements of ozone and nitrogen dioxide photolysis rates in the tropopause, *J. Geophys. Res.*, 87, 4933-4946, 1982.
- Dickerson, R.R., A.C. Delaney, and A.F. Wartburg, Further modification of a commercial NO<sub>x</sub> detector for higher sensitivity, *Rev. Sci. Instrum.*, 55, 1995-1998, 1984.

- Eliassen, A., A review of long-range transport modeling, *J. Appl. Meteorol.*, 19, 231-240, 1980.
- Eliassen, A., and J. Saltbones, Modelling of long-range transport of sulphur over Europe: a two-year model run and some model experiments, *Atmos. Environ.*, 17, 1457-1473, 1983.
- Evans, G., P. Finkelstein, B. Martin, N. Possiel and M. Graves, Ozone measurements from a network of remote sites, *J. Air Pollut. Contr. Assoc.*, 33, 291-296, 1983.
- Finlayson, B.J., and J.N. Pitts, Jr., Photochemistry of the polluted troposphere, *Science*, 192, 111-119, 1976.
- Fisher, B.E.A., A review of the processes and models of long-range transport of air pollutants, *Atmos. Environ.*, 17, 1865-1880, 1983.
- Garnett, A., Nitrogen oxides and carbon monoxide air pollution in the city of Sheffield, *Atmos. Environ.*, 13, 845-852, 1979.
- Glasson, W.A., Effect of hydrocarbons and  $\text{NO}_x$  on photochemical smog formation under simulated transport conditions, *J. Air Pollut. Contr. Assoc.*, 31, 1169-1172, 1981.
- Haagenson, P.L., Meteorological and climatological factors affecting Denver air quality, *Atmos. Environ.*, 13, 79-85, 1978.
- Hahn, J., and P.J. Crutzen, The role of fixed nitrogen in atmospheric photochemistry, *Atmos. Photochem.*, 296, 521-541, 1982.
- Haltiner, G.J., and F.L. Martin, *Dynamical and Physical Meteorology*, McGraw-Hill, New York, 1957.
- Hanst, P.L., Noxious trace gases in the air, *Chemistry*, 51, 8-15, 1978.
- Hogstrom, U., Air pollution in Swedish communities, *Ambio*, 4, 120-125, 1975.
- Hogstrom, U., Initial dry deposition and type of source in relation to long distance transport of air pollutants, *Atmos. Environ.*, 13, 295-301, 1978.

- Jones, F.L., R.W. Miksad, A.R. Laird, and P. Middleton,  
A simple method for estimating the influence of cloud  
cover on the  $\text{NO}_2$  photolysis rate constant, J. Air  
Pollut. Contr. Assoc., 31, 42-45, 1981.
- Kelly, T.J., D.H. Stedman, J.A. Ritter, and R.B. Harvey,  
Measurements of oxides of nitrogen and nitric acid in  
clean air, J. Geophys. Res., 85, 7417-7425, 1980.
- Lindsberg, H.E., World Survey of Climatology: Climates  
of Central and Southern Europe, edited by C.C.  
Wallen, vol. 6, Elsevier Scientific, Amsterdam, 1977.
- Leighton, P.A., Photochemistry of Air Pollution,  
Academic, New York, 1961.
- Levy II, H., Photochemistry of the lower troposphere,  
Planet. Space Sci., 20, 919-935, 1972.
- Levy II, H., Photochemistry of minor constituents in the  
troposphere, Planet. Space Sci., 21, 575-591, 1973.
- Logan, J.A., Nitrogen oxides in the troposphere: global  
and regional budgets, J. Geophys. Res., 88,  
10,785-10,807, 1983.
- Meszaros, E., Atmospheric Chemistry: Fundamental  
Aspects, Elsevier Scientific, Amsterdam, 1981.
- Milne, J.W., D.B. Roberts, and D.J. Williams, The dry  
deposition of sulfur dioxide - field measurements  
with a stirred chamber, Atmos. Environ., 13, 373-379,  
1978.
- Mukammal, E.I., H.H. Neumann, and T.J. Gillespie,  
Meteorological conditions associated with ozone in  
southwestern Ontario, Canada, Atmos. Environ., 16,  
2095-2106, 1982.
- Nieboer, H., W.P.L. Carter, A.C. Lloyd, and J.N. Pitts,  
Jr., The effect of latitude on the potential for  
information of photochemical smog, Atmos. Environ.,  
10, 731-734, 1976.
- O'Brien, R.J., Photostationary state in photochemical  
smog studies, Environ. Sci. Tech., 8, 579-583, 1974.

- Pack, D.H., G.J. Ferber, J.L. Heffter, K. Telegadas, J.K. Angell, and W.H. Hoecker, Meteorology of long-range transport, Atmos. Environ., 12, 425-444, 1977.
- Petterssen, S., Introduction to Meteorology, McGraw-Hill, New York, 1969.
- Richards, L.W., Comments on the oxidation of NO<sub>2</sub> to nitrate - day and night, Atmos. Environ., 17, 397-402, 1983.
- Rodhe, H., P. Crutzen, and A. Vanderpol, Formation of sulfuric and nitric acid in the atmosphere during long range transport, Tellus, 33, 132-141, 1981.
- Schjoldager, J., Observations of high ozone concentrations in Oslo, Norway, during the summer of 1977, Atmos. Environ., 33, 1689-1696, 1979.
- Schjoldager, J., Ambient ozone measurements in Norway 1975-1979, J. Air Pollut. Contr. Assoc., 31, 1187-1191, 1981.
- Schjoldager, J., B. Sivertsen, and J.E. Hanssen, On the occurrence of photochemical oxidants at high latitudes, Atmos. Environ., 12, 2461-2467, 1978.
- SCOPE 16, Carbon Cycle Modeling, edited by B. Bolin, John Wiley & Sons, Chichester, 1981.
- Sexton, K., and H. Westberg, Photochemical ozone formation from petroleum refinery emissions, Atmos. Environ., 17, 467-475, 1983.
- Shetter, R.E., D.H. Stedman, and D.H. West, The NO/NO<sub>2</sub>/O<sub>3</sub> photostationary state in Claremont, California, J. Air Pollut. Contr. Assoc., 33, 212-214, 1983.
- Slemr, F.R., R.R. Dickerson, and W. Seiler, Field measurements of NO and NO<sub>2</sub> emissions from soil, presented at the CACGP Symposium on Tropospheric Chemistry in Oxford, UK, August 28 - September 3, 1983.
- Smith, F.B., and G.H. Jeffrey, Airborne transport of sulfur dioxide from the U.K., Atmos. Environ., 643-659, 1975.

- Spedding, D.J., Air Pollution, Oxford University Press, London, 1974.
- U.S. Department of Energy, Handbook on atmospheric diffusion, Technical Information Center, DOE/TIC-11223, Springfield, Virginia, 1982.
- U.S. Environmental Protection Agency, Air quality criteria for ozone and other photochemical oxidants, EPA-600/8-78-004, Washington, D.C., 1978.
- Vukovich, F.M., W.D. Bach, Jr., B.W. Crissman, and W.J. King, On the relationship between high ozone in the rural surface layer and high pressure systems, Atmos. Environ., 11, 967-983, 1977.
- Wark, K., and C.F. Warner, Air Pollution: Its Origin and Control, Harper and Row, New York, 1981.
- Weber, E., Air pollution control strategy in the Federal Republic of Germany, J. Air Pollut. Contr. Assoc., 31, 24-30, 1981.
- Winer, A.M., G.M. Breur, W.P.L. Carter, K.R. Darnall, and J.N. Pitts, Jr., Effects of ultraviolet spectral distribution of the photochemistry of simulated polluted atmospheres, Atmos. Environ., 13, 989-998, 1979.
- Witz, S., A.M. Larm, B.M. Elvin, and A.B. Moore, The relationship between concentration of traffic-related pollutants and meteorology at a Los Angeles site, J. Air Pollut. Contr. Assoc., 32, 643-644, 1982.
- Zafonte, L., P.L. Rieger, and J.R. Holmes, Nitrogen dioxide photolysis in the Los Angeles atmosphere, Environ. Sci. Tech., 11, 483-487, 1977.


2

APPROVAL SHEET

Title of Thesis: Analysis of the Relationship Between  
Meteorology and Air Pollution at  
Deuselbach, West Germany

Name of Candidate: Stephen Robert Messina  
Master of Science, 1985

Thesis and Abstract Approved:

  
Russell R. Dickerson  
Assistant Professor  
Department of Meteorology

Date Approved:

8/2/85

## CURRICULUM VITAE

Name: Stephen Robert Messina.

PII Redacted

Degree and date to be conferred: MS, 1985.

Secondary education: Cardinal Spellman High School  
Bronx, New York, May 1971.

Collegiate institutions attended	Dates	Degree	Date of Degree
Manhattan College Bronx, New York	Sep 1971- May 1975	BCE	May 1975
St. Louis University St. Louis, Missouri	Aug 1975- Jul 1976	---	---
University of Maryland College Park, Maryland	Aug 1982- May 1984	MS	Aug 1985

Major: Meteorology.

Professional  
positions held:

- Officer-in-Charge  
OL-G, 2nd Weather Squadron  
Tyndall Air Force Base, Florida.
- Staff Weather Officer  
Detachment 2, HQ Air Weather Service  
Pentagon, Washington DC.
- Officer-in-Charge  
21st Air Force Weather Support Unit  
McGuire Air Force Base, New Jersey.
- Duty Forecaster  
21st Air Force Weather Support Unit  
McGuire Air Force Base, New Jersey.
- Duty Forecaster  
Detachment 10, 7th Weather Wing  
McGuire Air Force Base, New Jersey.